**T.C.**

**HASAN KALYONCU UNIVERSITY**

**GRADUATE EDUCATION INSTITUTE**

**CIVIL ENGINEERING DEPARTMENT**

# INVESTIGATION OF DRY AND WET PERIODS CHARACTERISTICS WITH DIFFERENT DROUGHT INDICES IN YEŞILIRMAK, KIZILIRMAK AND KONYA CLOSED BASINS

**MEHMET SELİM GEYİKLİ**

**Ph.D. THESIS**

**GAZİANTEP - 2023**

# Investigation of Dry and Wet Periods Characteristics With Different Drought Indices in Yeşilırmak, Kızılırmak and Konya Closed Basins

**Ph.D. THESIS**

**in**

**Civil Engineering Department**

**Hasan Kalyoncu University**

**Supervisor**

**Assoc. Prof. Dr. Mehmet Ali HINIS**

**by**

**Mehmet Selim GEYİKLİ**

**Gaziantep 2023**

# LİSANSÜSTÜ EĞİTİM ENSTİTÜSÜ

# DOKTORA TEZ KABUL VE ONAY FORMU

**İnşaat Mühendisliği** Anabilim Dalı Doktora Programı öğrencisi **Mehmet Selim GEYİKLİ** tarafından hazırlanan **"Investigation of Dry and Wet Periods Characteristics With Different Drought Indices in Yeşilırmak, Kızılırmak and Konya Closed Basins"** başlıklı tez, **12/06/2023** tarihinde yapılan savunma sınavı sonucu **başarılı** bulunarak jürimiz tarafından **Doktora Tezi** olarak kabul edilmiştir.

| **Görevi** | **Unvanı, Adı ve Soyadı** | **Kurumu/Üniversitesi** | **İmzası:** |
|---|---|---|---|
| **Tez Danışmanı** | Assoc. Prof. Dr. Mehmet Ali HINIS | Aksaray Üniversitesi | |
| **Jüri Başkanı** | Prof. Dr. Kadri YÜREKLİ | Tokat Gaziosmanpaşa Üniversitesi | |
| **Jüri Üyesi** | Prof. Dr. Hanifi ÇANAKÇI | Hasan Kalyoncu Üniversitesi | |
| **Jüri Üyesi** | Assoc. Prof. Dr. Adem YURTSEVER | İstanbul Üniversitesi Cerrahpaşa | |
| **Jüri Üyesi** | Asst. Prof. Dr. Amin GHAREHBAGHI | Hasan Kalyoncu Üniversitesi | |

**Bu tez Enstitü Yönetim Kurulunca belirlenen yukarıdaki jüri üyeleri tarafından uygun görülmüş ve Enstitü Yönetim Kurulu kararı ile onaylanmıştır.**

Prof. Dr. M. Serhat YENİCE

Enstitü Müdürü

## DECLARATION PAGE

**I hereby declare that all information in this document has been obtained and presented in accordance with academic rules and ethical conduct. I also declare that, as required by these rules and conduct, I have fully cited and referenced all material and results that are not original to this work.**

GEYİKLİ MEHMET SELİM

12.06.2023

**HASAN KALYONCU UNIVERSITY**
**GRADUATE EDUCATION INSTITUTE**
**CIVIL ENGINEERING DEPARTMENT**

# INVESTIGATION OF DRY AND WET PERIODS CHARACTERISTICS WITH DIFFERENT DROUGHT INDICES IN YEŞILIRMAK, KIZILIRMAK AND KONYA CLOSED BASINS

**Mehmet Selim GEYİKLİ**

**PHD THESIS**

**Advisor**
**Assoc. Prof. Dr. Mehmet Ali HINIS**

## ABSTRACT

Within the scope of this thesis, drought analyses were conducted using the SPI, RDI, SPEI, and SRI methods based on a total of 38 meteorological stations in the Yeşilırmak, Kızılırmak, and Konya closed basins. The SPI method was employed for drought analysis at 1, 3, 6, 9, 12, and 24-month accumulations. The Weibull and Generalized Extreme Value (GEV) distributions were determined as the most suitable distributions for the SPI index. In the analyses conducted using the RDI method, low correlations were observed, leading to the conclusion that the RDI index is not entirely reliable. For the analyses conducted using the SPEI method, critical situations were initially not detected, and D values were used to determine the most appropriate distribution methods. It was observed that the Generalized Extreme Value (GEV) distribution was generally suitable for SPEI 3 and 12-month accumulations. The SRI method was applied to a limited number of streamflow

stations, and significant results could not be obtained due to data insufficiency. After the completion of drought analyses, correlation calculations were performed to understand the relationships between the meteorological stations. Histograms were obtained for the 3-month and 12-month drought indices based on the classifications. Additionally, distribution maps of drought indices throughout the basin were created using the Inverse Distance Weighting (IDW) method. Trend analyses were conducted on precipitation data for meteorological stations using the SPI, RDI, and SPEI drought analysis results. Trend results were obtained using the Mann-Kendall (MK) and Innovative Şen Trend Analysis (ITA) methods and presented with maps. Magnitude-Duration-Frequency (MDF) analyses were performed to characterize drought and estimate the duration of drought magnitudes. MDF graphs revealed comparisons between stations for each method. Basin-specific MDF comparison maps were obtained, indicating higher drought magnitudes in the northern regions.

**Keywords:** Drought, Drought Indices, Trend Analysis, Magnitude-Duration-Frequency, Spatial Distribution Maps

**HASAN KALYONCU ÜNİVERSİTESİ**
**LİSANSÜSTÜ EĞİTİM ENSTİTÜSÜ**
**İNŞAAT MÜHENDİSLİĞİ ANABİLİM DALI**

# YEŞILIRMAK, KIZILIRMAK VE KONYA KAPALI HAVZALARINDA KURAK VE ISLAK DÖNEM KARAKTERISTIKLERININ FARKLI KURAKLIK INDISLERI ILE İNCELENMESI

**Mehmet Selim GEYİKLİ**

**DOKTORA TEZİ**

**Danışman**
**Doç. Dr. Mehmet Ali HINIS**

## ÖZET

Bu tez kapsamında, Yeşilırmak, Kızılırmak ve Konya kapalı havzalarında toplam 38 meteoroloji istasyonu kullanılarak SPI, RDI, SPEI ve SRI yöntemleriyle kuraklık analizleri gerçekleştirildi. SPI yöntemi, 1, 3, 6, 9, 12 ve 24 aylık toplamlar için kuraklık analizlerinde kullanıldı. Weibull ve Genelleştirilmiş Ekstrem Değer (GEV) dağılımları, SPI indeksinin en uygun dağılımları olarak belirlendi. RDI yöntemiyle yapılan analizlerde düşük korelasyonlar gözlendi ve RDI indeksinin tamamen güvenilir olmadığı sonucuna varıldı. SPEI yöntemiyle yapılan analizlerde, başlangıçta kritik durumlar tespit edilemedi ve en uygun dağılım yöntemleri belirlenmek için D değerleri kullanıldı. Genelleştirilmiş Ekstrem Değer (GEV) dağılımının SPEI 3 ve 12 aylık toplamlar için genellikle uygun olduğu gözlendi. SRI yöntemi ise sınırlı sayıda akım istasyonunda uygulandı ve veri yetersizliği nedeniyle anlamlı sonuçlar elde edilemedi. Kuraklık analizlerinin tamamlanmasının ardından

istasyonlar arasındaki ilişkileri anlamak için korelasyon hesaplamaları yapıldı. 3 aylık ve 12 aylık kuraklık indislerinin sınıflandırmalarına göre histogramlar elde edildi. Ayrıca, ters mesafe ağırlıklı yöntem (IDW) kullanılarak havza genelinde kuraklık indislerinin dağılım haritaları oluşturuldu. Meteoroloji istasyonları için yağış verileri, SPI, RDI ve SPEI kuraklık analiz sonuçları üzerinde trend analizleri gerçekleştirildi. Mann-Kendall (MK) ve İnovatif Şen Trend Analizi (ITA) yöntemleri kullanılarak trend sonuçları elde edildi ve haritalarla verildi. Büyüklük-Süre-Frekans (MDF) analizleri yapılarak kuraklık büyüklüklerinin süresi tahmin edildi. MDF grafikleri, her yöntem için istasyonlar arasında karşılaştırmaları gösterdi. Havza bazında MDF karşılaştırma haritaları elde edildi ve kuraklık büyüklüklerinin kuzey bölgelerinde yoğun olduğunu gösterdi.

**Anatar Kelimeler:** Kuraklık, Kuraklık İndeksleri, Trend Analizi, Büyüklük-Süre-Tekerrür, Bölgesel Dağılım Haritaları

## ACKNOWLEDGEMENTS

First and foremost, I would like to express my sincere gratitude to my esteemed advisor, Assoc. Prof. Dr. Mehmet Ali HINIS, and my esteemed thesis monitoring committee members, Prof. Dr. Kadri YÜREKLİ and Assoc. Prof. Dr. Adem YURTSEVER. I would also like to thank my sister, Şuanur GEYİKLİ, for the technical support. I extend my heartfelt thanks to my spouse and family for their financial and emotional support, and to everyone who has assisted me during the thesis process.

I dedicate this thesis to the victims of the earthquake on 06.02.2023.

Mehmet Selim GEYİKLİ

Gaziantep - 2023

**CONTENTS**

## LIST OF TABLES

## LIST OF FIGURES

## LIST OF SYMBOLS/ABBREVIATIONS

| | |
|---|---|
| **AGI:** | Flow Observation Station |
| **AI:** | Aridity Index |
| **ANN:** | Artificial Neural Network |
| **$Chi^2$:** | Chi-Square |
| **D1:** | Moderately Drought |
| **D2:** | Drought |
| **D3:** | Extremely Drought |
| **DEM:** | Digital Elevation Model |
| **DSİ:** | State Hydraulic Works |
| **$ET_0$:** | Evapotranspiration |
| **EV1:** | Extreme Value Type 1 |
| **FAO:** | Food and Agriculture Organization |
| **GAM:** | Gamma |
| **GEV:** | Generalized Extreme Value |
| **GIS:** | Geographic Information System |
| **GLOG**: | Generalized Logistic |
| **GPAR:** | Generalized Pareto |
| **GPCC:** | Global Precipitation Climatology Centre |
| **IDF:** | Intensity-Duration-Frequency |
| **ITA:** | Innovatife Şen Trend Analysis |
| **K–S:** | Kolmogorov–Smirnov |
| **LN2:** | Two Parameter Lognormal |
| **LN3:** | Three Parameter Lognormal |
| **LOG:** | Logistic |
| **LP3:** | Log Pearson Type 3 |
| **MDF:** | Magnitude-Duration-Frequency |
| **MGM:** | General Directorate of Meteorology |
| **MK:** | Mann-Kendall Trend Analysis |
| **MLM:** | Maximum Likelihood |
| **MOM:** | Methods of Moments |
| **N:** | Normal |
| **P3:** | Pearson Type 3 |

| | |
|---|---|
| **PDSI:** | Palmer Drought Severity Index |
| **PET:** | Potential evapotranspiration |
| **PWM:** | Probability Weighted Moments |
| **RDI:** | Reconnaissance Drought Index |
| **scPDSI:** | self-calibrating Palmer drought severity index |
| **SDI:** | Streamflow Drought Index |
| **SPEI:** | Standardized Precipitation Evapotranspiration Index |
| **SPEI G:** | Standardized Precipitation Evapotranspiration Index With GLOG Distribution |
| **SPEI bf:** | Standardized Precipitation Evapotranspiration Index With Best Fit Distribution |
| **SPI:** | Standardized Precipitation Index |
| **SPI G:** | Standardized Precipitation Index With Gamma Distribution |
| **SPI bf:** | Standardized Precipitation Index With Best Fit Distribution |
| **SRI:** | Standardized Runoff Index |
| **W:** | Weibull |
| **W1:** | Moderately Wet |
| **W2:** | Wet |
| **W3:** | Extremely Wet |

# CHAPTER 1

# INTRODUCTION

## 1.1.Drought

Drought is a slow-moving natural disaster that affects all living things negatively and whose exact origin and end cannot be predicted easily. Drought is a significant issue that has an impact on economic life and can reduce agricultural productivity, which can lead to famine, starvation, mortality, and migration. Due to its geographic position and organizational structure, our country has significantly distinct climatic zones. The largest influence on climate elements, and particularly on drought, is the precipitation factor, which exhibits significant temporal and regional variations.

The most pernicious natural calamity and the most dangerous among hydrological occurrences that cannot be directly quantified is the drought. Drought begins to pose its first threat when there is insufficient water available to meet the needs of all living creatures and habitat. Drought threatens societies and nations as a result of the rise in global population, urbanization, climate change, deforestation, environmental pollution, and desertification. Economic and societal aspects of drought exist. Additionally, it has a close connection to trade, psychology, and public health (Şen, 2001; Tosunoğlu, 2014).

One of the common accepted definitions of the drought is that it is a water shortage that lasts longer than usual relative to the typical mean level in an area that is experiencing drought. Apart from the broadest meaning given here, there are other definitions of drought that are given according to the location of the water such as precipitation, runoff, ground moisture, groundwater, and water in dam reservoirs, the time period chosen, the value that the deficiency must exceed, and the area that the drought must cover. First of all, it is important to understand the distinction between a drought and an area's climate being arid. Even in the middle of the day, water is scarce in arid areas. On the other hand, independent of the local environment, a drought is an extreme time-space process that occurs when the water supply falls below normal for a period of time (Bayazıt and Önöz, 2008; Tosunoğlu, 2014). In general, drought is characterized by the sudden onset of water shortages. Although the drought event is brought on by a deficit in precipitation, the greatest damages are

produced by the necessary decline in soil moisture, the inability to build up water in river flows and reservoirs (weirs, dams, and natural lakes), and poor management of these resources. Water resources do not decline at the same rate as precipitation does (Şen, 2009; Tosunoğlu, 2014). There are time laps among precipitation, streamflow and groundwater. The mechanism of these water bodies interrelated and influence each other with respect to drought occurrences.

The cumulative impacts of water scarcity over a variety of time periods result in drought. A natural occurrence of drought can have disastrous consequences. It should be identified how frequently the drought happens and in which locations it is more severe in order to lessen these negative impacts of drought (Gümüş, 2017). The identification of drought characteristics is essential for planning and taking protective measures against drought (Mishra and Nagarajan, 2011). The main barrier in determining the characteristics of extreme drought, however, is the lack of meteorological and hydrological data (Anisfeld, 2011). Drought indices, which are utilized as a drought monitoring tool, can be used to assess details like the impact area, severity, duration, and frequency of the drought. Giving analysts and decision-makers an understanding of the drought's characteristics, this information is utilized to develop drought risk management strategies and drought action plans. Drought interventions can be implemented more quickly and the consequences of drought are lessened with the aid of drought monitoring and forecasting (Katipoğlu, 2020).

### 1.2.Effects Of Drought

Drought’s effect can be categorized in three groups as following;

a) Economic impacts: The impacts can be seen in decrease in animal products, decrease in basic agricultural stocks, decrease in grazing and pasture areas, insufficient water for animals or too expensive, burning of farms, erosion and decrease in agricultural areas, plant and tree diseases, forest fires, decreases in tourism, unemployment increase, income-expenditure inequality, decrease in river transport, causing economic losses.
b) Environmental impacts: The impacts can be seen in reduced diversity of agricultural species, reduced drinking water, the onset of diseases, worsening water quality, worsening of land and soil quality.

c) Social effects: The impacts can be summarized as, increased pollution with increasing sewage water, social uncertainty, decrease in recreational areas, reuse of water in homes, decrease in entertainment, increase in migration to cities (Sırdaş, 2002; Hezerani, 2018).

Drought is a serious problem that causes significant damage worldwide and in Turkey, and these damages become more pronounced when expressed in numbers. For instance, according to the World Health Organization, approximately 2 million people worldwide lose their lives each year due to insufficient water resources. Furthermore, according to FAO data, the rate of unharvested crops due to global drought can reach up to 20%. In Turkey, agricultural production losses have been experienced in recent years due to drought, and the total cost of these losses amounts to billions of dollars. Additionally, forest fires also increase as a result of drought. In 2021, due to forest fires in Turkey, 10,000 hectares of forested area were destroyed, and millions of Turkish liras in material losses occurred. All of these figures demonstrate the magnitude of the damage caused by drought worldwide and in Turkey, emphasizing the severity of this issue.

The monetary value of losses caused by drought in Turkey is quite high. In 2018, the drought in Turkey resulted in a loss of 6 billion Turkish liras in the agricultural sector. Within the same year, the production of hydroelectric power plants decreased by 34%. The drought in Turkey resulted in an energy loss equivalent to approximately 2 billion Turkish Liras. However, the total amount of other material losses due to drought cannot be calculated.

The monetary value of losses caused by drought worldwide is also quite high. For instance, in 2011, the Somali economy suffered greatly due to drought. The drought affected the livestock sector, and millions of animals died. Additionally, agricultural production decreased significantly. The increase in food prices due to drought left many people facing hunger. The effects of this event resulted not only in economic losses for the country but also in a humanitarian aid cost of approximately 1.5 billion dollars.

### 1.3. Types of Drought

Although there are many definitions and classifications of drought in the literature, drought can be classified çoğunlukla dört sınıfa ayrılmaktadır. (URL-2)

These classes are: meteorological drought, hydrological drought, agricultural drought and socio-economic drought. Recently, ecological drought has been included in addition to these categories.

Meteorological drought: A meteorological drought is characterized by lower-than-average precipitation over an extended period of time. The first indication of drought is a decrease in precipitation, therefore the initial stage of the drought phase is meteorological drought. Persistent meteorological drought can have severe consequences. (Hejazizadeh and Javizadeh, 2011; Hezerani, 2018).

Hydrological drought, a long-term absence of precipitation causes a drop in surface water, reservoirs and ground water levels, which is referred to as a "hydrological drought." In other words, it can be said that a hydrological drought starts when a year's runoff is lower than its long-term average (Whipple, 1996). Due to the fact that hydrological drought frequently results from the combination of agricultural and meteorological drought (Şaylan et al., 1997), it can also lead to socio-economic drought. Long after the meteorological drought has subsided, the hydrological drought may continue (Linsley et al., 1958; Hezerani, 2018).

Agricultural drought, due to the depletion of water resources, agricultural drought—defined as a lack of water in the soil to meet plant needs—occurs. Different amounts of water are required by plants at different stages of development. A plant's root zone not having enough water to support growth and development is another way to describe an agricultural drought. Consequently, a drought in agriculture occurs when the soil does not have adequate moisture during the most crucial time when the plant needs water (Gibbs and Maher, 1967). Even when the soil is saturated, agricultural drought can significantly reduce crop production (Kadıoğlu, 2001). This decrease in output results in lower yields, leading to inadequate nourishment for animals (Bacanlı and Saf, 2005). Agricultural drought is one of the most common and hazardous types of drought (Wilhite, 2000; Hezerani, 2018).

Socioeconomic drought addresses how drought conditions, whether they be meteorological, agricultural or hydrological, affect the supply and demand for particular economic items, including produce, cereals, meat and other foods.

Water supply varies annually depending on precipitation and water resources. Among other natural hazards, droughts are potentially having the greatest economic impacts and affecting the greatest number of people.

### 1.4.Drought Indices Commonly Used

Drought indices are essential instruments for quantifying descriptions of drought and carrying out drought management (Wilhite et al., 2007). According to the quantity of hydro-meteorological variables used, there are three categories for hydro-meteorological drought indices. These are: univariate (such as the Standardized Precipitation Index (SPI)) (McKee et al., 1993); bivariate (such as the Reconnaissance Drought Index (RDI)) (Tsakiris and Vangelis, 2007; Tigkas et al., 2013); and multivariate (such as the Aggregated Drought Index (ADI)) (Keyantash and Dracup 2004).

The Palmer Drought Severity Index (PDSI) is used for drought analysis, providing a general guideline for evaluating meteorological exceptional circumstances, as well as aiding in the understanding of the quantity and distribution of drought severity Despite the limited and incomplete features of this drought analysis method in Canada and the USA, the PDSI has been proposed as a useful drought monitoring tool and a reliable drought analysis method when appropriately addressed. The PDSI is widely used in many regions (Alley, 1984).

The Erinç Index (EI) has been used by many researchers in our country at different times to determine drought-prone. This index is based on precipitation and temperature (Temel, 2016).

The Percent of Normal Index (PNI) is the easiest drought index to calculate. It can be calculated using monthly, seasonal, or annual precipitation data. The percentage is obtained by dividing the amount of precipitation during the given time period by the mean precipitation of the same series (Temel, 2016).

The Deciles Index (DI) method was developed by Gibbs and Maher in 1967 to overcome the deficiencies of the Percent of Normal method. It is widely used in drought analysis, especially in Australia. The method only utilizes precipitation data (Temel, 2016).

Lyon (2004) formed the Weighted Anomaly Standardized Precipitation Index (WASP) to track rainfall in tropical areas. Essentially, drought is referred to as a moisture deficit, so 6 or 12-month cumulative precipitation is typically used. (Akşan, 2021).

The Effective Drought Index (EDI) is a temporal reduction function of the daily precipitation total. The only data required for calculating the drought index are daily precipitation values for a period of 30 years or more (Kim et al., 2011; Akşan, 2021).

Also known as a standard index, The Z-Score Index (ZSI) indicates how many standard deviations a precipitation deviates from the mean. This index has been used in many studies (Morid et al., 2006; Afzali et al., 2016; Akşan, 2021).

Evaporative Demand Drought Index (EDDI) is calculated using the atmospheric evaporative demand (E0), and the index values can be obtained using multiple methods (Thornthwaite, Blaney-Criddle, Penman-Monteith, Hargreaves-Samani, etc.) (Dewes et al., 2017). The calculation steps are similar to the Standardized Precipitation Evapotranspiration Index (SPEI) (Hobbins et al., 2016; Akşan, 2021).

The Standardized Precipitation Index (SPI) is a drought index used for drought monitoring and management. SPI is particularly used in precipitation-based regions to determine how much deviation from normal precipitation occurs during a drought period. SPI uses a single parameter of precipitation data and measures the severity of drought by comparing it with a standard normal distribution function. SPI was developed by McKee et al., (1993).

Reconnaissance Drought Index (RDI), is a nother common drought index used for monitoring and managing drought. RDI measures drought by using two parameters namely evapotranspiration and precipitation data. Similar to SPI, RDI measures the severity of drought by comparing it to a standard normal distribution function. RDI was developed by Tsakiris and Vangelis (2007).

The Standardized Precipitation Evapotranspiration Index (SPEI) is a drought index used for drought monitoring and management. Similar to SPI, SPEI measures drought severity using precipitation data, but it also takes evapotranspiration into account. SPEI can be used in meteorological, hydrological, and agricultural applications. SPEI was developed by Vicente-Serrano et al., (2010).

The Standardized Runoff Index (SRI) is a drought index used to monitor and manage drought in water resources. SRI measures drought by using one or more hydrological parameters, such as streamflow data. This index is calculated based on hydrological models and measures the severity of drought using drops in streamflow levels. SRI is used in applications such as operations, planning, and water management decisions.

### 1.5. Purpose of The Thesis

Due to not being sufficiently rich in terms of water resources potential and being susceptible to the impacts of global climate change, our country is at risk of drought. Therefore, the optimal use of water resources is of great importance in minimizing the potential risks of drought and overcoming them with minimal damage. This study would help to understand the droughts prone in the basins of Yeşilırmak, Kızılırmak and Konya, and to make accurate and comprehensive plans for the future. The basic aims of this study are to enable the understanding of the droughts in the studied region and to assist in the preparation of drought disaster management plans. It is feasible to lessen the harmful consequences of agricultural and hydrological droughts by taking the right precautions prior to the drought and by properly preparing throughout the drought. Because of this, it is important to plan separately for the actions to be performed in the lead-up to and during the drought.

In this study, drought analyses were conducted on Turkey's major river basins, namely; Yeşilırmak, Kızılırmak, and Konya Closed basins. The data to be used in the study were obtained from the General Directorate of Meteorology and the General Directorate of State Hydraulic Works. The study consists of three main parts.

a) Drought analysis were carried out by using four drought indices namely: SPI, SPEI, RDI and SRI for the three basins.
b) Trend analysis of precipitation and drought indices for 38 stations of the basins for three- and twelve-monthly consecutive precipitation totals were realized.
c) Magnitude-Duration-Frequency analysis of three drought indices namely SPI, SPEI and RDI for three monthly total precipitation indexes was performed.

# CHAPTER 2

# LITERATURE REVIEW

Zhu et al. (2018) propose a new variant of the Palmer drought severity index (PDSI) that addresses the issues of moisture estimation and time scale by incorporating the Variable Infiltration Capacity (VIC) model into the hydrologic accounting module and modifying the standardization process. The novel Palmer variant was proven to be an effective indicator for monitoring soil moisture variation and the dynamics of plant growth after two remote sensing products of soil moisture and vegetation were used for comparison. This variant, known as the self-calibrating Palmer drought severity index (scPDSI), is specifically designed to monitor droughts at shorter time scales. The effectiveness of the new index was compared with the standardized precipitation index (SPI) and standardized precipitation evapotranspiration index (SPEI) at a 3-month time scale, and its performance was assessed over the Yellow River Basin (YRB) between 1961 and 2012. The new Palmer version has a more steady behavior in terms of drought frequency than the original scPDSI, according to the study, and it is closely linked with SPI and SPEI. Additionally, the new index exhibits a distinct spatial pattern from SPI and SPEI in the winter and is more likely to reflect all moisture conditions for identifying drought trends. Overall, the study emphasizes the novel Palmer variant's efficiency in tackling the moisture estimation and time scale difficulties in drought monitoring.

Akbaş (2014) determined the distribution of drought patterns for certain years using the Palmer Drought Severity Index (PDSI) and was conducted to evaluate how well this method represents drought. The Palmer Drought Severity Index was created using temperature and precipitation data obtained from 96 Turkish meteorological stations between 1929 and 2009. The drought index was then classified into seven classes according to the drought classification of NOAA. The results of the study show that the obtained results for drought years are similar to those in the literature. In this context, the Palmer Drought Severity Index is recommended as a useful tool for monitoring and reducing the impacts of drought in Turkey. The method used in the study was the calculation of the PDSI using meteorological and water availability data, and the results show that this approach can effectively represent drought patterns.

The standardized precipitation evapotranspiration index (SPEI), which considers the impacts of precipitation and temperature fluctuation on drought evaluation, is a novel drought measure that Serrano et al. (2009) present. The calculation procedure of the index includes the adjustment to a log-logistic probability distribution, the accumulation of deficit/surplus at various time scales, and a climatic water balance. The standardized precipitation index (SPI) and the SPEI are comparable, but the SPEI also takes temperature into account. The authors demonstrate that, under conditions of global warming, only the sc-PDSI and SPEI identify an increase in drought severity linked with increasing water demand owing to evapotranspiration. They compared the SPEI to the self-calibrated Palmer drought severity index (sc-PDSI). The authors showed that the SPEI's multiscalar character was essential for drought research and monitoring, and that one benefit of using it was that it may be compared to the sc-PDSI. Overall, the article offers a useful new method for assessing droughts that takes into account the effects of temperature variability and offers helpful insights for academics and professionals involved in the study of climate change and water management.

Using the Palmer Drought Severity Index (PDSI), Türkeş et al. (2009) detected significant drought episodes and their severity at Konya, Karaman, Aksaray, and Karapınar stations in the Central Anatolia Region. The PDSI considers evapotranspiration, precipitation, and the soil's available water capacity. From the start of the station records until 2006, monthly precipitation, computed evapotranspiration totals, and the soil's available water capacity were used to generate monthly PDSI values. They found that there were decreases in precipitation amounts ranging from 30% to 80% during common periods for all four stations, with these decreases being more pronounced in the winter and autumn seasons. Additionally, although there was no statistically significant trend in usable water amount (P-PE) and PDSI time-series, a general decreasing trend towards drier conditions was observed. The findings of the study showed that severe drought events occurred in 1972-1974 and 1999-2001. Overall, the study provides valuable insights into the severity and duration of drought periods in the region and highlights the need for effective water management strategies.

Bacanlı and Kargı (2019) analysed long-term rainfall data from Bursa, İznik, Keleş, Mustafa Kemalpaşa and Uludağ stations within the provincial borders of Bursa for

the period of 1969-2015. The trend of rainfall data was determined using linear regression analysis. The data were standardized and evaluated according to the runs analysis. Finally, the Standardized Precipitation Index (SPI) method, which is widely used in Turkey and worldwide, was used to analyse droughts for 1-, 3-, 6-, 9-, 12-, 24- and 48-month time periods. No significant trend was observed in annual and monthly rainfall data. It was found that İznik, Keleş, and Uludağ stations showed a decreasing trend in December, while Bursa station showed a decreasing trend in October. No statistically significant trend was found in other months at a confidence level of 5%. The results of the Standardized Precipitation Index (SPI) analysis showed that the stations had similar proportions of dry, normal, and wet periods. However, mild drought or normal periods were more common in short-term periods (3-6 months), while severe and extreme droughts were observed in long-term periods (12-,24-,48- months). Overall, the main objective of the study was to analyse the drought conditions in the Bursa region using the SPI method. In order to assess the data and establish the trend of the rainfall data, the study used linear regression analysis and runs analysis, respectively. The SPI method was applied for different time periods, and it was found that severe and extreme droughts were observed in long-term periods.

Using the Standardized Precipitation Index (SPI) at various timesacles, Caloiero et al. (2018) examined drought occurrences across a significant portion of the Northern Hemisphere, encompassing Europe, Ireland, the United Kingdom, and the Mediterranean basin. The data collection used covered the years 1951–2016 with spatial resolutions of 0.5 degrees longitude/latitude and was produced by the Global Precipitation Climatology Centre (GPCC). The percentage of grid points that fell into the severe and extreme drought categories, as well as their temporal development, were evaluated at the outset of the study. Then, a seasonal and annual scale trend analysis was carried out. The data demonstrate a general decrease in SPI values, especially over a long time period, with the Mediterranean basin and North Africa being the most continuously vulnerable regions. In order to help policymakers and water management develop policies to lessen the effects of drought, this study illustrates the importance of the SPI in detecting drought episodes and emphasizes the most drought-prone areas.

Ivrem et al. (2018) analysed the drought periods in the Göksu-Himmetli sub-basin of the Seyhan basin using the SPI and RUN methods based on monthly streamflow data obtained from the current observation station for the period between 1936 and 2011. The ReDIM software was utilized to carry out the analysis for 3- and 12-months periods. The severe drought periods were identified, and the longest drought durations were determined for each method. The SPI analysis revealed the most severe drought for the three months period between May 1989 and October 1989 and for the twelve months period between May 2001 and April 2002. The longest drought period was between September 1972 and March 1975 for the three months period and between April 1972 and April 1975 for the twelve months period. The RUN method indicated the longest drought period occurred between 2003 and 2008. The study also found that the maximum drought intensity was in 1994, and hydrological droughts that have a duration of 4 years or more occur in every 20 years in the basin. The cumulative water deficiency was also calculated, and it was found to be the highest between 1970 and 1974. The report also emphasized the significance of safeguarding the region's water supplies in view of the potential for drought in the years 2020–2023. Overall, the study was effective in analyzing the drought periods in the Göksu-Himmetli sub-basin of the Seyhan basin using the SPI and RUN methodologies. The study stresses the need for actions to lessen the effects of droughts on the region's water resources and offers useful information for the region's water management.

Başak (2017) used the Standardized Precipitation Index (SPI) approach to assess the temporal drought values in the lower Euphrates region of the Euphrates basin in Turkey. Twenty meteorological observation stations provided long-term monthly precipitation data to identify wet and dry periods. In order to forecast dryness and estimate SPI values, Artificial Neural Network (ANN) models were created using 16 different input parameters. The findings demonstrated that nearly all stations experienced the longest drought episodes between 1988 and 2004. In terms of forecasting current SPI levels, the ANN model that used past SPI values with rainfall data fared the best. Based on the 3-, 6-, 9-, and 12-month timescales, nearly half of the measurement periods of all stations examined were found to experiencing drought. Overall, the study provides important insights into the drought patterns and

trends in the lower Euphrates region and highlights the potential of using ANN models for forecasting drought conditions.

Dabanlı (2017) examined the evaluation of drought in Turkey and the impact of climate change on precipitation and temperature in the Akarcay Basin in three parts. The first section of the study focused on statistical downscaling, climate model setup, and predictions of future climate variables (precipitation and temperature). The statistical downscaling approach provided by the Water Foundation was used to predict monthly total precipitation and mean temperature data. The results showed that the amount of precipitation in the Akarçay Basin did not change on average, but extreme precipitation would increase. Additionally, it was concluded that temperatures would increase by 0.3% to 0.4% on average annually. The obtained prediction data was tested to demonstrate the validity of the model. The main subject of the second application section was a comprehensive trend analysis. The results showed the superiority of the Innovative-Sen method compared to other traditional methods. The Innovative-Sen approach was used to produce comprehensive trend analysis results demonstrating the applicability of the method to other places and different data types by applying it to flow, precipitation, temperature, and relative humidity data in the Ergene Basin. All trend analyses reached a common conclusion that all high precipitation and temperature values showed a rising trend, albeit at different rates. The standardized precipitation index (SPI) series with different time scales in the drought analysis, namely SPI-1, SPI-3, SPI-6, SPI-6N-E (SPI-6 April-September), and SPI-12 series, were conducted. The investigation showed that the smaller loadings (F3 and F4) were unstable loadings, and the correlation fields they represent were also unstable. It was observed that the loadings (F1 and F2) with a variance score more than 10% were more stable.

Oğuztürk (2017) looked at 21 dam basins in Turkey with various characteristics to determine how droughts affected river flows, dam reservoirs, and soil moisture. Weather-related, hydrological, and agricultural droughts were examined using the Standardized Precipitation Index (SPI) technique. In order to monitor the effects of the hydrological drought on river flows and reservoir storages, the study initially conducted a meteorological drought analysis using SPI time series at different scales. Next, it determined the best time scale for monitoring the effects of the agricultural drought on soil moisture. Maximum correlation coefficients were attained at short

time periods of 1-2 months by treating the standardized satellite-derived soil moisture levels as continuous data. The study also examined the relationship between river flows and soil moisture levels, and it found that reservoir characteristics and dam management goals have an impact on reservoir storages, while basin characteristics and climate have an impact on river flows. Furthermore, it was discovered that groundwater levels significantly influence soil moisture rates. The findings of the study have significant ramifications for preventing drought and managing water resources sustainably at the basin level.

In the North of the Haihe River Basin, Zhang et al. (2017) assessed the performance of three data-driven models, namely the ARIMA model, artificial neural network (ANN) model, and wavelet neural network (WANN), for drought forecasting based on standard precipitation index (SPI) of two-time scales (SPI-6 and SPI-12).The Kolmogorov-Smirnov (K-S) test, Kendall rank correlation, and correlation coefficients ($R^2$) were used in the study to examine the efficacy of various models. The study's findings demonstrated that the WANN model was the best one for predicting SPI-6 and SPI-12 values in the research area. In conclusion, the usefulness of various data-driven models for drought forecasting in the North of Haihe River Basin is the issue that this work attempts to solve. The methodology employed in the study involves using three data-driven models and evaluating their effectiveness using statistical tests. The results indicated that the WANN model was the most effective for forecasting SPI-6 and SPI-12 values.

Using rainfall and temperature data from 33 meteorological stations between 1960 and 2015, Oruç (2017) investigated drought in the Southeastern Anatolia Region. The drought analysis was conducted using the Standard Precipitation Index (SPI), the Erinç Index, and the De Mortanne Index. The 3-, 6-, 9-, 12-, and 24-month SPI time series calculations were made. The findings indicated that while very severe droughts were more frequently observed over longer durations (12–24 months), near-normal and moderate droughts were more common over shorter periods (3-6 months). The Pervari station had the greatest drought duration out of all the stations during the driest time, which was between 1971 and 1980. The most arid province was Şanlıurfa, and the driest station was Akçakale, according to the Erinç and De Mortanne Indices. In general, the study provides insights into the spatial and

temporal patterns of drought in the Southeastern Anatolia Region. It can be helpful for drought management and monitoring efforts in the area.

Arslan (2016) investigated droughts occurring in the Kizilirmak Basin using the standard precipitation index (SPI) method between 1973 and 2013. The SPI values for 1-, 3-, 6-, 9-, 12-, and 60-month periods were calculated, and the 60-month period was used for the first time in the drought analysis based on the SPI method. When compared to past droughts, significant increases were detected in the durations of the recent droughts in the basin for 12 and 60-month periods.

Keskiner et al. (2016) used the Standardized Precipitation Index (SPI) approach to make regional meteorological drought maps with return periods of 2 and 10 years in order to assess the drought risk in the Seyhan River Basin. The long-term annual precipitation statistics, which were necessary for the study, were provided by 41 meteorological observation sites located within and around the basin. Regression analysis was used to fill in missing precipitation data on a monthly basis, and SPI values were computed for both monthly and annual data. In the study, we determined the probability distribution models that provided the best fit for the SPI series of annual precipitation data, and calculated SPI values with return periods of two and ten years for each meteorological station. Using the Ordinary Cokriging method, regional meteorological drought maps of SPI values with return periods of 2 and 10 years were formed for the months of January through December. According to the study, if the return period is 10 years, a sizeable area of the Seyhan River Basin would be at great risk of drought. Overall, the study provides information about the drought risk in the region. It supports the use of the SPI approach for creating regional drought maps.

Gümüş et al. (2016) examined the drought analysis of Şanlıurfa meteorological station located in the southeast of Turkey, using 78 years (1937-2014) of rainfall data. The standardized Precipitation Index (SPI) method was used to identify drought events and to determine their severity, size, and distribution for various time scales, including 1-, 3-, 6-, and 12- months. The results indicated that extreme drought months were more frequent in the period of 1986-2014 (29 years) compared to the period of 1937-1985 (49 years). The highest SPI values were observed in the October-December 1972 period for all time scales, indicating the severity of drought

in that period. Overall, the study provides information about the drought characteristics of the Şanlıurfa meteorological station. It also contributes to drought management strategies in the region.

Dinç et al. (2016) focused on assessing drought features in meteorological stations located in various regions of Turkey using the Standardized Precipitation Index (SPI). The study spans a 40-year-long data period (1974–2014). The study's objectives were to determine the trend in SPI values for various time periods (3, 6, 12, and 24 months) and, to evaluate the likelihood that droughts would occur in both the summer and the winter. According to the findings, SPI levels have ranged from 0.99 (normal) to -0.99 (drought that is similar to normal), no discernible downward trend in SPI values has been seen. This has shown that the likelihood of a drought over the long term has not decreased. Additionally, it was discovered that droughts could happen in both the summer and winter months. The SPI approach, which was utilized in this study, was a trusted and popular way to track drought. Long-term data sets were utilized in this research to enhance the reliability of the findings. For decision-makers to take action to lessen the consequences of drought on agriculture, water resources, and other sectors, the study offers crucial information.

Yürekli et al. (2012) studied regional drought patterns in the Cekerek Watershed in Turkey, using the standardized precipitation index (SPI) method and the decision tree technique. Monthly rainfall data from 17 stations were used to constitute cumulative rainfall series for five reference periods, consisting of four seasonal and one annual series. Initially, stations were grouped according to discordancy criteria based on l-moment ratios to ensure homogeneity. The results indicated that the selected groups were homogeneous, except for the first reference period. Various regional distributions were tested based on goodness of fit criteria, and the Generalized Pareto, Generalized Extreme Values, Generalized Logistic, Pearson Type III, GEV, and 3-parameter Log Normal distributions were found to be the best candidates for the different reference periods. The decision tree method was used to predict drought categories for each region, and the results were compared with the conventional SPI algorithm. The study found no significant difference between the two methods, and the prediction accuracy for most reference periods was above 94%. However, the k3 and k5 reference periods had accuracy rates of 81.2% and 86.4% respectively. Overall, the study highlights the importance of using data-mining approaches for

drought analysis and provides insights into regional drought patterns in the Cekerek Watershed, which can inform future water management strategies.

According to Türkeş (2011), the Akhisar and Manisa plains have seen rising water scarcity and desertification over the past 30 years. This was accomplished by a thorough research of the region's hydro-climatologic features, climate, and fluctuation, as well as change over time. Long-term climatic data from meteorological stations in the area, including Manisa, Salihli, Turgutlu, and Akhisar, were used in the study. The nature and size (statistically significant) of the observed long-term trends in the SPI and AI time-series were investigated using the Mann-Kendall rank correlation coefficient ($\tau$) and least-squares linear regression methods. The Akhisar and Manisa districts have reportedly experienced an apparent drying trend, which has gotten stronger since the 1980s, according to the findings of trend studies conducted on the SPI and AI time-series. This trend has gotten worse as a result of the severe drought conditions that occurred between 2007 and 2008. The report contends that processes of desertification and growing water shortages in the area are a serious danger to the long-term viability of agriculture and the environment. In conclusion, a thorough analysis of the nature and severity of the water scarcity and desertification processes seen in the Akhisar and Manisa plains during the past 30 years was conducted as part of this study. The study's findings emphasize the urgent need for efficient and long-lasting water management methods to lessen the region's adverse effects of climate change and variability.

Aslan (2020), the NCEP/NCAR reanalysis data sets and station data sets, which are used to produce low-resolution grid data sets for variables including precipitation, temperature, and evaporation globally, were utilized to develop drought indices in this work. The Percentage Normal Precipitation Index (PNPI), Reconnaissance Drought Index (RDI), Standardized Precipitation Index (SPI), and Standardized Precipitation Evapotranspiration Index (SPEI) drought identification methods were used to evaluate the drought in the Northern Aegean Basin sub-basin using both station data and NCEP/NCAR datasets. It should be emphasized that there can be significant heterogeneity in the regional distribution of drought within the low-resolution grid cells of global climate models, which are used to forecast future climatic conditions. Hence, the drought indices obtained from the atmospheric estimates of the NCEP/NCAR reanalysis data may not accurately reflect the specific

conditions within the computation grid. Consequently, this study investigated the relationship between the SPI values obtained from the low-resolution NCEP/NCAR reanalysis data and the station-based SPI values within the same region using the quantile regression method. Additionally, the quantiles of drought indices at the stations were determined under known atmospheric conditions. As a result, it's possible that the drought indices derived from the atmospheric estimates of the NCEP/NCAR reanalysis data don't adequately reflect the particular circumstances present inside the computing grid. As a result, this study used the quantile regression method to examine the association between the SPI values generated from the low-resolution NCEP/NCAR reanalysis data and the station-based SPI values within the same region. Additionally, under known atmospheric circumstances, the quantiles of the drought indices at the locations were established.

Using the De Martonne Drought Index, Erinç Rainfall Efficiency Index, and Thornthwaite Climate Classification techniques, Akın (2019) evaluated the temporal and spatial aspects, as well as the severity, of the drought experienced in the Tuz Golu Basin during the process of climate change in Turkey. To achieve this, trends in long-term annual average temperature, annual minimum temperature, annual maximum temperature, and annual average total precipitation data were calculated, and drought index formulas were applied to long-term and uninterrupted measurements made at Kulu, Aksaray, Karapinar, and Cumra meteorology stations for the years 1975–2016. Drought in the Salt Lake Basin was evaluated according to the results based on meteorological data. According to the results of the study, the extent of the drought in Salt Lake Basin varies across the basin's several areas. Furthermore, this study emphasizes the importance of analyzing drought using different indices to achieve a comprehensive understanding of drought. The findings related to Salt Lake Basin revealed a significant increase in temperatures and a steady decrease in precipitation in recent years. These findings indicated that the climate characteristics of the Salt Lake Basin have been negatively affected and are gradually becoming arid. Based on these results, it is predicted that the basin will become an even more arid and desert-prone area in the coming years.

Anlı (2014) used the RDI (Reconnaissance Drought Index) approach to analyze the temporal change of reference evapotranspiration ($ET_0$) and the meteorological drought in the Southeast Anatolia Region. The reference crop water consumption for

the provinces in the area was calculated using the Penman-Monteith method and divided into four seasons (k1, k2, k3, and k4) per year. Dickey-Fuller and Mann Whitney U tests, both parametric and non-parametric, were used to analyze the temporal variation of reference crop water consumption over the four seasons. According to the RDI method used to estimate meteorological drought in the provinces, mild drought was generally dominant in the area, with a significant number of moderate and severe droughts occurring. As a result, significant increasing trends in reference crop water consumption were detected over time. Overall, this study provides important information for water resources management and drought mitigation strategies in the South-eastern Anatolia Region.

Ünlükara (2014) determined Angstrom coefficients of each month for Kayseri province using the sunshine duration data recorded between 1975 and 2009. Two different reference evapotranspiration series ($ET_0$1 and $ET_0$2) were obtained using these Angstrom coefficients, solar radiation intensity, and relative sunshine duration data. The variances and averages of the two series were compared. In addition, regression and correlation analyses were performed to obtain the relationship between the two series and to complete the missing data periods for one of the series. According to the results, it was determined that the variances were the same fort the months of January, April, July, and December. Based on the results of the t-test, there was no significant difference between the reference evapotranspiration averages for each month. The highest reference evapotranspiration was calculated in July, where $ET_0$1 = 169.55 mm and $ET_0$2 = 169.62 mm. It was concluded that there was no difference in the reference evapotranspiration values calculated from radiation intensity or relative sunshine duration data, provided that the Angstrom coefficients of the region were taken into consideration.

Using the SPI, RDI, and EDI indices, Yürekli et al. (2010) looked at the occurrence of drought in Karaman province. The data were monthly rainfall measurements made between 1975 and 2009 at the Karaman Meteorological Station and reference evapotranspiration (ETo) measurements based on the FAO56 Penman-Monteitht relationship for the same years. The SPI, RDI, and EDI values were computed based on the cumulative monthly rainfall and ETo data for four separate reference periods (k1, January-March; k2, January-June; k3, January-September; and k4, January-December) for each year. According to the findings, the province of Karaman has

recently experienced an increase in the frequency of drought times. The results of the indicators showed that the mild and severe drought categories occurred more frequently in the province. The study's conclusions can aid decision-makers and planners in taking the required steps to lessen the detrimental effects of drought on the area's water and agricultural resources.

Within the scope of the thesis by Aşkan (2021), meteorological drought analysis was conducted using daily and monthly total precipitation data, as well as monthly mean temperature data obtained from 81 central stations across Turkey. Potential evapotranspiration (PET) was calculated using the Thornthwaite method based on the monthly mean temperatures. According to the results, similar outcomes were observed in the WASP, CZI, SPI, and ZSI indices across all regions. The regions showed higher drought values based on the PNPI and RAI indices. The DI analysis generally indicated low rainfall during the months of July and August. The EDDI analysis mostly identified December as the month where Level 0 was observed. The SPEI and RDI indices indicated near-normal conditions in all stations. The IP and HTC indices yielded similar results. More detailed results were obtained through the monthly and annual assessment of the DMAI index.

The Standardized Precipitation Evapotranspiration Index (SPEI) and L moment techniques were used by Ney (2020) to analyze the regional drought using monthly average temperature and total monthly precipitation data from meteorological stations in the Gediz Basin, including Akhisar, Demirci, Gediz, Manisa, and Salihli. To divide the Potential Evapotranspiration (PET) amounts determined by the Thornthwaite technique using monthly average temperatures and monthly total precipitation amounts, reference periods were used. These reference periods were set as 1, 3, 6, 9, and 12 months. According to the water balance (Di) series, which measures the difference between precipitation and potential evapotranspiration, the 3-month period had a water surplus while the 9- and 12-month periods had deficits. The collected SPEI values were used to indicate that normal conditions generally prevailed in all stations, with occasional occurrences of moderate and severe drought and wet conditions, and rare instances of extreme wet and dry conditions. This was done after identifying the distributions that best fit the water balance series. The five stations were treated as a single region in the regional drought analysis carried out using SPEI values and L moment approaches, and the measures of discordancy and

heterogeneity showed that the basin was homogeneous to an acceptable degree. Based on regional SPEI values, the Generalized Extreme Values (GEV) distribution fit the reference periods of one and three months the best, the Generalized Normal (GNO) distribution fit the reference period of six months the best, the Generalized Logistics (GLO) distribution fit the reference period of nine months the best, and the Pearson Type 3 (PE3) distribution fit the reference period of twelve months the best.

Bakanoğullar (2020) used the Standardized Precipitation Evapotranspiration Index (SPEI) and the Standardized Precipitation Index (SPI) to compare the frequency and severity of droughts in the Damlıca Creek basin of the Istanbul-Büyükçekmece drinking water basin between 1982 and 2006. Evapotranspiration data were used to calculate the SPEI drought index using the Thornthwaite equation. The determination coefficient (R2) between the annual SPI and SPEI drought indices was determined to be 0.977 according to the second-degree polynomial, indicating a strong relationship between the two indices. The regression analysis conducted between the annual SPEI and SPI indices using a 25-year data set was found to be statistically significant. However, there were variations in the severity of the drought between the monthly, seasonal, and 6-month evaluations. The SPI index was used to determine two years of severe drought (1983, 1989), three years of moderate drought (1982, 2004, 2006), and two years of mild drought (1992, 1993), while the SPEI index was used to determine four years of moderate drought (1983, 1989, 2004, 2006) and seven years of mild drought (1982, 1992, 1993, 1994, 1999, 2000, and 2003). The SPEI drought index, which is derived from data on precipitation, temperature, and evapotranspiration, offered more accurate results in agricultural productivity and drought assessments, allowing decision-makers to develop policies to lessen drought with greater certainty.

Using values for the Standardized Precipitation Evapotranspiration Index (SPEI) and Vegetation Condition Index (VCI) for various time-scales, Jamal (2019) examined drought and wetness trends in several regions of Turkey. The purpose of the study is to evaluate the variation and trends in Turkey's drought and wetness conditions from 1901 to 2015. The study's technique entails dividing Turkey into 323 0.5° x 0.5° lat/lon grids. The SPEI values for the timescales of 1-, 3-, and 12- months for the periods of 1901-2015, 1901-1981, and 1982-2015 were calculated. The Normalized Difference Vegetation Index (NDVI) data from AVHRR sensors onboard NOAA

satellites were used to produce the monthly VCI values for the years 1982 to 2015. The Mann-Kendall's (MK) test was used to analyse the trend and significance of both SPEI and VCI data, and the Theil-Sen test was used to extract the trend slope value. Finally, the Pettitt-Whitney test was employed to determine the year of change in the trend. The spatial trend analysis was performed using GIS software. The results of the study pointed out that drought trends prevailed in most parts of Turkey, with some variations when the time scale changed from 1 to 12 months. However, some parts, such as northern, western, and some central parts of the country, showed a wetter trend, according to Mann-Kendall method. The difference between SPEI and VCI analysis results can be attributed to the source of raw data used to obtain each index. In conclusion, this study provides valuable insights into the drought and wetness trends in different parts of Turkey over a long-term period, using various statistical methods and spatial analysis techniques. The findings of this study have important implications for the water resource management and agricultural planning of the region.

Kermen (2019) conducted meteorological and hydrological drought analyses for the Küçük Menderes Basin in the Aegean Region using precipitation, temperature, and streamflow data. Meteorological analysis was carried out using monthly cumulative precipitation and mean temperature data from 11 selected meteorological stations in and around the basin, with missing data completed via regression analysis. Hydrological analysis was conducted using monthly cumulative streamflow data from 8 streamflow stations selected to represent the whole basin. Various drought indices such as SPI, SPEI, RDI, SDI, SSFI, and Self-calibrated Palmer Drought Severity Index (scPHDI) were calculated for both meteorological and hydrological analyses. The study also determined the drought dates and properties of the identified droughts for each index and examined the relationship between hydrological and meteorological indices by comparing the results. When the results of the analysis conducted using scPHDI in the scope of the thesis were examined, it was observed that although the drought severity calculated using scPHDI was slightly higher than the values calculated with meteorological indices, scPHDI could detect general drought trends in accordance with the results of meteorological drought analysis. When examined based on the selected meteorological and streamflow stations, it was observed that hydrological drought responded much faster to meteorological drought.

This is considered as an indication that hydrological drought is much more rapidly affected by meteorological droughts. It has been determined that hydrological droughts in the basin were more severe and longer-lasting than meteorological droughts. This increases the level of the basin's susceptibility to drought.

Using temperature and precipitation data recorded between 1981 and 2010 in the stations of the Turkish State Meteorological Service, Bayçınar (2019) evaluated the drought status and its effects on drought in the regions where 10 meteorological stations were located, including Cihanbeyli, Karapınar, Çumra, Seydişehir, Kulu, Ereğli, Niğde, Karaman, Beyşehir, and Aksaray. To assess the severity of the drought in the area, monthly calculations of the Standardized Precipitation Index (SPI), Percent of Normal Index (PNI), Aridity Index (AI), and Standardized Precipitation-Evapotranspiration Index (SPEI) were made. When comparing the results of SPI, PNI, AI, and SPEI each other, it was discovered that the drought situation was always in the normal or near-normal range. Factor and Cluster Analysis approaches were used for statistical analysis to merge various indices into a single index. The conclusion reached was that a general index may be exposed and used by averaging the SPI, SPEI, and aridity indices. According to the analysis, the drought situation was normal or close to normal over all time periods. Understanding the drought situation and its potential effects on the area's agriculture and other industries depends heavily on these findings.

Stagge et al. (2015) used the 0.5° 0.5° gridded Watch Forcing Dataset (WFD) for Europe to examine possible probability distributions for use in the Standardized Precipitation Index (SPI) and the Standardized Precipitation Evapotranspiration Index (SPEI) normalization at the continental scale. The study proposed a new approach based on the Shapiro-Wilk test for assessing the goodness of fit of SPI and SPEI. This approach provides a novel method for evaluating the compatibility of these indices with the underlying statistical assumptions. Based on their capacity to simulate either long-term accumulation (>3 months) or short-term accumulation (2 months), the candidate distributions for SPI were divided into two categories. All accumulation periods and regions of Europe should be calculated using the two-parameter gamma distribution, according to the study, which is in line with earlier research. In contrast to earlier recommendations, the study suggested the use of the generalized extreme value distribution for determining the SPEI. Particularly at the

continental scale, this study provides valuable insights into the selection of probability distributions for normalizing SPI and SPEI.

The standardized precipitation evapotranspiration index (SPEI) is computed using a variety of methods, as discussed by Begueria et al. (2014). The authors outline techniques for computing reference evapotranspiration ($ET_0$), weighting kernels used to calculate the SPEI at various time scales, and estimating parameters of the log-logistic distribution in order to achieve standardized values. Using observational data and globally gridded data, many choices for alternate $ET_0$ and actual evapotranspiration ($ET_a$) methodologies were also examined along with their effects on the resulting SPEI series. The study discovered that in certain regions of the world, the equation used to determine $ET_0$ can have a significant impact on SPEI. The authors advised against using plotting-positions PWM, which was employed in the SPEI's initial formulation, and instead suggest using unbiased Probability Weighted Moment (PWM). The study also provides updated worldwide gridded database, real-time drought monitoring system, and new software tools for computation and analysis of SPEI series. Overall, the study offers the SPEI and its applications in numerous industries versatile and reliable computing alternatives.

Stagge et al. (2014) tested the sensitivity of the Standardized Precipitation Evapotranspiration Index (SPEI) to the choice of potential evapotranspiration (PET) technique as well as if the SPEI significantly differs from the Standardized Precipitation Index (SPI). The analysis of the generated SPEI and SPI values across 3950 gridded land cells in Europe was done in order to compare the PET values obtained using five popular PET algorithms with various complexity and input requirements. According to the study, the SPI and SPEI values were significantly different from one another, and the PET and SPEI values were grouped by the PET radiation term. The study also found that the mass transfer term, which considers pressure, humidity, and wind speed, has a secondary impact on PET but no noticeable effect on SPEI.

Turhan et al. (2022) focused on the analysis of hydrological drought in Arsuz Plain, which is one of the agricultural areas in the Asi River Basin. Firstly, streamflow-duration curves (SDC) and flow-duration curves (FDC) were constructed using monthly average flow data obtained from three different Streamflow stations (SOS)

located close to each other, namely D19A021, D19A022 and D19A023, between 1990 and 2015. Additionally, Streamflow Drought Index (SDI) values were calculated for different time scales such as 3-, 6- and 12- months using the same data. As a result, it was observed that peak flow values were quite close to each other at all stations except for a few periods. Extreme drought and extreme wet periods began to occur in the basin as of 2000, which was observed for all stations. The wettest period occurred between 2009 and 2010, while the driest period was observed in 2014. The number of drought spells has grown recently, according to an analysis of drought trends at various time scales. These results are crucial for comprehending the regional hydrological drought condition and for creating successful drought management plans.

With an emphasis on the Western Black Sea region of Turkey, Albaqoul (2022) explored the application of the Reconnaissance Drought Index (RDI) and the Streamflow Drought Index (SDI) in drought analysis. The study used monthly average flow data from three flow monitoring stations and monthly total precipitation data from eight precipitation monitoring stations in the provinces of Sinop, Kastamonu, and Bartın to determine meteorological/agricultural and hydrological drought analyses, respectively. The indices were calculated using the DrinC software package, which has a module for calculating potential evapotranspiration (PET) using temperature-based techniques. The 2010–2011 drought was the most severe event during the study period, and it was discovered that both the RDI and SDI were useful for identifying drought conditions in the area. Additionally, it was discovered that drought analysis could benefit from the temperature-based PET estimation techniques.

Yıldız (2019) conducted hydrological drought analysis using flow data from 16 flow stations in the basin of the Euphrates River, which contains the most important water resources in the Middle East and falls under transboundary waters, located in the eastern and south-eastern regions of Turkey. The study used the Streamflow Drought Index (SDI) method to determine hydrological drought. Based on station-specific analyses, the most severe drought periods were found to be 58% at E21A058 and E21A064 stations based on the 12-month index values, while the least severe drought period was found to be 37% at E21A024 station. The study found that the drought between 1990 and 2011 was more severe than the droughts between 1968 and 1989

for nearly all time scales, and droughts increased. Additionally, the years with the highest drought rates were 1973, 1989, 2001, and 2008, while the years with the highest moisture levels were 1969 and 1988.

The effects of the Three Gorges Reservoir (TGR) on hydrological drought downstream during various operation stages were investigated by Yu et al. (2019). The case study location was chosen to be at Yichang and Cuntan stations, with Cuntan station serving as a point of reference. Based on long-term river discharge data series from 1950 to 2016, In the study, the occurrence, duration and frequency of hydrological droughts downstream of the TGR (Three Gorges Dam) were examined and compared with the periods before and after the dam. According to the study, TGR's operation changed the downstream seasonal fluctuation patterns of dry/wet periods, resulting in significantly more severe drought conditions from middle summer to middle winter and much wetter conditions in late winter and spring. Additionally, s reservoir water storage levels were increased, the effects on downstream hydrological drought became more severe. Hydrological droughts with significant sudden shifts were also found, and the abrupt changing years were strongly connected with the TGR's impoundment stages. The study's overall findings draw attention to the potential effects of extensive anthropogenic activity on downstream hydrological extremes, offering helpful examples for the ecological security and integrated water resources management of the Yangtze River basin and other sizable rivers affected by anthropogenic activity around the world. In conclusion, the study analyzed and compared drought occurrence, duration, and frequency downstream of the TGR (Three Gorges Reservoir) throughout various operation stages using long-term river discharge data. The findings demonstrated that TGR operation changed downstream dry/wet spell seasonal fluctuation patterns, amplified influences on downstream hydrological drought, and discovered significant abrupt changes in hydrological droughts that were associated with the TGR's impoundment phases.

Temel (2019) examined the drought in the Gediz Basin over the past 50 years using the streamflow drought index (SDI) and standardized precipitation index (SPI). The study utilized rainfall data organized by water year to match the flow data. SDI was applied to flow series of 3-, 6-, 9-, and 12-month periods. Normality tests were performed on the flow and rainfall series, and 3-month totals were excluded from the

study as they did not conform to normal distribution. The degree of drought was then determined by calculating the streamflow and precipitation indices, which revealed arid, very arid, and extremely dry years. Over the past 50 years, recurring droughts and wet and dry periods have been identified using water deficiency and redundancy graphs of consecutive years. Lastly, frequency analysis was done to calculate the frequency and intensity of droughts. Using these indices, 50- and 100-year drought indices as well as 50- and 100-year low flows were calculated. According to the study, this methodology can be used to assess low flows during particular return times and identify hydrological and meteorological droughts in broader regions.

Hezarani (2018) analysed drought in the Yeşilırmak basin between 1970-2014. The study utilizes 19 meteorological observation stations and various drought indices to assess the drought status of the basin. The first section of the paper discusses relevant studies, while the second section introduces the Yeşilırmak basin. The third section describes the Artificial Neural Network (ANN) model employed in the study, and the fourth section presents the application of the model, including the examination of long-term precipitation changes and the calculation of drought indices at different time intervals. In addition, the Streamflow Drought Index (SDI) has been applied to three current monitoring stations to examine both meteorological and hydrological drought. An ANN model has also been established to estimate drought in the basin. The results of the study indicated that the 12-month Standardized Precipitation Index (SPI) gave the best results for meteorological drought indices. Severe droughts were observed in the basin in 1974, 2001, and 2014, with droughts in the inner part being more severe and extreme. The results of SDI were compatible with those of SPI, with severe droughts being observed in 1973, 1974, 2001, 2003, and 2007 at 9 and 12-month intervals. Nine indices (Normal Precipitation Percentage, Precipitation Tails Index, Precipitation Anomaly Index, Z-Score Index, China Z-Index, Modified China Z-Index, Standard Precipitation Index (SRI), Erinc Index (EI), and SDI) were used in the study, and while the SPI using ANN predictions yielded successful results, the estimates of the SDI did not yield very successful results. The main problem addressed by the study is the extent of drought in the basin. The study used different indices to measure the severity of drought and ANN models to predict drought. The results show that severe droughts have occurred in the basin in various years, with the inner part being more severely affected. Overall, the study provides valuable

information on the extent of drought in the Yeşilırmak basin and can guide future drought management strategies.

Özfidaner (2018) investigated drought using the streamflow drought index (SDI) method based on the monthly mean flow data measured in the Seyhan Basin. Monthly mean flow data from the stations 1801 and 1818 in the Seyhan Basin between 1967 and 2007 were used. SDI index values expressing drought severity were obtained for 3-, 6-, 9-, and 12-month periods. Similar results were obtained for SDI values for 9- and 12-month reference periods at both stations. Drought values for 3 and 6-month periods have become significant after the year 2000. The study contributes to the understanding of drought in the Seyhan Basin and provides insights for water management and planning in the region.

At the streamflow station of 2102 in Turkey, Gümüş et al. (2018) conducted a study to evaluate the hydrological drought in the Euphrates basin using the Streamflow Drought Index (SDI). The study used station E21A002 data from 1968 to 2011 to calculate the temporal drought values. Water availability in all its forms throughout the land phase of the hydrological cycle is significantly reduced during a hydrological drought. The SDI was used to evaluate droughts over a range of time periods, including 1-, 3-, and 12-months. The most severe dry periods, with 36% each, occur in November, February, and March, while the lowest dry periods, with 18% each, occurred in May. The largest dry times in SDI-3 occurred in January with 34%, while the lowest dry periods in SDI-3 occurred in July with 23% when the 3-, 6-, and 12-month SDI values were analyzed for dry/wet periods. SDI-6 had a 34% dry period in October and a 30% dry period in April. For SDI-12, the dry time was calculated to be 32%. The study's findings shed light on the drought conditions in the Euphrates basin and can be used in regional water management plans.

Reis et al. (2016) realized the drought analysis of Kahramanmaraş city using the combined global drought index. The aim was to determine the suitability of the global drought index for monitoring drought in the region. Monthly average rainfall, heat, and flow data were used for the period of 1989-2011 to calculate the combined global drought index. The results were then compared with historical drought events that occurred in the years 1989-1994, 2001, and 2006-2008 to confirm the accuracy of the index. The findings revealed that the results of the general drought index were

compatible with the historical droughts in the region, pointing out that the index could be effectively used for drought monitoring in the area. To give a thorough evaluation of drought conditions, the index involved the Standardized Precipitation Index (SPI), Standardized Evapotranspiration Index (SPEI), and the Standardized Runoff Index (SRI). The index was constructed using average monthly rainfall, temperature, and flow data for the years 1989 through 2011. The index's ability to detect drought conditions was demonstrated by the fact that it correctly detected the region's past occurrences of drought. Therefore, the combined global drought index can be considered as a reliable tool for drought monitoring in the region. The study highlights the importance of using comprehensive drought indices that integrate various meteorological variables to provide a comprehensive assessment of drought conditions.

As a novel way for determining patterns in streamflow, Öztopal and Şen (2016) offered the partial trend methodology. The technique is intended to segregate and analyze the intensities, durations, and magnitudes of low, medium, and high cluster trends individually. The methodology was used to interpret the geographical and temporal trends at seven precipitation stations from seven different subclimatic zones of Turkey. The study revealed that the partial trend methodology is a valuable tool for analyzing patterns in water flow and can provide informative insights for managing water resources in various locations. Overall, the research emphasizes the value of employing cutting-edge and advanced techniques for trend analysis and identification in the context of water resource management.

Anlı et al. (2009) performed a regional analysis of annual maximum rainfall events that caused floods in Trabzon Province. For this purpose, annual maximum rainfall series were obtained for 10 rainfall stations with a duration of 10-78 years in Trabzon. Homogeneity tests, goodness-of-fit tests, and regional recurrence amounts were performed based on the assumption that the stations in the province was as a single region. Statistics based on L-moments were utilized for probability distribution parameter estimation and regional analysis. The homogeneity test indicated that the annual maximum rainfall events in Trabzon were hydrologically homogeneous. The General Logistic, General Extreme Value, General Normal, and Pearson Type 3 distributions were selected as appropriate regional distributions. Rainfall values for recurrence levels of 1%, 5%, 10%, 20%, 25%, 50%, 80%, 90%,

96%, 98%, and 99% were estimated based on these distributions. Furthermore, point and regional rainfall values were estimated for certain recurrence levels of the General Logistic and General Extreme Value distributions, which could be used in the design of flood control structures and urban drainage systems.

In order to find the best distribution for yearly peak flow data in the Konya Closed Basin, Turkey, Büyükkaracığan and Kahya (2009) looked into the viability of the independence assumption in flood frequency analysis. A baseflow study was done to determine the first-order autocorrelation coefficient of yearly peak flows. The results showed that just one of the thirteen streams displayed a dependence characteristic, and it was determined that the independence assumption is true for streams in the Konya Closed Basin. Additionally, they used a variety of distributions to analyze data from 12 stations in the Konya Closed Basin, including the two- and three-parameter log-normal, Gumbel, Pearson-3, log-Pearson-3, Log-Boughton, log-logistic, and general extreme value distributions. The best distribution for annual peak flow data was calculated using traditional goodness-of-fit tests like chi-squared and Kolmogorov-Smirnov. According to the results of the goodness-of-fit tests, the study found that the Log-Pearson-3 distribution provided the best fit to the data. The independence assumption's validity was assessed using a variety of statistical techniques in this study, and the best distribution for yearly peak flow data in the Konya Closed Basin was determined.

Hınıs (2013) analysed drought conditions in Aksaray province by utilizing the Aggregate Drought Index (ADI), which is a newly developed drought index. In addition, the commonly used Standardized Precipitation Index (SPI) was also calculated for Aksaray, and the differences between the two indices were compared. To evaluate the ADI, monthly precipitation, streamflow, evapotranspiration, and temperature data from 1969-2000 were used. Streamflow data was obtained from the monthly total volume of Karasu river near Aksaray. In the second part of the study, SPI analysis was conducted for the period of 1950-2008 for multiple time scales. The ADI series showed frequent crossings in both wet and dry seasons and presented more severe wet seasons than the SPI series. In the monthly comparison of ADI and Karasu flow data, the results were more consistent in the months of April and May, while February and October showed the poorest fit. Overall, the study found that ADI provides more comprehensive information on drought conditions compared to

SPI, as it incorporates multiple variables. The results of the study can be useful for drought monitoring and management in Aksaray province. In conclusion, this study highlights the importance of using comprehensive drought indices like ADI for effective drought monitoring and management. The findings of the study provide useful insights for policymakers and researchers in the field of drought management.

Şen et al. (2020) discussed the identification and characterization of wet and dry spells for hydro-meteorological records, including their duration, maximum surplus or deficit, amplitude, and intensity. As part of the process, each dry (wet) spell feature was shown graphically in relation to various risk levels that correlate to return durations. These charts were made for yearly discharge records for the Danube River and annual precipitation records in New Jersey, both of which had more than a century's worth of data. The study revealed the existence of an exponential function that governs the relationship between each wet and dry spell parameter and the return period, which appears as straight lines on semi-logarithmic paper. Other hydro-meteorological records in the research area can be generalized to show this exponential relationship.

Şişman (2019) discussed how climate change has affected dry and wet periods in hydrometeorological records. The paper offers a framework for analyzing the lengths of wet and dry spells, their frequency, and their connection to climate change impacts. The method entails splitting the hydro-meteorological data from various locations of Turkey into halves and plotting the lengths of wet and dry spells (months) against their values on semi-logarithmic paper. On the paper, the scatter points that arise have the appearance of decreasing straight lines, and their mathematical expressions resemble exponential functions. The slopes of these straight lines provide information about the climate change impacts on each meteorology station. By using pertinent tables and figures, the authors applied this approach to monthly rainfall records from different climate zones in Turkey and then offered physical interpretations and explanations. The findings demonstrated that climate change had a major impact on wet and dry spells. The methodology described in this work provides a straightforward and efficient tool for analyzing how climate change has affected dry and wet periods in hydro-meteorological records.

Şen (2017) put out a brand-new, non-parametric hydro-climatological time series trend identification method that is independent of constrictive premises. As a result, objective, quantitative trend assessments are produced, and their statistical significance may be determined. The essential statistical equations for the application of the statistical significance test and novel trend identification are derived. He used three different time series from around the world to show how well his method works: yearly temperature records from Southern New Jersey, annual discharge records from the Danube River, and annual total rainfall records from the Tigris River Diyarbakir meteorology station. Results indicated that each record has a substantial trend, with the New Jersey example showing a rising trend and the other two showing declining trends. Overall, without making any constricting assumptions, the suggested method underlines a straightforward and efficient way to find patterns in hydro-climatological time series. Hydrologists, climatologists, and other specialists in relevant subjects who want to analyze trends in time series data can benefit from this method.

The aim of Zhang et al. (2017) in their study was to investigate various data-driven models for drought forecasting in the North of Haihe River Basin. Three data-driven models were used in the study's methodology, and their efficiency was assessed using statistical tests. According to the findings, the WANN model was the most accurate for predicting SPI-6 and SPI-12 values.

Using the L-moments method, Seçkin and Topçu (2016) computed the probability distribution parameters for the investigation of regional flood frequency. The data was gathered from 53 precipitation stations run by the Turkish State of Meteorological Service and State Hydraulic Works Administration, with a minimum of 18 years of annual maximum precipitation peaks recorded. Plotting positions were calculated using a number of formulas, including the Median, Hosking, Cunnane, Gringorten, and Hazen formulas. For comparison and measurement error, three parameters—normalized absolute error (NAE), mean absolute error (MAE), and root mean square error (RMSE) were utilized. According to the measurement error value, the results showed that the Generalized Logistic distribution produced the most accurate results. Overall, the study estimated the probability distribution parameters for regional flood frequency analysis using the L-moments approach and various probability distributions.

According to Oğuz et al. (2011), the projected erosion index (R factor) in Tokat Province, Turkey, conforms best to the probability distribution with the highest accuracy. 596 values of the R factor computed from erosive rainfalls observed from 1972 to 1995 at the Tokat Soil and Water Resources Research Institute served as the basis for the analysis. For the frequency analysis of the R factor, six distributions were selected in the study: Generalized Extreme Value (GEV), 3-parameter Log Normal (LOGN3), Generalized Logistic (GLO), Generalized Pareto (GPA), and Pearson Type 3 (PE3). The Smirnov-Kolmogorov test was used to select the best fit distribution among the five distributions, and the LOGN3 distribution was found to be the most suitable. In the study, it was concluded that the LOGN3 distribution can be used in the estimation of the R factor in the province of Tokat.

Yürekli et al. (2011) performed a regional frequency analysis of daily maximum rainfall in the Tersakan Stream watershed. Daily rainfall data gathered from 8 rainfall gauging stations was used in the study. Using the L-moments approach, all ~~the~~ stations were treated as a single region for the purposes of regionalization, discordance, heterogeneity, goodness-of-fit tests, and regional quantile estimation. The goodness-of-fit test to determine the best fit regional distribution was taken into consideration. The findings showed that the absolute value of $Z^{DIST}$ (-0.24) in the generalized extreme values (GEV) distribution was the smallest. The study's findings could provide valuable insights for improving surface drainage systems in the Tersakan Stream watershed to reduce the risk of flooding and improve water management practices.

Hınıs (2009) examined the annual precipitation data that produced natural disasters such as droughts and floods, which are of great concern to society, for the Konya Closed Basin. The monthly total precipitation data for 54 years between 1950 and 2003 for a total of 21 meteorological stations in the Konya Closed Basin were used for the study, and the suitability of annual total precipitation for 8 probability distribution methods was investigated using the L-Moment method. To find the best fit distribution, these distributions were tested with the Chi-Square and Kolmogorov-Smirnov tests. As a result, it was observed that the Generalized Logistic distribution gave better results for some stations, while the Generalized Extreme and Log-Pearson Type III distributions gave better results for some other stations. Generally, it was concluded that the statistical distribution of annual precipitation values in the

Konya Closed Basin was more suitable for the Generalized Extreme distribution. In addition, the annual precipitation totals for the Konya Closed Basin were subjected to regional homogeneity testing, and it was found that the Konya Closed Basin was a homogeneous region for annual precipitation totals according to the Wiltshire statistic used for this purpose. The main issue addressed in this study was to determine the suitability of different probability distribution methods for annual total precipitation data in the Konya Closed Basin. The findings of this study can be useful for policymakers and researchers working in the field of water resource management and natural disaster mitigation in the Konya Closed Basin.

Using the L-moment method, Yürekli (2005) conducted a regional frequency study of the maximum daily rainfalls in the Tokat region. Initially, the Runs and Mann-Whitney statistics were used to test the homogeneity and randomness of the maximum daily rainfall.Then, using the mean absolute deviation index (MADI) and mean square deviation index (MSDI), the best-fit distribution for each of the four hydrologic homogenous regions, namely West-W, Central North-CN, Central South-CS, and East-E, of the Tokat region was determined According to MADI and MSDI measures, the results showed that generalized logistic (GLO) for W and CN, generalized pareto (GPA) for CS, and generalized extreme value type I (GEV) for E were the most suitable statistical distributions.

Using 117 years of rainfall data, Bhunia (2020) used the Standardized Precipitation Index (SPI) to analyze drought in three districts of West Bengal, India, that are prone to drought at the pre-monsoon, monsoon, post-monsoon The Mann-Kendall test was used to calculate trends and Gumbel–distribution was used to analyze drought frequency. The findings indicated that these regions regularly suffered drought with low SPI values and that the frequency of dry events was rising while that of wet and typical events was declining.

Using daily rainfall data from 9 meteorological stations, Ojara et al. (2020) examined the influence of shifting climatic trends on the incidence of dry spells in Uganda. A Markov chain method was used to determine the probability of rainfall and dry spell occurrence, and the direct method was used to determine the maximum length of dry spells. Sen's slope test and Mann-Kendall statistics were applied to determine the degree of change and evaluate trends in the length of maximum dry spells,

respectively. Five stations showed a rising tendency in the length of their maximum dry spells in March, while the remaining stations showed a negligible drop in the length of their maximum dry spells. Although not statistically significant at the 5% significance level for April and May, most stations showed a decreasing trend in the length of the maximum dry spells. All stations had an 8-day drought period in March, April and August. According to the study, it was reported that crop damage brought on by longer dry spells might be reduced by planting crops at the right time, using irrigation, and cultivating crop varieties that were resistant to heat and drought. These measures would be in line with the patterns of the changing weather and climate. It was emphasized in the study how crucial it was to keep an eye on alterations in weather patterns and put adaptation plans in place to lessen the effects of climate change on Uganda's rainfed agriculture.

For the Far-North region of Cameroon, Cheo (2016) examined trends in yearly seasonal rainfall data to offer ideas for designing water-gathering systems. The authors performed Time Series Analysis and the Mann-Kendall test on annual data for the dry and wet seasons between 1957 and 2006. The findings indicated a declining trend in rainfall throughout the rainy season and an upward trend during the research period's dry season. However, the null hypothesis was accepted for both seasons because the Mann-Kendall test did not detect any statistically significant trend for either season. The authors came to the conclusion that, particularly for water harvesting facilities in the Far-North region, climate change in the research area necessitates a fundamental rethinking of how water resources are designed and managed. In the study, it was emphasized the need for a proactive strategy for managing water resources in the face of climate change and the significance of looking at patterns in rainfall data when designing for water harvesting facilities.

The problem of trend detection and identification in hydro-meteorological time series data, which might include trend components primarily brought on by climate change in recent decades, was addressed by Dabanlı et al. (2016). The Mann-Kendall (MK) trend test and the Innovative-Şen Trend Method, two well-known trend identification techniques, were contrasted in terms of their theoretical underpinnings and practical use. While the Innovative-Şen technique provides category trend behavior based on cluster analysis, the MK test provides a comprehensive monotonic trend. These two methods in the study to analyse hydro-meteorological data from the Ergene drainage

basin in northwest Turkey, including records of temperature, precipitation, relative humidity, and runoff were used. It was discovered that while the innovative-Şen technique produced trend categorizations that should be taken into account in future flood and drought studies, the MK trend test almost always failed to reveal significant trends. The primary goal of the paper was to highlight key distinctions between these two methodologies as well as any potential overlaps, in order to improve trend detection and identification in the management of water resources.

Using data from the Tennessee Valley Authority rain gauge network and the National Weather Service, Jones et al. (2015) examined the temporal variation of precipitation in the Upper Tennessee River Basin by analyzing mean areal precipitation values for 78 subbasins. They used the Yamamoto Method, the Mann-Kendall-Sneyer's test, the Morlet's wavelet, and the Mann-Kendall trend test to identify precipitation trends and abrupt changes in annual precipitation volumes. It was discovered from the study that over a 50-year period, precipitation changed statistically significantly in 11% of the subbasins. According to a review of monthly volume-based seasonal precipitation changes, the summer and autumn series exhibited the biggest increases. In addition, subbasins with major El Niño episodes showed rapid shifts in yearly precipitation volumes, and numerous subbasins showed large periodicities of 1, 6, 18, and 22 years in monthly volumes. These results are essential for regional precipitation downscaling from global climate change models, especially for the steep Appalachian region, which has a significant impact on results. In conclusion, the study points out important new understandings of how precipitation varies through time in the Upper Tennessee River Basin.

Çeribaşı et al. (2013) studied the relationship between streamflow, sediment transport, and rainfall in the Sakarya River and the trend analysis of these parameters. The aim of the study was to estimate the future behaviour of water and sediment transport in the river and to identify the possible effects of rainfall on flooding and erosion. The Mann-Kendall and Spearman Rho tests were used to analyze the trends in these parameters. The analysis of the test results showed a decreasing trend in all three parameters, indicating that water and sediment transport in the Sakarya River will decrease in the future. Overall, the study highlights the importance of understanding the behaviour of water and sediment transport in rivers to manage water resources effectively.

By using a multi-duration trend analysis on monthly global temperature data, Mohorji et al. (2017) developed a novel method for precise computation of global warming. In order to present a thorough and improved trend application technique for global temperature increment calculation, the innovative trend template (ITT) approach was employed to detect monthly patterns of temperature increase. The ITT technique shows many aspects of the increases in global temperature over the course of the record, resulting in a set of verbal and numerical descriptions for each month, including "Low" (lowest), "High" (maximum), and "Medium" (moderate) temperature amounts. The findings showed that, in addition to an average incremental temperature of 1.33 °C, there were monthly temperature increments of 0.9 °C and 1.78 °C for "Low" and "High," respectively. The result of applying the ITT methodology to monthly global temperature records from 1881 to 2013 indicated that the global average warming was approximately 0.75 °C, which was compatible with the outcome of a different approach.

Şahaplıoğlu et al. (2014) examined the monthly and yearly flow rates of the streams in Turkey's Western Mediterranean Basin to look for any patterns. With a 95% confidence level, the Mann-Kendall trend test was used to determine whether any trends had altered or not. To ascertain the slopes of the trends and forecast the flow rates, scatter diagrams were made. The findings revealed a considerable monthly and yearly decline in the flow rates at all locations. Furthermore, the trend changes were more pronounced in the summer, when there was little rainfall and the majority of the rivers' flows came from underground. Angles less than 36 degrees were statically determined to suggest a strong trend change in the Sen diagram test's analysis of the angles between the x-axis and trendlines. In general, the study brought attention to the trend of declining flow rates in Turkey's Western Mediterranean Basin and the necessity for additional research into the underlying causes of this phenomena.

Using the L-moment method, Yürekli (2005) conducted a regional frequency analysis of monthly rainfalls measured over Amasya province. To satisfy the homogeneity criteria, the province's rain gauge stations (sites) were initially split into two groups (first and second) using the homogeneity (discordancy) metric. After that, a heterogeneity (H) test was used to determine whether the regions that had been suggested as homogeneous based on the discordancy measure of site characteristics could actually be treated as such. The homogeneity of the defined regions was

verified by this test. Based on the Z-statistic, the frequency distribution that fit the data from the sites of the selected regions the best was chosen. This statistic indicated that the Generalized Extreme Value Type I (GEV) for the first region and the Pearson Type Three (P3) or Generalized Extreme Value Type I for the second region were the best fit distributions.

Innovative Polygonal Trend Analysis (IPTA), a non-parametric approach, was introduced by Şen et al. (2019) to find the trend in hydro-meteorological time series without encountering the challenges of the conventional methods. The IPTA approach enables not only the trend but also the change in two equal segments from the original time series, forming a trend polygon, to be identified. When employing both linguistic and numerical interpretations to analyze and draw conclusions from a particular time series, the trend polygon offers a useful foundation. The IPTA approach was used to analyze rainfall data from New Jersey, USA, as well as discharge data from the Danube and Göksu rivers in Romania and Turkey. The results showed that the IPTA method was efficient in identifying trends and their transitions and provided a more informative and flexible approach for trend analysis in hydro-meteorological time series.

In order to obtain drought severity-duration-frequency curves using the Standardized Precipitation Index, Aksoy et al. (2019) determined drought characteristics for rainfall stations selected from the Meriç-Ergene in Thrace, Gediz in the Aegean region, and Seyhan and Ceyhan basins in the Mediterranean region. With the aid of this index, drought severity-duration-frequency curves for each station were created for return periods of 2, 5, 10, 25, 50, and 100 years. The problem addressed in this study is the need to understand drought characteristics and frequency in different regions of Turkey to effectively manage and plan for water resources. The methodology used in the study involves the calculation of the Standardized Precipitation Index and the use of this index to generate drought severity-duration-frequency curves for different return periods. After frequency analysis, it was determined that the Generalized Extreme Value (GEV) distribution mostly fits the SPI time series. Using the most suitable probability distribution function determined for each SPI at the Precipitation Monitoring Station, drought severity-duration-frequency curves were obtained. Based on these curves and SPI values calculated at 1-, 3-, 6-, 9-, 12-, and 24-month time scales, the intensity of drought can be estimated

for return periods of 2, 5, 10, 25, 50, and 100 years. The results of the study provide important information about the frequency and severity of droughts in the studied regions, which can be useful for water resource management and planning.

Çavuş and Aksoy~~'s~~ (2019) used the standardized precipitation index (SPI) at several time scales to analyze the drought at the Adana meteorological station. The duration and intensity of the crucial drought for each year were determined after identifying dry spells. The crucial drought sets were subjected to a frequency analysis to fit probability distribution functions, and intensity-duration-frequency (IDF) curves were drawn for each duration in terms of precipitation deficit. A logistic-type function for the regression between total precipitation and SPI was used and applied the method to the Seyhan River basin meteorological station. The results showed that longer return periods corresponded to higher drought intensities, but there was no significant difference in precipitation deficits for droughts with 25-year or longer return periods.

Yıldırım and Aksoy (2019) investigated the potential for transitioning between different drought classes, as defined by the Standardized Precipitation Index (SPI), in the Gediz Basin of Turkey. Monthly precipitation data from 1961 to 2015 were used to calculate the SPI, and the drought classes were determined based on threshold values. The probability of moving from one drought class to another was determined using a Markov Chain model, which allowed for the calculation of transition probabilities and the identification of the most likely future drought class. The results indicated that there was a significant probability of transitioning between different drought classes, with the most common transitions being between moderate and severe droughts. The Markov Chain model also provided insight into the future probabilities of drought class transitions, with the most likely scenario being a transition from moderate to severe drought. The study highlights the importance of understanding the potential for transitions between different drought classes and the need for effective drought management strategies in the Gediz Basin.

Aksoy et al. (2018) conducted in the Meriç-Ergene hydrological basin, and the Edirne meteorological ~~observation~~ station with number 17050 is selected for the application. Monthly precipitation data obtained from this station were used to calculate SPI for different periods of 1-, 3-, 6-, 9-, 12-, and 24- months, and drought

severity-duration-frequency curves corresponding to different return periods were obtained using the calculated indices. The main finding of this study was the determination of drought severity-duration-frequency curves for the Meriç-Ergene hydrological basin using SPI. Drought severity-duration-frequency curves were developed for the Edirne meteorological station. By using these curves, it is possible to determine the severity of drought for a certain duration and return interval. These curves are an important tool for taking necessary measures against future droughts. The results of the study can be used in sustainable water resources management and in the preparation of drought action plans and measures. The curves provide information about the severity, duration, and frequency of drought events that may occur in the basin in different return periods, and can aid in decision-making regarding water management strategies.

Through a literature review, it has been observed that various drought indices have been calculated in past studies, and the results of different drought indices have often been compared. Specifically, it has been observed that the SPI index is fitted to the Gamma distribution and the SPEI index is fitted to the Generalized Logistic (GLOG) distribution for drought analysis. Some studies have conducted trend analyses, while others have performed Intensity-Duration-Frequency (IDF) analyses. Drought analyses were conducted for SPI Gamma, SPI best fit distribution, SPEI GLOG, SPEI best fit distribution, RDI, and SRI indices. MK and ITA trend analyses were performed separately in some studies and together in others, with the ITA analysis combining statistical and graphical analyses in one study. Studies related to Intensity-Duration-Frequency exist in the literature, but no studies were found on Magnitude-Duration-Frequency (MDF).

In this study, drought analyses were conducted for the Yeşilırmak, Kızılırmak, and Konya Closed basins using SPI Gamma, SPI best fit distribution, SPEI GLOG, SPEI best fit distribution, RDI, and SRI indices. Maps were obtained and compared for SPI Gamma and the best fit distribution, and for SPEI GLOG and the best fit distribution. The trends of droughts were identified by applying MK, ITA statistical, and ITA graphical trend analyses, and maps were obtained for MK and ITA. The MDF graphs for the drought results were obtained, compared to each other, and MDF distribution graphs were provided.

# CHAPTER 3

# MATERIALS AND METHODS

## 3.1. Data Processing

In this thesis, it is aimed to make drought analysis of Yeşilırmak Basin, Kızılırmak Basin, Konya Closed Basin, which are among the major river basins of Turkey, according to various drought indices and to compare them with each other. These indexes are Standardized Precipitation Index (SPI), Standardized Precipitation Evapotranspiration Index (SPEI), Reconnaissance Drought Index (RDI), Standardized Runoff Index (SRI) indices. For this reason, monthly total precipitation, monthly average temperature, and monthly total evapotranspiration data calculated between 1975 and 2020 (46 years) for these basins are used and, the data required for calculation were obtained from the General Directorate of Meteorology (MGM). ~~unit,~~ On the other hand, the monthly total flow amounts measured by streamflow gauging stations (AGI) were taken from General Directorate of State Hydraulic Works. flow rate data were obtained from the State Hydraulic Works (DSI).

The first rule of thumb for an accurate drought analysis is to have at least 30 years of data. For this reason, stations with at least 30 years of precipitation data were determined among all station in the basins. According to meteorological data, a total of 38 precipitation stations, 9 stations in the Yeşilırmak basin, 20 stations in the Kızılırmak basin, and 9 stations in the Konya closed basin, met this condition. For the flow data, 9 flow stations in total, 5 stations in the Yeşilırmak basin and 4 stations in the Kızılırmak basin, met this condition. In the closed basin of Konya, no flow station that meets the 30-year flow data requirement was determined.

38 precipitation stations determined for drought analysis are shown in Table 3.1 with their basic statistical values, and 9 flow stations with some their statistical values are shown in Table 3.2.

**Table 3. 1.** Meteorology stations where drought analysis will be carried out

| | | | Monthly | | | Annual | | | |
|---|---|---|---|---|---|---|---|---|---|
| **Basin** | **Station No** | **Station Name** | **Mean (mm)** | **Deviation** | **Skewness** | **Mean (mm)** | **Deviation** | **Skewness** | **Duration Date** |
| **Yeşilırmak Basin** | 17030 | Samsun Bölge | 58.598 | 39.071 | 1.384 | 703.180 | 98.375 | 0.530 | 1975-2020 46 years |
| | 17083 | Merzifon | 37.275 | 26.820 | 1.014 | 447.303 | 188.523 | 0.970 | 1975-2012 37 years |
| | 17084 | Çorum | 37.760 | 29.503 | 1.441 | 453.115 | 84.195 | 0.006 | 1975-2020 46 years |
| | 17085 | Amasya | 38.618 | 28.669 | 0.942 | 463.415 | 84.518 | 0.601 | 1975-2020 46 years |
| | 17086 | Tokat | 36.862 | 27.588 | 0.905 | 442.339 | 70.151 | 0.161 | 1975-2020 46 years |
| | 17681 | Zile | 37.058 | 29.929 | 1.170 | 444.699 | 194.914 | 0.965 | 1984-2020 36 years |
| | 17683 | Turhal | 36.709 | 29.646 | 1.061 | 440.504 | 196.380 | 0.848 | 1984-2020 36 years |
| | 17684 | Suşehri | 34.829 | 27.214 | 1.195 | 417.949 | 186.929 | 0.956 | 1984-2020 36 years |
| | 17682 | Şebinkarahisar | 47.068 | 33.864 | 0.862 | 564.818 | 240.497 | 1.157 | 1985-2020 35 years |
| **Kızılırmak Basin** | 17074 | Kastamonu | 42.611 | 33.626 | 1.904 | 511.328 | 114.578 | 0.943 | 1975-2020 46 years |
| | 17080 | Çankırı | 35.019 | 27.242 | 1.113 | 420.224 | 94.839 | 0.441 | 1975-2020 46 years |
| | 17090 | Sivas | 37.947 | 28.438 | 0.899 | 455.370 | 73.178 | 0.004 | 1975-2020 46 years |
| | 17135 | Kırıkkale | 32.519 | 27.312 | 1.196 | 390.228 | 90.071 | 0.627 | 1975-2020 46 years |
| | 17140 | Yozgat | 50.376 | 38.065 | 0.865 | 604.515 | 107.055 | 0.625 | 1975-2020 46 years |
| | 17160 | Kırşehir | 32.757 | 26.321 | 1.115 | 393.083 | 77.170 | 0.327 | 1975-2020 46 years |
| | 17162 | Gemerek | 34.763 | 27.762 | 1.212 | 417.152 | 142.603 | 1.288 | 1975-2016 31 years |
| | 17193 | Nevşehir | 35.764 | 27.326 | 0.914 | 429.169 | 76.785 | 0.059 | 1975-2020 46 years |
| | 17196 | Kayseri Bölge | 34.217 | 26.372 | 1.003 | 410.602 | 80.480 | 0.311 | 1975-2020 45 years |
| | 17622 | Bafra | 62.142 | 43.737 | 1.235 | 745.703 | 380.359 | 0.274 | 1990-2020 30 years |
| | 17648 | Ilgaz | 37.005 | 26.748 | 0.876 | 444.063 | 203.249 | 0.743 | 1985-2020 35 years |
| | 17650 | Tosya | 39.549 | 28.547 | 0.978 | 474.583 | 206.705 | 0.861 | 1983-2020 37 years |
| | 17652 | Osmancık | 34.556 | 25.777 | 1.006 | 414.669 | 195.090 | 0.663 | 1984-2020 36 years |
| | 17716 | Zara | 42.482 | 32.354 | 0.976 | 509.787 | 230.131 | 0.790 | 1985-2020 35 years |
| | 17730 | Keskin | 34.086 | 27.808 | 1.050 | 409.030 | 192.290 | 0.726 | 1986-2020 34 years |
| | 17732 | Çiçekdağı | 29.655 | 24.025 | 1.215 | 355.862 | 159.178 | 0.841 | 1984-2020 36 years |
| | 17756 | Kaman | 39.094 | 32.601 | 1.328 | 469.126 | 95.276 | 0.054 | 1975-2020 46 years |

| | | | | | | | | | |
|---|---|---|---|---|---|---|---|---|---|
| | 17760 | Boğazlıyan | 30.654 | 24.370 | 1.138 | 367.849 | 80.300 | 0.126 | 1975-2020 46 years |
| | 17835 | Ürgüp | 30.908 | 24.800 | 1.090 | 370.899 | 81.292 | 0.176 | 1975-2020 46 years |
| | 17836 | Develi | 30.885 | 25.523 | 1.003 | 370.624 | 71.194 | 0.322 | 1975-2020 46 years |
| **Konya Closed Basin** | 17244 | Konya Havalimanı | 28.009 | 23.649 | 1.120 | 336.109 | 73.275 | 0.113 | 1975-2020 46 years |
| | 17246 | Karaman | 28.997 | 24.278 | 1.279 | 347.962 | 70.310 | 0.471 | 1975-2020 46 years |
| | 17248 | Ereğli | 26.033 | 21.466 | 1.086 | 312.390 | 57.787 | 0.302 | 1975-2020 46 years |
| | 17250 | Niğde | 28.965 | 23.172 | 0.873 | 347.578 | 64.143 | 0.214 | 1975-2020 46 years |
| | 17754 | Kulu | 32.333 | 26.074 | 1.020 | 387.998 | 71.130 | 0.056 | 1975-2020 46 years |
| | 17898 | Seydişehir | 64.358 | 65.035 | 1.973 | 772.293 | 143.455 | 0.568 | 1975-2020 46 years |
| | 17900 | Çumra | 27.524 | 24.193 | 1.149 | 330.287 | 73.207 | 0.056 | 1975-2020 46 years |
| | 17902 | Karapınar | 25.594 | 21.257 | 1.345 | 307.131 | 60.837 | 0.194 | 1975-2020 46 years |
| | 17192 | Aksaray | 29.870 | 23.655 | 0.858 | 358.437 | 71.453 | 0.189 | 1975-2020 46 years |

**Table 3. 2.** Flow stations for drought analysis

| | | | **Monthly** | | | **Annual** | | | |
|---|---|---|---|---|---|---|---|---|---|
| **Basin** | **Station No** | **Station Name** | **Mean** | **Deviation** | **Skewness** | **Mean** | **Deviation** | **Skewness** | **Duration Date** |
| **Yeşilırmak Basin** | E14A002 | Yeşilırmak Kale | 143.165 | 126.427 | 1.837 | 1717.974 | 596.913 | -0.303 | 1938-2015 77 years |
| | E14A012 | Çorum Çat Irmağı Şeyhoğlu Köprüsü | 6.302 | 7.844 | 2.581 | 75.619 | 49.291 | 0.664 | 1953-2015 62 years |
| | E14A014 | Yeşilırmak Sütlüce | 22.600 | 18.250 | 2.050 | 271.194 | 155.971 | 0.277 | 1955-2015 60 years |
| | E14A022 | Kelkit Çayı Çiçekbükü | 7.608 | 10.345 | 2.128 | 91.294 | 51.098 | 0.335 | 1968-2015 47 years |
| | E14A027 | Kelkit Çayı Yemişli Köprüsü | 43.963 | 49.101 | 2.524 | 527.561 | 311.896 | 0.823 | 1980-2015 35 years |
| **Kızılırmak Basin** | E15A001 | Kızılırmak Yamula | 63.385 | 73.584 | 2.421 | 760.624 | 263.442 | 0.285 | 1938-2015 77 years |
| | E15A017 | Karanlık Deresi Şefaatli | 9.764 | 10.784 | 2.078 | 117.172 | 75.159 | 0.553 | 1952-2015 63 years |
| | E15A039 | Kızılırmak Bulakbaşı | 13.268 | 19.803 | 2.416 | 159.215 | 88.618 | 0.293 | 1971-2015 44 years |
| | E15A041 | Delice Çayı Çadırhöyük | 19.304 | 19.958 | 1.774 | 231.645 | 137.372 | 1.247 | 1980-2013 33 years |

Missing data in the data sets were completed by Linear Regression method. The stations near the station interested with missing data were used. A formula was obtained by establishing a linear relationship between stations with complete data in the vicinity and stations with missing data, and all missing data were estimated by taking the average of the values obtained from all formulas. Missing data account for about 4% of all data. In Figure 3.1, an example of missing data completion using the Linear Regression method is shown.

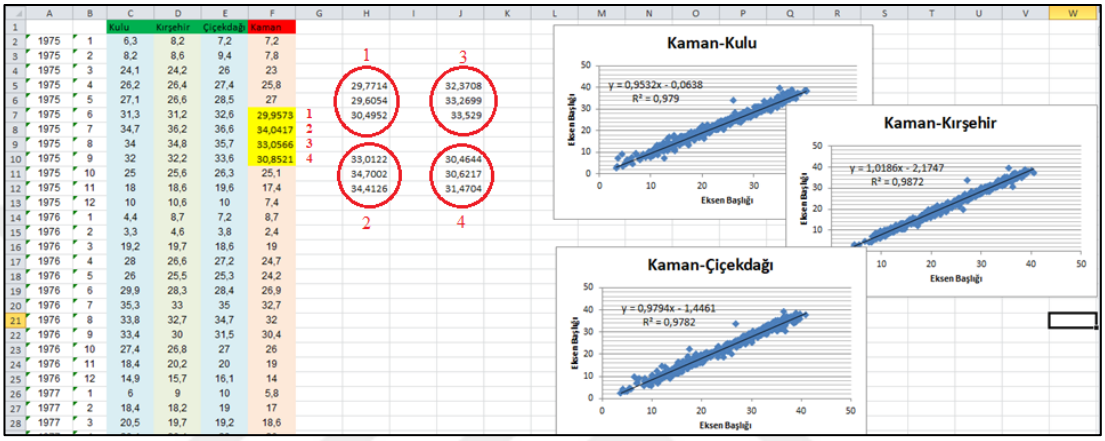


**Figure 3. 1.** Example of missing data completion

As shown in Figure 3.1., in order to estimate the missing data in the area marked with yellow in the total precipitation data of Kaman station, a Linear regression equation was found between Kaman-Kulu, Kaman-Kırşehir, Kaman-Çiçekdağı separately, and the results were written inside the circles marked in red. In order to estimate the missing data in the 1st row, the average of the data calculated in the 1st circle was taken, and for the other values, this process was repeated to complete the estimation of the missing data.

### 3.2. Study Area

The Digital Elevation Model (DEM) map of the Republic of Turkey was obtained from the website https://search.asf.alaska.edu/#/ . From this map, DEM maps of Yeşilırmak, Kızılırmak and Konya Closed basins were extracted separately by cutting with ArcGIS software from GIS software. Yeşilırmak basin is located between 39°-30' and 41°-21' north latitudes and 34°-40' and 39°-48' east longitudes. Kızılırmak Basin is located between 41°- 44' and 38°-25' north latitudes and 32°- 48' and 38°-25' east longitudes, Konya Closed Basin is located between 36°-51' and 39°-29' north latitudes. It is located between 31°36' North and 34°52' East longitudes.

The DEM map of Turkey is given in Figure 3.2, the DEM map of the Yeşilırmak Basin in Figure 3.3, the DEM map of the Kızılırmak Basin in Figure 3.4, and the DEM map of the Konya Closed basin in Figure 3.5. The unified DEM maps of all basins are shown in Figure 3.6.

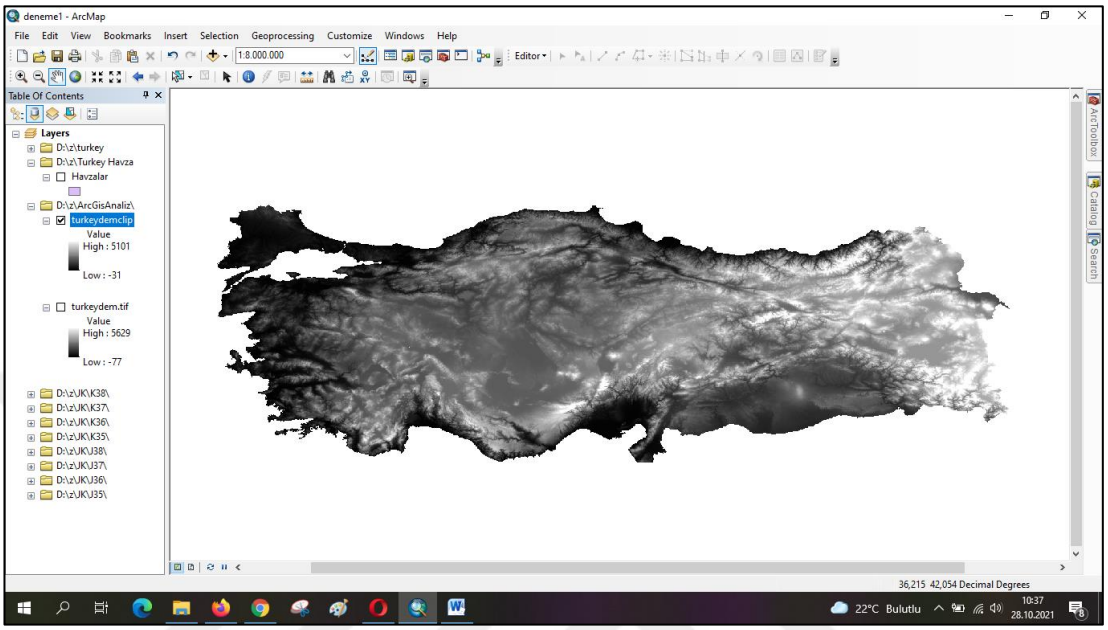


**Figure 3. 2.** Turkey DEM map

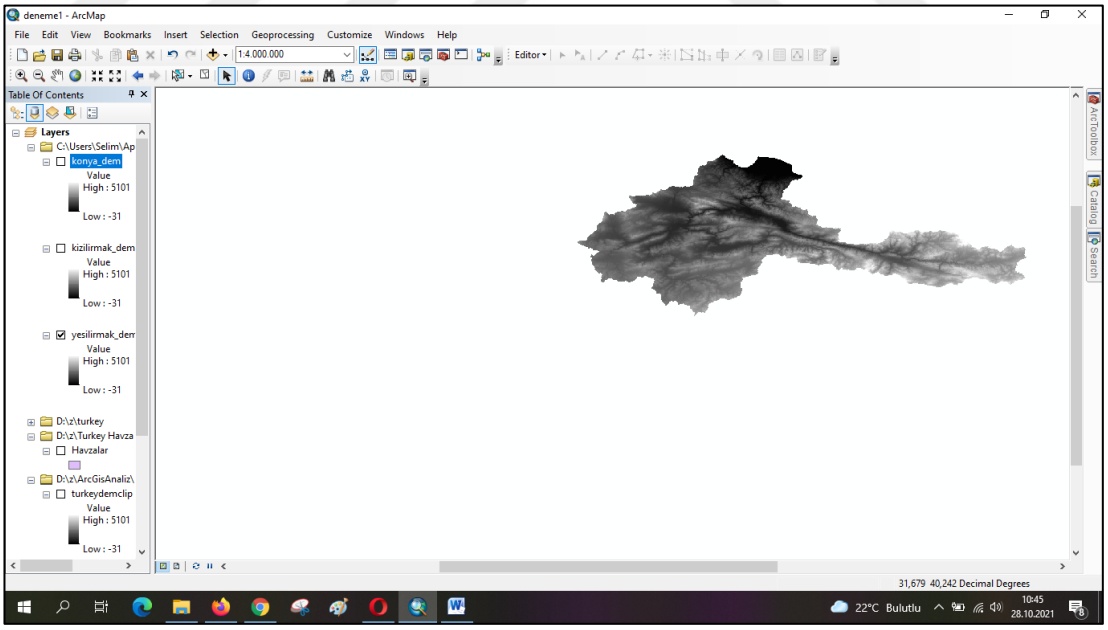


**Figure 3. 3.** Yeşilırmak basin DEM map

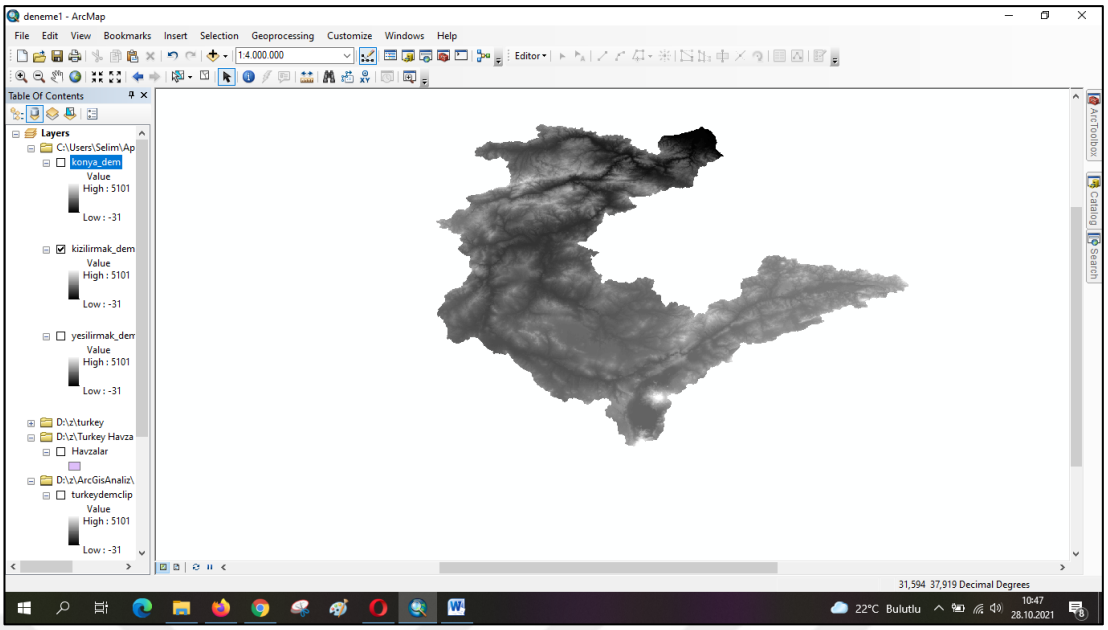


**Figure 3. 4.** Kızılırmak basin DEM map

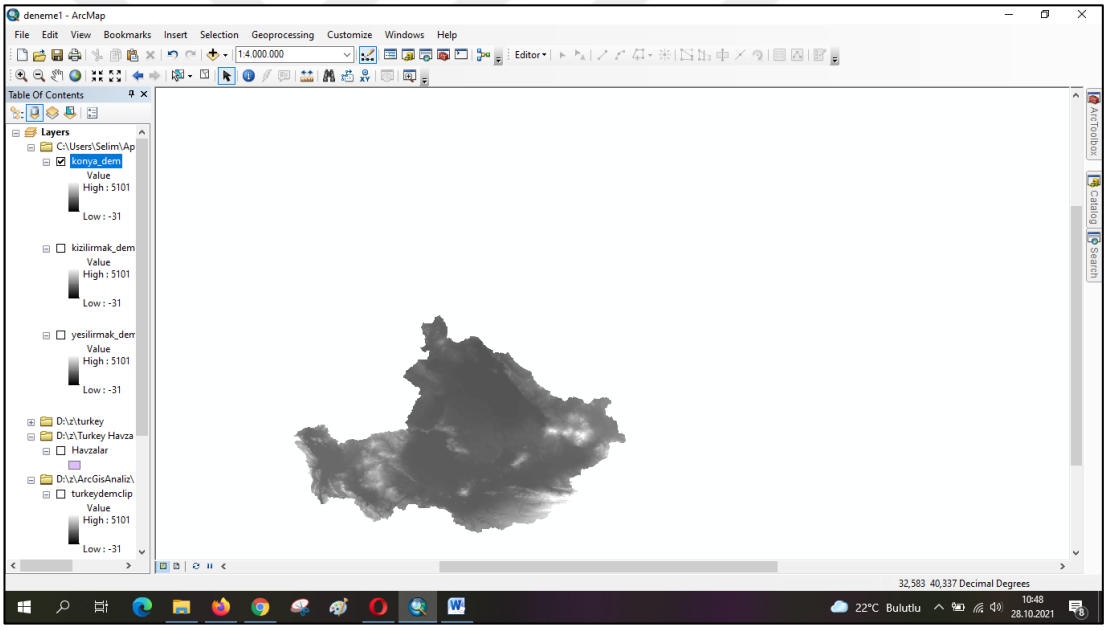


**Figure 3. 5.** Konya Closed basin DEM map

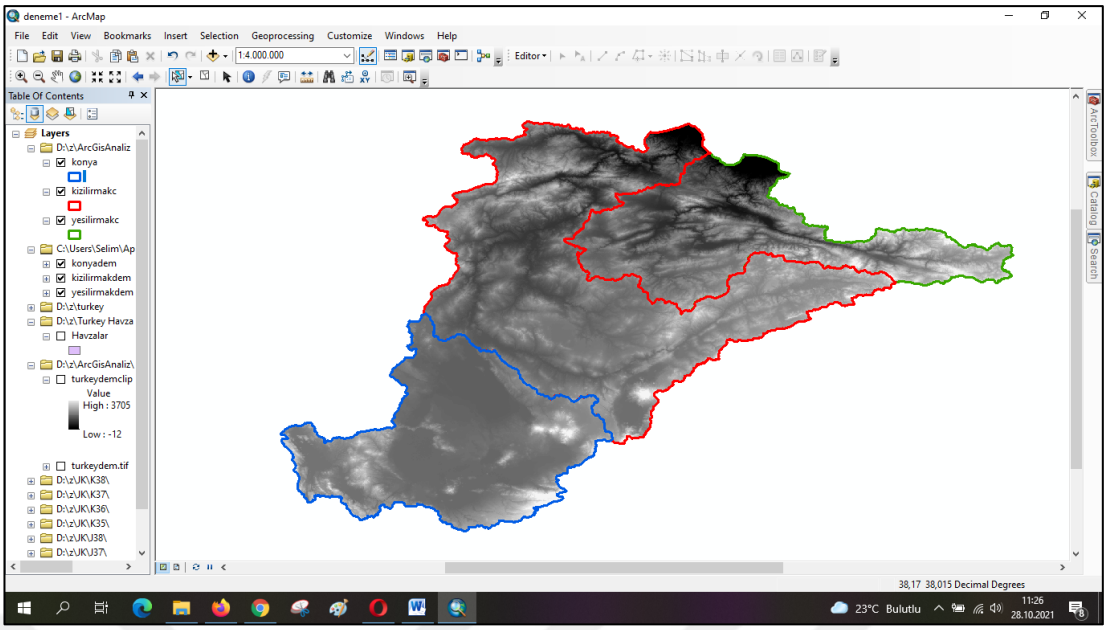


**Figure 3. 6.** DEM map of all basins

Coordinates of all Meteorology stations were determined and placed on the basin map. In Table 3.3., the coordinates of the stations are given together with their numbers in XY. In Figure 3.7., the locations of the stations are shown on the map.

**Table 3. 3.** Coordinates of meteorological stations

| Station Number and Name | Y | X |
|---|---|---|
| 17030 Samsun Bölge | 41.34417 | 36.25639 |
| 17083 Merzifon | 40.8793 | 35.4585 |
| 17084 Çorum | 40.5461 | 34.9362 |
| 17085 Amasya | 40.6668 | 35.8353 |
| 17086 Tokat | 40.3312 | 36.5577 |
| 17681 Zile | 40.296 | 35.8905 |
| 17683 Turhal | 40.3753 | 36.0988 |
| 17684 Suşehri | 40.1623 | 38.0752 |
| 17682 Şebinkarahisar | 40.2872 | 38.4193 |
| 17074 Kastamonu | 41.371 | 33.7756 |
| 17080 Çankırı | 40.6082 | 33.6102 |
| 17090 Sivas | 39.7437 | 37.002 |
| 17135 Kırıkkale | 39.8433 | 33.5181 |
| 17140 Yozgat | 39.8243 | 34.8159 |
| 17160 Kırşehir | 39.16393 | 34.1561 |
| 17162 Gemerek | 39.185 | 36.0805 |
| 17193 Nevşehir | 38.6163 | 34.7025 |
| 17196 Kayseri Bölge | 38.687 | 35.5 |
| 17622 Bafra | 41.5515 | 35.9247 |
| 17648 Ilgaz | 40.9156 | 33.6258 |

| | | |
|---|---|---|
| 17650 Tosya | 41.0132 | 34.0367 |
| 17652 Osmancık | 40.9787 | 34.8011 |
| 17716 Zara | 39.8829 | 37.72981 |
| 17730 Keskin | 39.6682 | 33.6118 |
| 17732 Çiçekdağı | 39.6067 | 34.4235 |
| 17756 Kaman | 39.3652 | 33.7064 |
| 17760 Boğazlıyan | 39.19395 | 35.25523 |
| 17835 Ürgüp | 38.6218 | 34.9144 |
| 17836 Develi | 38.3744 | 35.4797 |
| 17244 Konya Havalimanı | 37.9837 | 32.574 |
| 17246 Karaman | 37.1932 | 33.2202 |
| 17248 Ereğli | 37.5255 | 34.0485 |
| 17250 Niğde | 37.9585 | 34.6795 |
| 17754 Kulu | 39.0788 | 33.0657 |
| 17898 Seydişehir | 37.4267 | 31.849 |
| 17900 Çumra | 37.5658 | 32.79 |
| 17902 Karapınar | 37.71631 | 33.526 |
| 17192 Aksaray | 38.3705 | 33.9987 |

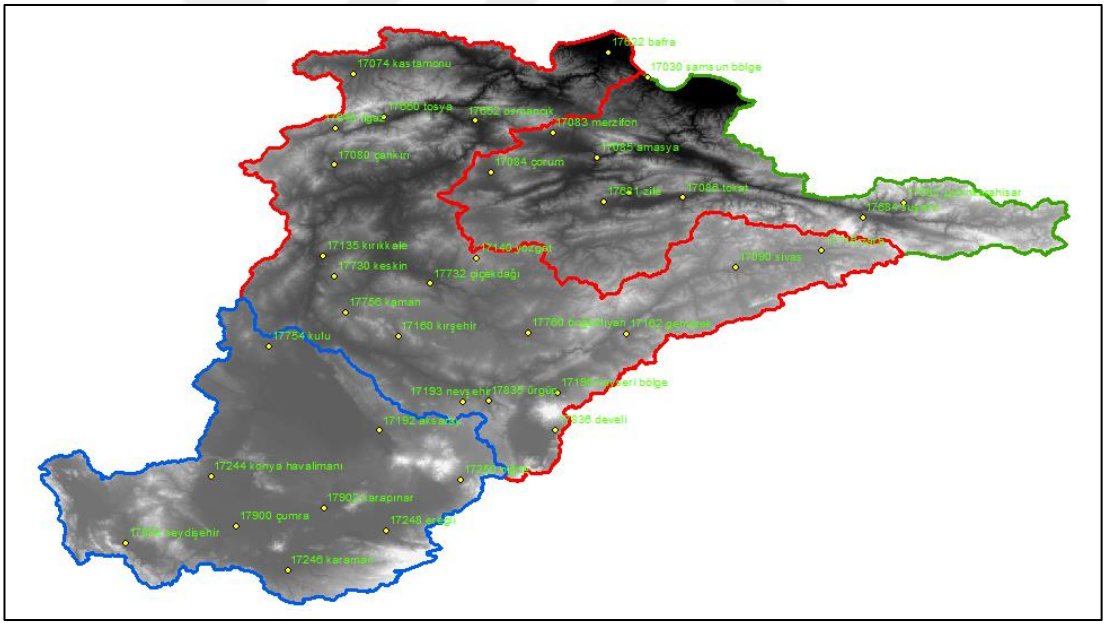


**Figure 3. 7.** Location of meteorological stations on the map. Konya Closed, Kızılırmak, and Yesilirmak basins were bounded by blue, red, and green lines, respectively.

### 3.3. Geographic Information System (GIS)

Geographic Information System (GIS) is a technique that is used to gather, organize, process, analyse, and report geographic and/or attribute information (such as maps, etc.). It is a supporting method that makes the user's life easier and lowers the margin

of error in a variety of arranging, analysis, and mapping tasks that cannot be completed manually, particularly in all engineering tasks that may be applied to the land. Maps were produced for three basins based on the results of drought analysis, trend analysis and Magnitude-Duration-Frequency analysis (Geyikli, 2015).

### 3.4. Drought Analysis

Four different drought indexes were used in this study and they were explained below.

#### 3.4.1. Standardized Precipitation Index (SPI)

Standardized Precipitation Index (SPI) proposed by McKee et al. (1993). It is a dimensionless indicator to assess drought.

Firstly, it is necessary to perform a normality analysis on the precipitation data that will be subjected to analysis. If the data satisfies the normality condition, the general relationship between the SPI and the data can be utilized. However, for data that does not meet the normality condition, SPI calculations should be conducted based on the two-parameter Gamma distribution. (McKee, Doesken, Kleist, 1993, 1995; Guttman, 1998, 1999; Wilks, 1999). According to Thom (1966), the use of the Gamma probability distribution is preferable to other distributions in investigations utilizing precipitation data sets, Equation 3.1;

$$f(x) = \frac{1}{\beta^{\alpha}\Gamma(\alpha)} x^{\alpha-1} exp^{\frac{-x}{\beta}} \tag{3.1}$$

Where, x is the monthly precipitation amount (mm/month), $\alpha$ and $\beta$ are the shape and scale parameters of the Gamma PDF, and $\Gamma(\alpha)$ is the Gamma function. The equation of the Gamma function is given by Equation 3.2;

$$\Gamma(\alpha) = \int_0^{\infty} t^{\alpha-1} e^{-t} dt \tag{3.2}$$

The $\alpha$ and $\beta$ shape and scale parameters of the Gamma distribution are calculated according to the number of data using Equation 3.3, Equation 3.4 and Equation 3.5 (Thom, 1966; Wilks, 1999);

$$D = \ln(\bar{x}) - \frac{\sum \ln(x)}{n} \tag{3.3}$$

$$\alpha = \frac{1}{4D}\left(1 + \sqrt{1 + \frac{4D}{3}}\right) \quad (3.4)$$

$$\beta = \frac{\bar{x}}{\alpha} \quad (3.5)$$

The cumulative probability of monthly sum of precipitation data can be calculated by Equation 3.6;

$$F(x) = \frac{1}{\beta^{\alpha}\Gamma(\alpha)} \int_0^x x^{\alpha-1} exp^{-x/\beta} dx, x > 0 \quad (3.6)$$

Since the Gamma Function is undefined for values zero, the cumulative probability values for periods without precipitation are calculated using Equation 3.7;

$$H(x) = q + (1 - q)F(x) \quad (3.7)$$

Where q=m/n and m=number of zero precipitation month n=total number of data, it is determined by dividing the number of data without precipitation by total number of data in the data set. H(x) is transferred to the standard normal distribution (Z) with mean 0 and variance 1. This transferred value correspond the SPI value;

$$t = \begin{pmatrix} \sqrt{\left\{\ln\left(\frac{1}{H(x)^2}\right)\right\}}, 0 < H(x) \leq 0.5 \\ \sqrt{\left\{\ln\left(\frac{1}{1-H(x)^2}\right)\right\}}, 0.5 < H(x) \leq 1 \end{pmatrix} \quad (3.8)$$

$$SPI = \begin{pmatrix} -\left(t - \frac{c_0 + c_1 t + c_2 t^2}{1 + d_1 t + d_2 t^2 + d_3 t^3}\right), 0 < H(x) \leq 0.5 \\ \left(t - \frac{c_0 + c_1 t + c_2 t^2}{1 + d_1 t + d_2 t^2 + d_3 t^3}\right), 0.5 < H(x) \leq 1 \end{pmatrix} \quad (3.9)$$

H(x) is the cumulative probability values of precipitation data; The coefficients c0, c1, c2, d1, d2, d3 are the coefficients that perform the equivalent normal distribution standardized variable transformation. These coefficients are 2,515517, 0.802853; 0.010328; 1.432788, 0.189269 and 0.001308, respectively (Gümüş and Algin 2017); (Wu et al. 2005; Aslan, 2020).

The Standardized Precipitation Index (SPI) values calculated by Mckee et al. (1993) are classified as droughts classes given in Table 3.4;

**Table 3. 4.** SPI drought classification

| **SPI Values** | **Drought Categories** |
|---|---|
| ≥ 2 | Extreme Wet (W3) |

| | |
|---|---|
| 1,50 ~ 1,99 | Wet (W2) |
| 1,00 ~ 1,49 | Moderate Wet (W1) |
| 0,99 ~ -0,99 | Normal (N) |
| -1,00 ~ -1,49 | Moderate Drought (D1) |
| -1,50 ~ -1,99 | Drought (D2) |
| ≤ - 2 | Extreme Drought (D3) |

### 3.4.2. Standardized Precipitation and Evapotranspiration Index (SPEI)

The Standardized Precipitation Evapotranspiration Index (SPEI) was proposed by Vicente Serrano et al (2010). It has been argued that the precipitation parameter should be included in drought assessments as well as other parameters such as temperature or $ET_0$.

Because of employing precipitation data as an only input parameter and the simple calculation procedure, the SPI approach is among the most popular indices in drought analysis. The SPI approach, however, ignores other factors impacting dryness because it only takes precipitation as an input parameter (Serrano et al. 2012). The fact that it is based only on precipitation data is considered as a lack of SPI analysis.

Hu and Wilson (2000) analysed the effects of precipitation and temperature using the Palmer Drought Severity Index (PDSI), and discovered that the index showed equal magnitude increases for drought in both variables. They came to the conclusion that it would be appropriate to assess the drought using precipitation data if temperature fluctuations were fewer than those of precipitation.

Empirical investigations revealed that the intensity of drought was influenced by the rise in temperature values. For instance, an experiment by Abramopoulos et al. (1988) using a general circulation model demonstrated that 80% of precipitation is lost to evaporation and transpiration. According to studies, heat-related droughts were just as bad as those brought on by precipitation.

The SPEI index was proposed to address the shortcomings of the SPI technique. It is an index that takes into account both the PDSI method's sensitivity to temperature and evaporation as well as the SPI method's ability to operate over a range of time periods (Serrano et al., 2012).

The SPI technique's calculation method serves as the foundation for SPEI. The index differs from the SPI technique in that it incorporates both the precipitation parameter and potential evapotranspiration data. (Anonymous, 2015).

Serrano et al. (2010) explained the SPEI calculation as follows; $D_i$ is the difference between precipitation and evapotranspiration;

$$D_i = P_i - PET_i \tag{3.10}$$

In this study PET calculation is calculated based on Thornthwaite method as follows.

$$PET_i = 16.\left(\frac{10.t}{I}\right)^a.G \tag{3.11}$$

$$a = 6{,}7510.10^{-7}.I^3 - 7{,}7110.10^{-5}.I^2 + 1{,}791210.10^{-2}.I + 0{,}492339 \tag{3.12}$$

$$I = \sum_1^{12}\left(\frac{t}{5}\right)^{1,514} \tag{3.13}$$

Where t: monthly average temperature, G: latitude correction coefficient.

SPEI can be calculated for various time scales using the same formula as SPI by using the $D_i$ determined by Equation 3.10. When calculating the SPEI index for the standardized D series, it is advised to utilize the Log-Logistic distribution. Equation 3.14 represents the three-parameter log-logistic probability density function (PDF).

$$f(x) = \frac{\beta}{\alpha}\left(\frac{x-\gamma}{\alpha}\right)^{\beta-1}(1+\left(\frac{x-\gamma}{\alpha}\right)^{\beta})^{-2} \tag{3.14}$$

In this expression, $\alpha$, $\beta$, $\gamma$, are the parameters of scale, shape, and origin within the range of $\gamma$>$D$<$\infty$. Several methods can be used to calculate the Log-logistic distribution's parameters. The L-moment approach is the simplest and most effective of these calculation techniques (Serrano et al. 2010). Log-logistic distribution parameters can be obtained when calculating L moments Equations 3.15, 3.16, 3.17;

$$\beta = \frac{2w_1 - w_0}{6w_1 - w_0 - 6w_2} \tag{3.15}$$

$$\alpha = \frac{(w_0 - 2w_1)\beta}{\Gamma(1+\frac{1}{\beta})\Gamma(1-\frac{1}{\beta})} \tag{3.16}$$

$$\gamma = w_0 - \alpha\Gamma(\frac{1+1}{\beta})\Gamma(\frac{1-1}{\beta}) \tag{3.17}$$

$\Gamma(\beta)$ in the equation is the gamma function of $\beta$. In Equation 3.18; The cumulative probability distribution of F(x) is calculated using the SPEI formulations given in Equation 3.19;

$$F(x) = \left[1 + \left(\frac{\alpha}{x-\gamma}\right)^{\beta}\right]^{-1} \quad (3.18)$$

$$SPEI = W - \frac{c_0 + c_1 W + c_2 W^2}{1 + d_1 W + d_2 W^2 + d_3 W^3} \quad (3.19)$$

P=1-F(x) is the probability of exceeding a certain precipitation value. W = $(-2 \ln(P))^{0.5}$ ; When P> 0.5, 1-P is used instead of P and the sign of the SPEI value is changed. $C_0$ = 2,515517; $C_1$= 0.802853; $C_2$=0.010328; $d_1$= 1.432788; $d_2$= 0.189269; $d_3$= 0.001308.

The calculation method described yields SPEI values with a mean value of 0 and a standard deviation of 1, and drought is categorised in accordance with Table 3.5 similar to SPI classification (Aslan, 2020).

**Table 3. 5.** SPEI drought classification

| **SPEI Values** | **Drought Categories** |
|---|---|
| ≥ 2 | Extreme Wet (W3) |
| 1,50 ~ 1,99 | Wet (W2) |
| 1,00 ~ 1,49 | Moderate Wet (W1) |
| 0,99 ~ -0,99 | Normal (N) |
| -1,00 ~ -1,49 | Moderate Drought (D1) |
| -1,50 ~ -1,99 | Drought (D2) |
| ≤ - 2 | Extreme Drought (D3) |

### 3.4.3. Reconnaissance Drought Index (RDI)

While performing the RDI analysis, the monthly precipitation totals and $ET_0$ values of the stations are used. This method was presented for the first time at the Mediterranean Drought Preparedness and Prevention Plan (MEDROPLAN) coordination meeting (Tsakiris, 2004). In essence, RDI drought analysis is a method calculated by proportioning precipitation data to $ET_0$ data. $ET_0$ values were calculated using the Thornthwaite method with a program called DRINC. In this study, the Thornthwaite climate classification system has been used. It is mostly based on the correlation between temperature- and precipitation-induced

evapotranspiration. Thornthwaite asserts that the soil is saturated and there is an excess of water in areas where precipitation exceeds evapotranspiration. Consequently, this area has a humid climate. Contrarily, water does not accumulate in the soil and cannot provide the plants with the water they require in areas where precipitation is less than evapotranspiration. In these locations, water is scarce. Consequently, this area has a dry climate. The distinctions made by Thornthwaite oscillate between these two ideas (Bölük, 2016).

Tsakiris et al. (2007) proposed RDI by taking under consideration $ET_0$ to under take the disadvantage of SPI. The first step is to calculate the formula. When calculating this value, monthly evaluations are made using monthly data and annual data for year i and month j are used as shown below:

$$\alpha_0^{(i)} \frac{\sum_{j=1}^{12} P_{ij}}{\sum_{j=1}^{12} PET_{ij}}, i = 1{:}\,N \; ve \; j = 1{:}\,12 \tag{3.20}$$

In Equation 3.10, Pij and PETij are expressed as the number of months in the dataset to be calculated and are the precipitation and potential evapotranspiration values for month j of year i, respectively. It should be noted that the water year in Mediterranean countries typically begins in October.

The second relationship to be calculated is the Normalized RDI ($RDI_n$) expression, which can also be calculated annually by Equation 3.21. The $\bar{\alpha}_0$ the arithmetic mean of the variables in the equation is $\alpha_0$ values calculated for N years of data.

$$RDI_n^{(i)} = \frac{\alpha_0^{(i)}}{\bar{\alpha}_0} - 1 \tag{3.21}$$

The third expression to be calculated is the standardized RDI (RDIst). The calculation of the $RDI_{st}$ parameter is done in a similar way to the SPI calculation method.

$$RDI_{st(k)}^{(i)} = \frac{y_k^{(i)} - \bar{y}_k}{\hat{\sigma}_{yk}} \tag{3.22}$$

The expression $y_k^{(i)}$ is $ln(\alpha_0^{(i)})$, $\bar{y}_k$ is the arithmetic mean of these $y_k^{(i)}$ values, and $\hat{\sigma}_{yk}$ is the standard deviation.

In the above expression, it is assumed that the $\alpha_o$ values fit the lognormal distribution. Standardized RDI gives similar results to SPI. For this reason, SPI and RDIst indices can be compared in studies conducted for the same region. The RDI drought index classification is similar to SPI, given in Table 3.6 (Aslan; 2020);

**Table 3. 6.** RDI drought classification

| **RDI Values** | **Drought Categories** |
|---|---|
| ≥ 2 | Extreme Wet (W3) |
| 1,50 ~ 1,99 | Wet (W2) |
| 1,00 ~ 1,49 | Moderate Wet (W1) |
| 0,99 ~ -0,99 | Normal (N) |
| -1,00 ~ -1,49 | Moderate Drought (D1) |
| -1,50 ~ -1,99 | Drought (D2) |
| ≤ - 2 | Extreme Drought (D3) |

### 3.4.4. Standardized Runoff Index (SRI)

Standardized Runoff Index (SRI) analysis is exactly the same as SPI. The only difference is that SPI uses precipitation data while SRI uses flow data. The SRI method is used for the drought calculations caused with a decrease in streamflow. The calculation method is the same as described in SPI. The drought classification table for the calculated SRI values is given in Table 3.7

**Table 3. 7.** SRI drought classification

| **SRI Values** | **Drought Categories** |
|---|---|
| ≥ 2 | Extreme Wet (W3) |
| 1,50 ~ 1,99 | Wet (W2) |
| 1,00 ~ 1,49 | Moderate Wet (W1) |
| 0,99 ~ -0,99 | Normal (N) |
| -1,00 ~ -1,49 | Moderate Drought (D1) |
| -1,50 ~ -1,99 | Drought (D2) |
| ≤ - 2 | Extreme Drought (D3) |

## 3.5. Frequency Analysis

Parameter estimation of theorical probability distributions were carried out by three different methods, namely; Method of Moments, L-Moments and Maximum Likelihood Methods. These are explained briefly in the following section.

### 3.5.1. Maximum Likelihood (ML) Method

The ML technique of estimation entails selecting parameter estimates that result in the highest possible chance of the observations occurring. The joint probability density function (pdf) of the observations conditional on the parameter values is known as the likelihood function $\alpha_1, \alpha_2, \dots, \alpha_k$, for a distribution with a probability density function (pdf) given by f(x) and parameters $\alpha_1, \alpha_2, \dots, \alpha_k$, in the form:

$$L(\alpha_1, \alpha_2, \dots, \alpha_k) = \prod_{i=1}^{n} f(x_i; \alpha_1, \alpha_2, \dots, \alpha_k) \quad (3.24)$$

By a limited differentiation in relation to $\alpha_1, \alpha_2, \dots, \alpha_k$ and setting these partial derivatives to zero as in Eq. 3.24, the values of $\alpha_1, \alpha_2, \dots, \alpha_k$ that maximize the probability function are determined. In Eq. 3.25, the values of $\alpha_1, \alpha_2, \dots, \alpha_k$ are then determined by simultaneously solving the set of equations that results.

$$\frac{\partial L(\alpha_1, \alpha_2, \dots, \alpha_k)}{\partial \alpha_i} = 0;\ i = 1,2,\dots,k \quad (3.25)$$

The likelihood function's natural logarithm is frequently easier to maximize by using (Rao & Hamed, 2000);

$$\frac{\partial \ln L(\alpha_1, \alpha_2, \dots, \alpha_k)}{\partial \alpha_i} = 0;\ i = 1,2,\dots,k \quad (3.26)$$

### 3.5.2. Methods of Moments (MOM)

In the MOM, estimates of a probability distribution function's parameters are produced by equating the sample's moments with the probability distribution function's moments. The initial k sample moments for a distribution with k parameters $\alpha_1, \alpha_2, \dots, \alpha_k$ that need to be estimated are set to equal the corresponding population moments defined in terms of the unknown parameters. The unknown parameters $\alpha_1, \alpha_2, \dots, \alpha_k$ are then simultaneously solved for in these k equations. Details can be found in Rao & Hamed 2020.

### 3.5.3. L-Moments (LM)

In this procedure, like in the case of MOM, parameter estimates are derived by equating distributional moments with matching sample moments. The first for a distribution with k estimated parameters, k sample moments, $\varphi_1, \varphi_2, \dots, \varphi_k$, are calibrated to match the relevant population moments. After that, the resulting

equations are simultaneously solved for the unknown parameters $\varphi_1, \varphi_2, \dots, \varphi_k,$. Details are given in Rao & Hamed, 2000.

The relationships of cumulative distribution function (CDF) used in this study are as follows;

**Generalized Extreme Value (GEV)**

$$F(x) = exp\left\{-\left[1 - k\left(\frac{x-u}{\alpha}\right)\right]^{1/k}\right\} \quad (3.27)$$

**Pearson Type 3 (P3)**

$$F(x) = \frac{1}{\alpha\Gamma(\beta)}\int_{\gamma}^{x}\left(\frac{x-\gamma}{\alpha}\right)^{\beta-1}.e^{-\left(\frac{x-\gamma}{\alpha}\right)}.dx \quad (3.28)$$

**Three Parameter Lognormal (LN3)**

$$F(x) = \frac{1}{(x-\alpha)\sigma_y\sqrt{2\pi}}.exp\left\{-\frac{1}{2\sigma_y^2}\left[\log(x-\alpha) - \mu_y\right]^2\right\} \quad (3.29)$$

**Generalized Logistic (GLOG)**

$$F(x) = \left[1 + \left\{1 - k\left(\frac{x-\varepsilon}{\alpha}\right)\right\}^{1/k}\right]^{-1} \quad (3.30)$$

**Extreme Value Type 1 (EV1)**

$$F(x) = exp\left[-e^{-\left(\frac{x-\beta}{\alpha}\right)}\right] \quad (3.31)$$

**Generalized Pareto (GPAR)**

$$F(x) = 1 - \left[1 - \frac{k}{\alpha}(x-\varepsilon)\right]^{1/k} \quad (3.32)$$

**Weibull (W)**

$$F(x) = 1 - e^{-\left(\frac{x-m}{\alpha}\right)^b} \quad (3.33)$$

**Normal (N)**

$$F(u) = \int_{-\infty}^{u} \frac{1}{\sqrt{2\pi}} . e^{-t^2/2} . dt$$

(3.34)

**Logistic (LOG)**

$$F(x) = \left[1 + \bar{e}^{\left(\frac{x-m}{a}\right)}\right]^{-1} \quad (3.35)$$

**Two Parameter Lognormal (LN2)**

$$F(x) = \frac{1}{x\sigma_y\sqrt{2\pi}} . exp\left\{\frac{[-\log x - \mu_y]^2}{2\sigma_y^2}\right\} \quad (3.36)$$

**Gamma (GAM)**

$$F(x) = \frac{(x-\beta)^{\alpha-1} exp(-\frac{x}{\beta})}{\beta.\Gamma(\alpha)} \quad (3.37)$$

**Log Pearson Type 3 (LP3)**

Same as Pearson Type III distribution, but data is logarithmically transformed x=ln(y).

**The Five-Parameter Wakeby Distribution (WAK(5))**

$$x = m + \alpha[1 - (1 - F)^b] - c[1 - (1 - F)^{-d}] \quad (3.38)$$

Where; $F = F(x) = P(X \leq x)$

**The Four-Parameter Wakeby Distribution (WAK(4))**

$$x = \alpha[1 - (1 - F)^b] - c[1 - (1 - F)^{-d}] \quad (3.39)$$

### 3.6. Goodness-Of-Fit Tests

There are two tests used to determine the best fit distributions.

**Kolmogorov-Smirnov**

$$D_N = max|F_N(x) - F_0(x)| \quad (3.46)$$

Where, $F_N(x)$ is cumulative theorical probability functions and $F_o(x)$ is the experienced cumulative distribution functions, which is calculated by Weibull formula in this study as given in previous section.

**Chi-Square**

$$\chi^2 = \sum_{j=1}^{j=k} \frac{(O_j - E_j)^2}{E_j} \quad (3.47)$$

$O_j$ is the observed number of events in the class interval j, $E_j$ is the number of events that would be expected from the theoretical distribution and k is an arbitrary number of classes to which the observed data are divided. This test is significant with 5% confidence intervals.

## 3.7. Trend Analysis

### 3.7.1. Mann-Kendall Trend Test

A common method for determining the importance of monotonic trends in hydrometeorological time series is the non-parametric Mann-Kendall (MK) trend test (Mann 1945; Kendall 1975). According to the sign of the difference between any two records, its statistic (S) is determined as follows:

$$S = \sum_{i=1}^{n-1} \sum_{j=1+1}^{n} sgn(x_j - x_i) \quad (3.48)$$

This is based on the phrase that follows,

$$sgn = (x_j - x_i) = \begin{cases} 1\ ;\ x_j > x_i \\ 0\ ;\ x_j = x_i \\ -1\ ;\ x_j < x_i \end{cases} \quad (3.49)$$

$x_i$ and $x_j$ are the recorded data at times i and j, respectively, and n is the length of the time series. S's positive (negative) number denotes an upward (downward) trend. If n is more than 10 and the time series is somewhat normally distributed, the slope's variance is as follows:

$$Var(S) = \frac{n(n-1)(2n+5) - \sum_{i=1}^{p} t_i(t_i-1)(2t_i)}{18} \quad (3.50)$$

where $t_i$ is the length of the data in the $p^{th}$ cluster and p is the number of dependent clusters. If there is any form of dependent cluster, the summary method should not be applied. The standard Z value for the MK test is finally determined as follows:

$$Z = \begin{cases} \frac{S-1}{\sqrt{Var(S)}} & if \;\; S > 0 \\ 0 & if \;\; S = 0 \\ \frac{S+1}{\sqrt{Var(S)}} & if \;\; S < 0 \end{cases} \tag{3.51}$$

The value ( $\left|Z_{1-\alpha/2}\right|$) from the standard normal distribution table is compared with this Z value at two-tailed confidence levels ($\alpha = 95\%$). The null hypothesis ($H_0$) of an insignificant trend is invalid if |Z| is greater than ( $\left|Z_{1-\alpha/2}\right|$); otherwise, the alternative hypothesis ($H_1$) indicates a statistically significant trend.

### 3.7.2. Innovative Şen Trend Analysis (ITA)

The observation data is split into two equal lengths from the start date and arranged in this fashion from smallest to largest. The two sub-series are positioned in the Cartesian coordinate plane against each other (Figure 3.8.). It is accepted that the analysed series does not exhibit a trend if the data lies on or very nearly touches the 1:1 (45°) line. The upward or downward trend is appeared depending on which direction the data diverges from the 1:1 (45°) line: if it diverges upward (toward the y-axis), the trend is increasing; if it diverges downward (toward the x-axis), the trend is decreasing (Dabanlı 2017).

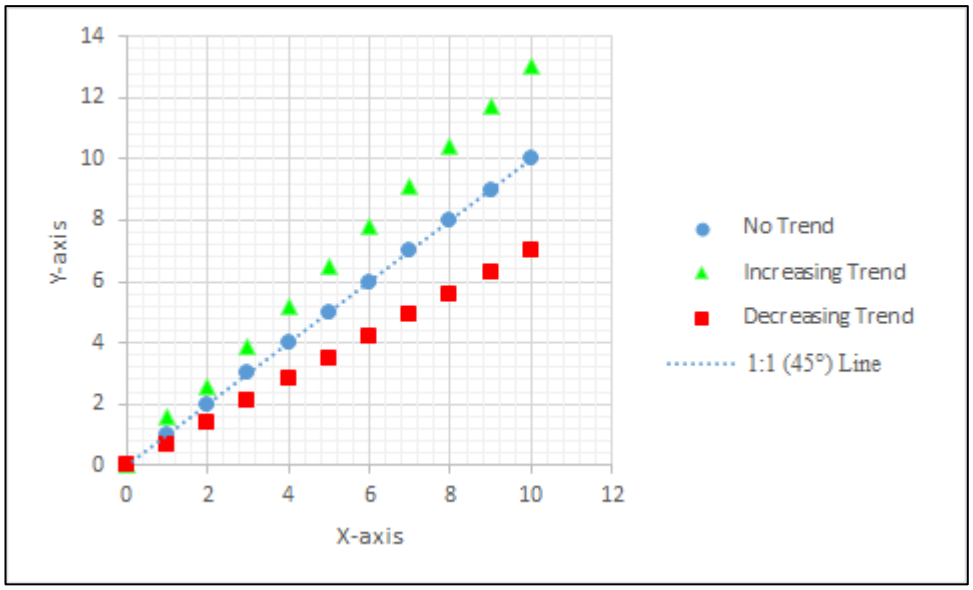


**Figure 3. 8.** Display of increasing, decreasing and no-trend series.

In the ITA method, as explained above, we can detect the trend of the data with the graphical method, as well as the trend of the data with statistical analysis. After the number of data in the whole data set is determined, the standard deviation and correlation of the data are calculated. The standard deviation of the slope of the whole data set is calculated using the number of data, standard deviation and correlation values calculated above. The data is then divided into two equal lengths from the start date and sorted from smallest to largest. The mean of both ranked data sets is taken. For slope calculation, the average of the 1st data set is taken from the average of the 2nd data data set, divided by the total number of data and multiplied by 2. In the next step, the confidence interval is calculated using the standard deviation of the slope. If the slope is higher than the confidence interval, the trend is increasing; if the slope is lower than the confidence interval, the trend is decreasing; if the slope is within the confidence interval, there is no trend. This method can be used as a supplement to the graphic method described above. This calculation is expressed by the following formulas.

The statistical significance of the trend in the given data is determined by comparing the calculated slope value ($S_{cal}$) with the critical slope value ($S_{crit}$), and deciding whether the ~~observed~~ variation is significant or not.

$$S_{cal} = \frac{2(\bar{y}_2 - \bar{y}_1)}{n} \tag{3.52}$$

The $\bar{y_1}$ and $\bar{y_2}$ in the equation represent the means of the two divided series of the original data, and "n" indicates the number of observations. The standard deviation of the calculated slope ($\sigma_s$) is calculated using the following relationship.

$$\sigma_s = \frac{2\sqrt{2}}{n\sqrt{n}}\sigma\sqrt{1-\rho_{\bar{y}_1.\bar{y}_2}} \tag{3.53}$$

The terms "$\rho_{\bar{y}1\bar{y}2}$" and "σ" in the equation represent the correlation coefficient and the standard deviation of the original data, respectively. The confidence interval of the calculated slope at a 5% significance level is obtained using the following relationship.

$$CI_{(1-\alpha)} = 0 \pm S_{crit}\sigma_s \tag{3.54}$$

The value of critical S ("Scrit") in the Equation 3.54 is equal to the value of ±1.960 obtained from the standard normal distribution table for a 5% significance level. (Yürekli, 2023).

### 3.8. Magnitude-Duration-Frequency (MDF) Analysis

Curves of drought magnitude-duration-frequency are one way to describe drought. Studies on drought magnitude-duration-frequency curves that describe the magnitude, length, and return interval of drought are available for diverse locations of the world. These studies are similar to the precipitation magnitude-duration-frequency curve technique used in infrastructure estimates (Aksoy et al. 2018).

In order to characterize the drought, it is necessary to determine the drought severity, drought magnitude and drought frequency from the drought parameters and to obtain the Magnitude-Duration-Frequency (MDF) curves. MDF curves express the relationship between drought magnitude, drought duration, and frequency (recurrence) obtained from the analysis of a calculated set of drought data. Sometimes, magnitude values can be used instead of intensity. Magnitude is obtained by summing SPI values for drought duration. Magnitude-Duration-Frequency (MDF) curves can be obtained. In Figure 3.9 and 3.10 explanatory visuals about drought severity, magnitude and duration are given.

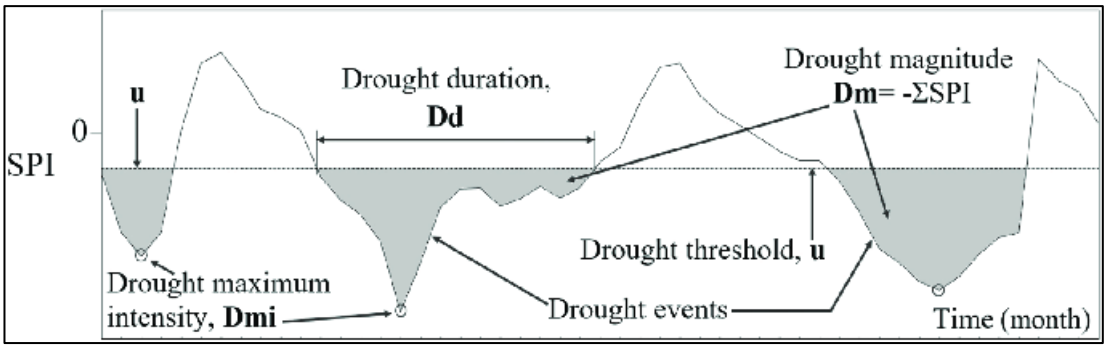


**Figure 3. 9.** Drought Magnitude, frequency and duration (Aksoy et al., 2019)

# CHAPTER 4

# FINDINGS AND DISCUSSION

Drought analysis for Yeşilırmak, Kızılırmak and Konya Closed basin were carried out by using SPI, SPEI, RDI and SRI indices for the 38 selected stations. SPI is based only on precipitation values, SPEI is based on the difference between the precipitation and evapotranspiration and RDI is based on the ratio of precipitation to evapotranspiration function. SRI is based on the streamflow values. The results histograms of some selected stations were given and results of SPI, SPEI and RDI for whole basins were mapped and given in this chapter.

The procedure for drought analysis for each indices were carried out firstly as suggested in the literature. SPI analysis were based on Gamma distribution function in the literature. In this study SPI analysis were followed by using Gamma distribution, then the most suitable distributions were sought for each station and for each monthly total precipitation values. Our analysis show that Gamma distribution does not represent the best distribution for most of stations in study area. Similar procedure were followed for SPEI analysis in the literature. Generalized Logistic (GLOG) distribution was suggested for SPEI analysis, SPEI was calculated by GLOG distribution for the study area and the most suitable distribution was sought. The results for SPEI showed that GLOG was not the best distribution function. The best distribution for SPEI was sought and the results were mapped for the study area for 3 and 12 month precipitation totals.

## 4.1. Standardized Precipitation Index (SPI)

### 4.1.1. Standardized Precipitation Index (SPI) with Gamma Distribution Analysis

Thom (1966) suggested that the Gamma distribution in the analyses made with climatic data. SPI is a drought analysis method that can only use precipitation data. In this SPI analysis study, the total precipitation data of 38 meteorology stations between 1975 and 2020 were analysed by adapting them with Gamma distribution function for 1-month, 3 month, 6 month, 9 month, 12 month and 24 months totals precipitation. Drought analysis results of SPI with Gamma distribution for the selected Samsun station are given in Figure 4.1 to 4.6.

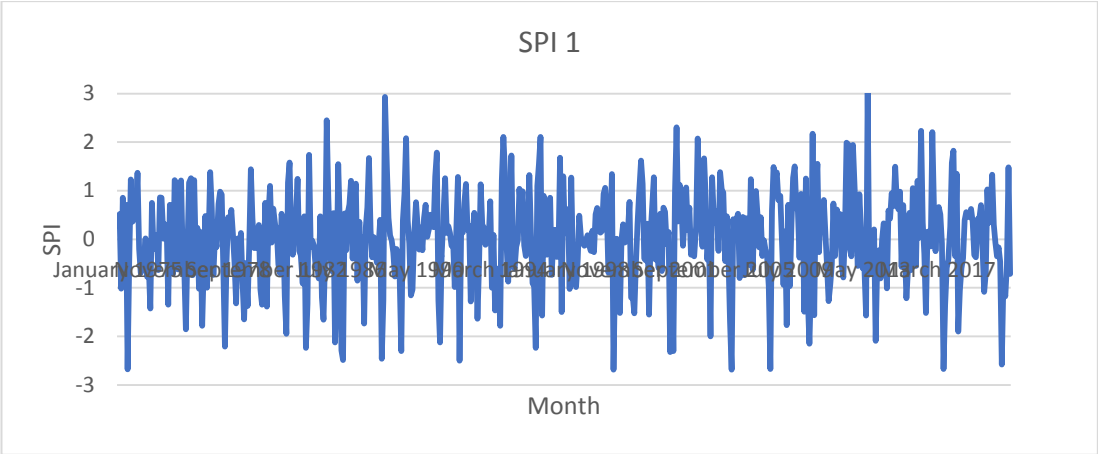


**Figure 4. 1.** Samsun station SPI1 result graph (Gamma disrtibution)

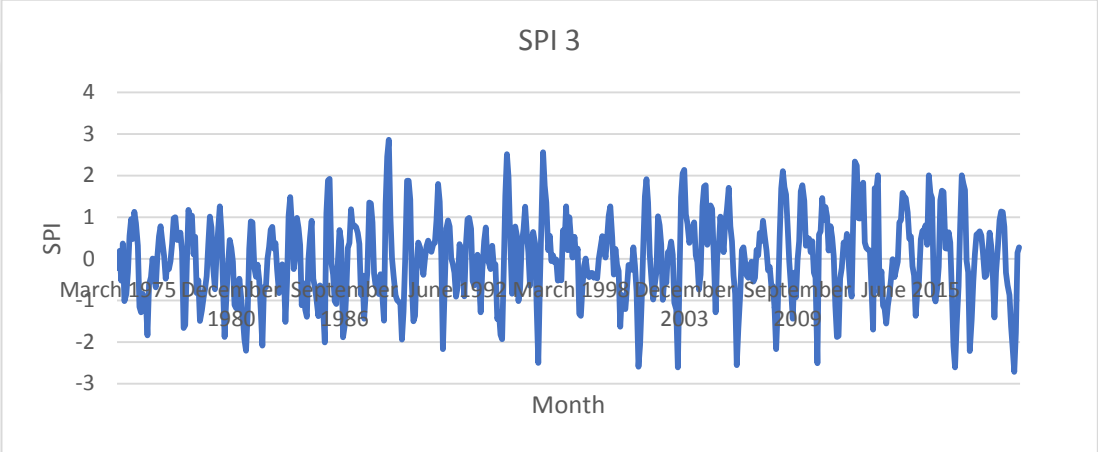


**Figure 4. 2.** Samsun station SPI3 result graph (Gamma disrtibution)

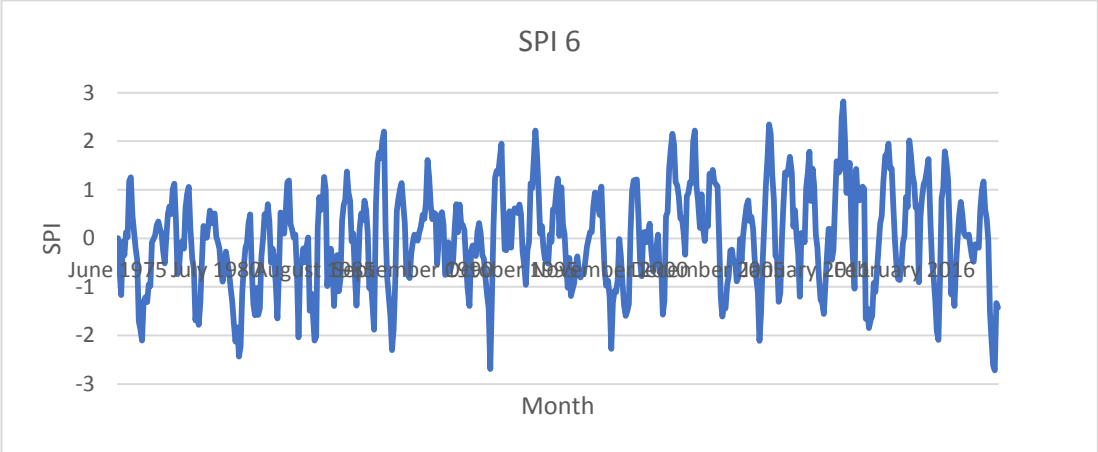


**Figure 4. 3.** Samsun station SPI6 result graph (Gamma disrtibution)

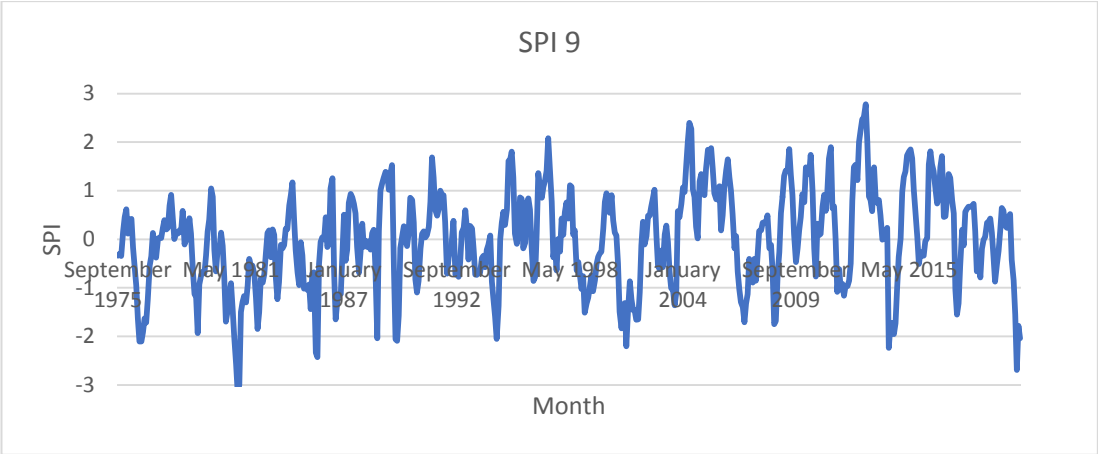


**Figure 4. 4.** Samsun station SPI9 result graph (Gamma disrtibution)

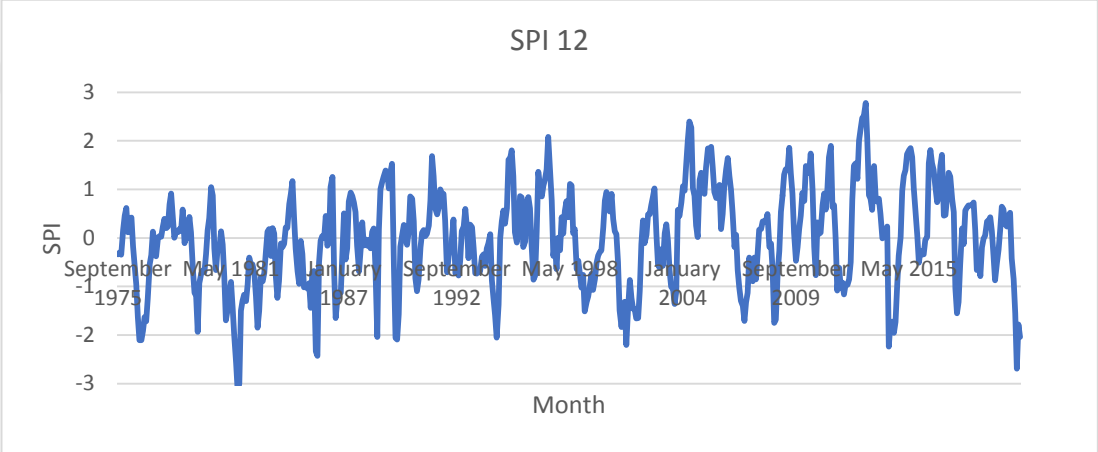


**Figure 4. 5.** Samsun station SPI12 result graph (Gamma disrtibution)

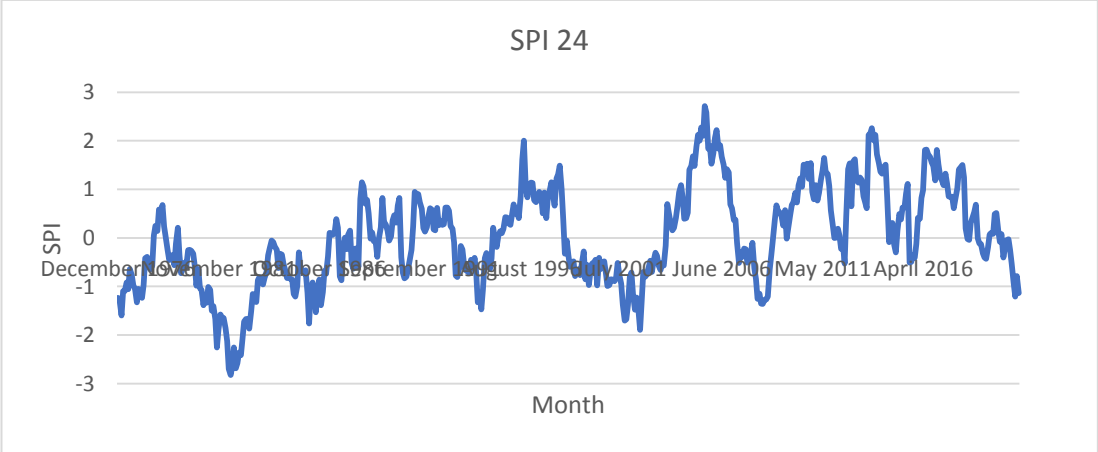


**Figure 4. 6.** Samsun station SPI24 result graph (Gamma disrtibution)

### 4.1.2. Standardized Precipitation Index (SPI) with Best Fit Distribution Analysis

Contrary to the idea of Thom (1966) that "in analyses with climatic data, the data should be analysed by fitting the Gamma distribution", it was thought that climate data would not always fit the Gamma distribution under all conditions and each data set could fit for best distribution methods. In this study, the total precipitation data of 38 meteorology stations used in SPI analysis between 1975 and 2020 were determined for 1 month, 3 months, 6 months, 9 months, 12 months and 24 months precipitation totals, and the most appropriate distribution method for each station is investigated. The best fit distribution was sought by using three different methods namely: Methods of Moment, L-Moment and Maximum Likelihood methods. Kolmogorov-Smirnov (K-S) and Chi Square methods were used to determine the best-fit theoretical probability distribution function for each methods. The detected methods were validated with additional frequency plots as well. A MATLAB software written by A. Ramachandra RAO and Khaled H. HALED was used to determine the most suitable distributions (Rao and Hamed, 2000). Drought analysis results of the SPI for selected stations calculated based on the best fit distribution were given as an example Figure 4.7 to 4.12. The best fit distributions determined in the SPI 3-month and SPI 12-month drought analyses are shown in Table 4.1.

**Table 4. 1.** Best fit distributions for SPI analysis

| St. No | St. Name | 1 Month | 3 Month | 6 Month | 9 Month | 12 Month | 24 Month |
|---|---|---|---|---|---|---|---|
| 17030 | Samsun | GEV-LM | P3-ML | GEV-LM | P3-ML | N-ML | LN2-LM |
| 17083 | Merzifon | W-LM | W-ML | GEV-M | P3-M | LN3-ML | LN3-ML |
| 17084 | Çorum | W-LM | W-LM | LOG-ML | GAM-LM | P3-ML | GEV-M |
| 17085 | Amasya | W-LM | W-LM | W-LM | LN3-M | LN3-M | GLOG-ML |
| 17086 | Tokat | W-LM | W-LM | N-ML | LOG-ML | W-M | W-ML |
| 17681 | Zile | W-M | W-LM | GEV-LM | GAM-M | GAM-LM | GLOG-ML |
| 17683 | Turhal | GPAR-LM | W-LM | GEV-LM | W-M | LOG-ML | GLOG-M |
| 17684 | Suşehri | W-M | W-LM | GEV-M | W-LM | N-ML | GLOG-ML |
| 17682 | Şebinkarahisar | W-LM | W-M | W-LM | LN3-M | LOG-ML | W-M |
| 17074 | Kastamonu | GEV-LM | LN2-LM | P3-M | GAM-M | LN2-ML | GLOG-ML |
| 17080 | Çankırı | W-LM | P3-M | GEV-M | P3-M | N-ML | EV1-ML |

| | | | | | | | |
|---|---|---|---|---|---|---|---|
| 17090 | Sivas | W-M | P3-M | GEV-ML | P3-M | N-LM | GEV-ML |
| 17135 | Kırıkkale | GPAR-LM | W-LM | W-LM | GAM-LM | LOG-ML | EV1-ML |
| 17140 | Yozgat | GPAR-M | W-LM | GEV-ML | GEV-LM | GAM-ML | GEV-LM |
| 17160 | Kırşehir | GPAR-LM | W-M | GEV-LM | W-M | GAM-M | GEV-M |
| 17162 | Gemerek | W-LM | W-LM | GEV-LM | GLOG-LM | LOG-LM | LN3-ML |
| 17193 | Nevşehir | GPAR-ML | W-LM | W-ML | GEV-ML | GAM-LM | GEV-M |
| 17196 | Kayseri | W-M | W-LM | GEV-ML | LN3-LM | LOG-LM | LN3-ML |
| 17622 | Bafra | LN3-LM | P3-ML | LN3-ML | GAM-M | LN3-ML | GLOG-ML |
| 17648 | Ilgaz | W-LM | W-LM | W-M | GLOG-ML | W-M | LN2-ML |
| 17650 | Tosya | W-M | GEV-M | W-LM | GEV-M | W-LM | GLOG-ML |
| 17652 | Osmancık | W-LM | P3-ML | P3-ML | W-LM | W-M | P3-ML |
| 17716 | Zara | W-M | W-M | P3-M | GLOG-ML | LOG-LM | GEV-LM |
| 17730 | Keskin | GPAR-LM | W-LM | W-M | W-M | LN3-ML | GLOG-ML |
| 17732 | Çiçekdağı | W-M | W-LM | GEV-LM | GEV-M | EV1-M | GEV-ML |
| 17756 | Kaman | W-M | W-M | P3-ML | P3-ML | W-M | LN3-ML |
| 17760 | Boğazlıyan | W-M | GEV-LM | LN3-LM | GLOG-ML | LOG-ML | GLOG-LM |
| 17835 | Ürgüp | GPAR-LM | W-LM | W-ML | W-M | W-LM | GEV-LM |
| 17836 | Develi | GPAR-M | LN3-ML | GEV-ML | GEV-ML | GLOG-ML | W-M |
| 17244 | Konya | GPAR-LM | P3-ML | W-M | W-LM | W-LM | GEV-LM |
| 17246 | Karaman | GPAR-LM | P3-ML | P3-ML | LN3-ML | P3-ML | P3-ML |
| 17248 | Ereğli | GPAR-LM | W-M | P3-ML | GEV-M | W-M | GLOG-ML |
| 17250 | Niğde | GPAR-M | W-LM | GEV-LM | GEV-ML | LN3-ML | LN3-ML |
| 17754 | Kulu | GPAR-LM | W-LM | LN3-ML | GEV-LM | GEV-M | GEV-ML |
| 17898 | Seydişehir | P3-M | GAM-ML | W-M | W-M | GLOG-ML | GAM-LM |
| 17900 | Çumra | GPAR-LM | W-M | GEV-LM | GAM-LM | W-M | P3-LM |
| 17902 | Karapınar | W-LM | W-LM | GAM-M | P3-ML | LN2-LM | W-LM |
| 17192 | Aksaray | GPAR-LM | W-LM | GEV-ML | GEV-ML | GEV-M | W-LM |

As an example, Table 4.1 illustrates that the best distribution for SPI 3 at Samsun station is determined as Pearson Type-3 using the Maximum Likelihood method. And for SPI 12 the best distribution is Normal distribution determined by Maximum Likelihood method.

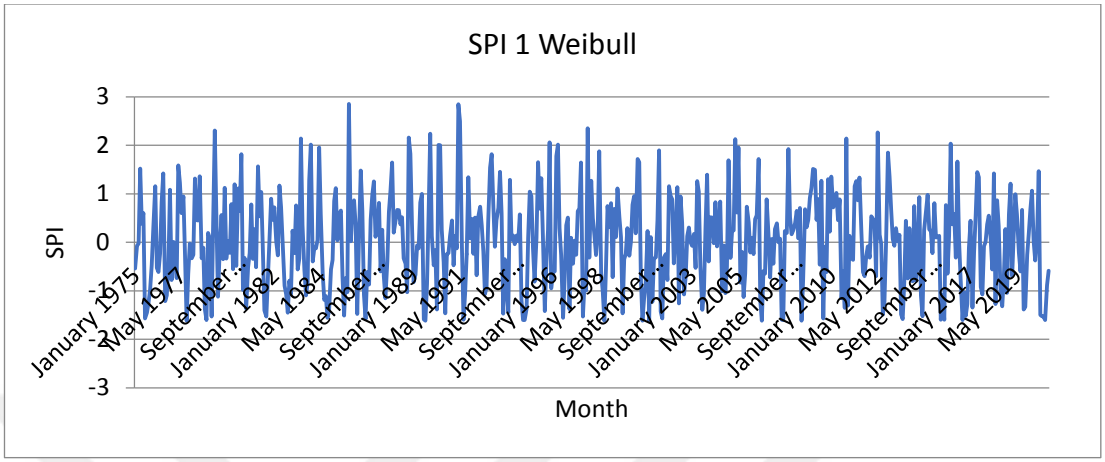


**Figure 4. 7.** Tokat station SPI1 result graph (Best Fit distribution)

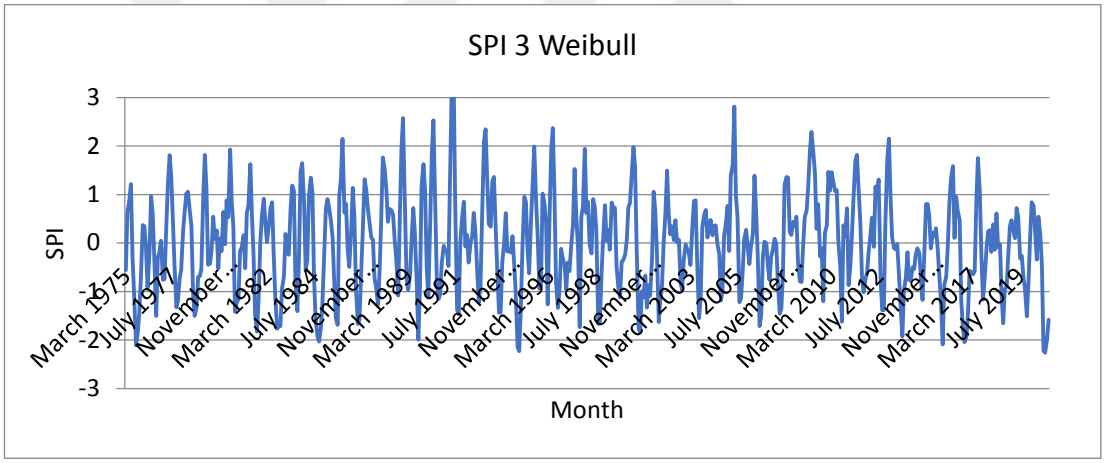


**Figure 4. 8.** Tokat station SPI3 result graph (Best Fit distribution)

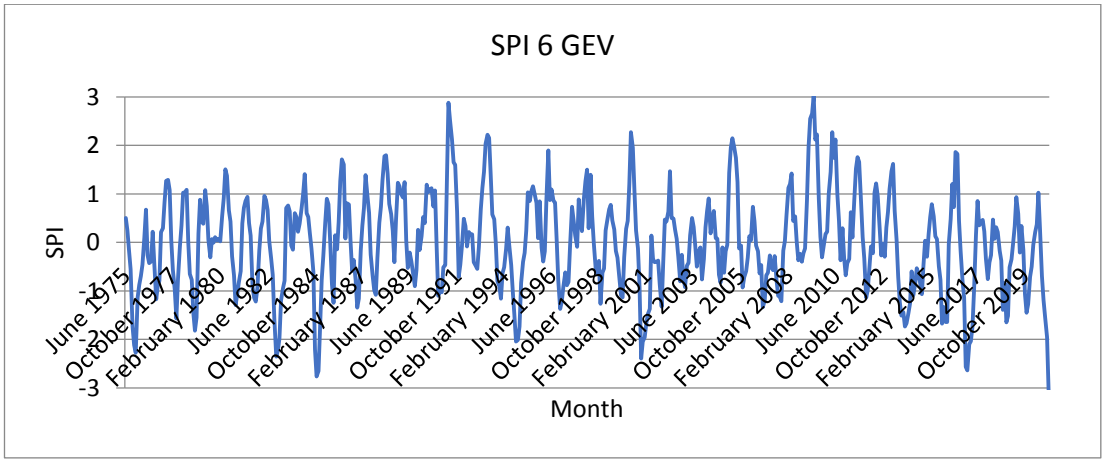


**Figure 4. 9.** Tokat station SPI6 result graph (Best Fit distribution)

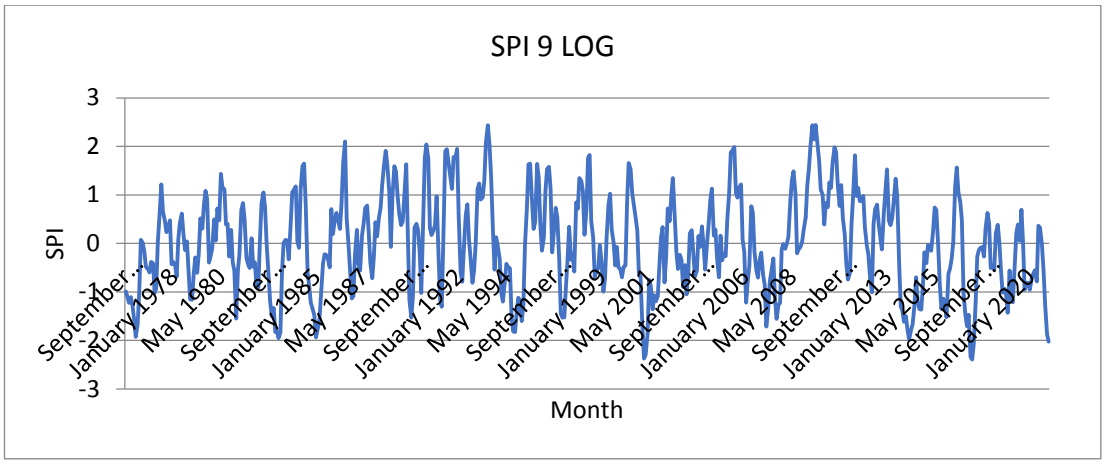


**Figure 4. 10.** Tokat station SPI19 result graph (Best Fit distribution)

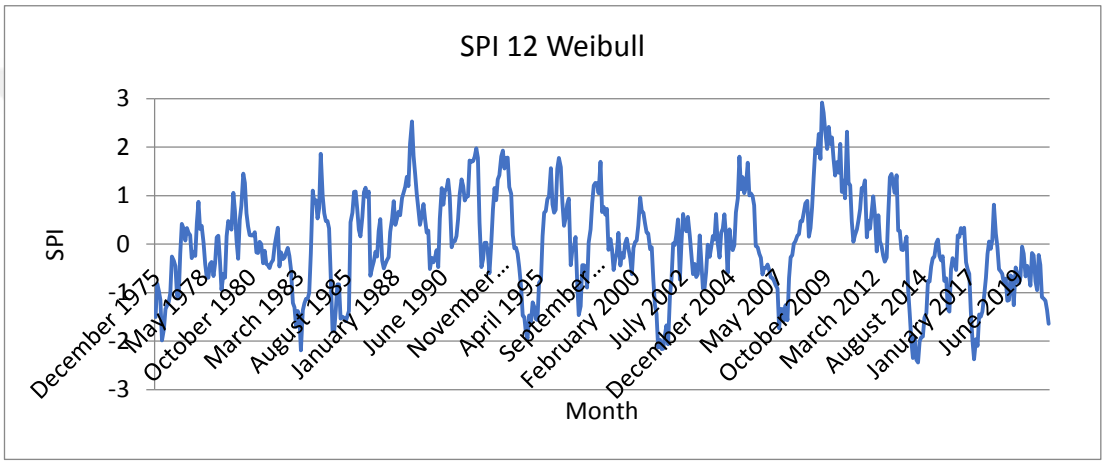


**Figure 4. 11.** Tokat station SPI12 result graph (Best Fit distribution)

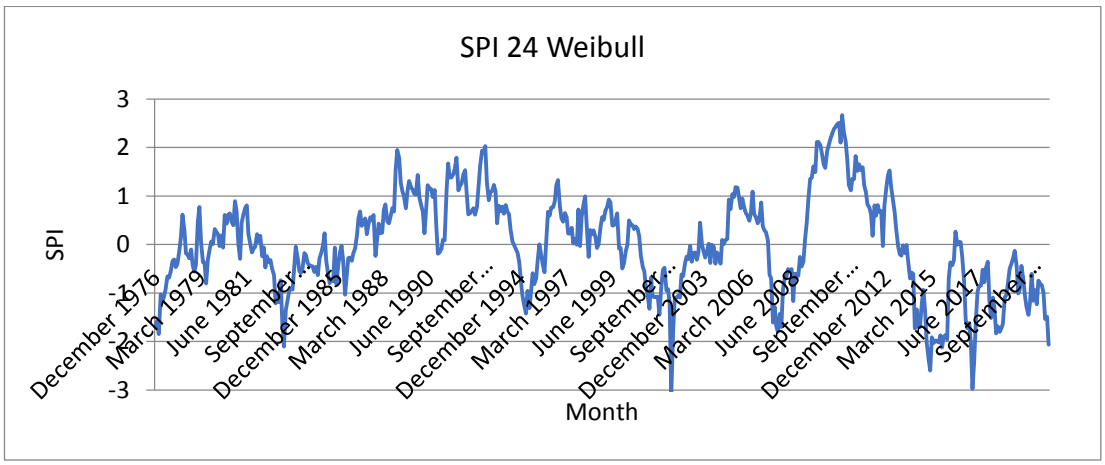


**Figure 4. 12.** Tokat station SPI24 result graph (Best Fit distribution)

The Figures 13-15 the relationship between the ~~observed~~ values of SPI 3 drought calculation, the results obtained by the Gamma distribution, and the results obtained by the most appropriate distribution for selected stations Tokat, Sivas and Konya. The best distribution function determined based on the K-S test and Chi Squared tests.

Upon examining the graphs and results of K-S and Chi Squared tests, in most of the stations for SPI3 and SPI12, it was determined that the calculations based on the Gamma distribution is not the most appropriate distribution to represent the drought analysis. Therefore, it is not correct to fit the precipitation values to the Gamma distribution when performing the SPI drought calculations. The correct approach is to identify the most appropriate distribution for each station first, and perform the drought calculation accordingly.

### 4.1.3. SPI comparison

Comparison of SPI analysis methods by using Gamma distribution and best fit distribution were given in this section. The comparison of Gamma distribution and the best distribution for SPI 3 and SPI 12 analysis for some selected stations were given in Figure 4.13 to 4.15. Subsequently, by combining the results of the best-fit distribution for each station, drought analysis maps were obtained by aggregating them for all basins.

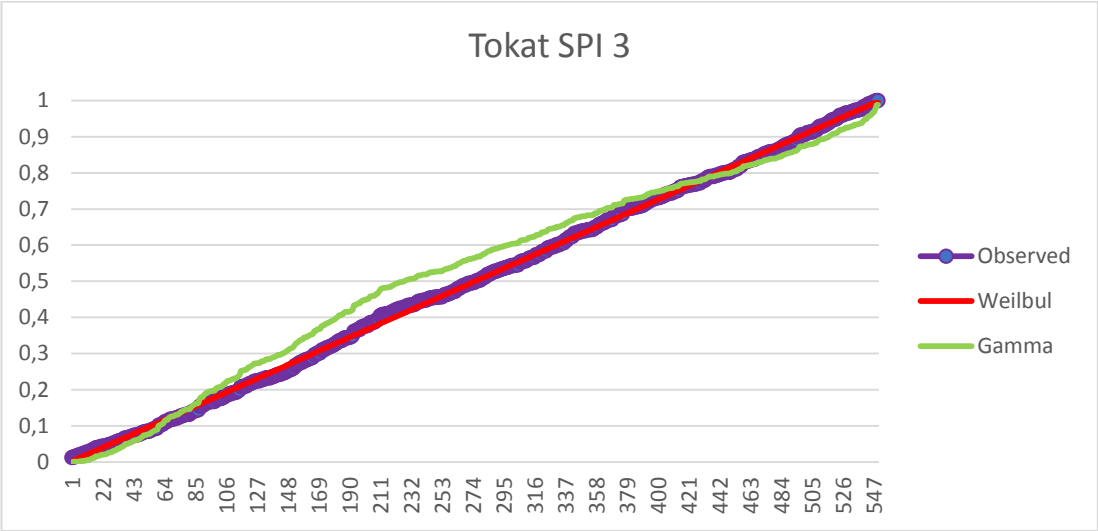


**Figure 4. 13.** Comparison of observed, Gamma distribution, and Best Fit distribution for SPI 3 at Tokat station.

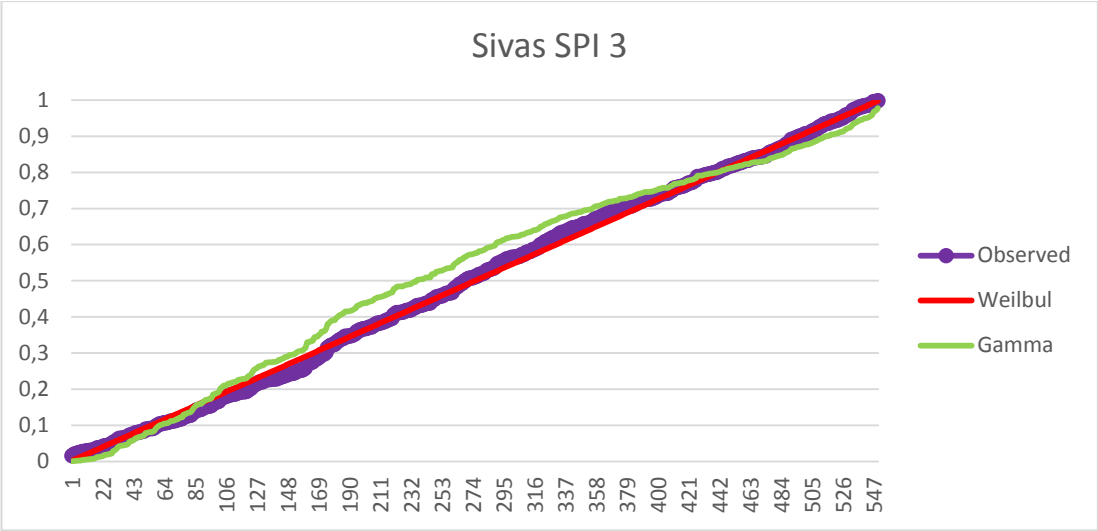


**Figure 4. 14.** Comparison of observed, Gamma distribution, and Best Fit distribution for SPI 12 at Sivas station.

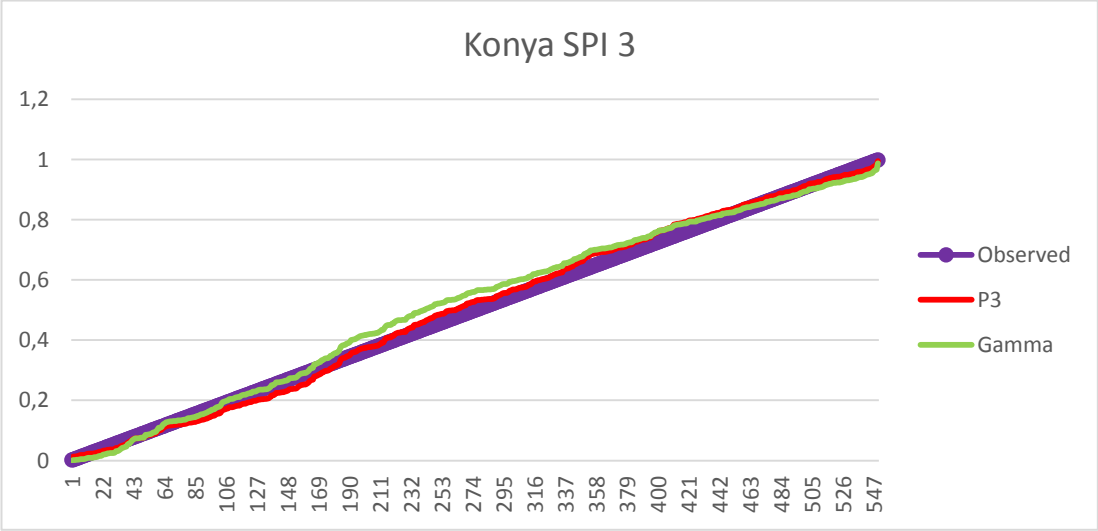


**Figure 4. 15.** Comparison of observed, Gamma distribution, and Best Fit distribution for SPI 3 at Konya station.

The spatial variability of the best-fit probability distributions over the study area for 3-month and 12-month SPI results is shown in the following figures. Figure 4.16-4.21 shows the spatial distributions for Yeşilırmak, Kızılırmak and Konya closed basins separately.

When Yesilırmak and Kızılırmak basins for SPI3 analysis investigated from Table 4.1, Figure 4.18, Figure 4.18 and Figure 4.20, it is shown that Weibull distribution is dominant except for Konya basin. In Konya basin, Pearson Type 3 is dominant distribution for SPI3 analysis as well as Weibull. On the other hand, for SPI12 analysis Weibull as well as other distributions were seemed to be in effect for all

three basins. When the Figure 4.22 and Figure 4.23 examined, the importance of frequency distributions should not to be evaluated separately for each basins is revealed. Figure 4.22-4.23 shows the study area for all basins together for SPI 3 and SPI 12 analysis. These Figures indicated that there was a boundary condition affects for the calculated drought values when mapping basins separately. This effect appears when mapping the whole basin all together. Therefore, drought analysis should be carried out for greater areas to assess the impact and spatial variations of drought and to consider the areal effects of drought.

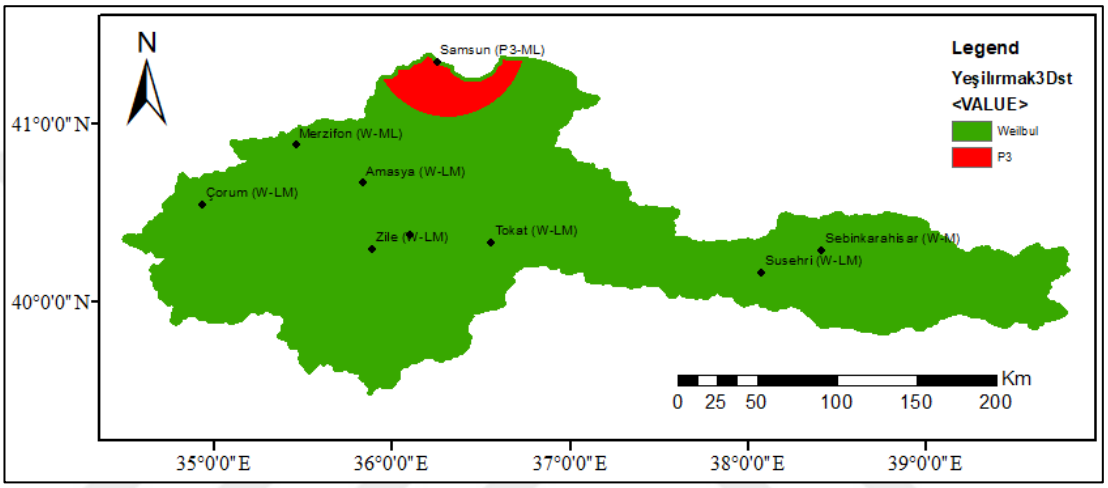


**Figure 4. 16.** SPI 3 spatial representation of the best-fit probability distribution for Yeşilırmak Basin

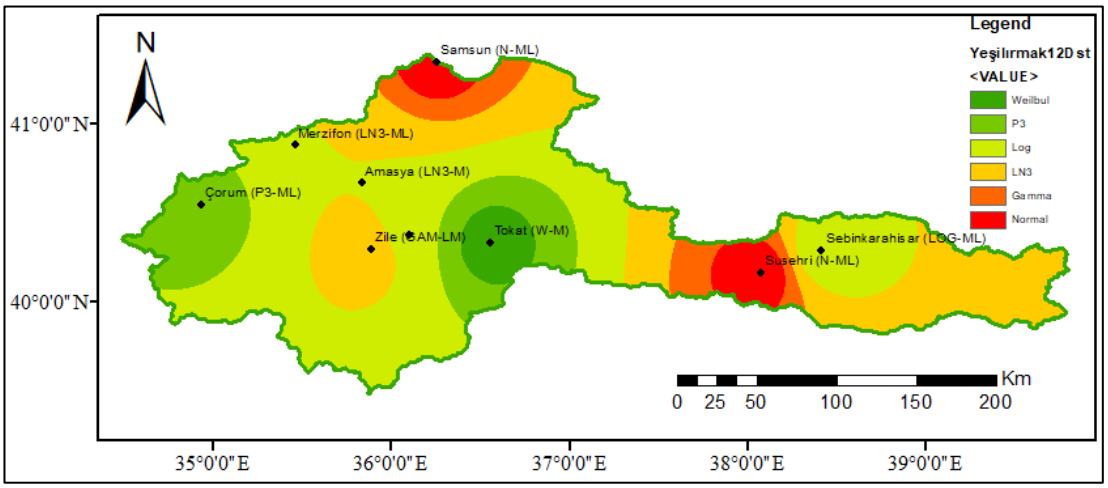


**Figure 4. 17.** SPI 12 spatial representation of the best-fit probability distribution for Yeşilırmak Basin

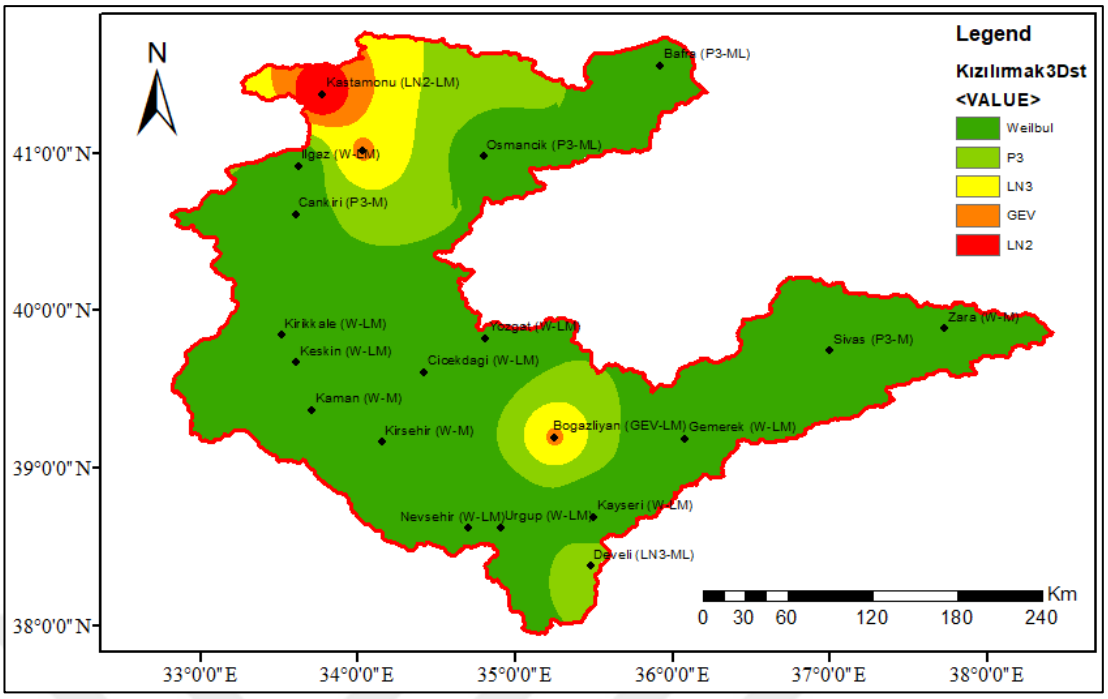


**Figure 4. 18.** SPI 3 spatial representation of the best-fit probability distribution for Kızılırmak Basin

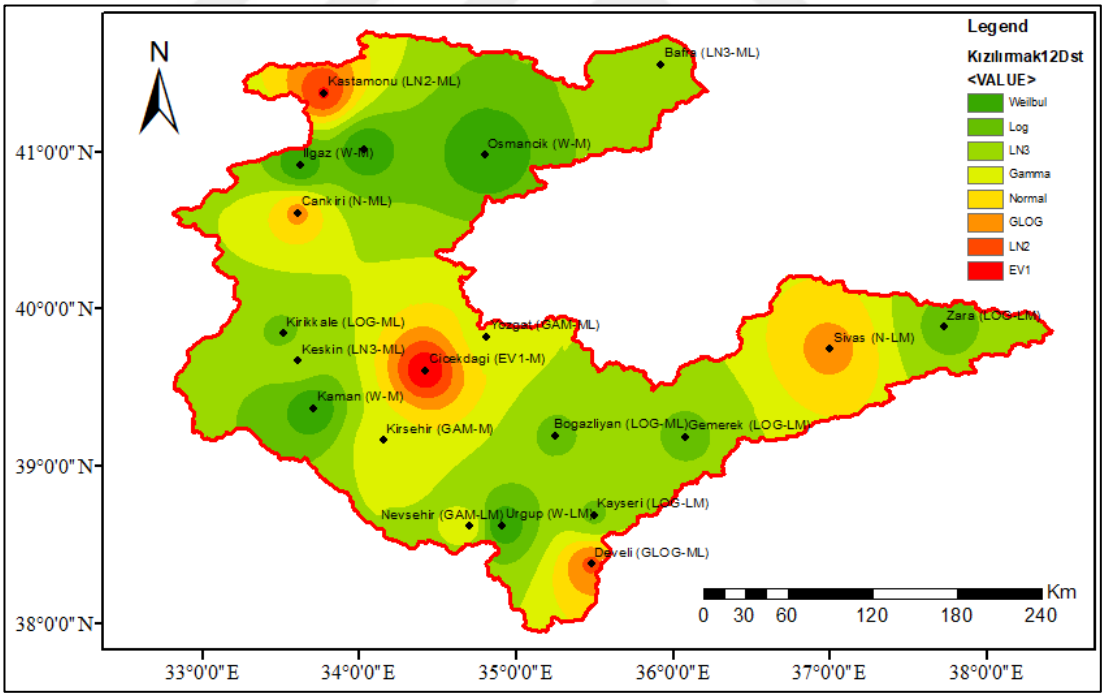


**Figure 4. 19.** SPI 12 spatial representation of the best-fit probability distribution for Kızılırmak Basin

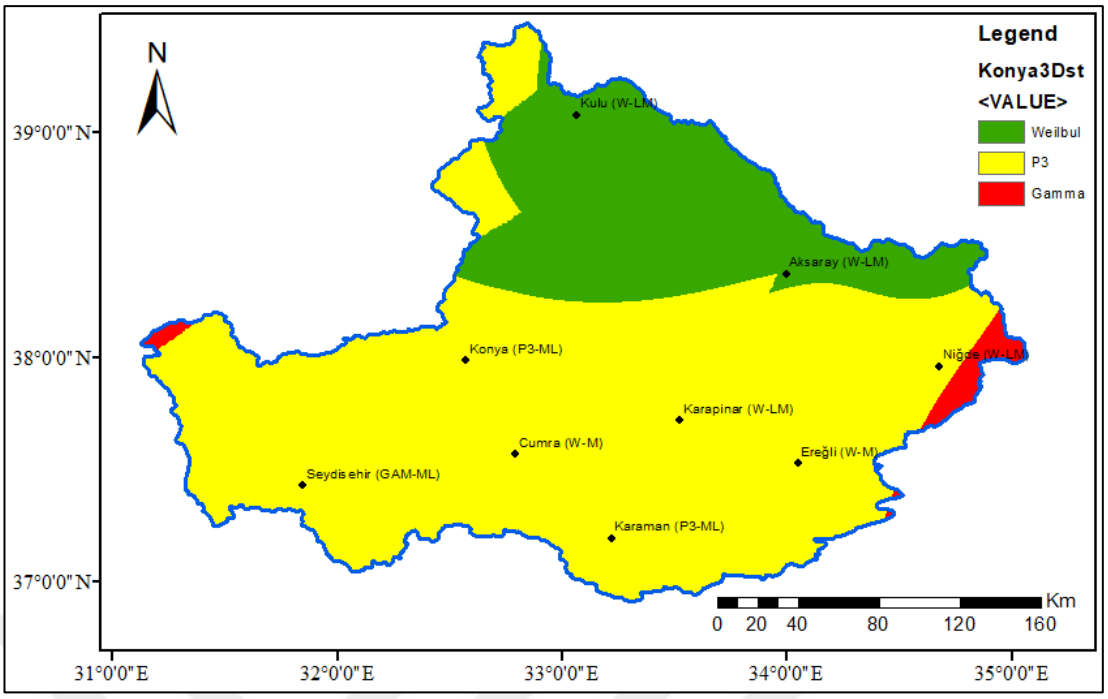


**Figure 4. 20.** SPI 3 spatial representation of the best-fit probability distribution for Konya Closed Basin

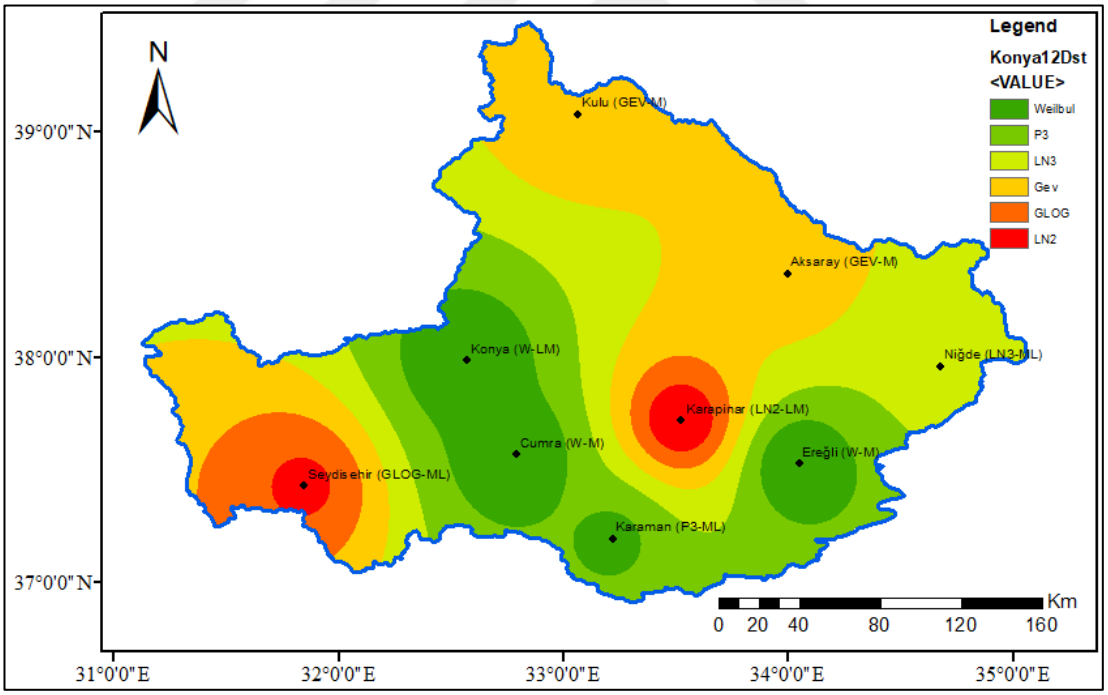


**Figure 4. 21.** SPI 12 spatial representation of the best-fit probability distribution for Konya Closed Basin

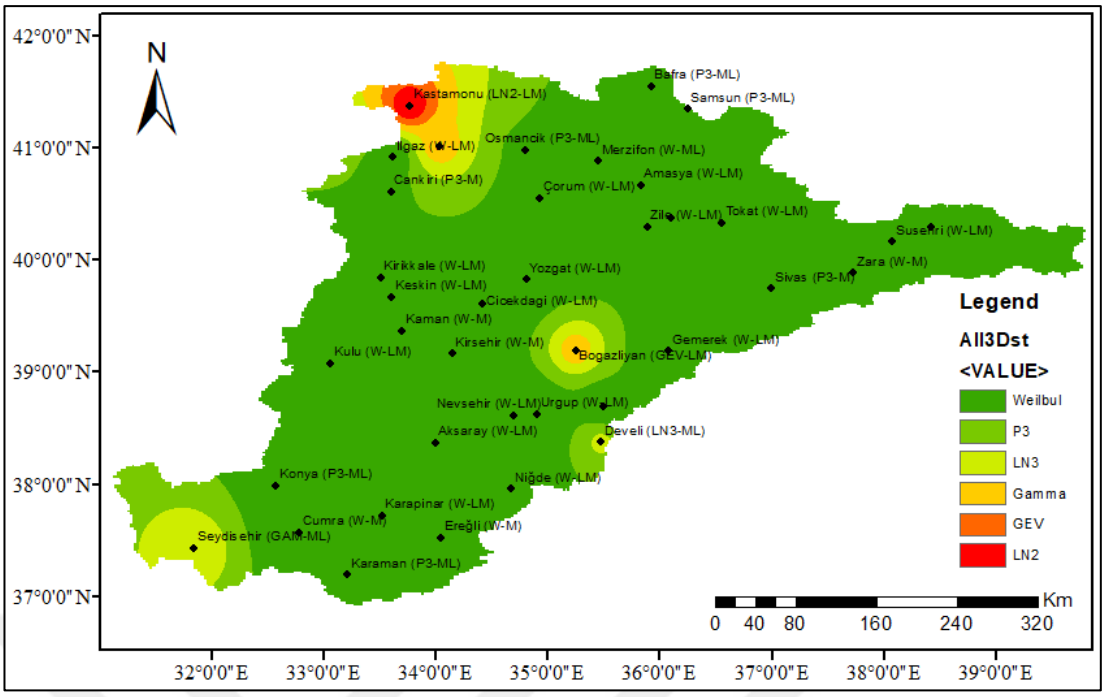


**Figure 4. 22.** Spatial representation of the best-fit probability distribution for SPI 3

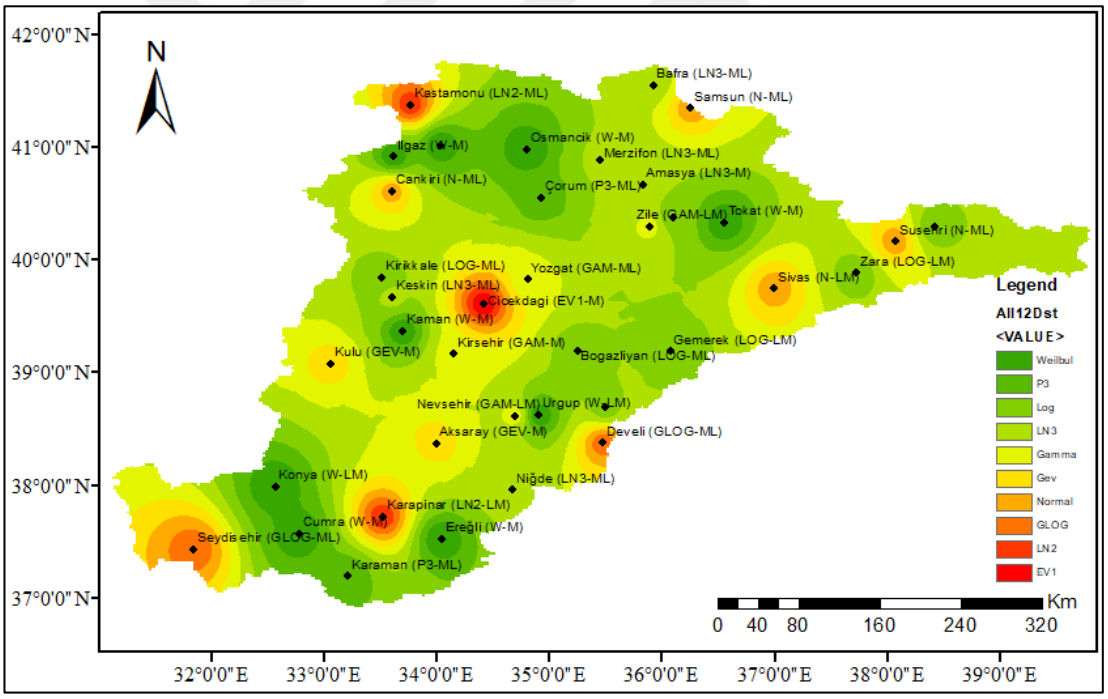


**Figure 4. 23.** Spatial representation of the best-fit probability distribution for SPI 12

Table 4.2 shows the percent areas of the best fit distributions in the study area for the SPI 3 and SPI 12 drought calculations.

**Table 4. 2.** Areal percentage of the best fit distributions for SPI

| Probability distribution | SPI 3 Area % (Amount of Station ) | SPI 12 Area % (Amount of Station) |
|---|---|---|
| Weibull | 68.42 (26) | 23.68 (9) |
| P-3 | 18.42 (7) | 5.26 (2) |
| Log | 0 (0) | 18.42 (7) |
| LN-3 | 2.63 (1) | 13.16 (5) |
| Gamma | 2.63 (1) | 10.53 (4) |
| GEV | 5.26 (2) | 5.26 (2) |
| Normal | 0 (0) | 10.53 (4) |
| GLOG | 0 (0) | 5.26 (2) |
| LN-2 | 2.63 (1) | 5.26 (2) |
| EV1 | 0 (0) | 2.63 (1) |

The Weibull distribution was the dominant distribution for SPI 3, dominating 68.42% (26 stations) of the entire study area. The P-3 distribution was the second most used distribution with sites of 18.42% (7 stations), and the GEV distribution was the third most used distribution with a 5.26% (2 stations). While GAM, LN-2, and LN-3 were the least used distributions with 2.63% (1 station), LOG, NORM, and EV-1 distributions were not found in any area as the most appropriate distribution. On the other hand, in the SPI 12 drought calculation, the best-fit distribution was the Weibull distribution with a rate of 23.68% (9 stations) in the study area, as in the SPI 3 calculation. The LOG distribution, which is not seen in the SPI 3 calculation, took the second place as the best-fit distribution with 18.42% (7 stations). This was followed by LN-3 distribution with 13.16% (5 stations), GAM and NORM with 10.53% (4 stations). P- 3, GEV, GLOG, and LN2 distributions were seen in sites of 5.26% (2 stations), and the least used distribution was EV1 with 2.63% (1 station). In the SPI3 and SPI12 drought calculations, although different distributions were brought out as the best distribution on an aerial basis, the Weibull distribution was determined to be the most appropriate distribution in common. Table 4.3 shows the numbers of the most successful parameter estimation approaches used in the best-fit distributions.

**Table 4. 3.** The numbers of the most successful parameter estimation approaches

| Methods | SPI 3 Amount of Station | SPI 12 Amount of Station |
|---|---|---|
| ML | 8 | 17 |
| M | 9 | 11 |
| LM | 21 | 10 |

As can be seen in the table, the LM (21 stations) has been identified as the most frequently used method for SPI 3, while the ML (8 stations) method is the least. For SPI 12, the ML (17 stations) has been identified as the most frequently used, while the LM (10 stations) method is the least. It can be stated that the most suitable method for SPI 3 is LM, while the most suitable method for SPI 12 is ML.

### 4.2. Reconnaissance Drought Index (RDI) Analysis

In this part of the study, the total precipitation and Potential Evapotranspiration $ET_0$ values of 37 meteorology stations between 1975 and 2020 were used to calculate the droughts for 3-months, 6 months, 9 months and 12 months based on the RDI method. Drought analysis results of the RDI for the selected Kastamonu station are given in Figure 4.24 to 4.27. Since the lack of temperature data was abundant in Bafra station, this station was not considered in RDI analysis.

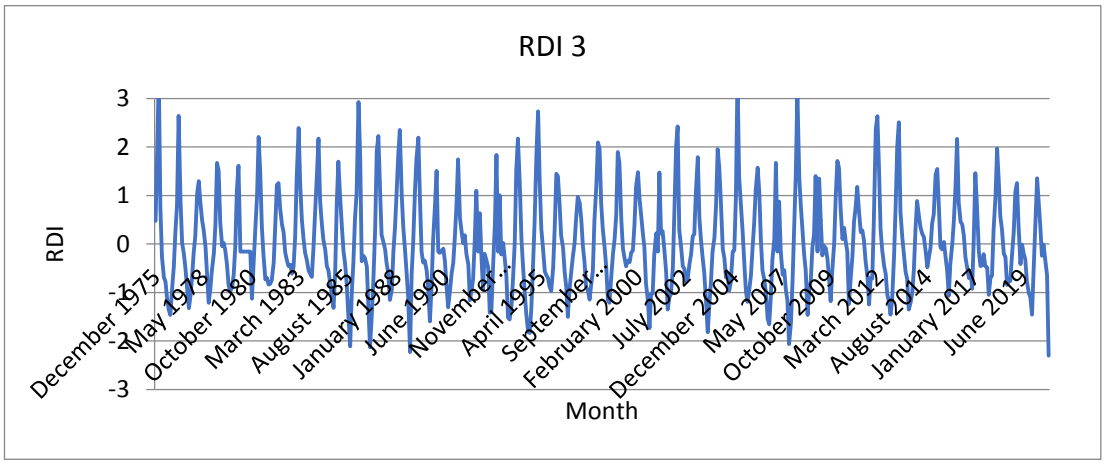


**Figure 4. 24.** Kastamonu station RDI3 result graph

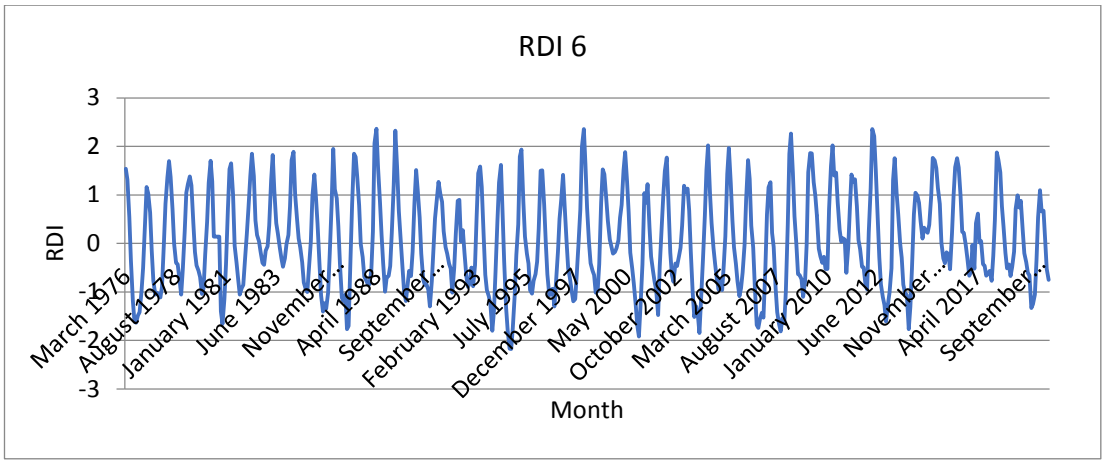


**Figure 4. 25.** Kastamonu station RDI6 result graph

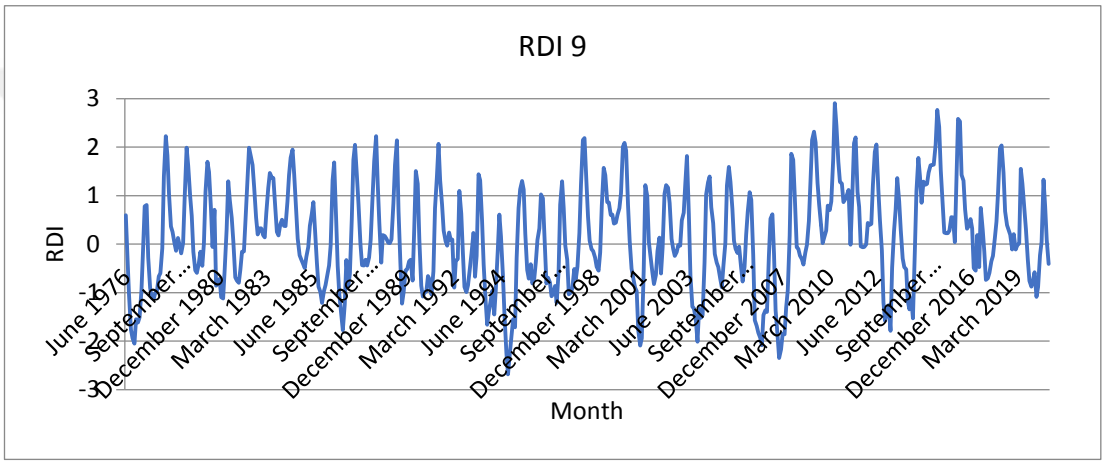


**Figure 4. 26.** Kastamonu station RDI9 result graph

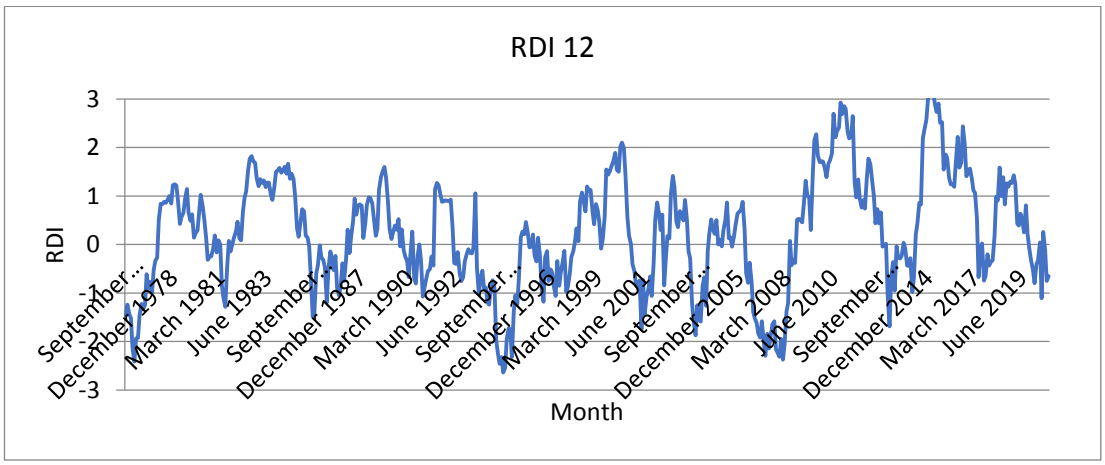


**Figure 4. 27.** Kastamonu station RDI12 result graph

The RDI results were evaluated and the histograms for each drought classes of the RDI results and spatial variations were mapped and given in comparison with SPI and SPEI best fit distributions in the next sections.

### 4.3. Standardized Precipitation and Evapotranspiration Index (SPEI)

#### 4.3.1. Standardized Precipitation and Evapotranspiration Index (SPEI) With GLOG Distribution Analysis

While performing the SPEI analysis, the precipitation and $ET_0$ values of the stations are used. Since the lack of temperature data was abundant in Karaman station, this station was not considered in SPEI analysis. SPEI is essentially a method based on the differences (D) calculated by subtracting potential evapotranspiration (PET) data from precipitation data. Serrano et al. (2010) assumed that D values fit the Log-Logistic distribution in their SPEI analysis. The Generalized Logistic distribution is equivalent to Log-logistic distribution (Rao and Hamed, 2000). Therefore, the analysis is carried out by Generalized Logistic distribution in this study. PET values were calculated by Thorntwaite method by using DRINC program. In this study, the total precipitation and monthly average $ET_0$ values of 37 meteorology stations between 1975 and 2020 were calculated for 3-months, 6 months, 9 months, 12 months and 24 months. Drought analysis results of the SPEI for the selected station based on the GLOG distribution are given in Figure 4.28 to 4.32.

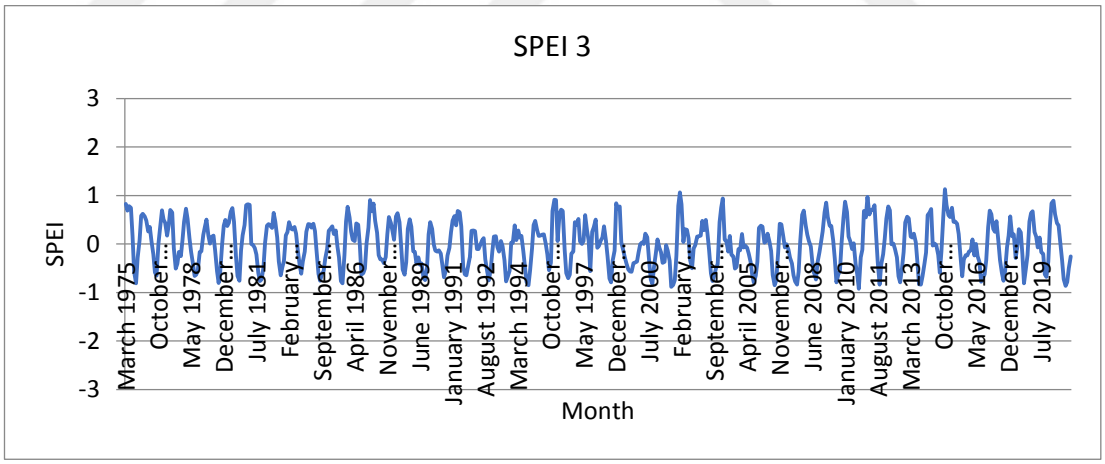


**Figure 4. 28.** Konya station SPEI3 result graph (GLOG distribution)

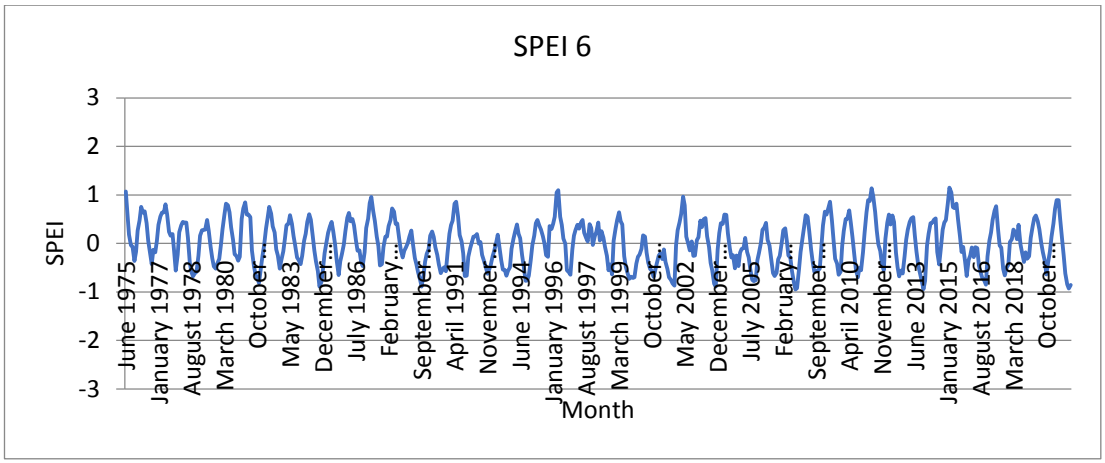


**Figure 4. 29.** Konya station SPEI6 result graph (GLOG distribution)

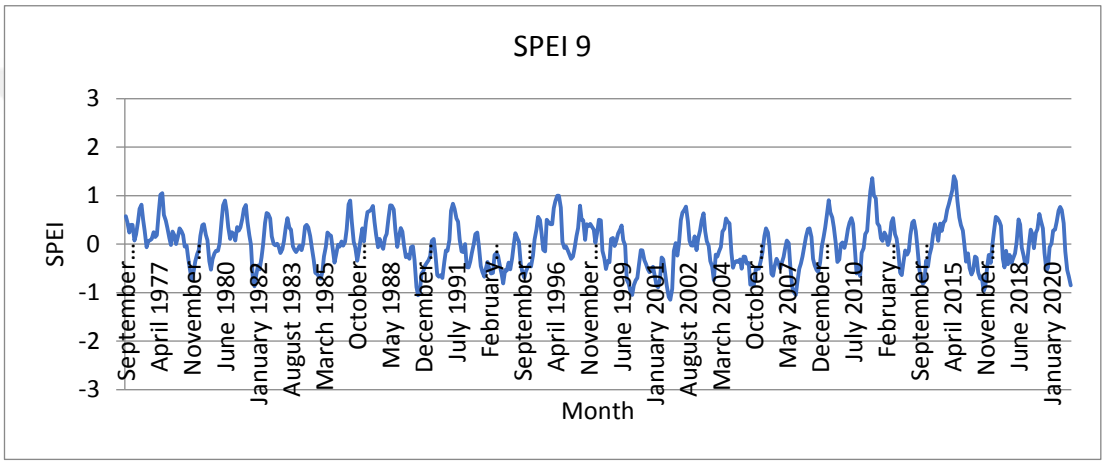


**Figure 4. 30.** Konya station SPEI9 result graph (GLOG distribution)

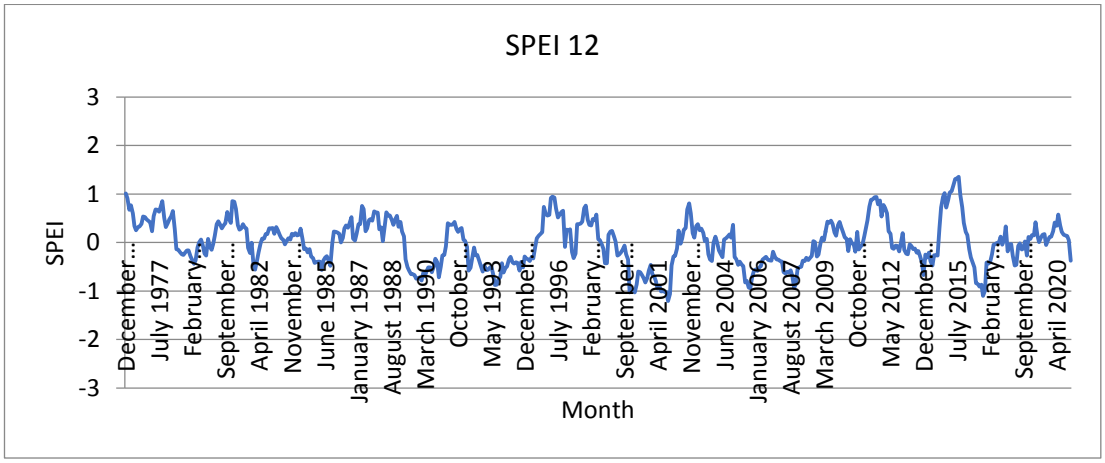


**Figure 4. 31.** Konya station SPEI12 result graph (GLOG distribution)

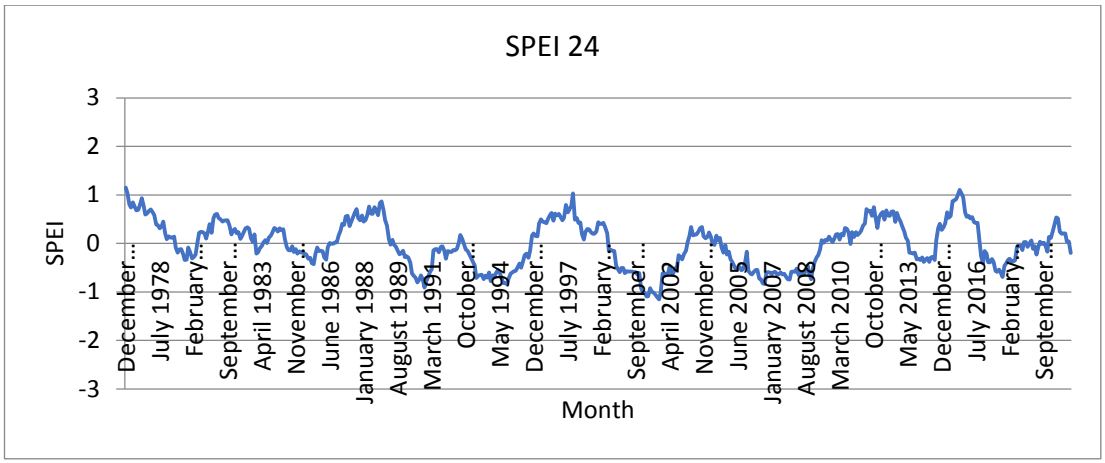


**Figure 4. 32.** Konya station SPEI24 result graph (GLOG disrtibution)

### 4.3.2. Standardized Precipitation and Evapotranspiration Index (SPEI) With Best-Fit Distribution Analysis

As observed in the previous analysis, when assessing the fit of the GLOG distribution for SPEI, no critical drought results were obtained for any station.

The best-fit distribution to describe SPEI was sought, which was conceptually similar to the SPI analysis that was previously conducted in this study. The program used to determine the best fit distribution in SPI analysis was also considered to determine the best-fit one for the difference between precipitation and potential evapotranspiration, D. Analysis were carried out for SPEI 3 and SPEI 12. The results of best fit distribution are given in Table 4.4

Some of the results of the SPEI calculated based on the best fit distribution are given in the following figures. The results for best fit distributions and parameter estimation method for each stations were given in Table 4.4 for SPEI 3-month and 12-month.

**Table 4. 4.** SPEI best fit distributions

| Station No | Station Name | 3 Month | 12 Month |
|---|---|---|---|
| 17030 | Samsun | GEV-LM | N-LM |
| 17083 | Merzifon | LN3-LM | LN3-M |
| 17084 | Çorum | GEV-LM | N-LM |
| 17085 | Amasya | W-M | LN3-LM |
| 17086 | Tokat | GEV-LM | N-M |
| 17681 | Zile | GEV-LM | LOG-ML |
| 17683 | Turhal | GEV-LM | LN3-M |
| 17684 | Suşehri | GEV-LM | GEV-LM |

| | | | |
|---|---|---|---|
| 17682 | Şebinkarahisar | GEV-LM | GEV-ML |
| 17074 | Kastamonu | GEV-M | GEV-ML |
| 17080 | Çankırı | GEV-LM | GAM-ML |
| 17090 | Sivas | GEV-LM | N-LM |
| 17135 | Kırıkkale | GEV-LM | GEV-LM |
| 17140 | Yozgat | GEV-LM | GEV-LM |
| 17160 | Kırşehir | GEV-LM | GEV-M |
| 17162 | Gemerek | GEV-LM | GAM-LM |
| 17193 | Nevşehir | GEV-LM | GEV-M |
| 17196 | Kayseri | GEV-LM | LOG-ML |
| 17622 | Bafra | GEV-M | LN3-ML |
| 17648 | Ilgaz | GEV-LM | GEV-LM |
| 17650 | Tosya | GEV-LM | GEV-LM |
| 17652 | Osmancık | GEV-LM | GEV-LM |
| 17716 | Zara | GEV-LM | LOG-LM |
| 17730 | Keskin | GEV-LM | GEV-M |
| 17732 | Çiçekdağı | GEV-LM | GAM-LM |
| 17756 | Kaman | GEV-LM | GEV-LM |
| 17760 | Boğazlıyan | GEV-LM | LOG-ML |
| 17835 | Ürgüp | GEV-LM | N-LM |
| 17836 | Develi | GEV-LM | GEV-LM |
| 17244 | Konya | GEV-LM | GEV-M |
| 17248 | Ereğli | GEV-LM | GEV-LM |
| 17250 | Niğde | GLOG-M | GEV-LM |
| 17754 | Kulu | GEV-LM | GEV-M |
| 17898 | Seydişehir | GEV-LM | LN3-M |
| 17900 | Çumra | GEV-LM | LOG-ML |
| 17902 | Karapınar | GEV-LM | GAM-ML |
| 17192 | Aksaray | GEV-LM | N-M |

Table 4.4 shows the best-fit distribution for SPEI 3 for Samsun station is found as Generalized Extreme Value distribution determined by L-Moments method. For SPI 12 the best-fit distribution is Normal distribution determined by L-Moments method as well. 33 stations determined by L-Moments, 4 stations determined by Methods of Moments for SPEI 3. For SPEI 12 analysis; 18 stations determined by L-Moments, 10 stations determined by Methods of Moments and 9 stations determined by Maximum Likelihood methods.

Drought analysis results of the SPEI for the selected Aksaray station based on the best- fit distributions are given in Figure 4.33 and Figure 4.34.

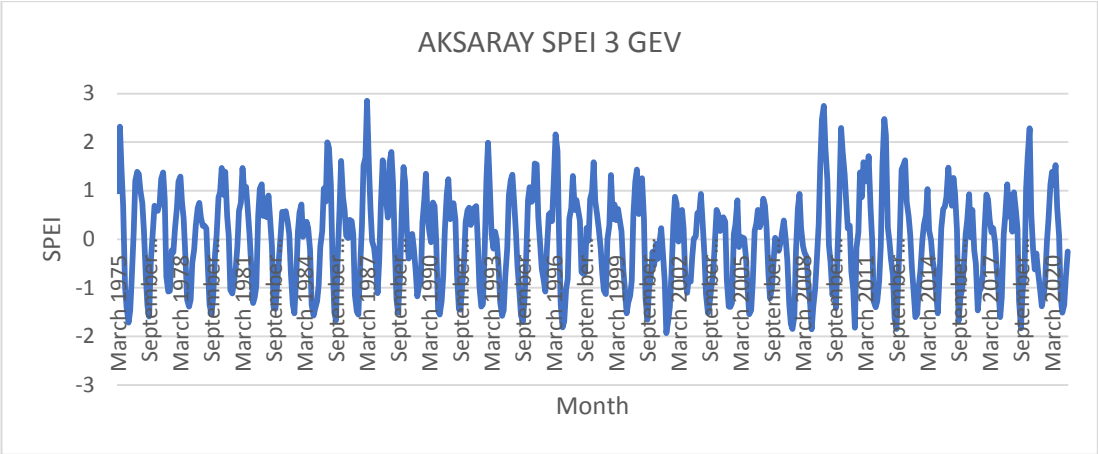


**Figure 4. 33.** Aksaray station SPEI3 result graph (Best-Fit distribution)

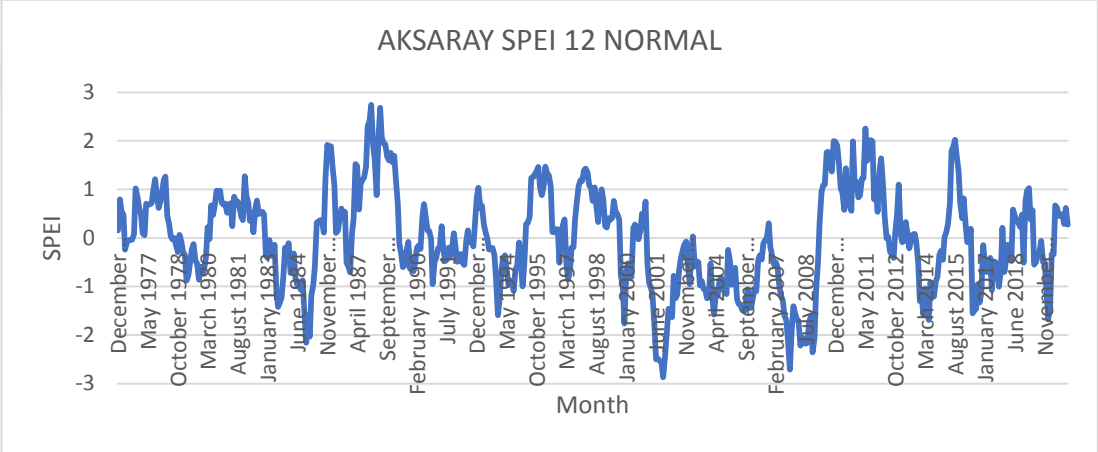


**Figure 4. 34.** Aksaray station SPEI12 result graph (Best-Fit distribution)

### 4.3.3. SPEI Comparison

The graphs (Figure 4.35, Figure 4.36, and Figure 4.37) presented below indicate the relationship between the observed value of SPEI drought calculation, the results obtained by the GLOG distribution, and the results obtained by the most appropriate distribution. Upon examining the graphs, it was determined that the calculation based on the GLOG distribution is significantly different from the observed value, while the most appropriate distribution is nearly identical to the observed value. Therefore, it is not correct to fit the D values to the GLOG distribution when performing the SPEI drought calculation. The correct approach is to identify the most appropriate distribution and perform the drought calculation accordingly.

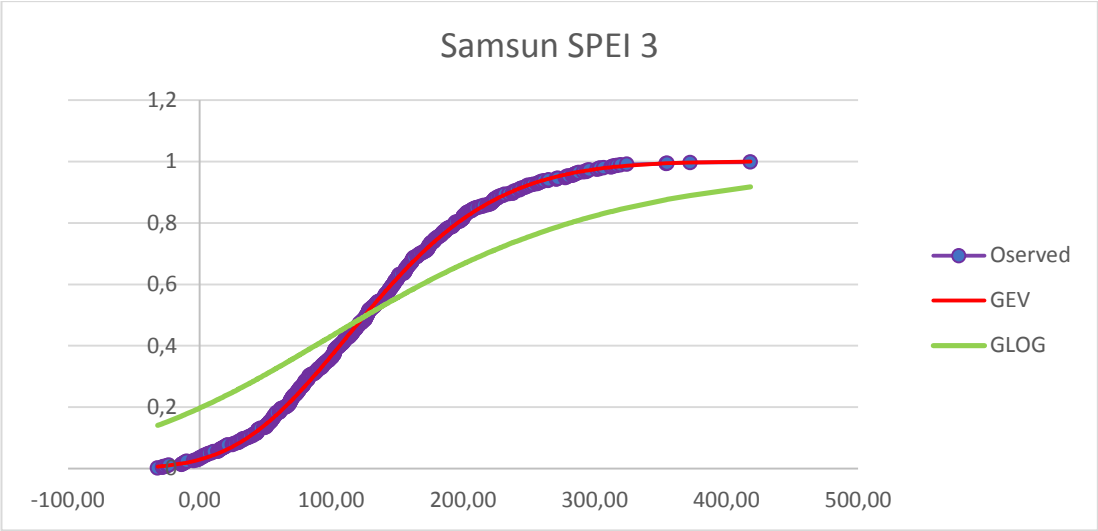


**Figure 4. 35.** Comparison of observed, GLOG distribution, and Best-Fit distribution for SPEI 3 at Samsun station.

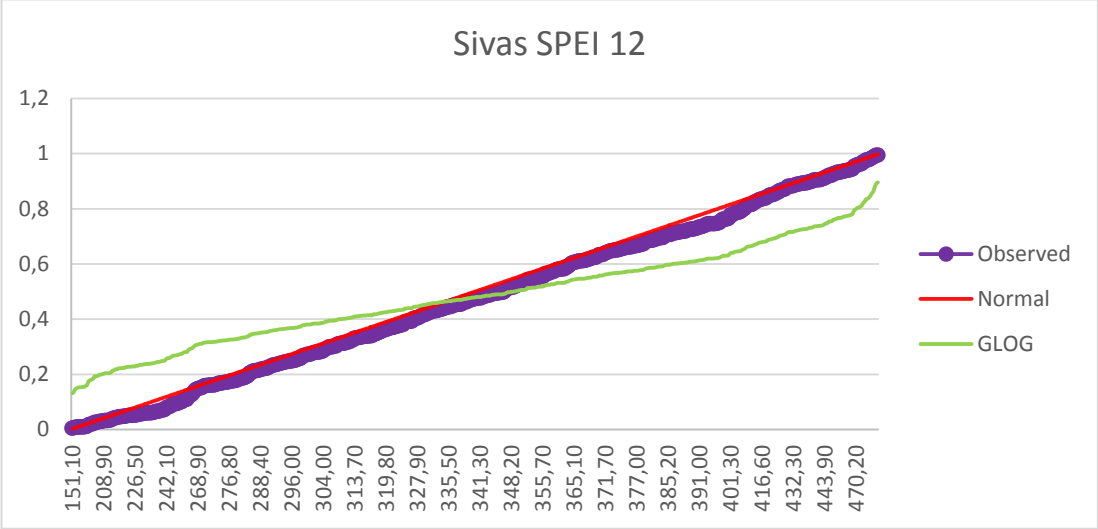


**Figure 4. 36.** Comparison of observed, GLOG distribution, and Best Fit distribution for SPEI 12 at Sivas station.

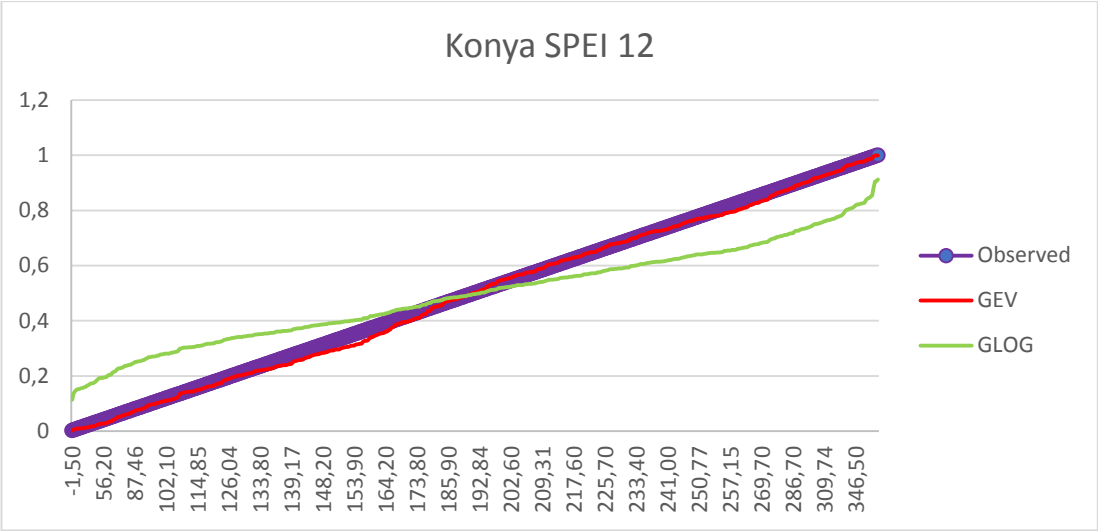


**Figure 4. 37.** Comparison of observed, GLOG distribution, and Best Fit distribution for SPEI 12 at Konya station.

The spatial variability of the best-fit probability distributions over the study area for 3-month and 12-month SPEI results is shown in Figure 4.38 and Figure 4.39.

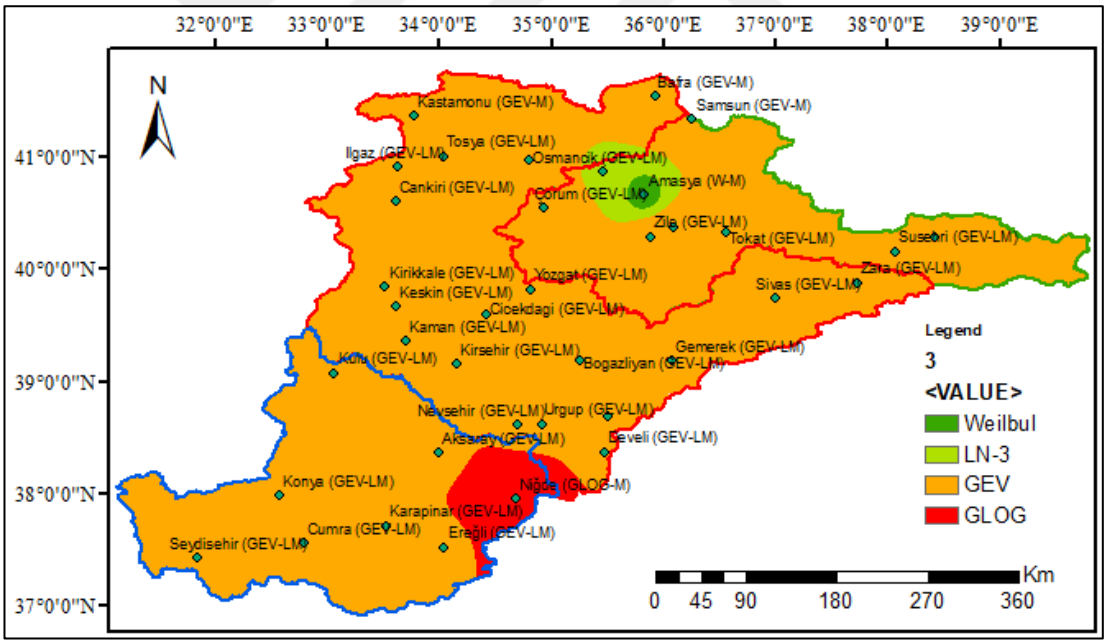


**Figure 4. 38.** Spatial representation of the best-fit probability distribution for SPEI 3

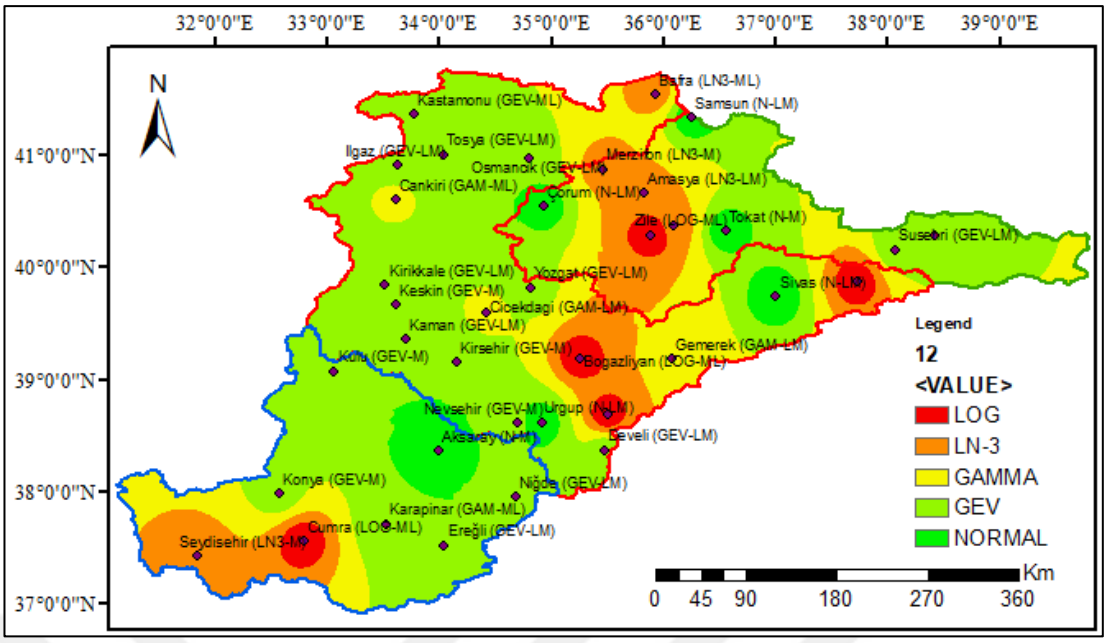


**Figure 4. 39.** Spatial representation of the best-fit probability distribution for SPEI12

Table 4.5 shows the percentiles of the best distributions in the study area for the SPEI 3 and SPEI 12 drought calculations.

**Table 4. 5.** Areal percentage of the best fit distributions for SPEI

| Probability distribution | SPEI 3 Area % (Amount of Station) | SPEI 12 Area % (Amount of Station) |
|---|---|---|
| Weibull | 2.7 (1) | 0 (0) |
| P-3 | 0 (0) | 0 (0) |
| Log | 0 (0) | 13.51 (5) |
| LN-3 | 2.7 (1) | 13.51 (5) |
| Gamma | 0 (0) | 8.11 (3) |
| GEV | 91.89 (34) | 46.65 (18) |
| Normal | 0 (0) | 16.22 (6) |
| Glog | 2.7 (1) | 0 (0) |
| LN-2 | 0 (0) | 0 (0) |
| EV1 | 0 (0) | 0 (0) |

For SPEI 3, the GEV distribution dominated 91.89% (34 stations) of the entire study area, making it the most common distribution. The Weibull, LN3, and GLOG distributions were the second most used distributions, each covering an area of 2.7% (1 station). On the other hand, for the SPEI 12 drought calculation, the GEV distribution was again the most dominant and best-fit distribution, involving 46.65% (18 stations) of the study area. The Normal distribution, which was not selected as

the best-fit distribution in the SPEI 3 calculation, ranked as the second-best distribution, covering an area of 16.22% (6 stations). This was followed by the LN-3 and Log distributions with 13.51% (5 stations) each, while GAM accounted for 8.11% (3 stations). Although different distributions were selected as the best distribution in the SPEI 3 and SPEI 12 drought calculations, the GEV distribution appeared to be the most appropriate distribution in common. Table 4.6 shows the numbers of the most successful parameter estimation approaches used in the best-fit distributions.

**Table 4. 6.** The the numbers of the most successful parameter estimation approaches

| Methods | SPEI 3 Amount of Station | SPEI 12 Amount of Station |
|---|---|---|
| ML | 0 | 9 |
| M | 4 | 10 |
| LM | 33 | 18 |

As can be seen in the table, the LM (33 stations) method has been identified as the most frequent method for SPEI 3, while the ML (0 stations) method was the least frequent. For SPEI 12, the LM (18 stations) method has been identified as the most frequent approach, while the ML (9 stations) method is the least frequent. It can be stated that the most suitable method for both SPEI 3 and SPEI 12 is LM.

### 4.4. Standardized Runoff Index (SRI) Analysis

The Standardized Runoff Index (SRI) drought analysis method is the calculated same as the SPI method. The only difference is that while precipitation data is used in SPI as input data, stream flow data is used in SRI calculation. In this study, the average flow data of 9 Flow Observation Stations (FOS) used for SRI analysis between the years 1975-2020 were determined as 3-month, 6-month, 9-month, 12-month, and 24-month sums. The best fit distribution method for each station was determined accordingly. The best-fit probability distribution models were validated with additional frequency plots. Drought analysis results of the SRI for the selected stations based on the best-fit distribution are given in Figure 4.40 and Figure 4.41. The best-fit distributions identified for SRI are presented in Table 4.7.

**Table 4. 7.** Best fit distributions for SRI

| St. No | St. Name | 1-Month | 3-Month | 6-Month | 9-Month | 12-Month | 24-Month |
|---|---|---|---|---|---|---|---|
| E15A001 | Kızılırmak Yamula | EV1-ML | LN2-ML | GAM-ML | W-ML | GLOG-ML | LOG-ML |
| E15A017 | Karanlık Deresi Şefaatli | GPAR-ML | LN3-ML | P3-ML | GPAR-ML | GAM-ML | LN2-ML |
| E15A039 | Kızılırmak Bulakbaşı | LN3-ML | LN3-ML | GPAR-ML | N-ML | GAM-ML | W-ML |
| E15A041 | Delice Çayı Çadırhöyük | LN2-ML | LN3-ML | LN3-ML | GAM-ML | GPAR-ML | GPAR-ML |
| E14A002 | Yeşilırmak Kale | LN3-ML | LN2-ML | GAM-ML | LOG-ML | GLOG-ML | LN2-ML |
| E14A012 | Çorum Çat Irmağı | GPAR-ML | GPAR-ML | LN3-ML | P3-ML | GAM-ML | GAM-ML |
| E14A014 | Yeşilırmak Sütlüce | LN2-ML | LN2-ML | GAM-ML | GAM-ML | LN2-ML | GAM-ML |
| E14A022 | Kelkit Çayı Çiçekbükü | LOG-ML | LN3-ML | GPAR-ML | N-ML | GLOG-ML | EV1-ML |
| E14A027 | Kelkit Çayı Yemişli Köprüsü | GAM-ML | GAM-ML | EV1-ML | N-ML | GLOG-ML | GLOG-ML |

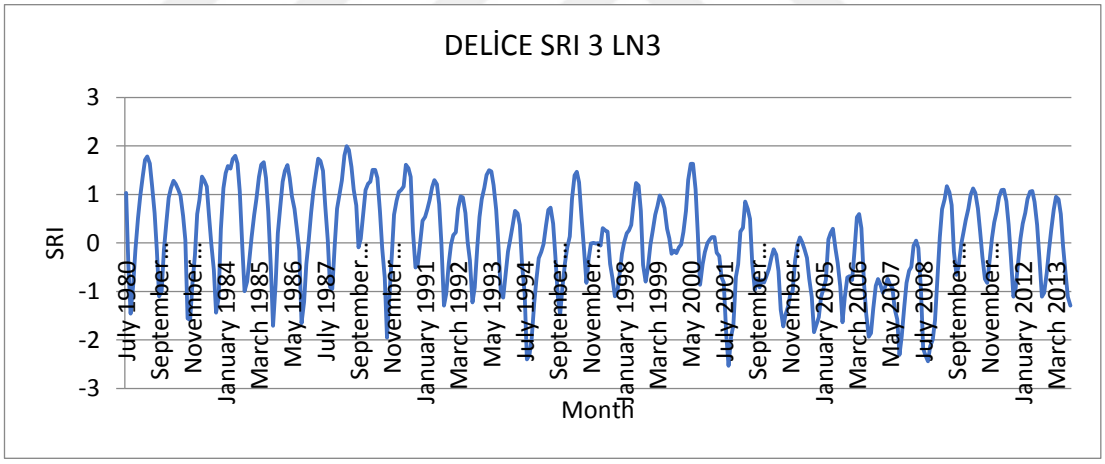


**Figure 4. 40.** Delice Çayı Çadırhöyük station SRI3 result graph

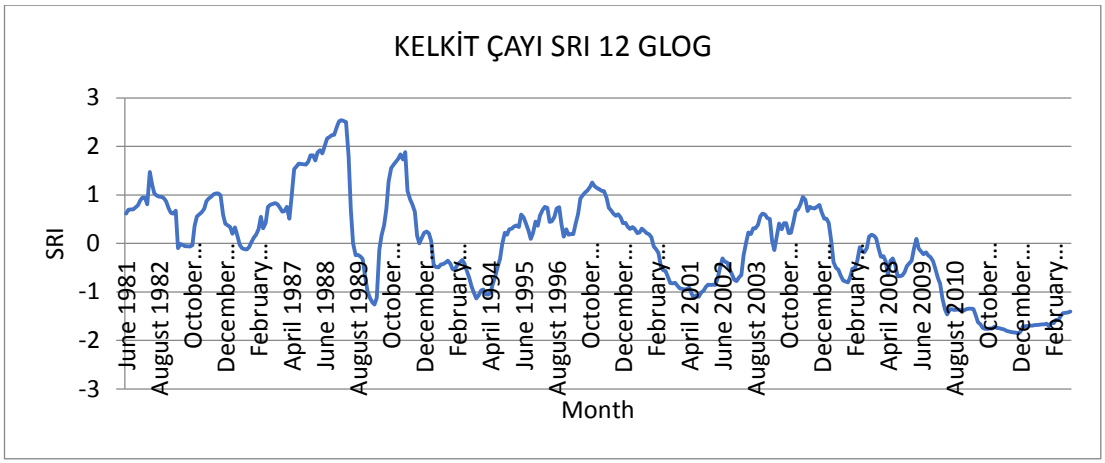


**Figure 4. 41.** Kelkit Çayı Yemişli Köprüsü station SRI12 result graph

### 4.5. Comparison of Drought indices results

Results of drought indices used in this study were assessed in this section. First the correlation matrices were conducted. Secondly histogram of drought results for each station and for each drought classes were evaluated. Drought histograms for some of selected stations were given and the rest of stations were given in appendices. Thirdly spatial variations of results for each drought indices were assessed by mapping the drought results for each station for the study area. Spatial variation of Extreme Wet (W3), Moderate Drought (D1), Drought (D2) and Extreme Drought (D3) drought classes were mapped. Comparisons of areal development for drought for each drought classes were given.

Correlations (Pearson) were calculated among the results of SPI Gamma distribution (SPI G), SPI Best Fit distribution (SPI bf), SPEI GLOG distribution (SPEI G), SPEI Best Fit distribution (SPEI bf), and RDI drought methods for each station to understand the relationship between them. Some of the selected stations correlations are shown in the Tables 4.8-4.11 below. The areas highlighted in dark red in the tables indicate the highest correlation, while the areas highlighted in dark blue indicate the lowest correlation.

**Table 4. 8.** Samsun station drought analysis correlation

| | SPI 1 G | SPI 3 G | SPI 6 G | SPI 9 G | SPI 12 G | SPI 24 G | SPI 1 bf | SPI 3 bf | SPI 6 bf | SPI 9 bf | SPI 12 bf | SPI 24 bf |
|---|---|---|---|---|---|---|---|---|---|---|---|---|
| **SPI 1 G** | 1.000 | 0.595 | 0.369 | 0.250 | 0.241 | 0.180 | 0.993 | 0.594 | 0.366 | 0.249 | 0.241 | 0.180 |
| **SPI 3 G** | 0.595 | 1.000 | 0.675 | 0.486 | 0.413 | 0.311 | 0.599 | 1.000 | 0.670 | 0.483 | 0.411 | 0.311 |
| **SPI 6 G** | 0.369 | 0.675 | 1.000 | 0.744 | 0.581 | 0.455 | 0.369 | 0.675 | 0.999 | 0.742 | 0.579 | 0.454 |
| **SPI 9 G** | 0.250 | 0.486 | 0.744 | 1.000 | 0.772 | 0.572 | 0.251 | 0.486 | 0.742 | 0.999 | 0.770 | 0.572 |
| **SPI 12 G** | 0.241 | 0.413 | 0.581 | 0.772 | 1.000 | 0.701 | 0.249 | 0.414 | 0.582 | 0.772 | 0.998 | 0.701 |
| **SPI 24 G** | 0.180 | 0.311 | 0.455 | 0.572 | 0.701 | 1.000 | 0.188 | 0.313 | 0.458 | 0.575 | 0.704 | 1.000 |
| **SPI 1 bf** | 0.993 | 0.599 | 0.369 | 0.251 | 0.249 | 0.188 | 1.000 | 0.598 | 0.367 | 0.250 | 0.249 | 0.188 |
| **SPI 3 bf** | 0.594 | 1.000 | 0.675 | 0.486 | 0.414 | 0.313 | 0.598 | 1.000 | 0.670 | 0.483 | 0.413 | 0.313 |
| **SPI 6 bf** | 0.366 | 0.670 | 0.999 | 0.742 | 0.582 | 0.458 | 0.367 | 0.670 | 1.000 | 0.741 | 0.581 | 0.457 |
| **SPI 9 bf** | 0.249 | 0.483 | 0.742 | 0.999 | 0.772 | 0.575 | 0.250 | 0.483 | 0.741 | 1.000 | 0.771 | 0.574 |
| **SPI 12 bf** | 0.241 | 0.411 | 0.579 | 0.770 | 0.998 | 0.704 | 0.249 | 0.413 | 0.581 | 0.771 | 1.000 | 0.703 |
| **SPI 24 bf** | 0.180 | 0.311 | 0.454 | 0.572 | 0.701 | 1.000 | 0.188 | 0.313 | 0.457 | 0.574 | 0.703 | 1.000 |
| **SPEI 3 G** | 0.568 | 0.979 | 0.709 | 0.490 | 0.375 | 0.285 | 0.569 | 0.979 | 0.705 | 0.487 | 0.373 | 0.285 |
| **SPEI 6 G** | 0.304 | 0.610 | 0.974 | 0.735 | 0.520 | 0.404 | 0.300 | 0.609 | 0.974 | 0.734 | 0.519 | 0.404 |
| **SPEI 9 G** | 0.190 | 0.414 | 0.701 | 0.983 | 0.731 | 0.536 | 0.191 | 0.413 | 0.700 | 0.985 | 0.731 | 0.535 |
| **SPEI 12 G** | 0.242 | 0.413 | 0.577 | 0.764 | 0.994 | 0.689 | 0.250 | 0.415 | 0.579 | 0.766 | 0.996 | 0.688 |
| **SPEI 24 G** | 0.181 | 0.317 | 0.459 | 0.573 | 0.700 | 0.994 | 0.190 | 0.319 | 0.462 | 0.576 | 0.703 | 0.993 |
| **SPEI 3 bf** | 0.568 | 0.980 | 0.708 | 0.488 | 0.372 | 0.282 | 0.569 | 0.980 | 0.703 | 0.486 | 0.369 | 0.282 |
| **SPEI 12 bf** | 0.242 | 0.414 | 0.577 | 0.765 | 0.995 | 0.688 | 0.250 | 0.415 | 0.579 | 0.766 | 0.996 | 0.687 |
| **RDI 3** | 0.402 | 0.713 | 0.653 | 0.364 | 0.187 | 0.130 | 0.388 | 0.709 | 0.648 | 0.360 | 0.181 | 0.131 |
| **RDI 6** | 0.125 | 0.329 | 0.693 | 0.525 | 0.236 | 0.175 | 0.109 | 0.324 | 0.689 | 0.525 | 0.234 | 0.175 |
| **RDI 9** | -0.011 | 0.139 | 0.448 | 0.739 | 0.429 | 0.299 | -0.016 | 0.136 | 0.443 | 0.740 | 0.427 | 0.299 |
| **RDI 12** | 0.231 | 0.403 | 0.550 | 0.725 | 0.954 | 0.625 | 0.240 | 0.403 | 0.549 | 0.723 | 0.945 | 0.625 |

There is a continuation of this table on the next page.

| SPEI 3 G | SPEI 6 G | SPEI 9 G | SPEI 12 G | SPEI 24 G | SPEI 3 bf | SPEI 12 bf | RDI 3 | RDI 6 | RDI 9 | RDI 12 | |
|---|---|---|---|---|---|---|---|---|---|---|---|
| 0.568 | 0.304 | 0.190 | 0.242 | 0.181 | 0.568 | 0.242 | 0.402 | 0.125 | -0.011 | 0.231 | **SPI 1 G** |
| 0.979 | 0.610 | 0.414 | 0.413 | 0.317 | 0.980 | 0.414 | 0.713 | 0.329 | 0.139 | 0.403 | **SPI 3 G** |
| 0.709 | 0.974 | 0.701 | 0.577 | 0.459 | 0.708 | 0.577 | 0.653 | 0.693 | 0.448 | 0.550 | **SPI 6 G** |
| 0.490 | 0.735 | 0.983 | 0.764 | 0.573 | 0.488 | 0.765 | 0.364 | 0.525 | 0.739 | 0.725 | **SPI 9 G** |
| 0.375 | 0.520 | 0.731 | 0.994 | 0.700 | 0.372 | 0.995 | 0.187 | 0.236 | 0.429 | 0.954 | **SPI 12 G** |
| 0.285 | 0.404 | 0.536 | 0.689 | 0.994 | 0.282 | 0.688 | 0.130 | 0.175 | 0.299 | 0.625 | **SPI 24 G** |
| 0.569 | 0.300 | 0.191 | 0.250 | 0.190 | 0.569 | 0.250 | 0.388 | 0.109 | -0.016 | 0.240 | **SPI 1 bf** |
| 0.979 | 0.609 | 0.413 | 0.415 | 0.319 | 0.980 | 0.415 | 0.709 | 0.324 | 0.136 | 0.403 | **SPI 3 bf** |
| 0.705 | 0.974 | 0.700 | 0.579 | 0.462 | 0.703 | 0.579 | 0.648 | 0.689 | 0.443 | 0.549 | **SPI 6 bf** |
| 0.487 | 0.734 | 0.985 | 0.766 | 0.576 | 0.486 | 0.766 | 0.360 | 0.525 | 0.740 | 0.723 | **SPI 9 bf** |
| 0.373 | 0.519 | 0.731 | 0.996 | 0.703 | 0.369 | 0.996 | 0.181 | 0.234 | 0.427 | 0.945 | **SPI 12 bf** |
| 0.285 | 0.404 | 0.535 | 0.688 | 0.993 | 0.282 | 0.687 | 0.131 | 0.175 | 0.299 | 0.625 | **SPI 24 bf** |
| 1.000 | 0.674 | 0.423 | 0.377 | 0.293 | 0.999 | 0.377 | 0.819 | 0.450 | 0.171 | 0.373 | **SPEI 3 G** |
| 0.674 | 1.000 | 0.724 | 0.521 | 0.412 | 0.673 | 0.521 | 0.698 | 0.827 | 0.563 | 0.504 | **SPEI 6 G** |
| 0.423 | 0.724 | 1.000 | 0.732 | 0.544 | 0.423 | 0.732 | 0.314 | 0.576 | 0.837 | 0.703 | **SPEI 9 G** |
| 0.377 | 0.521 | 0.732 | 1.000 | 0.697 | 0.374 | 1.000 | 0.186 | 0.239 | 0.436 | 0.966 | **SPEI 12 G** |
| 0.293 | 0.412 | 0.544 | 0.697 | 1.000 | 0.290 | 0.695 | 0.138 | 0.183 | 0.313 | 0.652 | **SPEI 24 G** |
| 0.999 | 0.673 | 0.423 | 0.374 | 0.290 | 1.000 | 0.374 | 0.821 | 0.453 | 0.174 | 0.371 | **SPEI 3 bf** |
| 0.377 | 0.521 | 0.732 | 1.000 | 0.695 | 0.374 | 1.000 | 0.188 | 0.240 | 0.436 | 0.968 | **SPEI 12 bf** |
| 0.819 | 0.698 | 0.314 | 0.186 | 0.138 | 0.821 | 0.188 | 1.000 | 0.705 | 0.163 | 0.204 | **RDI 3** |
| 0.450 | 0.827 | 0.576 | 0.239 | 0.183 | 0.453 | 0.240 | 0.705 | 1.000 | 0.677 | 0.249 | **RDI 6** |
| 0.171 | 0.563 | 0.837 | 0.436 | 0.313 | 0.174 | 0.436 | 0.163 | 0.677 | 1.000 | 0.443 | **RDI 9** |
| 0.373 | 0.504 | 0.703 | 0.966 | 0.652 | 0.371 | 0.968 | 0.204 | 0.249 | 0.443 | 1.000 | **RDI 12** |

As can be seen in the correlation in Table 4.8 for Samsun station, a very high correlation was detected among SPEI 3 G-SPI 3 G (0.979), SPEI 6 G-SPI 6 G (0.974), SPEI 9 G-SPI 9 G (0.983), SPEI 12 G-SPI 12 G (0.994), SPEI 24 G-SPI 24 G (0.994), RDI 12-SPI 12 G (0.954), RDI 12-

SPEI 12 G (0.966), and RDI 12-SPEI 12 bf (0.968), while the lowest correlation is observed between RDI 9-SPI 1 G (0.011) and RDI 9-SPI 1 bf (0.016).

**Table 4. 9.** Kayseri station drought analysis correlation

| | SPI 1 G | SPI 3 G | SPI 6 G | SPI 9 G | SPI 12 G | SPI 24 G | SPI 1 bf | SPI 3 bf | SPI 6 bf | SPI 9 bf | SPI 12 bf | SPI 24 bf |
|---|---|---|---|---|---|---|---|---|---|---|---|---|
| **SPI 1 G** | 1.000 | 0.613 | 0.265 | 0.141 | 0.197 | 0.123 | 0.977 | 0.608 | 0.267 | 0.141 | 0.191 | 0.128 |
| **SPI 3 G** | 0.613 | 1.000 | 0.603 | 0.412 | 0.349 | 0.225 | 0.626 | 0.981 | 0.607 | 0.414 | 0.339 | 0.227 |
| **SPI 6 G** | 0.265 | 0.603 | 1.000 | 0.742 | 0.582 | 0.384 | 0.309 | 0.644 | 0.998 | 0.743 | 0.576 | 0.380 |
| **SPI 9 G** | 0.141 | 0.412 | 0.742 | 1.000 | 0.796 | 0.541 | 0.188 | 0.464 | 0.750 | 1.000 | 0.792 | 0.537 |
| **SPI 12 G** | 0.197 | 0.349 | 0.582 | 0.796 | 1.000 | 0.709 | 0.229 | 0.383 | 0.590 | 0.797 | 0.995 | 0.708 |
| **SPI 24 G** | 0.123 | 0.225 | 0.384 | 0.541 | 0.709 | 1.000 | 0.152 | 0.254 | 0.393 | 0.545 | 0.714 | 0.996 |
| **SPI 1 bf** | 0.977 | 0.626 | 0.309 | 0.188 | 0.229 | 0.152 | 1.000 | 0.634 | 0.313 | 0.188 | 0.225 | 0.156 |
| **SPI 3 bf** | 0.608 | 0.981 | 0.644 | 0.464 | 0.383 | 0.254 | 0.634 | 1.000 | 0.652 | 0.467 | 0.378 | 0.252 |
| **SPI 6 bf** | 0.267 | 0.607 | 0.998 | 0.750 | 0.590 | 0.393 | 0.313 | 0.652 | 1.000 | 0.752 | 0.585 | 0.388 |
| **SPI 9 bf** | 0.141 | 0.414 | 0.743 | 1.000 | 0.797 | 0.545 | 0.188 | 0.467 | 0.752 | 1.000 | 0.795 | 0.540 |
| **SPI 12 bf** | 0.191 | 0.339 | 0.576 | 0.792 | 0.995 | 0.714 | 0.225 | 0.378 | 0.585 | 0.795 | 1.000 | 0.709 |
| **SPI 24 bf** | 0.128 | 0.227 | 0.380 | 0.537 | 0.708 | 0.996 | 0.156 | 0.252 | 0.388 | 0.540 | 0.709 | 1.000 |
| **SPEI 3 G** | 0.655 | 0.937 | 0.527 | 0.313 | 0.334 | 0.224 | 0.670 | 0.955 | 0.534 | 0.316 | 0.329 | 0.224 |
| **SPEI 6 G** | 0.365 | 0.706 | 0.939 | 0.602 | 0.494 | 0.330 | 0.401 | 0.739 | 0.944 | 0.605 | 0.488 | 0.326 |
| **SPEI 9 G** | 0.152 | 0.482 | 0.820 | 0.966 | 0.731 | 0.494 | 0.200 | 0.532 | 0.827 | 0.967 | 0.727 | 0.490 |
| **SPEI 12 G** | 0.194 | 0.342 | 0.574 | 0.788 | 0.993 | 0.703 | 0.226 | 0.377 | 0.582 | 0.790 | 0.991 | 0.701 |
| **SPEI 24 G** | 0.123 | 0.221 | 0.375 | 0.529 | 0.698 | 0.989 | 0.151 | 0.249 | 0.383 | 0.532 | 0.701 | 0.990 |
| **SPEI 3 bf** | 0.652 | 0.935 | 0.531 | 0.328 | 0.348 | 0.235 | 0.670 | 0.957 | 0.540 | 0.331 | 0.343 | 0.234 |
| **SPEI 12 bf** | 0.191 | 0.337 | 0.569 | 0.785 | 0.989 | 0.705 | 0.224 | 0.374 | 0.578 | 0.787 | 0.993 | 0.700 |
| **RDI 3** | 0.508 | 0.627 | 0.152 | -0.094 | 0.131 | 0.093 | 0.482 | 0.570 | 0.148 | -0.092 | 0.122 | 0.099 |
| **RDI 6** | 0.423 | 0.626 | 0.673 | 0.220 | 0.243 | 0.167 | 0.436 | 0.628 | 0.666 | 0.220 | 0.235 | 0.170 |
| **RDI 9** | 0.210 | 0.551 | 0.811 | 0.765 | 0.483 | 0.330 | 0.255 | 0.595 | 0.816 | 0.764 | 0.476 | 0.328 |
| **RDI 12** | 0.188 | 0.334 | 0.559 | 0.767 | 0.970 | 0.699 | 0.220 | 0.367 | 0.566 | 0.768 | 0.963 | 0.698 |

There is a continuation of this table on the next page.

| SPEI 3 G | SPEI 6 G | SPEI 9 G | SPEI 12 G | SPEI 24 G | SPEI 3 bf | SPEI 12 bf | RDI 3 | RDI 6 | RDI 9 | RDI 12 | |
|---|---|---|---|---|---|---|---|---|---|---|---|
| 0.655 | 0.365 | 0.152 | 0.194 | 0.123 | 0.652 | 0.191 | 0.508 | 0.423 | 0.210 | 0.188 | **SPI 1 G** |
| 0.937 | 0.706 | 0.482 | 0.342 | 0.221 | 0.935 | 0.337 | 0.627 | 0.626 | 0.551 | 0.334 | **SPI 3 G** |
| 0.527 | 0.939 | 0.820 | 0.574 | 0.375 | 0.531 | 0.569 | 0.152 | 0.673 | 0.811 | 0.559 | **SPI 6 G** |
| 0.313 | 0.602 | 0.966 | 0.788 | 0.529 | 0.328 | 0.785 | -0.094 | 0.220 | 0.765 | 0.767 | **SPI 9 G** |
| 0.334 | 0.494 | 0.731 | 0.993 | 0.698 | 0.348 | 0.989 | 0.131 | 0.243 | 0.483 | 0.970 | **SPI 12 G** |
| 0.224 | 0.330 | 0.494 | 0.703 | 0.989 | 0.235 | 0.705 | 0.093 | 0.167 | 0.330 | 0.699 | **SPI 24 G** |
| 0.670 | 0.401 | 0.200 | 0.226 | 0.151 | 0.670 | 0.224 | 0.482 | 0.436 | 0.255 | 0.220 | **SPI 1 bf** |
| 0.955 | 0.739 | 0.532 | 0.377 | 0.249 | 0.957 | 0.374 | 0.570 | 0.628 | 0.595 | 0.367 | **SPI 3 bf** |
| 0.534 | 0.944 | 0.827 | 0.582 | 0.383 | 0.540 | 0.578 | 0.148 | 0.666 | 0.816 | 0.566 | **SPI 6 bf** |
| 0.316 | 0.605 | 0.967 | 0.790 | 0.532 | 0.331 | 0.787 | -0.092 | 0.220 | 0.764 | 0.768 | **SPI 9 bf** |
| 0.329 | 0.488 | 0.727 | 0.991 | 0.701 | 0.343 | 0.993 | 0.122 | 0.235 | 0.476 | 0.963 | **SPI 12 bf** |
| 0.224 | 0.326 | 0.490 | 0.701 | 0.990 | 0.234 | 0.700 | 0.099 | 0.170 | 0.328 | 0.698 | **SPI 24 bf** |
| 1.000 | 0.685 | 0.380 | 0.333 | 0.225 | 0.997 | 0.330 | 0.737 | 0.688 | 0.462 | 0.328 | **SPEI 3 G** |
| 0.685 | 1.000 | 0.732 | 0.492 | 0.328 | 0.686 | 0.488 | 0.364 | 0.849 | 0.823 | 0.482 | **SPEI 6 G** |
| 0.380 | 0.732 | 1.000 | 0.733 | 0.493 | 0.393 | 0.730 | -0.050 | 0.385 | 0.888 | 0.716 | **SPEI 9 G** |
| 0.333 | 0.492 | 0.733 | 1.000 | 0.705 | 0.346 | 0.998 | 0.132 | 0.243 | 0.485 | 0.978 | **SPEI 12 G** |
| 0.225 | 0.328 | 0.493 | 0.705 | 1.000 | 0.236 | 0.706 | 0.102 | 0.176 | 0.338 | 0.716 | **SPEI 24 G** |
| 0.997 | 0.686 | 0.393 | 0.346 | 0.236 | 1.000 | 0.344 | 0.724 | 0.678 | 0.467 | 0.339 | **SPEI 3 bf** |
| 0.330 | 0.488 | 0.730 | 0.998 | 0.706 | 0.344 | 1.000 | 0.127 | 0.238 | 0.480 | 0.973 | **SPEI 12 bf** |
| 0.737 | 0.364 | -0.050 | 0.132 | 0.102 | 0.724 | 0.127 | 1.000 | 0.589 | 0.024 | 0.141 | **RDI 3** |
| 0.688 | 0.849 | 0.385 | 0.243 | 0.176 | 0.678 | 0.238 | 0.589 | 1.000 | 0.618 | 0.254 | **RDI 6** |
| 0.462 | 0.823 | 0.888 | 0.485 | 0.338 | 0.467 | 0.480 | 0.024 | 0.618 | 1.000 | 0.495 | **RDI 9** |
| 0.328 | 0.482 | 0.716 | 0.978 | 0.716 | 0.339 | 0.973 | 0.141 | 0.254 | 0.495 | 1.000 | **RDI 12** |

As can be seen in the correlation in Table4.9 for Kayseri station, a very high correlation was detected among SPEI 3 bf-SPEI 3 G (0.997), SPEI 12 bf-SPI 12 G (0.989), SPEI 12 bf-SPI 12 bf (0.993), SPEI 12 bf-SPEI 12 G (0.998), RDI 12-SPI 12 G (0.970), RDI 12-SPEI 12 G (0.978), and

RDI 12-SPEI 12 bf (0.973), while the lowest correlation is observed between RDI 3-SPI 9 G (0.094), RDI 3-SPI 9 bf (0.092), and RDI 3-SPEI 9 G (0.050).

**Table 4. 10.** Çankırı station drought analysis correlation

| | SPI 1 G | SPI 3 G | SPI 6 G | SPI 9 G | SPI 12 G | SPI 24 G | SPI 1 bf | SPI 3 bf | SPI 6 bf | SPI 9 bf | SPI 12 bf | SPI 24 bf |
|---|---|---|---|---|---|---|---|---|---|---|---|---|
| **SPI 1 G** | 1.000 | 0.589 | 0.359 | 0.306 | 0.294 | 0.184 | 0.990 | 0.588 | 0.362 | 0.306 | 0.292 | 0.185 |
| **SPI 3 G** | 0.589 | 1.000 | 0.667 | 0.551 | 0.479 | 0.332 | 0.598 | 0.994 | 0.668 | 0.552 | 0.479 | 0.335 |
| **SPI 6 G** | 0.359 | 0.667 | 1.000 | 0.790 | 0.684 | 0.511 | 0.372 | 0.674 | 0.996 | 0.790 | 0.682 | 0.516 |
| **SPI 9 G** | 0.306 | 0.551 | 0.790 | 1.000 | 0.844 | 0.660 | 0.318 | 0.561 | 0.796 | 1.000 | 0.838 | 0.658 |
| **SPI 12 G** | 0.294 | 0.479 | 0.684 | 0.844 | 1.000 | 0.784 | 0.305 | 0.489 | 0.693 | 0.844 | 0.993 | 0.778 |
| **SPI 24 G** | 0.184 | 0.332 | 0.511 | 0.660 | 0.784 | 1.000 | 0.193 | 0.342 | 0.522 | 0.661 | 0.771 | 0.991 |
| **SPI 1 bf** | 0.990 | 0.598 | 0.372 | 0.318 | 0.305 | 0.193 | 1.000 | 0.602 | 0.376 | 0.318 | 0.302 | 0.194 |
| **SPI 3 bf** | 0.588 | 0.994 | 0.674 | 0.561 | 0.489 | 0.342 | 0.602 | 1.000 | 0.678 | 0.562 | 0.485 | 0.344 |
| **SPI 6 bf** | 0.362 | 0.668 | 0.996 | 0.796 | 0.693 | 0.522 | 0.376 | 0.678 | 1.000 | 0.796 | 0.686 | 0.524 |
| **SPI 9 bf** | 0.306 | 0.552 | 0.790 | 1.000 | 0.844 | 0.661 | 0.318 | 0.562 | 0.796 | 1.000 | 0.838 | 0.659 |
| **SPI 12 bf** | 0.292 | 0.479 | 0.682 | 0.838 | 0.993 | 0.771 | 0.302 | 0.485 | 0.686 | 0.838 | 1.000 | 0.774 |
| **SPI 24 bf** | 0.185 | 0.335 | 0.516 | 0.658 | 0.778 | 0.991 | 0.194 | 0.344 | 0.524 | 0.659 | 0.774 | 1.000 |
| **SPEI 3 G** | 0.606 | 0.927 | 0.533 | 0.410 | 0.419 | 0.294 | 0.615 | 0.935 | 0.537 | 0.410 | 0.414 | 0.295 |
| **SPEI 6 G** | 0.425 | 0.726 | 0.923 | 0.656 | 0.599 | 0.450 | 0.434 | 0.731 | 0.928 | 0.656 | 0.593 | 0.454 |
| **SPEI 9 G** | 0.319 | 0.604 | 0.834 | 0.967 | 0.798 | 0.625 | 0.331 | 0.614 | 0.840 | 0.968 | 0.792 | 0.623 |
| **SPEI 12 G** | 0.287 | 0.470 | 0.672 | 0.838 | 0.996 | 0.777 | 0.298 | 0.479 | 0.681 | 0.838 | 0.993 | 0.773 |
| **SPEI 24 G** | 0.178 | 0.324 | 0.502 | 0.651 | 0.774 | 0.996 | 0.187 | 0.334 | 0.511 | 0.651 | 0.766 | 0.994 |
| **SPEI 3 bf** | 0.605 | 0.925 | 0.532 | 0.413 | 0.424 | 0.296 | 0.614 | 0.935 | 0.537 | 0.414 | 0.418 | 0.297 |
| **SPEI 12 bf** | 0.287 | 0.471 | 0.673 | 0.836 | 0.996 | 0.776 | 0.298 | 0.480 | 0.681 | 0.836 | 0.994 | 0.774 |
| **RDI 3** | 0.381 | 0.511 | 0.113 | -0.011 | 0.153 | 0.095 | 0.370 | 0.489 | 0.107 | -0.011 | 0.155 | 0.096 |
| **RDI 6** | 0.380 | 0.548 | 0.569 | 0.228 | 0.282 | 0.207 | 0.376 | 0.537 | 0.557 | 0.228 | 0.288 | 0.216 |
| **RDI 9** | 0.340 | 0.614 | 0.775 | 0.729 | 0.539 | 0.419 | 0.349 | 0.619 | 0.775 | 0.729 | 0.544 | 0.427 |
| **RDI 12** | 0.285 | 0.470 | 0.674 | 0.830 | 0.981 | 0.762 | 0.296 | 0.478 | 0.681 | 0.830 | 0.983 | 0.765 |

There is a continuation of this table on the next page.

| SPEI 3 G | SPEI 6 G | SPEI 9 G | SPEI 12 G | SPEI 24 G | SPEI 3 bf | SPEI 12 bf | RDI 3 | RDI 6 | RDI 9 | RDI 12 | |
|---|---|---|---|---|---|---|---|---|---|---|---|
| 0.606 | 0.425 | 0.319 | 0.287 | 0.178 | 0.605 | 0.287 | 0.381 | 0.380 | 0.340 | 0.285 | **SPI 1 G** |
| 0.927 | 0.726 | 0.604 | 0.470 | 0.324 | 0.925 | 0.471 | 0.511 | 0.548 | 0.614 | 0.470 | **SPI 3 G** |
| 0.533 | 0.923 | 0.834 | 0.672 | 0.502 | 0.532 | 0.673 | 0.113 | 0.569 | 0.775 | 0.674 | **SPI 6 G** |
| 0.410 | 0.656 | 0.967 | 0.838 | 0.651 | 0.413 | 0.836 | -0.011 | 0.228 | 0.729 | 0.830 | **SPI 9 G** |
| 0.419 | 0.599 | 0.798 | 0.996 | 0.774 | 0.424 | 0.996 | 0.153 | 0.282 | 0.539 | 0.981 | **SPI 12 G** |
| 0.294 | 0.450 | 0.625 | 0.777 | 0.996 | 0.296 | 0.776 | 0.095 | 0.207 | 0.419 | 0.762 | **SPI 24 G** |
| 0.615 | 0.434 | 0.331 | 0.298 | 0.187 | 0.614 | 0.298 | 0.370 | 0.376 | 0.349 | 0.296 | **SPI 1 bf** |
| 0.935 | 0.731 | 0.614 | 0.479 | 0.334 | 0.935 | 0.480 | 0.489 | 0.537 | 0.619 | 0.478 | **SPI 3 bf** |
| 0.537 | 0.928 | 0.840 | 0.681 | 0.511 | 0.537 | 0.681 | 0.107 | 0.557 | 0.775 | 0.681 | **SPI 6 bf** |
| 0.410 | 0.656 | 0.968 | 0.838 | 0.651 | 0.414 | 0.836 | -0.011 | 0.228 | 0.729 | 0.830 | **SPI 9 bf** |
| 0.414 | 0.593 | 0.792 | 0.993 | 0.766 | 0.418 | 0.994 | 0.155 | 0.288 | 0.544 | 0.983 | **SPI 12 bf** |
| 0.295 | 0.454 | 0.623 | 0.773 | 0.994 | 0.297 | 0.774 | 0.096 | 0.216 | 0.427 | 0.765 | **SPI 24 bf** |
| 1.000 | 0.685 | 0.463 | 0.413 | 0.288 | 0.998 | 0.414 | 0.715 | 0.642 | 0.494 | 0.412 | **SPEI 3 G** |
| 0.685 | 1.000 | 0.764 | 0.591 | 0.444 | 0.680 | 0.592 | 0.337 | 0.803 | 0.827 | 0.591 | **SPEI 6 G** |
| 0.463 | 0.764 | 1.000 | 0.796 | 0.618 | 0.464 | 0.795 | 0.012 | 0.382 | 0.861 | 0.788 | **SPEI 9 G** |
| 0.413 | 0.591 | 0.796 | 1.000 | 0.772 | 0.417 | 0.999 | 0.151 | 0.279 | 0.538 | 0.984 | **SPEI 12 G** |
| 0.288 | 0.444 | 0.618 | 0.772 | 1.000 | 0.291 | 0.772 | 0.095 | 0.208 | 0.421 | 0.766 | **SPEI 24 G** |
| 0.998 | 0.680 | 0.464 | 0.417 | 0.291 | 1.000 | 0.418 | 0.710 | 0.633 | 0.490 | 0.417 | **SPEI 3 bf** |
| 0.414 | 0.592 | 0.795 | 0.999 | 0.772 | 0.418 | 1.000 | 0.151 | 0.281 | 0.539 | 0.985 | **SPEI 12 bf** |
| 0.715 | 0.337 | 0.012 | 0.151 | 0.095 | 0.710 | 0.151 | 1.000 | 0.579 | 0.040 | 0.155 | **RDI 3** |
| 0.642 | 0.803 | 0.382 | 0.279 | 0.208 | 0.633 | 0.281 | 0.579 | 1.000 | 0.631 | 0.290 | **RDI 6** |
| 0.494 | 0.827 | 0.861 | 0.538 | 0.421 | 0.490 | 0.539 | 0.040 | 0.631 | 1.000 | 0.552 | **RDI 9** |
| 0.412 | 0.591 | 0.788 | 0.984 | 0.766 | 0.417 | 0.985 | 0.155 | 0.290 | 0.552 | 1.000 | **RDI 12** |

As can be seen in the correlation in Table4.10 for Çankırı station, a very high correlation was detected among SPEI 12 G-SPI 12 G (0.996), SPEI 12 G-SPI 12 bf (0.993), SPEI 12 bf-SPI 12 G (0.996), SPEI 12 bf-SPI 12 bf (0.994), RDI 12-SPEI 12 G (0.984), RDI 12-SPEI 12 bf (0.985) and RDI 12-SPI 12 bf (0.983), while the lowest correlation is observed between RDI 3-SPI 9 G (0.011) and RDI 3-SPI 9 bf (0.011).

**Table 4. 11.** Konya station drought analysis correlation

| | SPI 1 G | SPI 3 G | SPI 6 G | SPI 9 G | SPI 12 G | SPI 24 G | SPI 1 bf | SPI 3 bf | SPI 6 bf | SPI 9 bf | SPI 12 bf | SPI 24 bf |
|---|---|---|---|---|---|---|---|---|---|---|---|---|
| **SPI 1 G** | 1.000 | 0.603 | 0.375 | 0.276 | 0.248 | 0.164 | 0.986 | 0.602 | 0.378 | 0.272 | 0.245 | 0.158 |
| **SPI 3 G** | 0.603 | 1.000 | 0.644 | 0.529 | 0.414 | 0.286 | 0.611 | 0.991 | 0.641 | 0.523 | 0.409 | 0.274 |
| **SPI 6 G** | 0.375 | 0.644 | 1.000 | 0.776 | 0.653 | 0.450 | 0.380 | 0.661 | 0.998 | 0.772 | 0.648 | 0.437 |
| **SPI 9 G** | 0.276 | 0.529 | 0.776 | 1.000 | 0.826 | 0.602 | 0.285 | 0.538 | 0.775 | 0.995 | 0.818 | 0.586 |
| **SPI 12 G** | 0.248 | 0.414 | 0.653 | 0.826 | 1.000 | 0.734 | 0.258 | 0.428 | 0.653 | 0.820 | 0.992 | 0.722 |
| **SPI 24 G** | 0.164 | 0.286 | 0.450 | 0.602 | 0.734 | 1.000 | 0.174 | 0.289 | 0.449 | 0.594 | 0.725 | 0.972 |
| **SPI 1 bf** | 0.986 | 0.611 | 0.380 | 0.285 | 0.258 | 0.174 | 1.000 | 0.613 | 0.384 | 0.281 | 0.255 | 0.168 |
| **SPI 3 bf** | 0.602 | 0.991 | 0.661 | 0.538 | 0.428 | 0.289 | 0.613 | 1.000 | 0.660 | 0.535 | 0.426 | 0.280 |
| **SPI 6 bf** | 0.378 | 0.641 | 0.998 | 0.775 | 0.653 | 0.449 | 0.384 | 0.660 | 1.000 | 0.775 | 0.652 | 0.439 |
| **SPI 9 bf** | 0.272 | 0.523 | 0.772 | 0.995 | 0.820 | 0.594 | 0.281 | 0.535 | 0.775 | 1.000 | 0.821 | 0.585 |
| **SPI 12 bf** | 0.245 | 0.409 | 0.648 | 0.818 | 0.992 | 0.725 | 0.255 | 0.426 | 0.652 | 0.821 | 1.000 | 0.724 |
| **SPI 24 bf** | 0.158 | 0.274 | 0.437 | 0.586 | 0.722 | 0.972 | 0.168 | 0.280 | 0.439 | 0.585 | 0.724 | 1.000 |
| **SPEI 3 G** | 0.603 | 0.928 | 0.612 | 0.402 | 0.338 | 0.226 | 0.605 | 0.944 | 0.613 | 0.399 | 0.336 | 0.221 |
| **SPEI 6 G** | 0.375 | 0.652 | 0.931 | 0.643 | 0.490 | 0.337 | 0.370 | 0.660 | 0.934 | 0.645 | 0.488 | 0.331 |
| **SPEI 9 G** | 0.213 | 0.493 | 0.789 | 0.953 | 0.721 | 0.520 | 0.217 | 0.497 | 0.791 | 0.957 | 0.721 | 0.513 |
| **SPEI 12 G** | 0.244 | 0.404 | 0.637 | 0.812 | 0.988 | 0.722 | 0.252 | 0.417 | 0.639 | 0.811 | 0.990 | 0.720 |
| **SPEI 24 G** | 0.150 | 0.263 | 0.423 | 0.573 | 0.709 | 0.980 | 0.158 | 0.267 | 0.424 | 0.569 | 0.707 | 0.972 |
| **SPEI 3 bf** | 0.601 | 0.930 | 0.610 | 0.402 | 0.339 | 0.227 | 0.603 | 0.945 | 0.612 | 0.400 | 0.337 | 0.221 |
| **SPEI 12 bf** | 0.243 | 0.405 | 0.638 | 0.813 | 0.989 | 0.721 | 0.250 | 0.418 | 0.640 | 0.812 | 0.991 | 0.718 |
| **RDI 3** | 0.462 | 0.706 | 0.435 | 0.147 | 0.165 | 0.110 | 0.445 | 0.692 | 0.429 | 0.135 | 0.155 | 0.102 |
| **RDI 6** | 0.327 | 0.518 | 0.745 | 0.386 | 0.263 | 0.185 | 0.312 | 0.514 | 0.744 | 0.382 | 0.255 | 0.177 |
| **RDI 9** | 0.181 | 0.444 | 0.727 | 0.800 | 0.500 | 0.373 | 0.182 | 0.440 | 0.727 | 0.799 | 0.492 | 0.363 |

| | | | | | | | | | | | | |
|---|---|---|---|---|---|---|---|---|---|---|---|---|
| **RDI 12** | 0.245 | 0.408 | 0.641 | 0.808 | 0.978 | 0.729 | 0.254 | 0.420 | 0.639 | 0.799 | 0.963 | 0.715 |

There is a continuation of this table on the next page.

| SPEI 3 G | SPEI 6 G | SPEI 9 G | SPEI 12 G | SPEI 24 G | SPEI 3 bf | SPEI 12 bf | RDI 3 | RDI 6 | RDI 9 | RDI 12 | |
|---|---|---|---|---|---|---|---|---|---|---|---|
| 0.603 | 0.375 | 0.213 | 0.244 | 0.150 | 0.601 | 0.243 | 0.462 | 0.327 | 0.181 | 0.245 | **SPI 1 G** |
| 0.928 | 0.652 | 0.493 | 0.404 | 0.263 | 0.930 | 0.405 | 0.706 | 0.518 | 0.444 | 0.408 | **SPI 3 G** |
| 0.612 | 0.931 | 0.789 | 0.637 | 0.423 | 0.610 | 0.638 | 0.435 | 0.745 | 0.727 | 0.641 | **SPI 6 G** |
| 0.402 | 0.643 | 0.953 | 0.812 | 0.573 | 0.402 | 0.813 | 0.147 | 0.386 | 0.800 | 0.808 | **SPI 9 G** |
| 0.338 | 0.490 | 0.721 | 0.988 | 0.709 | 0.339 | 0.989 | 0.165 | 0.263 | 0.500 | 0.978 | **SPI 12 G** |
| 0.226 | 0.337 | 0.520 | 0.722 | 0.980 | 0.227 | 0.721 | 0.110 | 0.185 | 0.373 | 0.729 | **SPI 24 G** |
| 0.605 | 0.370 | 0.217 | 0.252 | 0.158 | 0.603 | 0.250 | 0.445 | 0.312 | 0.182 | 0.254 | **SPI 1 bf** |
| 0.944 | 0.660 | 0.497 | 0.417 | 0.267 | 0.945 | 0.418 | 0.692 | 0.514 | 0.440 | 0.420 | **SPI 3 bf** |
| 0.613 | 0.934 | 0.791 | 0.639 | 0.424 | 0.612 | 0.640 | 0.429 | 0.744 | 0.727 | 0.639 | **SPI 6 bf** |
| 0.399 | 0.645 | 0.957 | 0.811 | 0.569 | 0.400 | 0.812 | 0.135 | 0.382 | 0.799 | 0.799 | **SPI 9 bf** |
| 0.336 | 0.488 | 0.721 | 0.990 | 0.707 | 0.337 | 0.991 | 0.155 | 0.255 | 0.492 | 0.963 | **SPI 12 bf** |
| 0.221 | 0.331 | 0.513 | 0.720 | 0.972 | 0.221 | 0.718 | 0.102 | 0.177 | 0.363 | 0.715 | **SPI 24 bf** |
| 1.000 | 0.684 | 0.369 | 0.333 | 0.211 | 0.999 | 0.333 | 0.847 | 0.616 | 0.330 | 0.336 | **SPEI 3 G** |
| 0.684 | 1.000 | 0.732 | 0.485 | 0.323 | 0.682 | 0.487 | 0.574 | 0.914 | 0.757 | 0.485 | **SPEI 6 G** |
| 0.369 | 0.732 | 1.000 | 0.724 | 0.508 | 0.369 | 0.725 | 0.123 | 0.516 | 0.921 | 0.712 | **SPEI 9 G** |
| 0.333 | 0.485 | 0.724 | 1.000 | 0.719 | 0.334 | 0.999 | 0.160 | 0.256 | 0.494 | 0.972 | **SPEI 12 G** |
| 0.211 | 0.323 | 0.508 | 0.719 | 1.000 | 0.212 | 0.715 | 0.103 | 0.177 | 0.364 | 0.724 | **SPEI 24 G** |
| 0.999 | 0.682 | 0.369 | 0.334 | 0.212 | 1.000 | 0.334 | 0.847 | 0.613 | 0.330 | 0.337 | **SPEI 3 bf** |
| 0.333 | 0.487 | 0.725 | 0.999 | 0.715 | 0.334 | 1.000 | 0.162 | 0.259 | 0.498 | 0.975 | **SPEI 12 bf** |
| 0.847 | 0.574 | 0.123 | 0.160 | 0.103 | 0.847 | 0.162 | 1.000 | 0.637 | 0.115 | 0.174 | **RDI 3** |
| 0.616 | 0.914 | 0.516 | 0.256 | 0.177 | 0.613 | 0.259 | 0.637 | 1.000 | 0.645 | 0.274 | **RDI 6** |
| 0.330 | 0.757 | 0.921 | 0.494 | 0.364 | 0.330 | 0.498 | 0.115 | 0.645 | 1.000 | 0.513 | **RDI 9** |
| 0.336 | 0.485 | 0.712 | 0.972 | 0.724 | 0.337 | 0.975 | 0.174 | 0.274 | 0.513 | 1.000 | **RDI 12** |

As can be seen in the correlationin Table4.11 for Konya station, a very high correlation was detected among SPEI 12 G-SPI 12 G (0.988), SPEI 12 G-SPI 12 bf (0.990), SPEI 12 bf-SPI 12 G (0.989), SPEI 12 bf-SPI 12 bf (0.991), and RDI 12-SPI 12 G (0.978), while the lowest correlation is observed between RDI 3-SPEI 24 G (0.103), RDI 3-SPI 24 G (0.110), and RDI 3-SPI 24 bf (0.102). Similar evaluations were made for the other stations.

When the correlation tables are examined as a whole, it can be generally observed that SPI 1 G is the least correlated with other drought indices and provides the least reliable results for Samsun station, while SPI 9 G is highly correlated with other indices and provides the most reliable results. Therefore, if a reliable drought index for this station should be selected, SPI 9 G should be considered. For Kayseri station, RDI 3 is the least correlated with other drought indices and provides the least reliable results, while SPI 6 bf is highly correlated with other indices and provides the most reliable results. Hence, if we want to choose a reliable drought index for this station, SPI 6 bf should be considered. For Çankırı station, RDI 3 is the least correlated with other drought indices and provides the least reliable results, while SPEI 9 G is highly correlated with other indices and provides the most reliable results. Therefore, if we want to select a reliable drought index for this station, SPEI 9 G should be considered. For Konya station, RDI 3 is the least correlated with other drought indices and provides the least reliable results, while SPI 6 bf is highly correlated with other indices and provides the most reliable results. If we want to choose a reliable drought index for this station, SPI 6 bf should be considered. The RDI results generally provided the least reliable outcomes. Similar evaluations can be made for all other stations.

To better understand the relationship between the 3-month and 12-month drought classifications of the SPI gamma distribution (SPI g), SPI best fit distribution (SPI bf), SPEI GLOG distribution (SPEI g), SPEI best fit distribution (SPEI bf), and RDI drought results were given as histograms. Histograms were prepared as percentages for the extremely wet (W3), wet (W2), moderately wet (W1), normal (N), moderately drought (D1), drought (D2), and extremely drought (D3) drought categories. Some of the selected stations of calculated histogram graphs are shown in Figures 4.42 to 4.47.

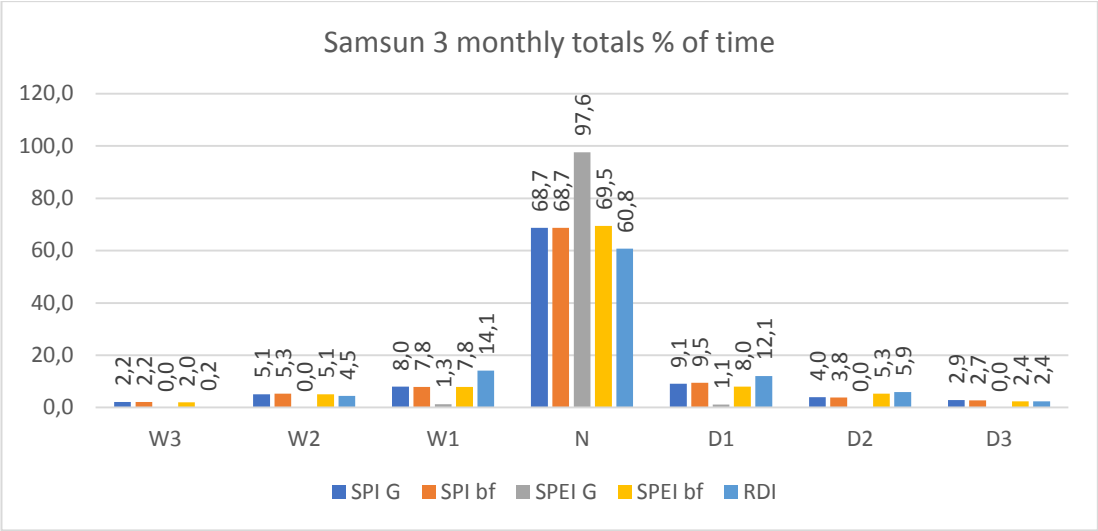


**Figure 4. 42.** Samsun station 3-month drought histogram percent of time graph

As can be seen in the graph, the highest percentage of D3 was given by SPI g, the highest percentage of D2 was given by RDI, the highest percentage of D1 was given by RDI, and the highest percentage of W3 was given by SPI and SPI g drought indices.

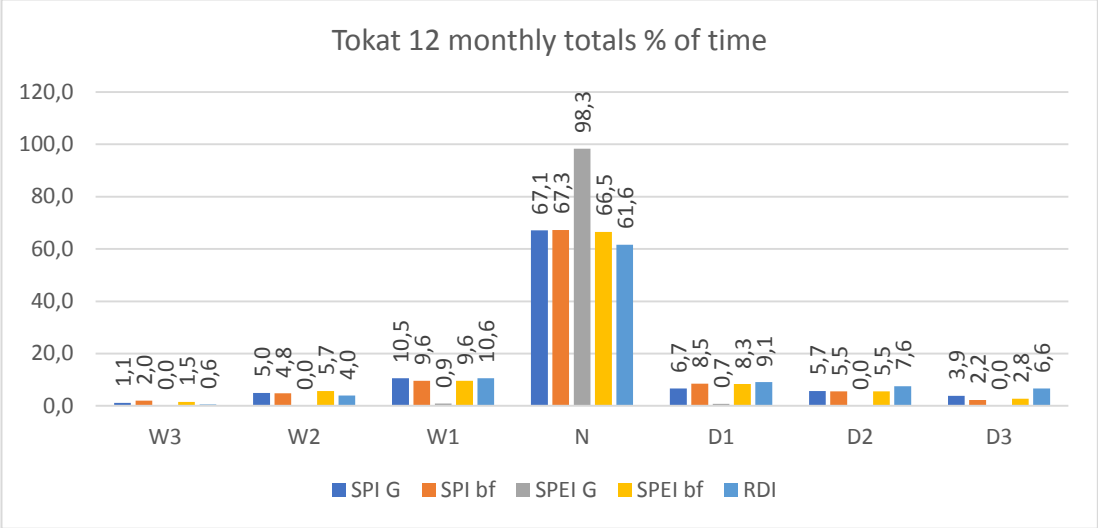


**Figure 4. 43.** Tokat station 12-month drought histogram percentage graph

As can be seen in the graph, the highest percentage of D3 was given by RDI, the highest percentage of D2 was given by RDI, the highest percentage of D1 was given by RDI, and the highest percentage of W3 was given by SPI drought indices.

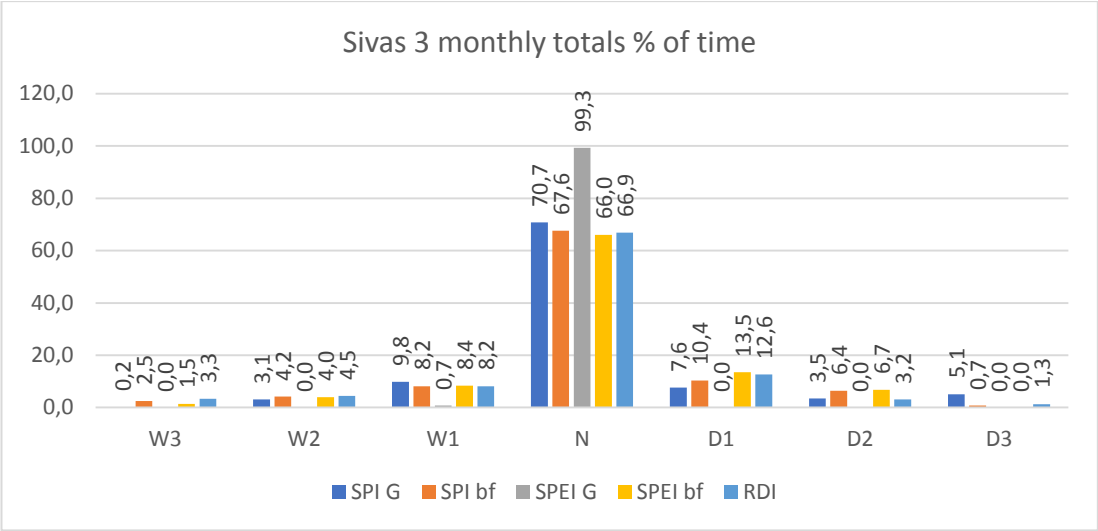


**Figure 4. 44.** Sivas station 3-month drought histogram percentage graph

As can be seen in the graph, the highest percentage of D3 was given by SPI g, the highest percentage of D2 was given by SPEI, the highest percentage of D1 was given by SPEI, and the highest percentage of W3 was given by SPI drought indices.

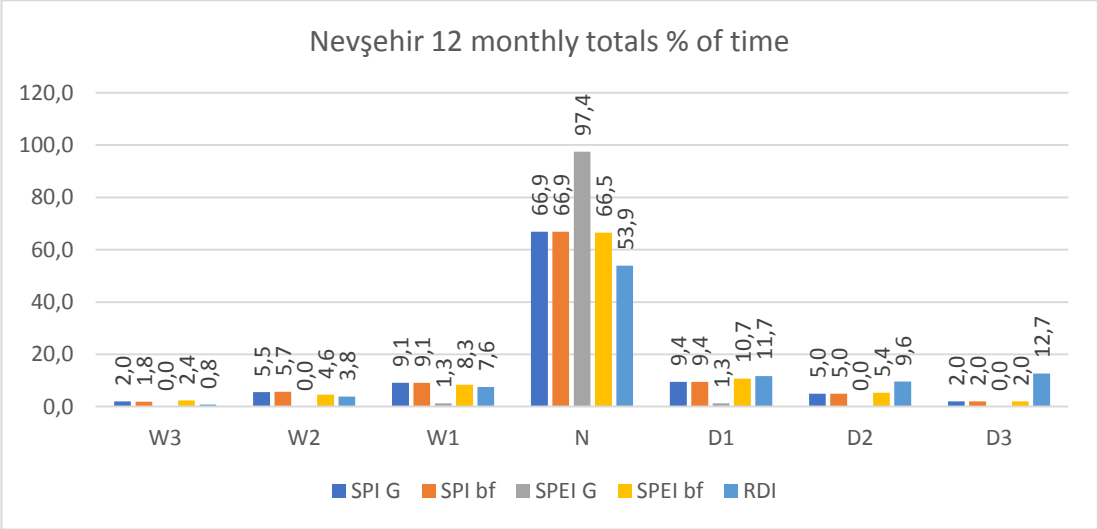


**Figure 4. 45.** Nevşehir station 12-month drought histogram percentage graph

As can be seen in the graph, the highest percentage of D3 was given by RDI, the highest percentage of D2 was given by RDI, the highest percentage of D1 was given by RDI, and the highest percentage of W3 was given by SPEI drought indices.

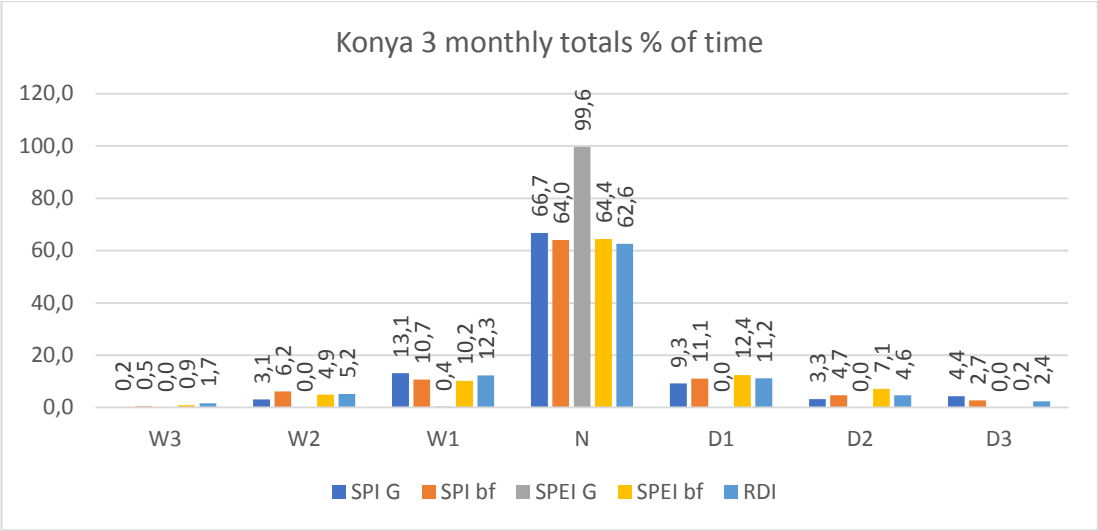


**Figure 4. 46.** Konya station 3-month drought histogram percentage graph

As can be seen in the graph, the highest percentage of D3 was given by SPI g, the highest percentage of D2 was given by SPEI, the highest percentage of D1 was given by SPEI, and the highest percentage of W3 was given by RDI drought indices.

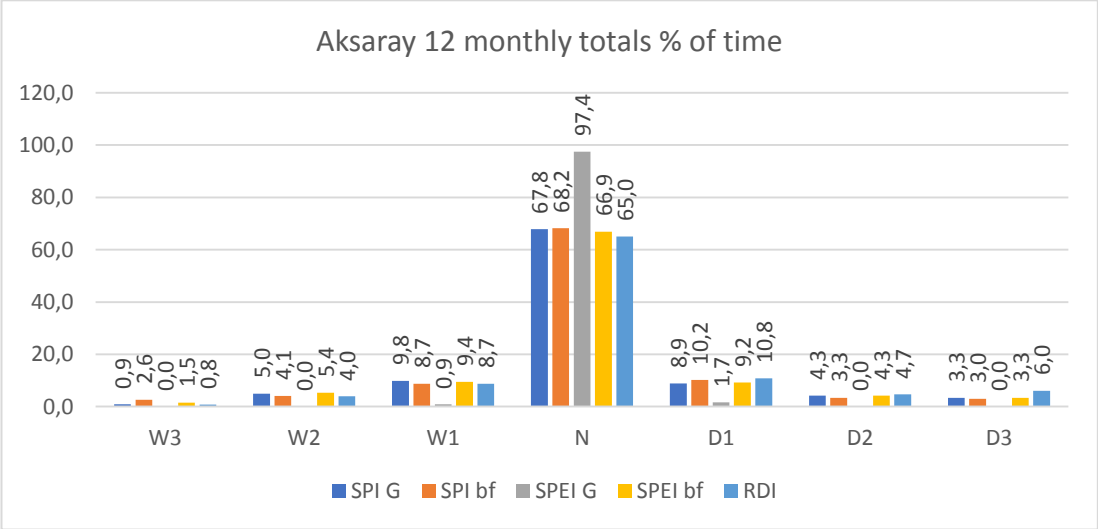


**Figure 4. 47.** Aksaray station 12-month drought histogram percentage graph

As can be seen in the graph, the highest percentage of D3 was given by RDI, the highest percentage of D2 was given by RDI, the highest percentage of D1 was given by RDI, and the highest percentage of W3 was given by SPI drought indices. Similar evaluations were made for the other stations. As can be seen in the Figures for all other stations, SPEI g (SPEI index calculated by GLOG) gives only near-Normal wet/dry periods in all graphs, and zero values in other periods.

Based on the histograms, all 3-month and 12-month drought results were mapped for the Yeşilırmak Basin, Kızılırmak Basin, and Konya Closed Basin and given according to the D3, D2, D1, and W3 classifications as shown in the figures below.

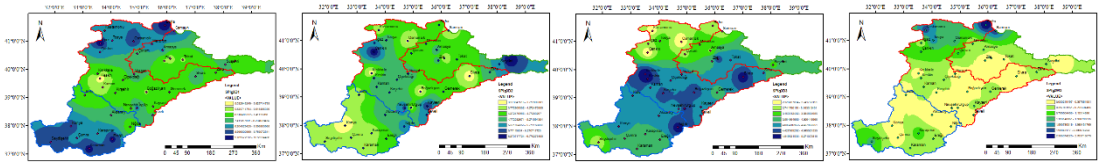

**Figure 4. 48.** SPI gamma distribution for all basins 3-month D1, D2, D3, W3 histogram maps

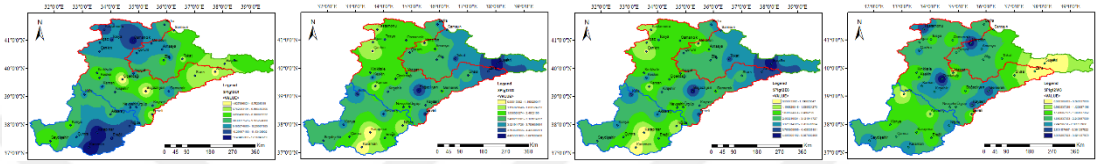

**Figure 4. 49.** SPI gamma distribution for all basins 12-month D1, D2, D3, W3 histogram maps

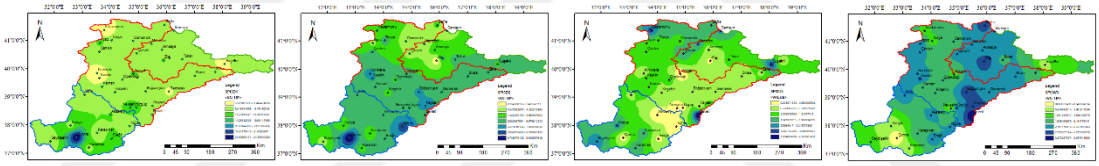

**Figure 4. 50.** SPI best fit distribution for all basins 3-month D1, D2, D3, W3 histogram maps

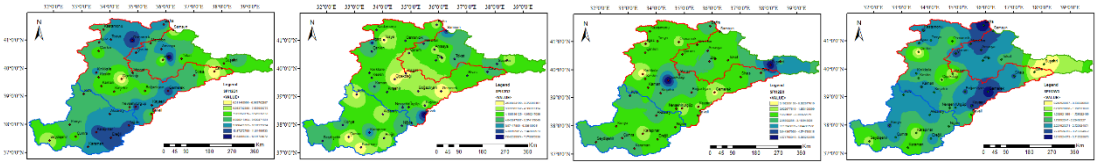

**Figure 4. 51.** SPI best fit distribution for all basins 12-month D1, D2, D3, W3 histogram maps

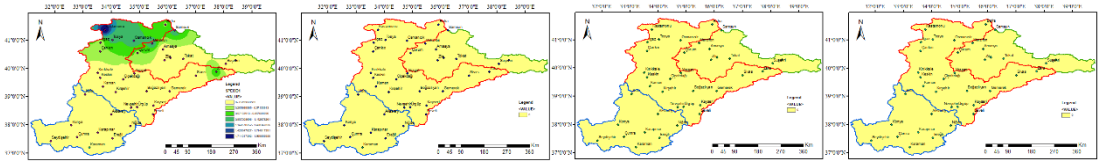

**Figure 4. 52.** SPEI GLOG distribution for all basins 3-month D1, D2, D3, W3 histogram maps

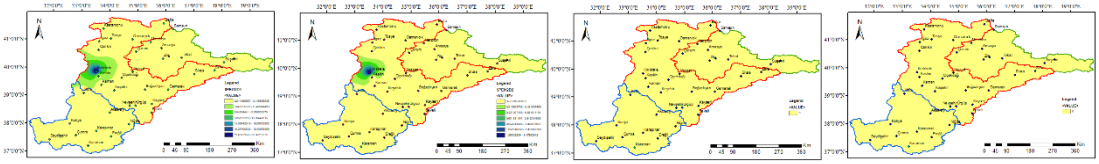

**Figure 4. 53.** SPEI glog distribution for all basins 12-month D1, D2, D3, W3 histogram maps

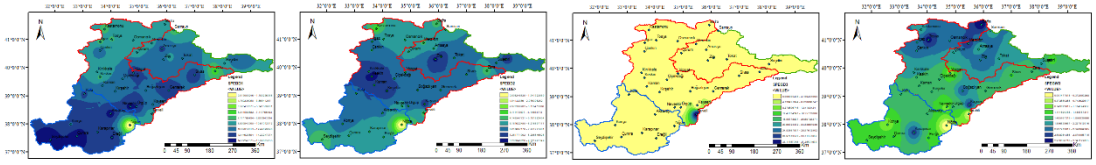

**Figure 4. 54.** SPEI best fit distribution for all basins 3-month D1, D2, D3, W3 histogram maps

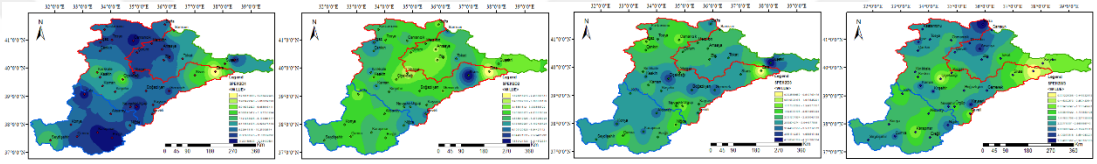

**Figure 4. 55.** SPEI best fit distribution for all basins 12-month D1, D2, D3, W3 histogram maps

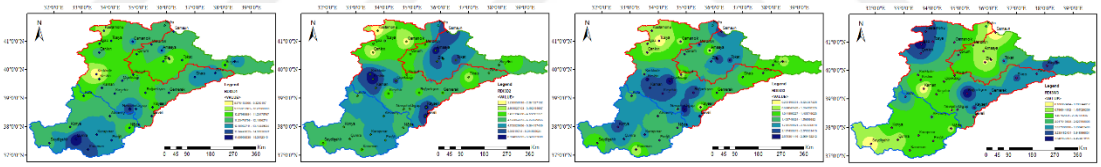

**Figure 4. 56.** RDI for all basins 3-month D1, D2, D3, W3 histogram maps

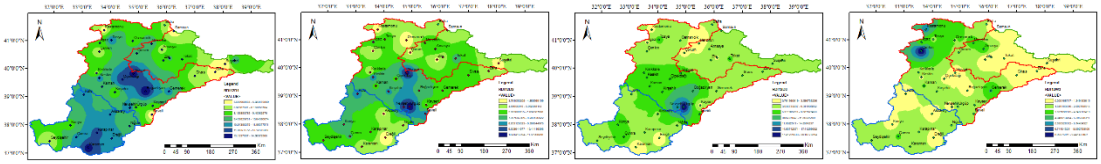

**Figure 4. 57.** RDI for all basins 12-month D1, D2, D3, W3 histogram maps

The spatial representation of all probability distribution maps shown above for all drought classifications (D1, D2, D3, W3) according to the distribution percentages for all drought indices is given in Table 4.12.

**Table 4. 12.** Distribution percentages of drought classifications.

| | % Area | | | |
|---|---|---|---|---|
| **Drought Indices** | **D1** | **D2** | **D3** | **W3** |
| **SPI 3 G** | 46.14 | 27.44 | 22.71 | 3.72 |
| **SPI 3 BF** | 53.61 | 28.29 | 7.77 | 10.33 |
| **SPEI 3 G** | 100.00 | 0.00 | 0.00 | 0.00 |
| **SPEI 3 BF** | 53.42 | 30.01 | 7.76 | 8.82 |
| **RDI 3** | 58.11 | 22.90 | 8.20 | 10.78 |
| **SPI 12 G** | 49.35 | 25.63 | 14.86 | 10.16 |
| **SPI 12 BF** | 51.68 | 24.41 | 12.36 | 11.55 |
| **SPEI 12 G** | 98.11 | 1.89 | 0.00 | 0.00 |
| **SPEI 12 BF** | 51.29 | 24.68 | 13.07 | 10.96 |
| **RDI 12** | 39.87 | 27.34 | 24.46 | 8.34 |

Since the SPEI calculated by GLOG had only classes in Normal wet/dry periods, the evaluation of Table 4.12 was realized by taking the other indices into consideration. When evaluated based on the results of the 3-month total precipitations in Table 4.12, RDI 3 yielded the highest percentage for D1 classification (58.51 %), while SPI 3 G had the lowest percentage (46.14 %). SPEI 3 bf provided the highest percentage for D2 classification (30.01 %), whereas RDI 3 had the lowest percentage (22.90). SPI 3 G yielded the highest percentage for D3 classification (22.71 %), while SPEI 3 bf provided the lowest percentage (7.76 %). RDI 3 had the highest percentage for W3 classification (10.78 %), while SPI 3 G had the lowest percentage (3.72 %). SPI 3 G provided the best results for extreme drought periods, while RDI 3 performed the best for extreme wet periods.

When evaluated based on the results of the 12-month total precipitations, SPI 12 bf provided the highest percentage for D1 classification (51.68 %), while RDI 12 had the lowest percentage (39.87). RDI 12 yielded the highest percentage for D2 classification (27.34 %), while SPI 12 bf provided the lowest percentage (11.55 %). RDI 12 also had the highest percentage for D3 classification (24.46 %), while SPI 12 bf provided the lowest percentage (12.36 %). SPI 12 bf yielded the highest percentage for W3 classification (11.55 %), while RDI 12 had the lowest percentage (8.34 %). RDI 12 showed successful results for drought periods, while SPI 12 bf performed the best for extreme drought periods.

### 4.6. Trend Analysis

In this study, 38 precipitation stations were taken as a basis. Trend analysis was performed for the total precipitation data, SPI, SPEI, RDI drought results of these stations. In addition, trend analysis was performed for the SRI drought results of 9 flow stations. Two methods were used in trend analysis, these are Mann-Kendall (MK) and Innovative Sen Trend (ITA) methods. The results of the trend analysis are given in the tables below. Trend results for each basin are shown in the maps below.

#### 4.6.1. Mann Kendall (MK) Trend Analysis

Trend analysis was performed by applying Mann-Kendall (MK) trend analysis to the results of 4 different drought indexes and precipitation data. An application called XLSTAT, which can be added and run as an add-on to Excel software, was used while performing trend analysis. %1, 5% and %10 levels of significance were taken into account while performing trend analysis.

Trend test results of precipitation are given in Table 4.13, trend test results of SPI bf method are given in Table 4.14, trend test results of RDI method are given in Table 4.15, trend test results of SPEI bf method are given in Table 4.16, trend test results of SRI method i are given in Table 4.17.

**Table 4. 13.** MK trend test results for precipitation

| St. No. | Yeşilırmak Basin | Trend MK | St. No. | Kızılırmak Basin | Trend MK | St. No. | Konya Closed Basin | Trend MK |
|---|---|---|---|---|---|---|---|---|
| 17030 | Samsun | No Trend* | 17074 | Kastamonu | No Trend* | 17244 | Konya | No Trend** |
| 17083 | Merzifon | No Trend** | 17080 | Çankırı | No Trend** | 17246 | Karaman | No Trend** |
| 17084 | Çorum | No Trend* | 17090 | Sivas | No Trend* | 17248 | Ereğli | No Trend* |
| 17085 | Amasya | No Trend* | 17135 | Kırıkkale | No Trend* | 17250 | Niğde | No Trend* |
| 17086 | Tokat | No Trend* | 17140 | Yozgat | No Trend** | 17754 | Kulu | Decreasing Trend** |
| 17681 | Zile | No Trend** | 17160 | Kırşehir | No Trend** | 17898 | Seydişehir | No Trend* |
| 1768 | Turhal | No | 1716 | Gemerek | No | 1790 | Çumra | No |

| | | | | | | | | |
|---|---|---|---|---|---|---|---|---|
| 4 | | Trend* | 2 | | Trend** | 0 | | Trend** |
| 17682 | Suşehri | No Trend** | 17193 | Nevşehir | No Trend** | 17902 | Karapınar | No Trend** |
| 17683 | Şebinkarahisar | No Trend** | 17196 | Kayseri | No Trend* | 17192 | Aksaray | No Trend** |
| | | | 17622 | Bafra | No Trend* | | | |
| | | | 17648 | Ilgaz | No Trend* | | | |
| | | | 17650 | Tosya | No Trend* | | | |
| | | | 17652 | Osmancık | Increasing Trend** | | | |
| | | | 17716 | Zara | Decreasing Trend*** | | | |
| | | | 17730 | Keskin | No Trend* | | | |
| | | | 17732 | Çiçekdağı | No Trend* | | | |
| | | | 17756 | Kaman | No Trend* | | | |
| | | | 17760 | Boğazlıyan | Decreasing Trend*** | | | |
| | | | 17835 | Ürgüp | Decreasing Trend*** | | | |
| | | | 17836 | Develi | No Trend** | | | |

(*: Significant at 5-10 %, **: significant at 1-5 %, ***: Significant at a level less than 1 %)

**Table 4. 14.** MK trend test results for SPI bf

| Order | **St. No.** | **Name** | **1** | **3** | **6** | **9** | **12** | **24** |
|---|---|---|---|---|---|---|---|---|
| 1 | 17030 | Samsun | No Trend* | Increasing Trend*** | Increasing Trend*** | Increasing Trend*** | Increasing Trend*** | Increasing Trend*** |
| 2 | 17083 | Merzifon | No Trend* | Increasing Trend*** | Increasing Trend*** | Increasing Trend*** | Increasing Trend*** | Increasing Trend*** |
| 3 | 170 | Çorum | No | No | No | No | No | No |

| | | | | | | | | |
|---|---|---|---|---|---|---|---|---|
| | 84 | | Trend* | Trend* | Trend* | Trend* | Trend* | Trend* |
| 4 | 17085 | Amasya | No Trend* | No Trend* | No Trend* | Increasing Trend*** | Increasing Trend*** | Increasing Trend*** |
| 5 | 17086 | Tokat | No Trend* | No Trend* | No Trend* | No Trend* | No Trend* | No Trend*** |
| 6 | 17681 | Zile | No Trend* | Decreasing Trend** | Decreasing Trend*** | Increasing Trend** | Decreasing Trend*** | Decreasing Trend*** |
| 7 | 17683 | Turhal | No Trend* | No Trend* | Decreasing Trend** | Decreasing Trend*** | Decreasing Trend*** | Decreasing Trend*** |
| 8 | 17684 | Suşehri | No Trend** | Decreasing Trend*** | Decreasing Trend*** | Decreasing Trend*** | Decreasing Trend*** | Decreasing Trend*** |
| 9 | 17682 | Şebinkarahisar | No Trend* | Decreasing Trend** | Decreasing Trend*** | Decreasing Trend*** | Decreasing Trend*** | Decreasing Trend*** |
| 10 | 17074 | Kastamonu | No Trend* | No Trend* | Increasing Trend*** | Increasing Trend*** | Increasing Trend*** | Increasing Trend*** |
| 11 | 17080 | Çankırı | No Trend* | Increasing Trend** | Increasing Trend*** | Increasing Trend*** | Increasing Trend*** | Increasing Trend*** |
| 12 | 17090 | Sivas | No Trend* | No Trend* | No Trend* | No Trend* | No Trend* | No Trend* |
| 13 | 17135 | Kırıkkale | No Trend* | No Trend* | No Trend* | No Trend** | Increasing Trend** | Increasing Trend*** |
| 14 | 17140 | Yozgat | No Trend* | No Trend* | No Trend** | No Trend* | Decreasing Trend** | Decreasing Trend*** |
| 15 | 17160 | Kırşehir | No Trend* | No Trend* | No Trend* | No Trend* | No Trend* | No Trend* |
| 16 | 17162 | Gemerek | No Trend* | No Trend* | No Trend* | Increasing Trend** | Increasing Trend*** | Increasing Trend*** |
| 17 | 17193 | Nevşehir | No Trend* | No Trend* | No Trend* | No Trend* | No Trend* | Decreasing Trend*** |
| 18 | 17196 | Kayseri | No Trend* | No Trend* | No Trend* | No Trend* | Increasing | Increasing |

| | | | | | | | | |
|---|---|---|---|---|---|---|---|---|
| | | | | | | | Trend** | Trend*** |
| 19 | 17622 | Bafra | No Trend* | Increasing Trend*** | Decreasing Trend*** | Decreasing Trend*** | Decreasing Trend*** | Decreasing Trend*** |
| 20 | 17648 | Ilgaz | No Trend* | No Trend* | No Trend* | No Trend* | No Trend* | No Trend* |
| 21 | 17650 | Tosya | No Trend* | No Trend* | No Trend* | No Trend* | No Trend* | No Trend* |
| 22 | 17652 | Osmancık | Increasing Trend** | Increasing Trend*** | Increasing Trend*** | Increasing Trend*** | Increasing Trend*** | Increasing Trend*** |
| 23 | 17716 | Zara | Decreasing Trend*** | Decreasing Trend*** | Decreasing Trend*** | Decreasing Trend*** | Decreasing Trend*** | Decreasing Trend*** |
| 24 | 17730 | Keskin | No Trend* | Decreasing Trend*** | Decreasing Trend*** | Decreasing Trend*** | Decreasing Trend*** | Decreasing Trend*** |
| 25 | 17732 | Çiçekdağı | No Trend* | Decreasing Trend** | Decreasing Trend*** | Decreasing Trend*** | Decreasing Trend*** | Decreasing Trend*** |
| 26 | 17756 | Kaman | No Trend* | No Trend* | No Trend* | No Trend* | No Trend* | No Trend* |
| 27 | 17760 | Boğazlıyan | Decreasing Trend*** | Decreasing Trend*** | Decreasing Trend*** | Decreasing Trend*** | Decreasing Trend*** | Decreasing Trend*** |
| 28 | 17835 | Ürgüp | Decreasing Trend*** | Decreasing Trend*** | Decreasing Trend*** | Decreasing Trend*** | Decreasing Trend*** | Decreasing Trend*** |
| 29 | 17836 | Develi | No Trend* | No Trend* | Decreasing Trend** | Decreasing Trend** | Decreasing Trend*** | Decreasing Trend*** |
| 30 | 17244 | Konya | No Trend* | No Trend* | No Trend* | No Trend* | No Trend* | No Trend* |
| 31 | 17246 | Karaman | No Trend* | No Trend* | No Trend* | No Trend** | No Trend** | No Trend* |
| 32 | 17248 | Ereğli | No Trend* | No Trend* | Increasing Trend*** | No Trend* | No Trend* | Increasing Trend*** |
| 33 | 17250 | Niğde | No Trend* | No Trend* | No Trend* | Increasing Trend** | Increasing Trend** | Increasing Trend*** |
| 34 | 17754 | Kulu | Decreasing | Decreasing | Decreasing | Decreasing | Decreasing | Decreasing |

| | | | | | | | | |
|---|---|---|---|---|---|---|---|---|
| | | | Trend** | Trend*** | Trend*** | Trend*** | Trend*** | Trend*** |
| 35 | 17898 | Seydişehir | No Trend* | No Trend* | No Trend* | No Trend* | No Trend* | Increasing Trend** |
| 36 | 17900 | Çumra | No Trend* | No Trend* | Decreasing Trend** | No Trend** | No Trend*** | No Trend*** |
| 37 | 17902 | Karapınar | No Trend* | No Trend* | No Trend* | No Trend* | No Trend* | No Trend* |
| 38 | 17192 | Aksaray | No Trend* | No Trend* | No Trend* | No Trend* | No Trend* | Decreasing Trend** |

(*: Significant at 5-10 %, **: significant at 1-5 %, ***: Significant at a level less than 1 %)

**Table 4. 15.** MK trend test results for RDI

| Order | St. No. | Name | 3 | 6 | 9 | 12 |
|---|---|---|---|---|---|---|
| 1 | 17030 | Samsun | No Trend* | No Trend* | No Trend* | Increasing Trend*** |
| 2 | 17083 | Merzifon | No Trend* | No Trend* | No Trend* | Increasing Trend*** |
| 3 | 17084 | Çorum | No Trend* | No Trend* | No Trend* | Decreasing Trend*** |
| 4 | 17085 | Amasya | No Trend* | No Trend* | No Trend* | No Trend* |
| 5 | 17086 | Tokat | No Trend* | No Trend** | Decreasing Trend*** | Decreasing Trend*** |
| 6 | 17681 | Zile | No Trend* | Decreasing Trend*** | Decreasing Trend*** | Decreasing Trend*** |
| 7 | 17683 | Turhal | No Trend* | No Trend** | Decreasing Trend*** | Decreasing Trend*** |
| 8 | 17684 | Suşehri | No Trend* | Decreasing Trend** | Decreasing Trend*** | Decreasing Trend*** |
| 9 | 17682 | Şebinkarahisar | No Trend* | Decreasing Trend*** | Decreasing Trend*** | Decreasing Trend*** |
| 10 | 17074 | Kastamonu | No Trend* | No Trend* | Increasing Trend* | Increasing Trend* |
| 11 | 17080 | Çankırı | No Trend* | No Trend* | No Trend** | Increasing Trend* |
| 12 | 17090 | Sivas | No Trend* | No Trend* | No Trend* | Decreasing Trend*** |
| 13 | 17135 | Kırıkkale | No Trend* | No Trend* | No Trend* | No Trend** |
| 14 | 17140 | Yozgat | No Trend* | No Trend* | Decreasing Trend** | Decreasing Trend*** |
| 15 | 17160 | Kırşehir | No Trend* | No Trend* | No Trend* | Decreasing Trend* |
| 16 | 17162 | Gemerek | No Trend* | No Trend* | No Trend* | No Trend** |
| 17 | 17193 | Nevşehir | No | No Trend* | Decreasing | Decreasing |

| | | | | | | |
|---|---|---|---|---|---|---|
| | | | Trend* | | Trend* | Trend** |
| 18 | 17196 | Kayseri | No Trend* | No Trend* | No Trend*** | No Trend*** |
| 20 | 17648 | Ilgaz | No Trend* | No Trend* | No Trend* | No Trend*** |
| 21 | 17650 | Tosya | No Trend* | No Trend* | No Trend* | Decreasing Trend*** |
| 22 | 17652 | Osmancık | No Trend* | No Trend* | Increasing Trend*** | Increasing Trend*** |
| 23 | 17716 | Zara | No Trend* | Decreasing Trend*** | Decreasing Trend*** | Decreasing Trend*** |
| 24 | 17730 | Keskin | No Trend** | Decreasing Trend*** | Decreasing Trend*** | Decreasing Trend*** |
| 25 | 17732 | Çiçekdağı | No Trend* | Decreasing Trend*** | Decreasing Trend*** | Decreasing Trend*** |
| 26 | 17756 | Kaman | No Trend* | No Trend* | Decreasing Trend*** | Decreasing Trend*** |
| 27 | 17760 | Boğazlıyan | No Trend* | Decreasing Trend*** | Decreasing Trend*** | Decreasing Trend*** |
| 28 | 17835 | Ürgüp | No Trend** | Decreasing Trend*** | Decreasing Trend*** | Decreasing Trend*** |
| 29 | 17836 | Develi | No Trend* | No Trend** | Decreasing Trend*** | Decreasing Trend*** |
| 30 | 17244 | Konya | No Trend* | No Trend* | No Trend* | Decreasing Trend*** |
| 31 | 17246 | Karaman | No Trend* | No Trend* | Decreasing Trend** | Decreasing Trend*** |
| 32 | 17248 | Ereğli | No Trend* | No Trend* | No Trend* | Decreasing Trend*** |
| 33 | 17250 | Niğde | No Trend* | No Trend* | No Trend* | No Trend* |
| 34 | 17754 | Kulu | No Trend* | Decreasing Trend** | Decreasing Trend*** | Decreasing Trend*** |
| 35 | 17898 | Seydişehir | No Trend* | No Trend* | No Trend* | No Trend* |
| 36 | 17900 | Çumra | No Trend* | No Trend* | Decreasing Trend** | Decreasing Trend*** |
| 37 | 17902 | Karapınar | No Trend*** | No Trend*** | No Trend*** | No Trend*** |
| 38 | 17192 | Aksaray | No Trend* | No Trend* | Decreasing Trend** | Decreasing Trend*** |

(*: Significant at 5-10 %, **: significant at 1-5 %, ***: Significant at a level less than 1 %)

**Table 4. 16.** MK trend test results for SPEI bf

| Order | St. No. | Name | 3 | 12 |
|---|---|---|---|---|
| 1 | 17030 | Samsun | No trend** | Increasing Trend** |
| 2 | 17083 | Merzifon | No trend* | Increasing Trend* |
| 3 | 17084 | Çorum | No trend* | No trend* |
| 4 | 17085 | Amasya | Increasing Trend*** | Increasing Trend*** |
| 5 | 17086 | Tokat | No trend* | No trend* |
| 6 | 17681 | Zile | Decreasing Trend** | Decreasing Trend** |
| 7 | 17683 | Turhal | No trend** | No trend** |
| 8 | 17684 | Suşehri | Decreasing Trend** | Decreasing Trend** |
| 9 | 17682 | Şebinkarahisar | Decreasing Trend** | Decreasing Trend** |
| 10 | 17074 | Kastamonu | No trend*** | No trend*** |
| 11 | 17080 | Çankırı | No trend*** | No trend*** |
| 12 | 17090 | Sivas | No trend*** | No trend*** |
| 13 | 17135 | Kırıkkale | No trend*** | No trend*** |
| 14 | 17140 | Yozgat | No trend*** | No trend*** |
| 15 | 17160 | Kırşehir | No trend*** | No trend*** |
| 16 | 17162 | Gemerek | No trend*** | No trend*** |
| 17 | 17193 | Nevşehir | No trend* | No trend* |
| 18 | 17196 | Kayseri | No trend* | No trend* |
| 19 | 17622 | Bafra | No trend*** | No trend*** |
| 20 | 17648 | Ilgaz | No trend** | No trend** |
| 21 | 17650 | Tosya | No trend*** | No trend*** |
| 22 | 17652 | Osmancık | No trend** | Increasing Trend** |
| 23 | 17716 | Zara | No trend** | No trend** |
| 24 | 17730 | Keskin | Decreasing Trend** | Decreasing Trend** |
| 25 | 17732 | Çiçekdağı | No trend** | Decreasing Trend** |
| 26 | 17756 | Kaman | No trend** | No trend** |
| 27 | 17760 | Boğazlıyan | Decreasing Trend*** | Decreasing Trend*** |
| 28 | 17835 | Ürgüp | Decreasing Trend** | Decreasing Trend** |
| 29 | 17836 | Develi | Decreasing Trend** | Decreasing Trend** |
| 30 | 17244 | Konya | No trend*** | No trend*** |
| 32 | 17248 | Ereğli | No trend*** | No trend*** |
| 33 | 17250 | Niğde | No trend*** | No trend*** |
| 34 | 17754 | Kulu | Decreasing Trend* | Decreasing Trend* |
| 35 | 17898 | Seydişehir | No trend*** | No trend*** |
| 36 | 17900 | Çumra | No trend* | No trend* |
| 37 | 17902 | Karapınar | No trend* | No trend* |
| 38 | 17192 | Aksaray | No trend** | No trend** |

(*: Significant at 5-10 %, **: significant at 1-5 %, ***: Significant at a level less than 1 %)

**Table 4. 17.** MK trend test results for SRI

| Order | St. No. | Name | 3 | 6 | 9 | 12 | 24 |
|---|---|---|---|---|---|---|---|
| 1 | E15A001 | Kızılırmak Yamula | Increasing Trend*** | Increasing Trend*** | Increasing Trend*** | Increasing Trend*** | Increasing Trend*** |
| 2 | E15A017 | Karanlık Deresi Şefaatli | Decreasing Trend*** | Decreasing Trend*** | Decreasing Trend*** | Decreasing Trend*** | Decreasing Trend*** |
| 3 | E15A039 | Kızılırmak Bulakbaşı | No Trend* | No Trend* | No Trend* | No Trend* | Decreasing Trend** |
| 4 | E15A041 | Delice Çayı Çadırhöyük | Decreasing Trend*** | Decreasing Trend*** | Decreasing Trend*** | Decreasing Trend*** | Decreasing Trend*** |
| 5 | E14A002 | Yeşilırmak Kale | Increasing Trend*** | No Trend* | No Trend* | No Trend* | No Trend*** |
| 6 | E14A012 | Çorum Çat Irmağı | Decreasing Trend*** | Decreasing Trend*** | Decreasing Trend*** | Decreasing Trend*** | Decreasing Trend*** |
| 7 | E14A014 | Yeşilırmak Sütlüce | No Trend* | No Trend* | Increasing Trend** | Increasing Trend** | No Trend* |
| 8 | E14A022 | Kelkit Çayı Çiçekbükü | No Trend* | No Trend* | No Trend* | No Trend* | No Trend* |
| 9 | E14A027 | Kelkit Çayı Yemişli Köprüsü | Decreasing Trend*** | Decreasing Trend*** | Decreasing Trend*** | Decreasing Trend*** | Decreasing Trend*** |

(*: Significant at 5-10 %, **: significant at 1-5 %, ***: Significant at a level less than 1 %)

### 4.6.2. Innovative Şen Trend Analysis (ITA)

In this study, trend analysis was performed by applying Innovative Şen Trend (ITA) analysis to the results of 4 different drought analysis (SPI bf, SPEI bf, RDI, SRI) and precipitation data. The 5% significance level was taken into account while performing the trend analysis. While performing this trend analysis, results were obtained according to both the graphical method and the statistical method. The results obtained according to the statistical method are given in the tables below. Some of the results of the graphic method are given below the tables. The results of both methodologies support each other.

Trend test results of precipitation are given in Table 4.18, trend test results of SPI bf method are given in Table 4.19, trend test results of RDI method are given in Table

4.20, trend test results of SPEI bf method are given in Table 4.21, trend test results of SRI method are given in Table 4.22.

**Table 4. 18.** ITA trend test results for precipitation

| St. No. | Yeşilırmak Basin | Trend ITA | St. No. | Kızılırmak Basin | Trend ITA | St. No. | Konya Closed Basin | Trend ITA |
|---|---|---|---|---|---|---|---|---|
| 17030 | Samsun | No Trend | 17074 | Kastamonu | Increasing Trend | 17244 | Konya | No Trend |
| 17083 | Merzifon | No Trend | 17080 | Çankırı | Increasing Trend | 17246 | Karaman | No Trend |
| 17084 | Çorum | Increasing Trend | 17090 | Sivas | No Trend | 17248 | Ereğli | No Trend |
| 17085 | Amasya | No Trend | 17135 | Kırıkkale | No Trend | 17250 | Niğde | No Trend |
| 17086 | Tokat | No Trend | 17140 | Yozgat | No Trend | 17754 | Kulu | Decreasing Trend |
| 17681 | Zile | Decreasing Trend | 17160 | Kırşehir | No Trend | 17898 | Seydişehir | No Trend |
| 17684 | Turhal | No Trend | 17162 | Gemerek | No Trend | 17900 | Çumra | No Trend |
| 17682 | Suşehri | No Trend | 17193 | Nevşehir | No Trend | 17902 | Karapınar | No Trend |
| 17683 | Şebinkarahisar | No Trend | 17196 | Kayseri | No Trend | 17192 | Aksaray | No Trend |
| | | | 17622 | Bafra | Decreasing Trend | | | |
| | | | 17648 | Ilgaz | No Trend | | | |
| | | | 17650 | Tosya | No Trend | | | |
| | | | 17652 | Osmancık | Increasing Trend | | | |
| | | | 17716 | Zara | Decreasing Trend | | | |
| | | | 17730 | Keskin | Decreasing Trend | | | |
| | | | 17732 | Çiçekdağı | No Trend | | | |
| | | | 17756 | Kaman | No Trend | | | |
| | | | 17760 | Boğazlıyan | Decreasing Trend | | | |
| | | | 17835 | Ürgüp | Decreasing Trend | | | |
| | | | 17836 | Develi | No Trend | | | |

**Table 4. 19.** ITA trend test results for SPI bf

| Ord | St. | Name | 1 | 3 | 6 | 9 | 12 | 24 |
|---|---|---|---|---|---|---|---|---|

| er | No. | | | | | | | |
|---|---|---|---|---|---|---|---|---|
| 1 | 17030 | Samsun | Increasing Trend | Increasing Trend | Increasing Trend | Increasing Trend | Increasing Trend | Increasing Trend |
| 2 | 17083 | Merzifon | No Trend | Increasing Trend | Increasing Trend | Increasing Trend | Increasing Trend | Increasing Trend |
| 3 | 17084 | Çorum | No Trend | No Trend | No Trend | Increasing Trend | Increasing Trend | Increasing Trend |
| 4 | 17085 | Amasya | No Trend | Increasing Trend | Increasing Trend | Increasing Trend | Increasing Trend | Increasing Trend |
| 5 | 17086 | Tokat | No Trend | No Trend | No Trend | Decreasing Trend | Decreasing Trend | Decreasing Trend |
| 6 | 17681 | Zile | Decreasing Trend | Decreasing Trend | Decreasing Trend | Decreasing Trend | Decreasing Trend | Decreasing Trend |
| 7 | 17683 | Turhal | No Trend | Decreasing Trend | Decreasing Trend | Decreasing Trend | Decreasing Trend | Decreasing Trend |
| 8 | 17684 | Suşehri | No Trend | Decreasing Trend | Decreasing Trend | Decreasing Trend | Decreasing Trend | Decreasing Trend |
| 9 | 17682 | Şebinkarahisar | No Trend | Decreasing Trend | Decreasing Trend | Decreasing Trend | Decreasing Trend | Decreasing Trend |
| 10 | 17074 | Kastamonu | Increasing Trend | Increasing Trend | Increasing Trend | Increasing Trend | Increasing Trend | Increasing Trend |
| 11 | 17080 | Çankırı | No Trend | Increasing Trend | Increasing Trend | Increasing Trend | Increasing Trend | Increasing Trend |
| 12 | 17090 | Sivas | No Trend | No Trend | No Trend | No Trend | No Trend | No Trend |
| 13 | 17135 | Kırıkkale | No Trend | No Trend | No Trend | No Trend | Increasing Trend | Increasing Trend |
| 14 | 17140 | Yozgat | No Trend | Decreasing Trend | Decreasing Trend | Decreasing Trend | Decreasing Trend | Decreasing Trend |
| 15 | 17160 | Kırşehir | No Trend | No Trend | No Trend | Decreasing Trend | Decreasing Trend | Decreasing Trend |
| 16 | 17162 | Gemerek | No Trend | No Trend | Increasing Trend | Increasing Trend | Increasing Trend | Increasing Trend |
| 17 | 17193 | Nevşehir | No Trend | No Trend | Increasing Trend | Increasing Trend | Increasing Trend | Increasing Trend |
| 18 | 17196 | Kayseri | No Trend | No Trend | No Trend | No Trend | No Trend | No Trend |
| 19 | 176 | Bafra | Decreas | Decreas | Decreas | Increasi | Decreas | Decreas |

| | | | | | | | | |
|---|---|---|---|---|---|---|---|---|
| | 22 | | ing Trend | ing Trend | ing Trend | ng Trend | ing Trend | ing Trend |
| 20 | 17648 | Ilgaz | No Trend | No Trend | No Trend | Decreasing Trend | No Trend | Decreasing Trend |
| 21 | 17650 | Tosya | No Trend | No Trend | No Trend | Decreasing Trend | No Trend | Decreasing Trend |
| 22 | 17652 | Osmancık | Increasing Trend | Increasing Trend | Increasing Trend | Increasing Trend | Increasing Trend | Increasing Trend |
| 23 | 17716 | Zara | Decreasing Trend | Decreasing Trend | Decreasing Trend | Decreasing Trend | Decreasing Trend | Decreasing Trend |
| 24 | 17730 | Keskin | Decreasing Trend | Decreasing Trend | Decreasing Trend | Decreasing Trend | Decreasing Trend | Decreasing Trend |
| 25 | 17732 | Çiçekdağı | Decreasing Trend | Decreasing Trend | Decreasing Trend | Decreasing Trend | Decreasing Trend | Decreasing Trend |
| 26 | 17756 | Kaman | No Trend | No Trend | Decreasing Trend | Decreasing Trend | Decreasing Trend | Decreasing Trend |
| 27 | 17760 | Boğazlıyan | Decreasing Trend | Decreasing Trend | Decreasing Trend | Decreasing Trend | Decreasing Trend | Decreasing Trend |
| 28 | 17835 | Ürgüp | Decreasing Trend | Decreasing Trend | Decreasing Trend | Decreasing Trend | Decreasing Trend | Decreasing Trend |
| 29 | 17836 | Develi | No Trend | No Trend | No Trend | No Trend | No Trend | No Trend |
| 30 | 17244 | Konya | Decreasing Trend | Decreasing Trend | Decreasing Trend | Decreasing Trend | Decreasing Trend | Decreasing Trend |
| 31 | 17246 | Karaman | No Trend | No Trend | No Trend | Decreasing Trend | Decreasing Trend | Decreasing Trend |
| 32 | 17248 | Ereğli | No Trend | No Trend | No Trend | Increasing Trend | Increasing Trend | Increasing Trend |
| 33 | 17250 | Niğde | No Trend | Increasing Trend | Increasing Trend | Increasing Trend | Increasing Trend | Increasing Trend |
| 34 | 17754 | Kulu | Decreasing Trend | Decreasing Trend | Decreasing Trend | Decreasing Trend | Decreasing Trend | Decreasing Trend |
| 35 | 17898 | Seydişehir | No Trend | No Trend | Increasing Trend | Increasing Trend | Increasing Trend | Increasing Trend |
| 36 | 17900 | Çumra | No Trend | No Trend | Decreasing Trend | Decreasing Trend | Decreasing Trend | Decreasing Trend |
| 37 | 17902 | Karapınar | No Trend | No Trend | No Trend | No Trend | No Trend | Decreasing |

| | | | | | | | | |
|---|---|---|---|---|---|---|---|---|
| | | | | | | | | Trend |
| 38 | 17192 | Aksaray | No Trend | Decreasing Trend | Decreasing Trend | Decreasing Trend | Decreasing Trend | Decreasing Trend |

**Table 4. 20.** ITA trend test results for RDI

| Order | St. No. | Name | 3 | 6 | 9 | 12 |
|---|---|---|---|---|---|---|
| 1 | 17030 | Samsun | No Trend | No Trend | No Trend | No Trend |
| 2 | 17083 | Merzifon | Decreasing Trend | No Trend | No Trend | No Trend |
| 3 | 17084 | Çorum | No Trend | No Trend | Decreasing Trend | Decreasing Trend |
| 4 | 17085 | Amasya | No Trend | No Trend | No Trend | No Trend |
| 5 | 17086 | Tokat | No Trend | No Trend | Decreasing Trend | Decreasing Trend |
| 6 | 17681 | Zile | No Trend | Decreasing Trend | Decreasing Trend | Decreasing Trend |
| 7 | 17683 | Turhal | No Trend | No Trend | Decreasing Trend | Decreasing Trend |
| 8 | 17684 | Suşehri | Decreasing Trend | Decreasing Trend | Decreasing Trend | Decreasing Trend |
| 9 | 17682 | Şebinkarahisar | No Trend | Decreasing Trend | Decreasing Trend | Decreasing Trend |
| 10 | 17074 | Kastamonu | No Trend | No Trend | Increasing Trend | Increasing Trend |
| 11 | 17080 | Çankırı | No Trend | No Trend | No Trend | Increasing Trend |
| 12 | 17090 | Sivas | No Trend | No Trend | Decreasing Trend | Decreasing Trend |
| 13 | 17135 | Kırıkkale | No Trend | No Trend | Decreasing Trend | Decreasing Trend |
| 14 | 17140 | Yozgat | No Trend | Decreasing Trend | Decreasing Trend | Decreasing Trend |
| 15 | 17160 | Kırşehir | No Trend | No Trend | Decreasing Trend | Decreasing Trend |
| 16 | 17162 | Gemerek | No Trend | No Trend | No Trend | No Trend |
| 17 | 17193 | Nevşehir | No Trend | Decreasing Trend | Decreasing Trend | Decreasing Trend |
| 18 | 17196 | Kayseri | No Trend | Decreasing Trend | Decreasing Trend | Decreasing Trend |
| 20 | 17648 | Ilgaz | No Trend | No Trend | No Trend | No Trend |
| 21 | 17650 | Tosya | No Trend | No Trend | Decreasing Trend | Decreasing Trend |
| 22 | 17652 | Osmancık | No Trend | No Trend | Increasing Trend | Increasing Trend |
| 23 | 17716 | Zara | Decreasing Trend | Decreasing Trend | Decreasing Trend | Decreasing Trend |
| 24 | 17730 | Keskin | Decreasing Trend | Decreasing Trend | Decreasing Trend | Decreasing Trend |
| 25 | 17732 | Çiçekdağı | Decreasing Trend | Decreasing Trend | Decreasing Trend | Decreasing Trend |

| | | | | | | |
|---|---|---|---|---|---|---|
| 26 | 17756 | Kaman | No Trend | Decreasing Trend | Decreasing Trend | Decreasing Trend |
| 27 | 17760 | Boğazlıyan | No Trend | Decreasing Trend | Decreasing Trend | Decreasing Trend |
| 28 | 17835 | Ürgüp | No Trend | Decreasing Trend | Decreasing Trend | Decreasing Trend |
| 29 | 17836 | Develi | No Trend | No Trend | Decreasing Trend | Decreasing Trend |
| 30 | 17244 | Konya | No Trend | Decreasing Trend | Decreasing Trend | Decreasing Trend |
| 31 | 17246 | Karaman | No Trend | Decreasing Trend | Decreasing Trend | Decreasing Trend |
| 32 | 17248 | Ereğli | No Trend | No Trend | No Trend | Decreasing Trend |
| 33 | 17250 | Niğde | No Trend | No Trend | No Trend | No Trend |
| 34 | 17754 | Kulu | No Trend | Decreasing Trend | Decreasing Trend | Decreasing Trend |
| 35 | 17898 | Seydişehir | Decreasing Trend | Decreasing Trend | Decreasing Trend | Decreasing Trend |
| 36 | 17900 | Çumra | No Trend | Decreasing Trend | Decreasing Trend | Decreasing Trend |
| 37 | 17902 | Karapınar | No Trend | No Trend | Decreasing Trend | Decreasing Trend |
| 38 | 17192 | Aksaray | No Trend | Decreasing Trend | Decreasing Trend | Decreasing Trend |

**Table 4. 21.** ITA trend test results for SPEI bf

| Order | St. No. | Name | 3 | 12 |
|---|---|---|---|---|
| 1 | 17030 | Samsun | No Trend | Decreasing Trend |
| 2 | 17083 | Merzifon | No Trend | Increasing Trend |
| 3 | 17084 | Çorum | No Trend | No Trend |
| 4 | 17085 | Amasya | No Trend | Increasing Trend |
| 5 | 17086 | Tokat | Decreasing Trend | Decreasing Trend |
| 6 | 17681 | Zile | Decreasing Trend | Decreasing Trend |
| 7 | 17683 | Turhal | Decreasing Trend | Decreasing Trend |
| 8 | 17684 | Suşehri | Decreasing Trend | Decreasing Trend |
| 9 | 17682 | Şebinkarahisar | Decreasing Trend | Decreasing Trend |
| 10 | 17074 | Kastamonu | Increasing Trend | Increasing Trend |
| 11 | 17080 | Çankırı | Increasing Trend | Increasing Trend |

| | | | | |
|---|---|---|---|---|
| 12 | 17090 | Sivas | No Trend | Decreasing Trend |
| 13 | 17135 | Kırıkkale | No Trend | No Trend |
| 14 | 17140 | Yozgat | Decreasing Trend | Decreasing Trend |
| 15 | 17160 | Kırşehir | Decreasing Trend | Decreasing Trend |
| 16 | 17162 | Gemerek | No Trend | No Trend |
| 17 | 17193 | Nevşehir | Decreasing Trend | Decreasing Trend |
| 18 | 17196 | Kayseri | No Trend | Decreasing Trend |
| 19 | 17622 | Bafra | Decreasing Trend | Decreasing Trend |
| 20 | 17648 | Ilgaz | Decreasing Trend | Decreasing Trend |
| 21 | 17650 | Tosya | Decreasing Trend | Decreasing Trend |
| 22 | 17652 | Osmancık | Increasing Trend | Increasing Trend |
| 23 | 17716 | Zara | Decreasing Trend | Decreasing Trend |
| 24 | 17730 | Keskin | Decreasing Trend | Decreasing Trend |
| 25 | 17732 | Çiçekdağı | Decreasing Trend | Decreasing Trend |
| 26 | 17756 | Kaman | Decreasing Trend | Decreasing Trend |
| 27 | 17760 | Boğazlıyan | Decreasing Trend | Decreasing Trend |
| 28 | 17835 | Ürgüp | Decreasing Trend | Decreasing Trend |
| 29 | 17836 | Develi | Decreasing Trend | Decreasing Trend |
| 30 | 17244 | Konya | Decreasing Trend | Decreasing Trend |
| 32 | 17248 | Ereğli | No Trend | No Trend |
| 33 | 17250 | Niğde | No Trend | No Trend |
| 34 | 17754 | Kulu | Decreasing Trend | Decreasing Trend |
| 35 | 17898 | Seydişehir | No Trend | Decreasing Trend |
| 36 | 17900 | Çumra | Decreasing Trend | Decreasing Trend |
| 37 | 17902 | Karapınar | Decreasing Trend | Decreasing Trend |
| 38 | 17192 | Aksaray | Decreasing Trend | Decreasing Trend |

**Table 4. 22.** ITA trend test results for SRI

| **Order** | **St. No.** | **Name** | **3** | **6** | **9** | **12** | **24** |
|---|---|---|---|---|---|---|---|
| 1 | E15A001 | Kızılırmak Yamula | No Trend | No Trend | Decreasing Trend | Decreasing Trend | Decreasing Trend |
| 2 | E15A017 | Karanlık Deresi Şefaatli | Decreasing Trend | Decreasing Trend | Decreasing Trend | Decreasing Trend | Decreasing Trend |
| 3 | E15A039 | Kızılırmak Bulakbaşı | No Trend | No Trend | Decreasing Trend | Decreasing Trend | Decreasing Trend |
| 4 | E15A041 | Delice Çayı Çadırhöyük | Decreasing Trend | Decreasing Trend | Decreasing Trend | Decreasing Trend | Decreasing Trend |
| 5 | E14A00 | Yeşilırma | Increasin | Increasin | Increasin | Increasin | Increasin |

| | | | | | | | |
|---|---|---|---|---|---|---|---|
| | 2 | k Kale | g Trend | g Trend | g Trend | g Trend | g Trend |
| 6 | E14A012 | Çorum Çat Irmağı | Decreasing Trend | Decreasing Trend | No Trend | Decreasing Trend | Decreasing Trend |
| 7 | E14A014 | Yeşilırmak Sütlüce | Decreasing Trend | Decreasing Trend | Decreasing Trend | Decreasing Trend | Decreasing Trend |
| 8 | E14A022 | Kelkit Çayı Çiçekbükü | Decreasing Trend | Decreasing Trend | Decreasing Trend | No Trend | Decreasing Trend |
| 9 | E14A027 | Kelkit Çayı Yemişli Köprüsü | Decreasing Trend | Decreasing Trend | Decreasing Trend | Decreasing Trend | Decreasing Trend |

The results of the ITA graphical method are presented in the Figure 4.58-4.61. If the data is very close to the 1:1 line, it means there is no trend, if the data is in the upper part of the 1:1 line, it means there is an increasing trend, if the data is in the lower part of the 1:1 line, it means there is a decreasing trend.

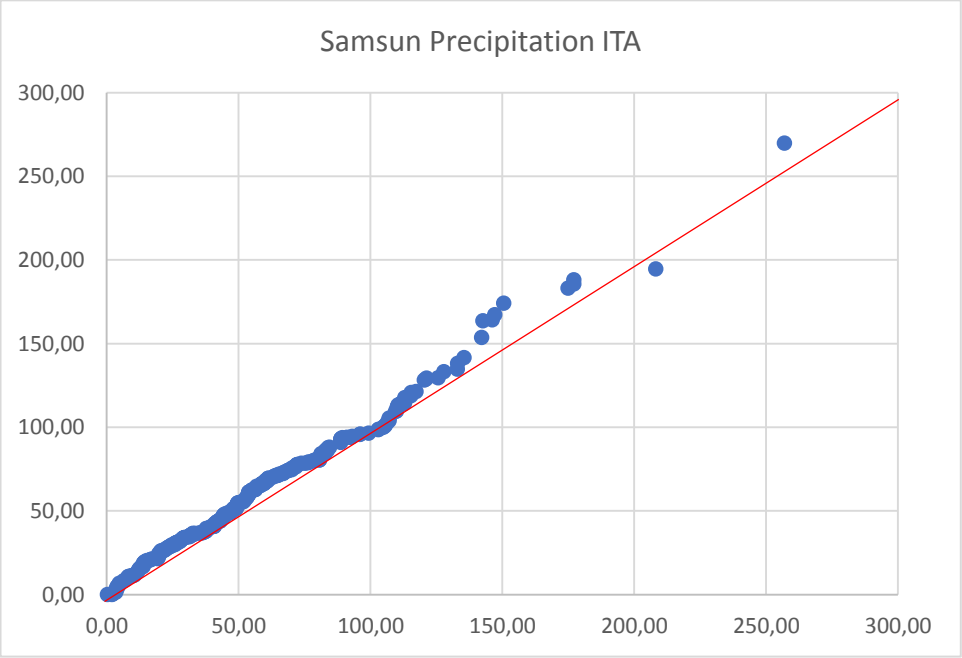


**Figure 4. 58.** Samsun Station Precipitation ITA result graph (no trend)

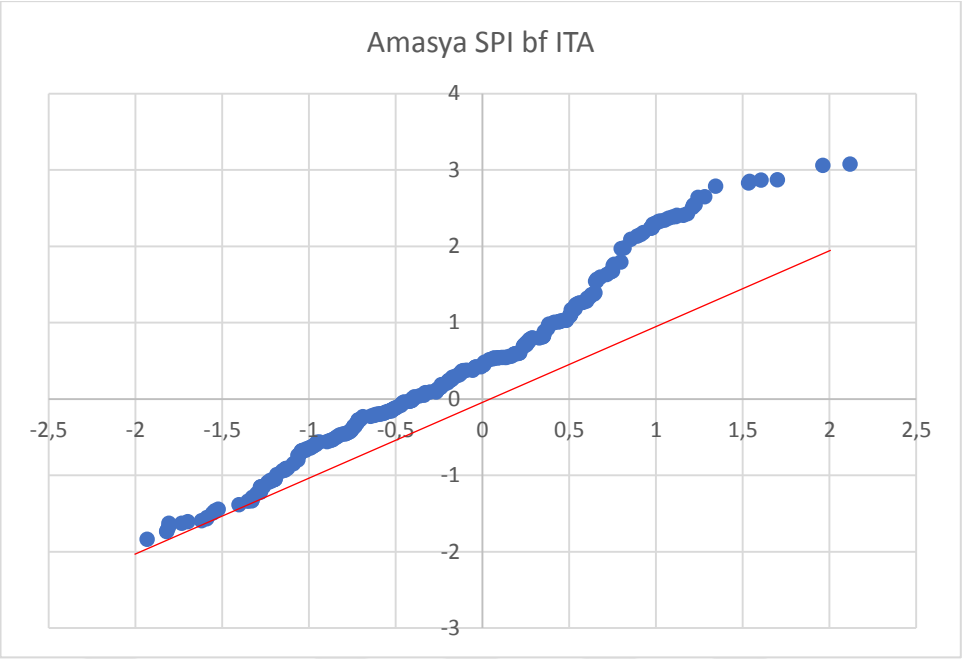


**Figure 4. 59.** Amasya Station SPI bf ITA result graph (increasing trend)

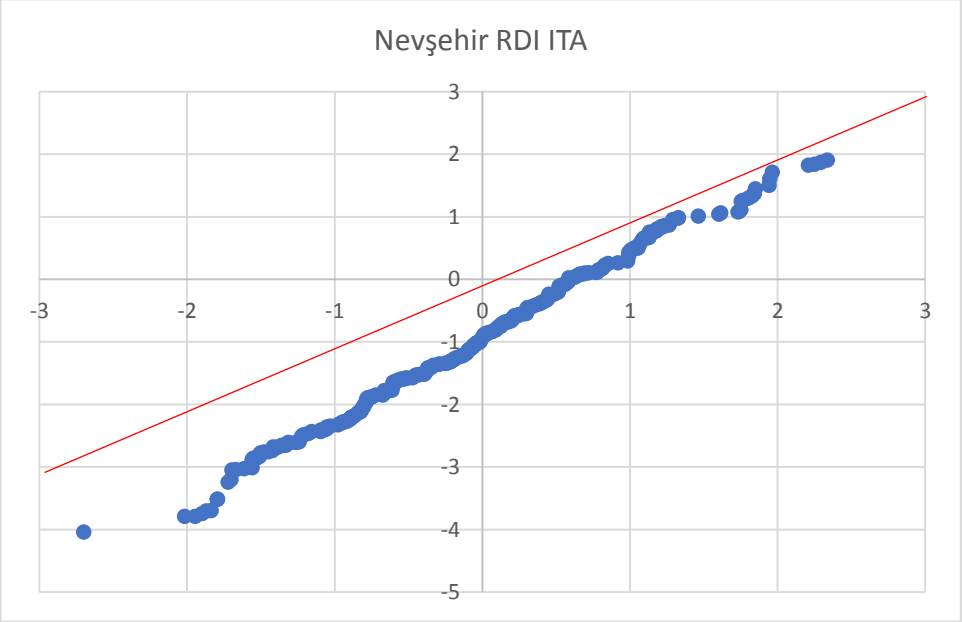


**Figure 4. 60.** Nevşehir Station RDI ITA result graph (decreasing trend)

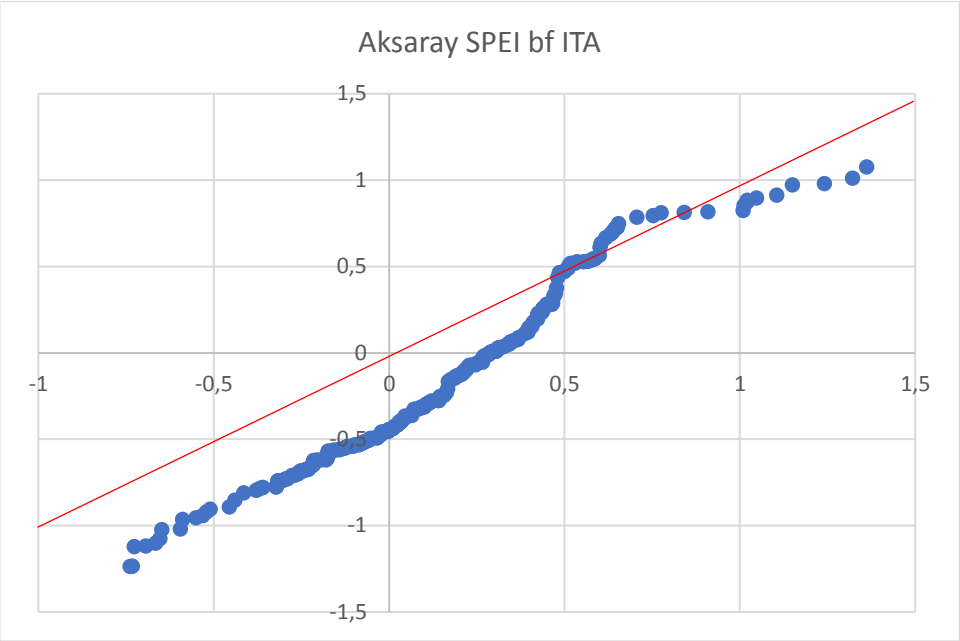


**Figure 4. 61.** Aksaray Station SPEI bf ITA result graph (decreasing trend)

### 4.6.3. Trend Analysis Comparison

The MK and ITA trend test analyses results were presented comparatively on basin maps according to the coordinates of each station.

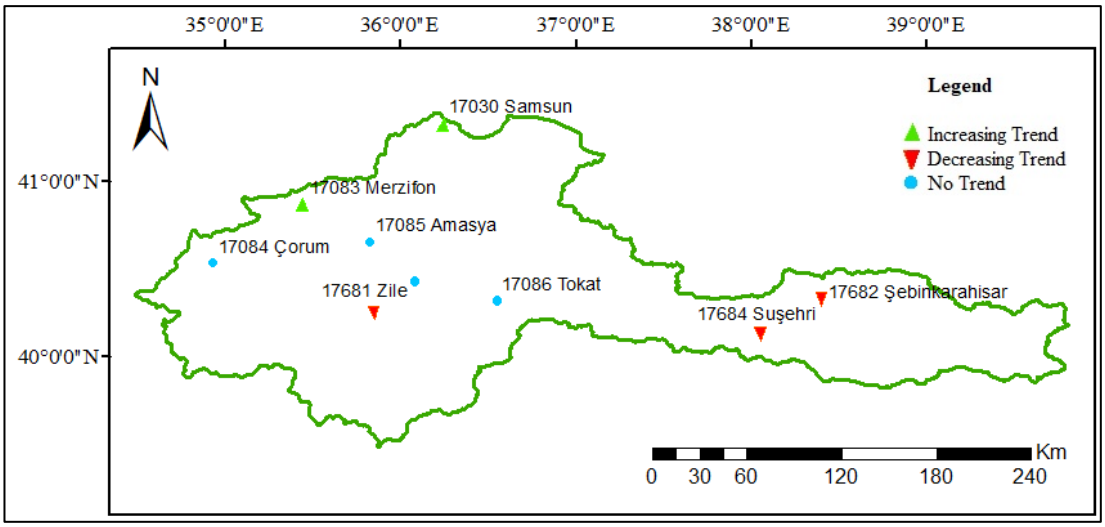

**Figure 4. 62.** Yeşilırmak basin SPI 3 bf MK trend distribution map

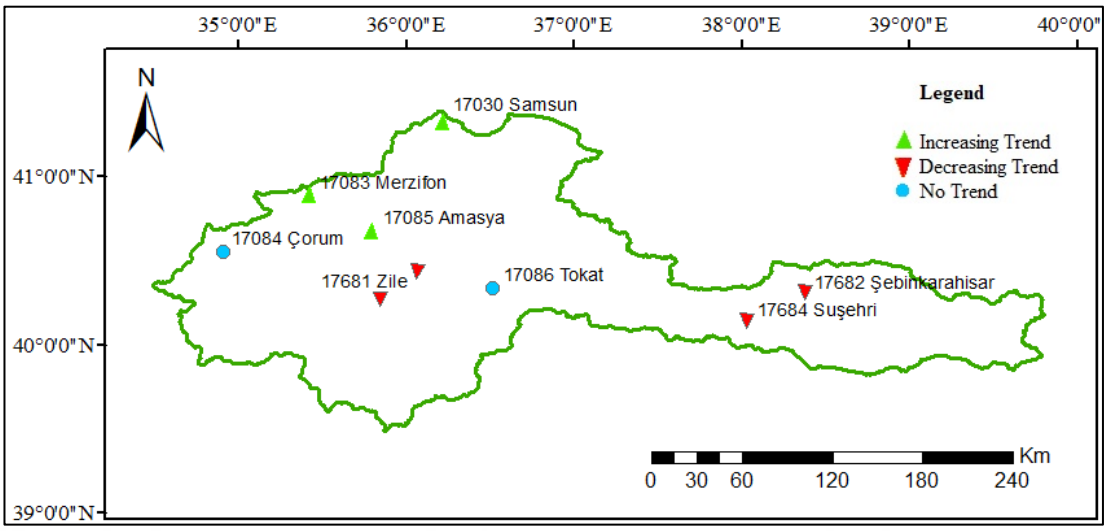


**Figure 4. 63.** Yeşilırmak basin SPI 3 bf ITA trend distribution map

As can be seen in the figures, for the SPI 3-month bf trend analysis in the Yeşilırmak basin, with the MK (Mann-Kendall) method, "no trend" was found in the middle regions of the basin, while the ITA (Integrated Trend Analysis) method identified a "decreasing trend." Both methods found the same results in other regions of the basin.

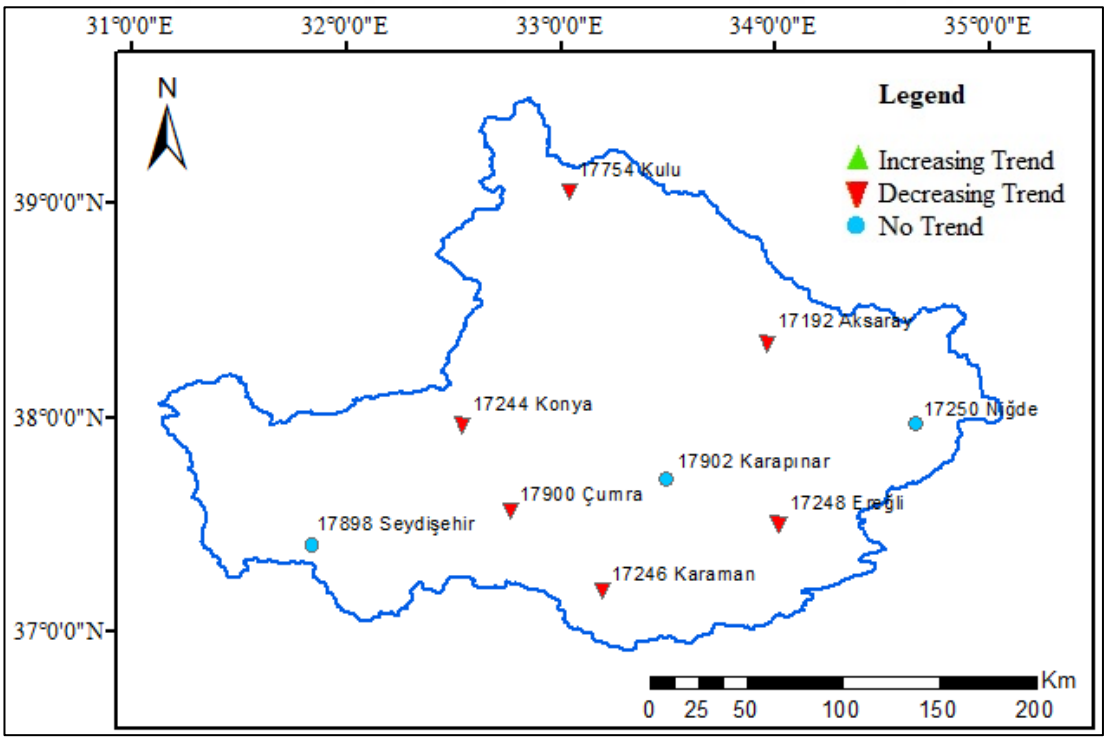


**Figure 4. 64.** Konya basin SPEI 12 bf MK trend distribution map

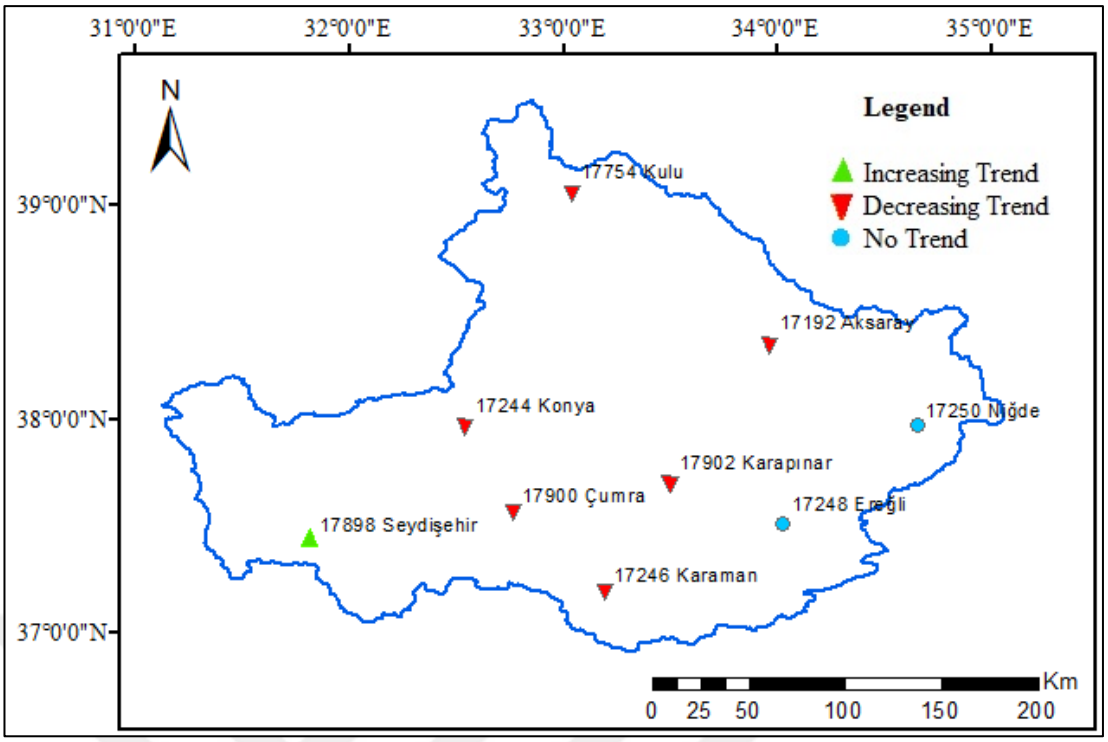


**Figure 4. 65.** Konya basin SPEI 12 bf ITA trend distribution map

As can be seen in the figures, the MK and ITA methods have produced almost identical results in the trend analysis of SPEI 12-month bf in the Konya basin. The only difference is that at the Seydişehir station, the MK method detected "no trend," while the ITA method identified an "increasing trend."

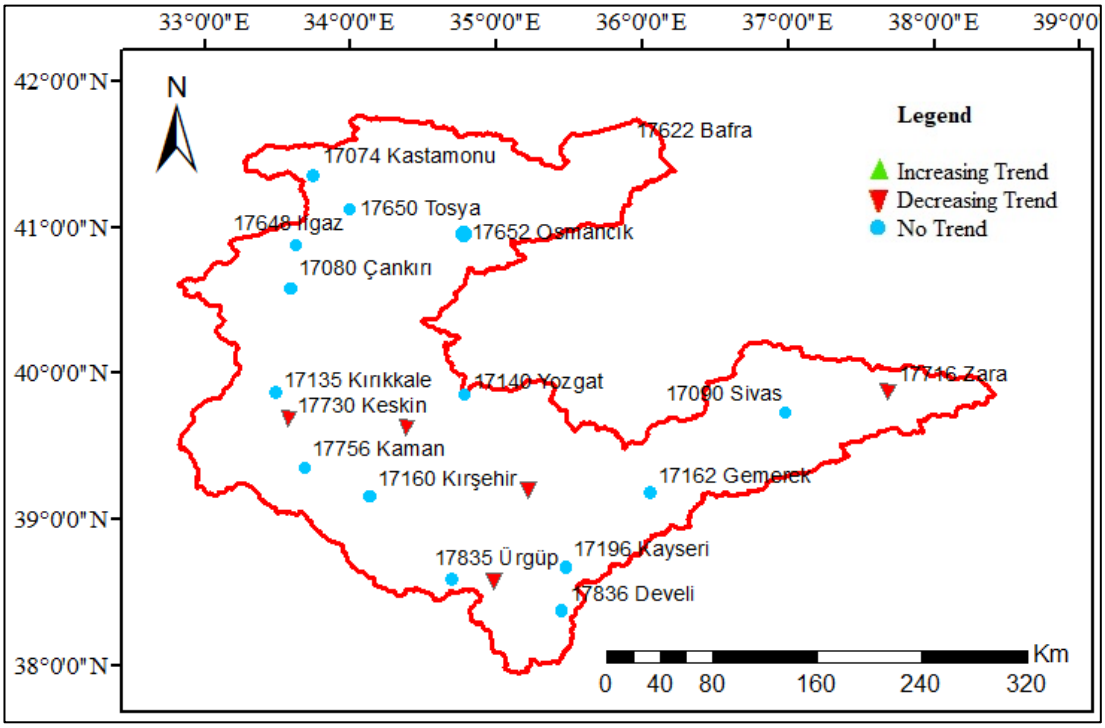


**Figure 4. 66.** Kızılırmak basin RDI 6 MK trend distribution map

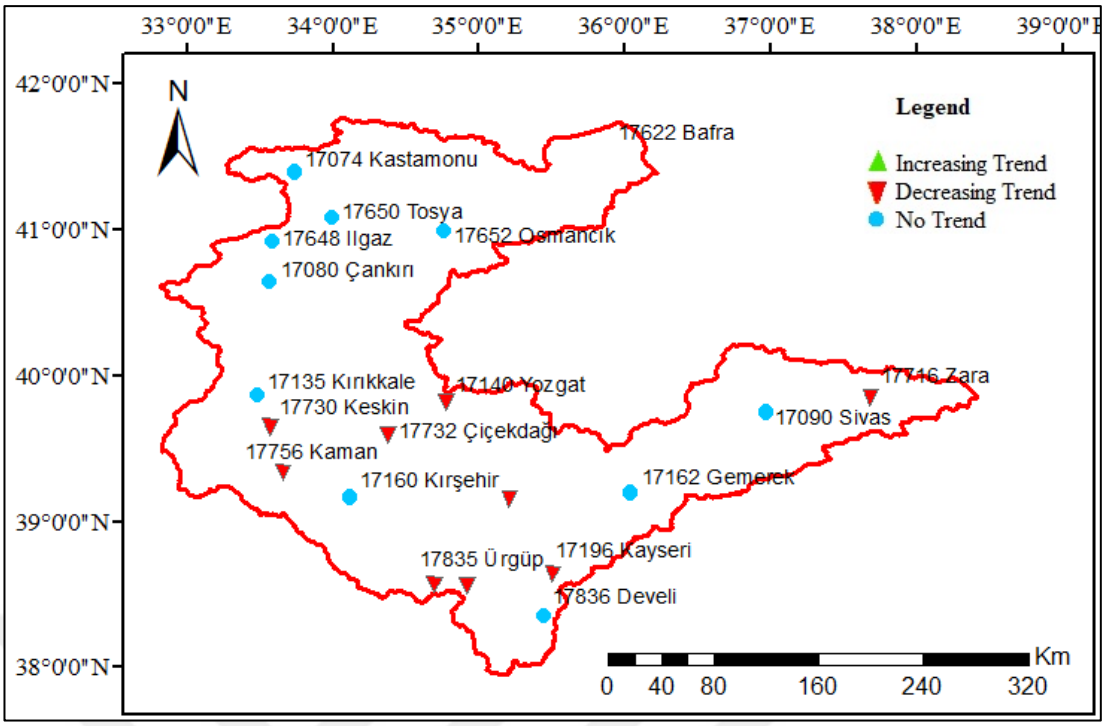


**Figure 4. 67.** Kızılırmak basin RDI 6 ITA trend distribution map

As can be seen in the figures, the trend analysis of RDI 6 months for Kızılırmak basin using the MK method mainly yielded "no trend" results. In contrast, the ITA method resulted in a higher number of "decreasing trends."

The following tables show the number of trend types found for each basin and drought index. These tables help to better understand the difference between MK and ITA methods.

**Table 4. 23.** MK Precipitation trend numbers for the basins

| MK Precipitation | No Trend | Increasing Trend | Decreasing Trend |
|---|---|---|---|
| Yeşilırmak | 9 | 0 | 0 |
| Kızılırmak | 16 | 1 | 3 |
| Konya | 8 | 0 | 1 |

**Table 4. 24.** ITA Precipitation trend numbers for the basins

| ITA Precipitation | No Trend | Increasing Trend | Decreasing Trend |
|---|---|---|---|
| Yeşilırmak | 7 | 1 | 1 |
| Kızılırmak | 12 | 3 | 5 |
| Konya | 8 | 0 | 1 |

As can be seen in the precipitation trend tables, the MK method mostly found "no trend," while the ITA method found more "increasing trend" and "decreasing trend."

**Table 4. 25.** MK 3-month trend numbers for the basins

| **MK** | **No Trend** | | | **Increasing Trend** | | | **Decreasing Trend** | | |
|---|---|---|---|---|---|---|---|---|---|
| 3 Month | SPI bf | SPEI bf | RDI | SPI bf | SPEI bf | RDI | SPI bf | SPEI bf | RDI |
| Yeşilırmak | 4 | 5 | 9 | 2 | 1 | 0 | 3 | 3 | 0 |
| Kızılırmak | 12 | 16 | 19 | 3 | 0 | 0 | 5 | 4 | 0 |
| Konya | 8 | 7 | 9 | 0 | 0 | 0 | 1 | 1 | 0 |

**Table 4. 26.** ITA 3-month trend numbers for the basins

| **ITA** | **No Trend** | | | **Increasing Trend** | | | **Decreasing Trend** | | |
|---|---|---|---|---|---|---|---|---|---|
| 3 Month | SPI bf | SPEI bf | RDI | SPI bf | SPEI bf | RDI | SPI bf | SPEI bf | RDI |
| Yeşilırmak | 2 | 4 | 7 | 3 | 0 | 0 | 4 | 5 | 2 |
| Kızılırmak | 10 | 4 | 16 | 3 | 3 | 0 | 7 | 13 | 3 |
| Konya | 5 | 3 | 8 | 1 | 0 | 0 | 3 | 5 | 1 |

As can be seen in the tables, in the MK method, "no trend" was mostly found for each of the three drought indices, while in the ITA method, "decreasing trend" was found more frequently.

**Table 4. 27.** MK 12-month trend numbers for the basins

| **MK** | **No Trend** | | | **Increasing Trend** | | | **Decreasing Trend** | | |
|---|---|---|---|---|---|---|---|---|---|
| 12 Month | SPI bf | SPEI bf | RDI | SPI bf | SPEI bf | RDI | SPI bf | SPEI bf | RDI |
| Yeşilırmak | 2 | 3 | 1 | 3 | 3 | 2 | 4 | 3 | 6 |
| Kızılırmak | 6 | 14 | 4 | 6 | 1 | 3 | 8 | 5 | 12 |
| Konya | 7 | 7 | 3 | 1 | 0 | 0 | 1 | 1 | 6 |

**Table 4. 28.** ITA 12-month trend numbers for the basins

| **ITA** | **No Trend** | | | **Increasing Trend** | | | **Decreasing Trend** | | |
|---|---|---|---|---|---|---|---|---|---|
| 12 Month | SPI bf | SPEI bf | RDI | SPI bf | SPEI bf | RDI | SPI bf | SPEI bf | RDI |
| Yeşilırmak | 0 | 1 | 3 | 4 | 2 | 0 | 5 | 6 | 6 |
| Kızılırmak | 5 | 2 | 2 | 6 | 3 | 3 | 9 | 15 | 14 |
| Konya | 1 | 2 | 1 | 3 | 0 | 0 | 5 | 6 | 8 |

As can be seen in the tables, MK and ITA methods found almost the same results.

### 4.7. Magnitude-Duration-Frequency (MDF)

Magnitude-Duration-Frequency (MDF) analyses are performed to characterize drought and predict the duration of future drought magnitudes. MDF curves of each station were obtained for each drought method. In order to obtain MDF curves, first, the magnitude, duration and frequency values of the 3-month drought values were extracted, and the magnitude values from these extracted data was classified into 2-month durations (0-2, 2-4, 4-6, 6-8) and sorted out. It was not possible to obtain enough results to calculate frequency in 6-, 9- and 12- month of drought data, so frequency calculation was made according to only 3 months of drought results. Accordingly, the frequency intervals of 2, 5, 10, 25, 50, 100 years were calculated and the result were given. The MDF graphics for the selected station are given in the Figures 4.68- 4.76.

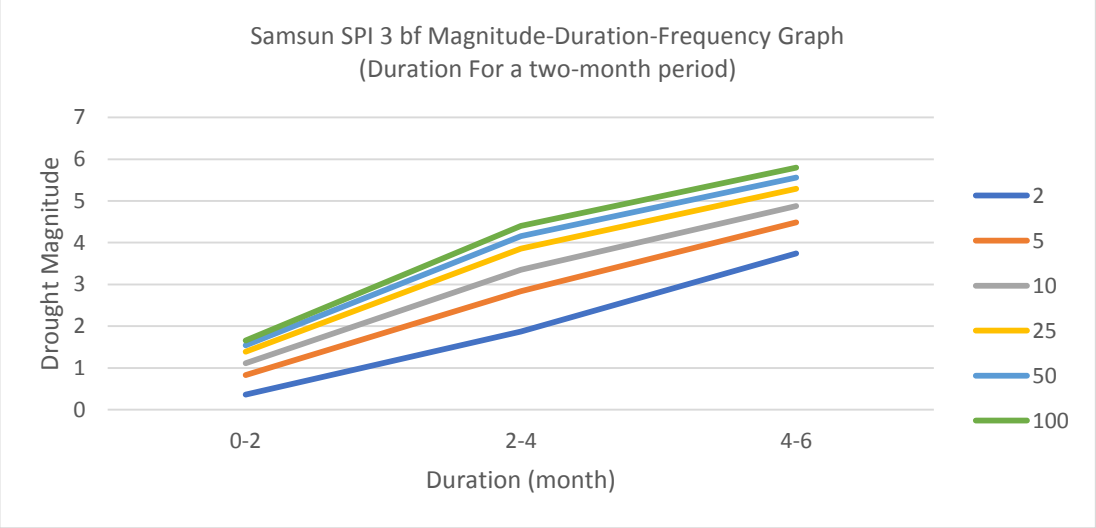


**Figure 4. 68.** Samsun SPI 3 bf MDF graph

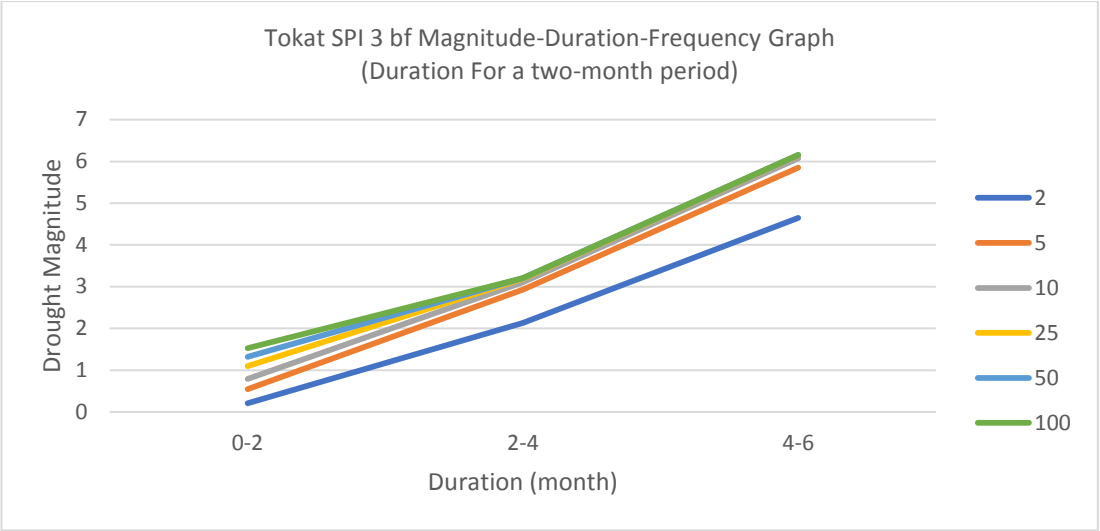


**Figure 4. 69.** Tokat SPI 3 bf MDF graph

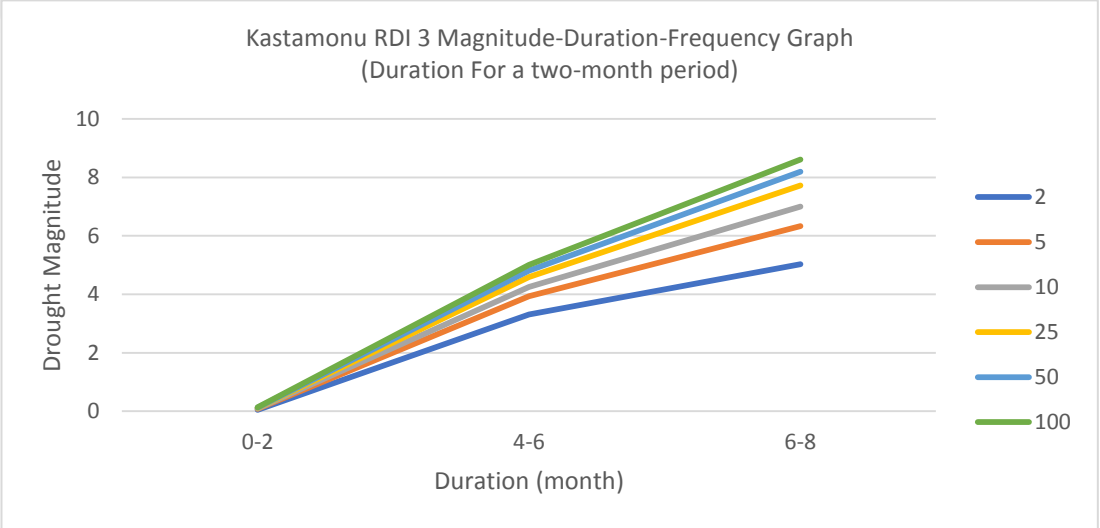


**Figure 4. 70.** Kastamonu RDI3 MDF graph

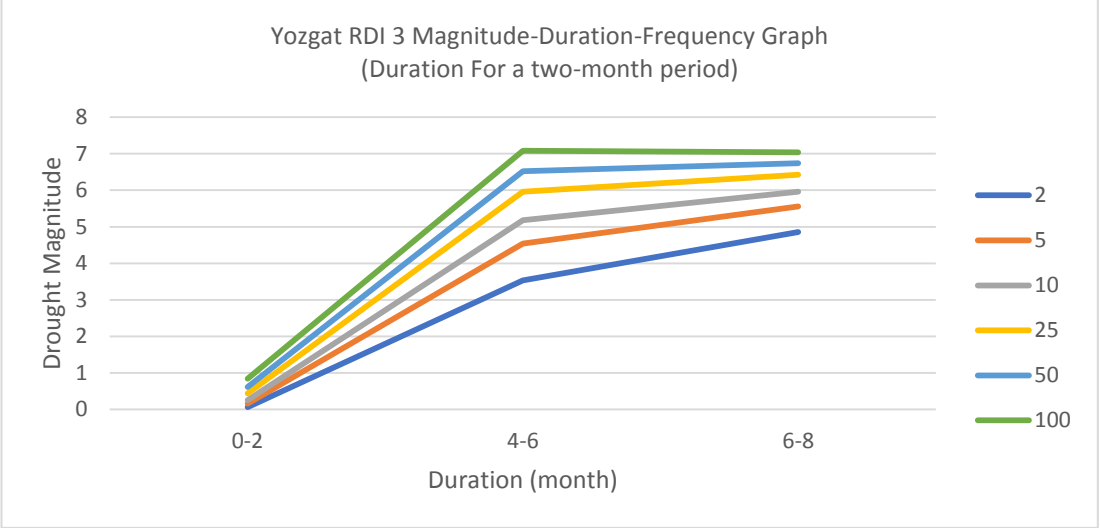


**Figure 4. 71.** Yozgat RDI3 MDF graph

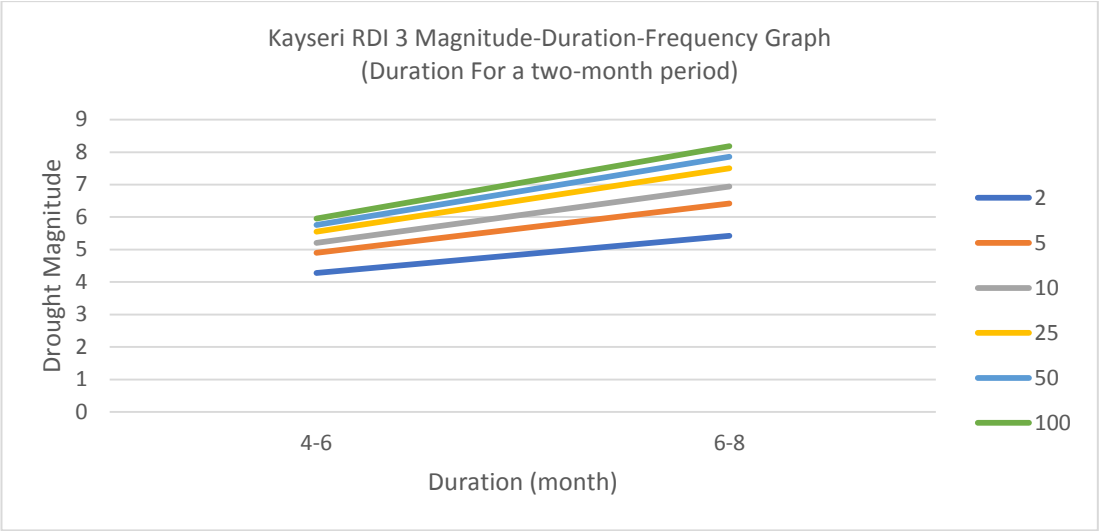


**Figure 4. 72.** Kayseri RDI3 MDF graph

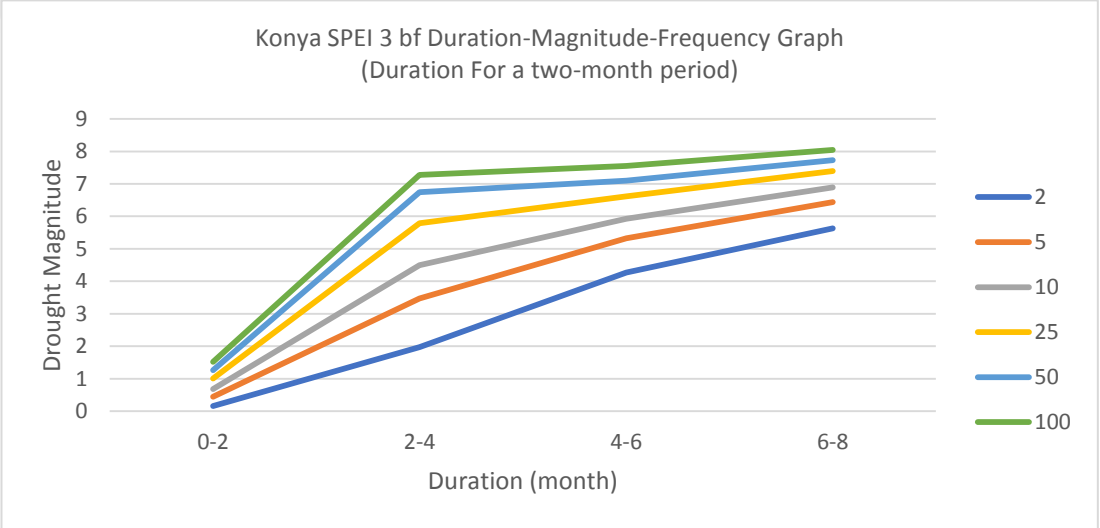


**Figure 4. 73.** Konya SPEI 3 bf MDF graph

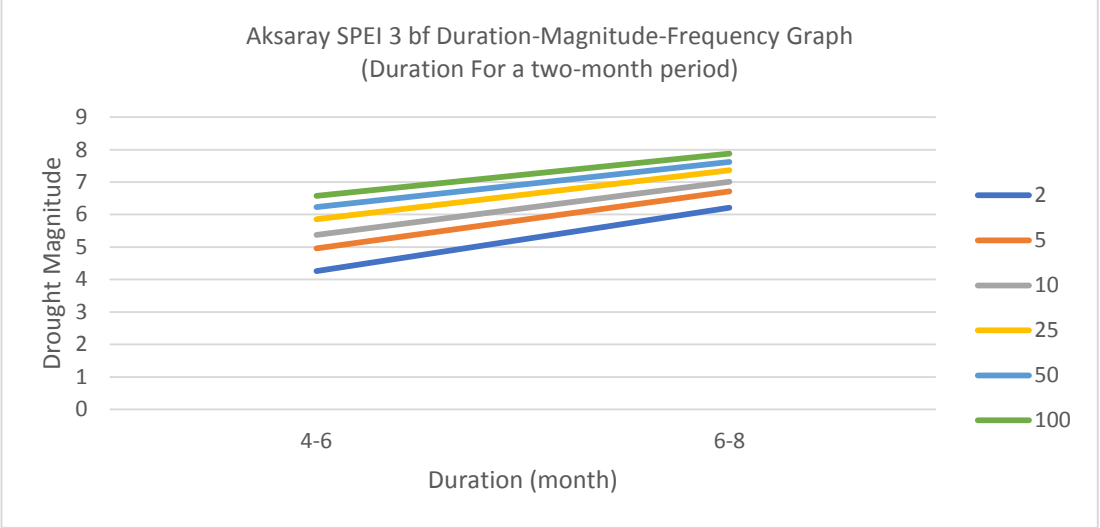


**Figure 4. 74.** Aksaray SPEI 3 bf MDF graph

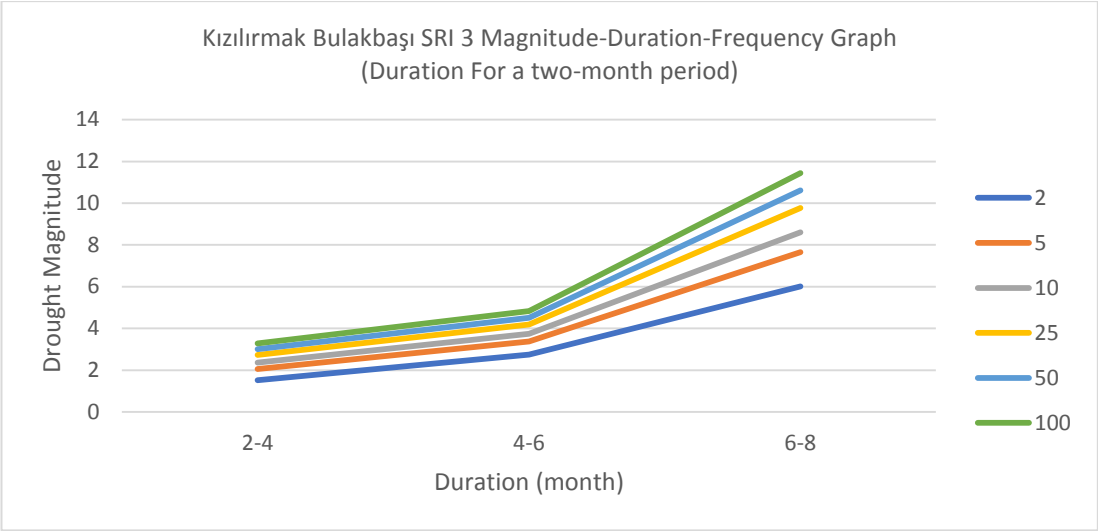


**Figure 4. 75.** Kızılırmak Bulakbaşı SRI3 MDF graph

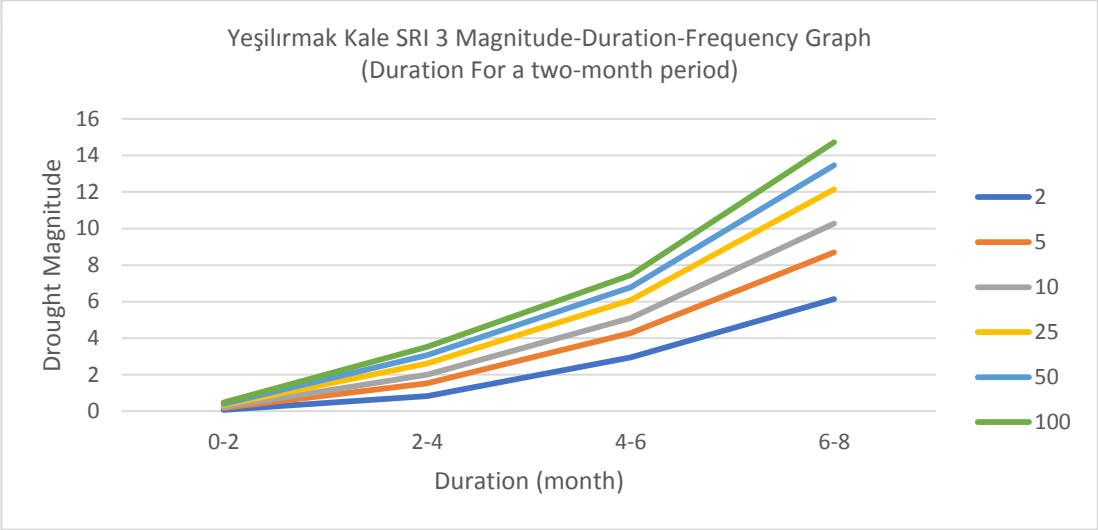


**Figure 4. 76.** Yeşilırmak Kale SRI3 MDF graph

The MDF analyses presented in Figure 4.68- 4.76 can be interpreted as follows: For the 3-month SPI bf analysis at the Samsun station, a drought with a magnitude of 4, corresponding to a 25-year recurrence interval, will last between 2-4 months. For the 3-month RDI analysis at the Kayseri station, a drought with a magnitude of 5, corresponding to a 5-year recurrence interval, will last between 4-6 months. For the 3-month SPEI bf analysis at the Aksaray station, a drought with a magnitude of 3.6, corresponding to a 100-year recurrence interval, will last between 6-8 months. Similar evaluations are conducted for the other stations.

### 4.1. Magnitude-Duration-Frequency (MDF) Comparison

MDF results were classified based on the recurrence intervals and Drought indices in order to compare the differences for each stations. The MDF comparison graphics for the selected stations are given in the Figures 4.77 - 4.84.

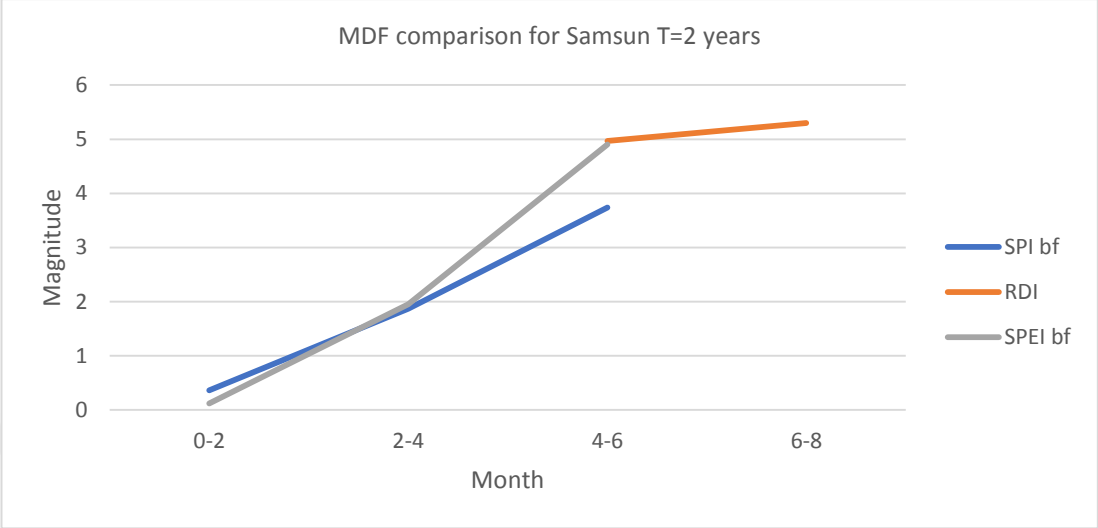


**Figure 4. 77.** MDF comparison for Samsun T=2 years

When examining the MDF comparison graph for the Samsun station for 2-year recurrence, it can be observed that for short and medium-term periods, SPEI bf (0.12-4.9) yields higher magnitudes compared to SPI bf (0.36-3.74), while RDI (4.97-5.3) yields very high magnitudes for longer periods.

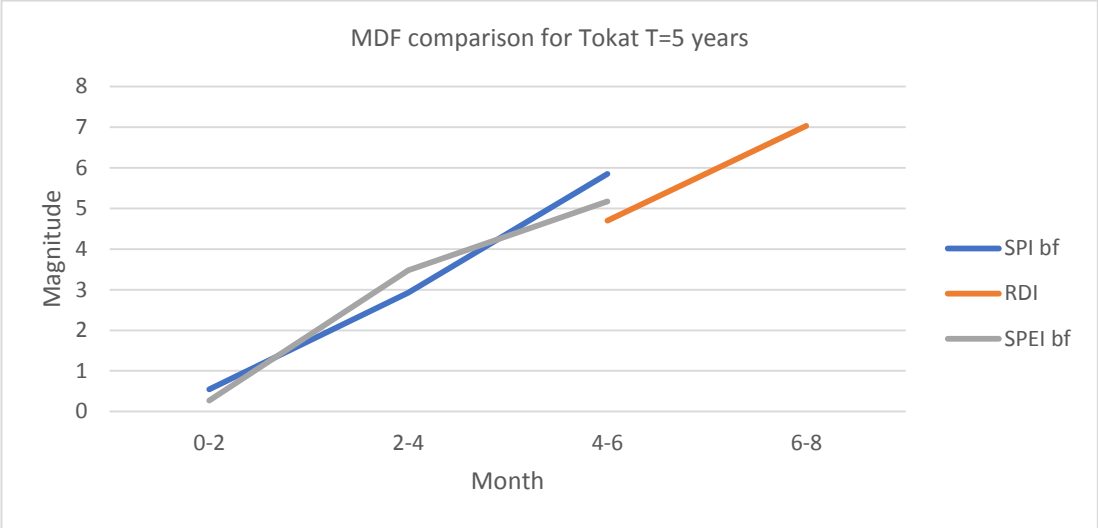


**Figure 4. 78.** MDF comparison for Tokat T=5 years

When examining the MDF comparison graph for the Tokat station for 5-year recurrence, it can be observed that for short and medium-term periods, SPEI bf

(0.27-5.17) and SPI bf (0.55-5.85) yield similar magnitudes, while RDI (4.7-7.03) yields higher magnitudes for longer periods.

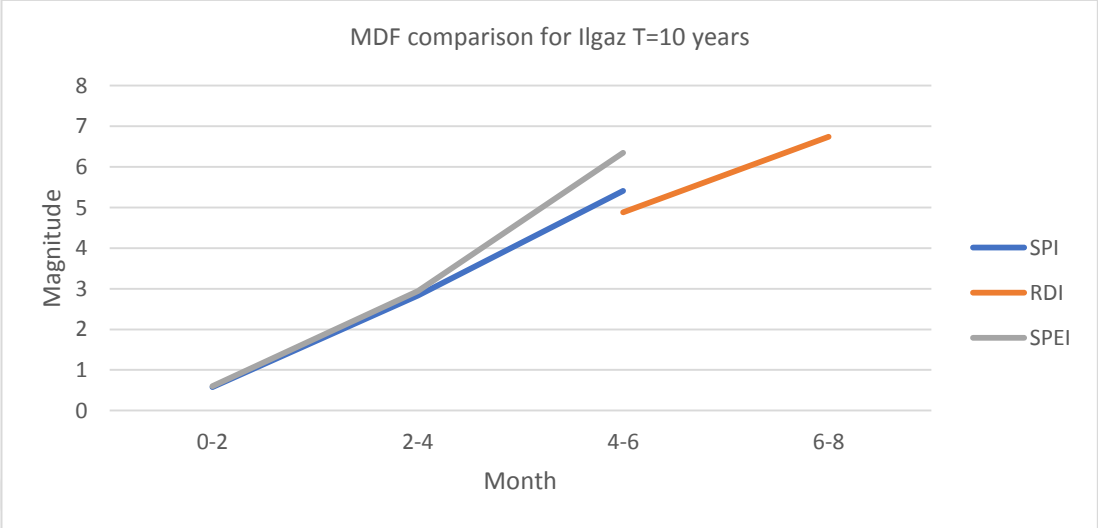


**Figure 4. 79.** MDF comparison for Ilgaz T=10 years

When examining the graph for the Ilgaz station, it can be observed that for short-term periods, SPEI bf (0.6-2.94) and SPI bf (0.58-2.83) yield similar magnitudes. However, for medium-term periods, SPEI bf (2.94-6.35) yields higher magnitudes compared to SPI bf (2.83-5.41). In contrast, for long-term periods, only RDI (6.04-7.99) yields significantly higher magnitudes. SPI bf and SPEI bf do not yield any results for the long-term period.

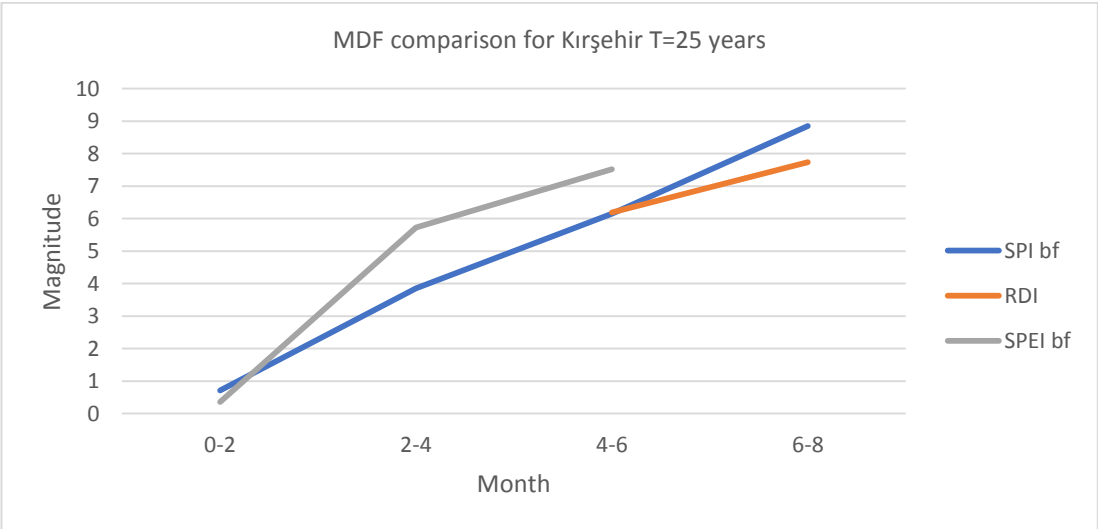


**Figure 4. 80.** MDF comparison for Kırşehir T=25 years

When examining the MDF comparison graph for the Kırşehir station, it can be observed that for short and medium-term periods, SPEI bf (0.36-7.52) yields higher

magnitudes than SPI bf (0.71-6.15), while for long-term periods, SPI bf (6.15-8.85) yields higher magnitudes than RDI (6.19-7.74).

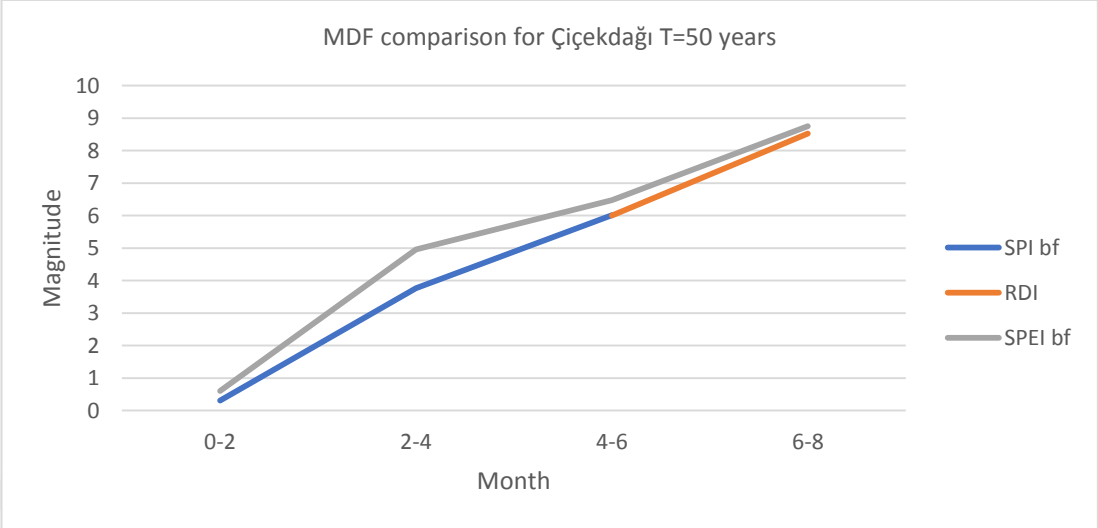


**Figure 4. 81.** MDF comparison for Çiçekdağı T=50 years

When examining the graph for Çiçekdağı station, it is observed that for short and medium-term periods, SPEI bf (0.6-6.48) yields higher magnitudes than SPI bf (0.31-6.01), while for long-term periods, SPEI bf (6.48-8.75) yields higher magnitudes than RDI (6-8.53).

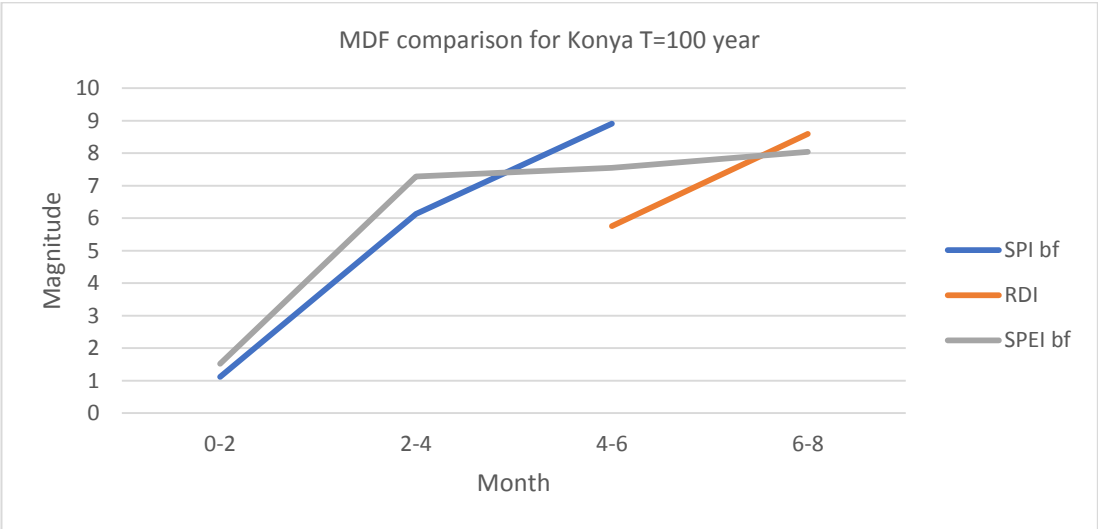


**Figure 4. 82.** MDF comparison for Konya T=100 year

When examining the graph for the Konya station, it can be observed that for short-term periods, SPEI bf (1.52-7.28) yielded higher magnitudes compared to SPI bf (1.12-6.13), while for medium-term periods, SPI bf (6.13-8.91) provided higher

magnitudes compared to SPEI bf (7.28-7.55). For long-term periods, SPEI bf (7.55-8.04) resulted in higher magnitudes compared to RDI (5.76-8.59).

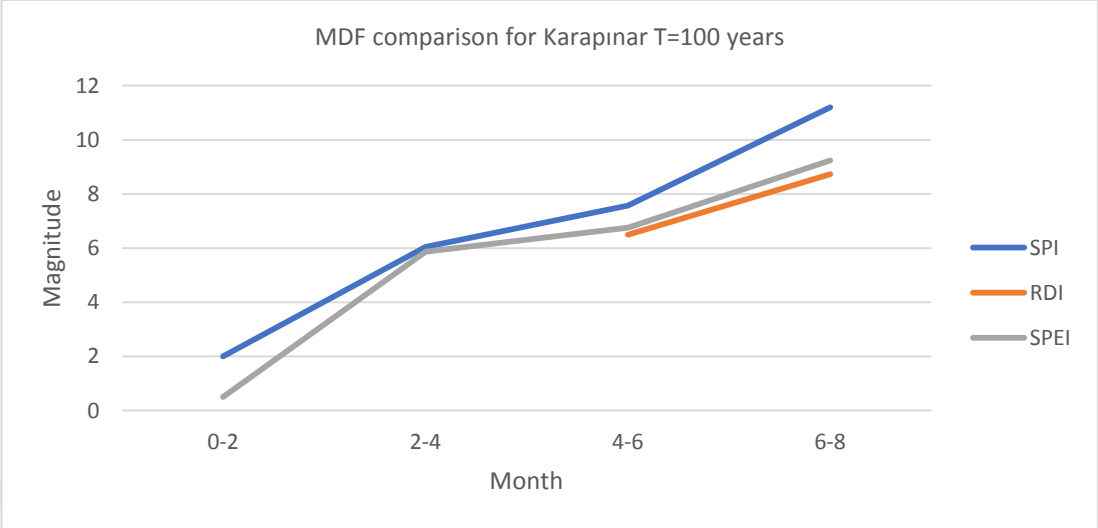


**Figure 4. 83.** MDF comparison for Karapınar T=100 years

When examining the graph for the Karapınar station, it can be observed that for short and medium-term periods, SPI bf (2-7.57) yields higher magnitudes compared to SPEI bf (0.5-6.76). However, for long-term periods, only SPI bf (7.57-11.2) yields the highest magnitudes, while SPEI bf (6.76-9.24) yields moderate magnitudes, and RDI (6.5-8.73) yields the lowest magnitudes.

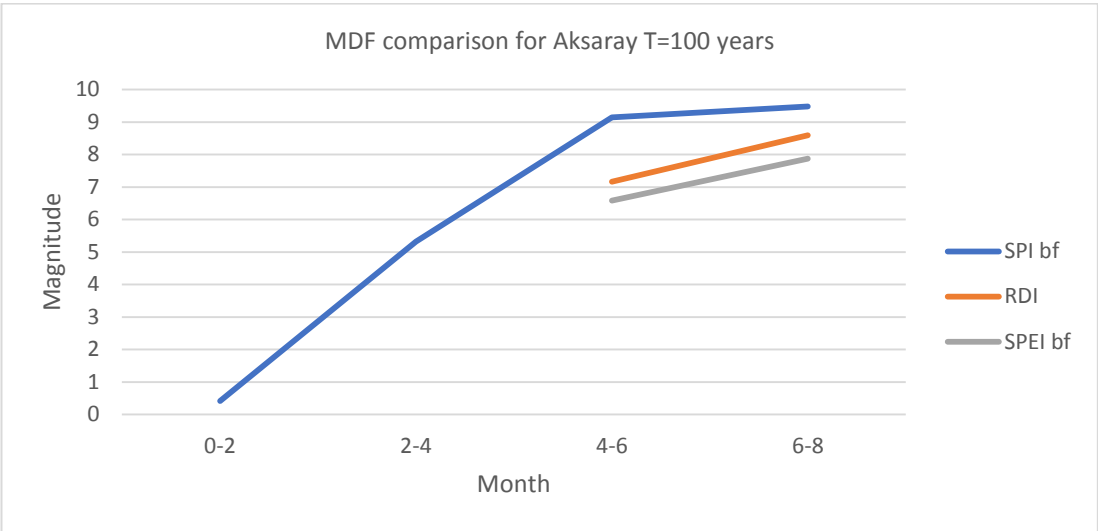


**Figure 4. 84.** MDF comparison for Aksaray T=100 years

When examining the graph for the Aksaray station, it can be observed that for short and medium-term periods, both SPEI bf and RDI did not yield any results, only SPI bf (0.42-9.15) provided results. For long-term periods, SPI bf (9.15-9.48) resulted in

the highest magnitudes, RDI in (7.17-8.59) moderate magnitudes, and SPEI bf (6.58-7.88) in the lowest magnitudes. Similar interpretations can be made for all other stations.

The MDF comparison graphs presented above can be interpreted as follows: For the Tokat station, a drought with a magnitude of 3 and a recurrence interval of 5 years will last between 2-4 months for SPI, 4-6 months for RDI, and 6-8 months for SPEI bf. For the Konya station, a drought with a magnitude of 6 and a recurrence interval of 100 years will last between 2-4 months for SPI, 4-6 months for RDI, and 6-8 months for SPEI bf. Similar evaluations are conducted for the other stations.

After these results, as an example, SPEI 3 bf method 4-6 months and 5 years magnitude duration frequency distribution maps were obtained by IDW method. The MDF distribution map of each basin is given in Figures 4.85 - 4.91.

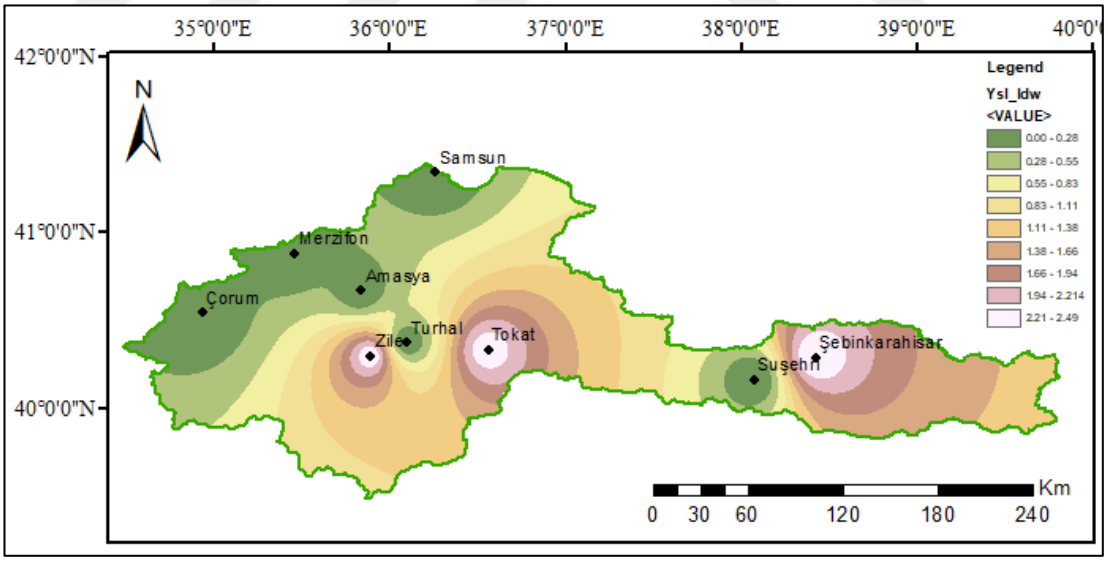


**Figure 4. 85.** Yeşilırmak basin SPEI 3 bf, 4-6 months, 5 years recurrence MDF distribution map

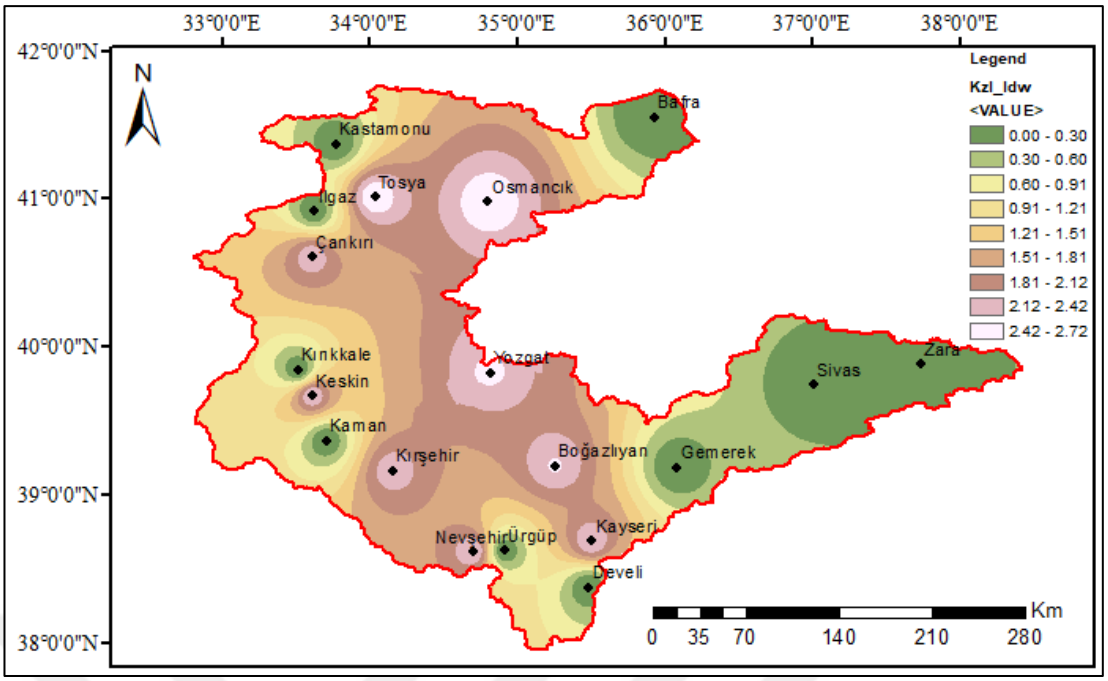


**Figure 4. 86.** Kızılırmak basin SPEI 3 bf, 4-6 months, 5 years recurrence MDF distribution map

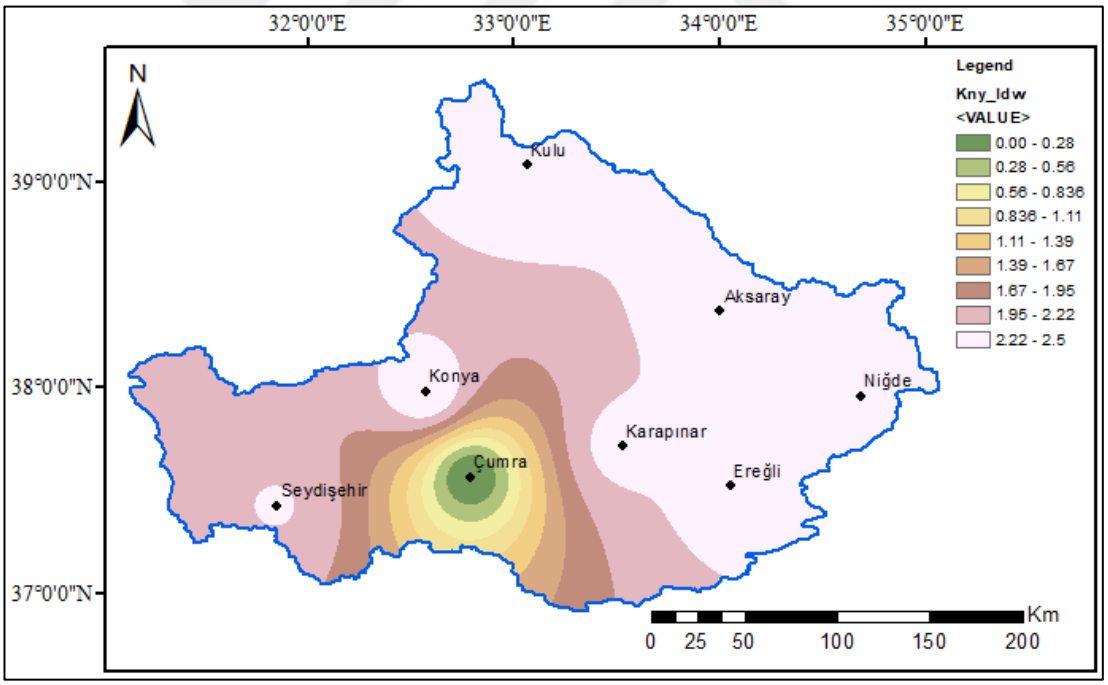


**Figure 4. 87.** Konya Closed basin SPEI 3 bf, 4-6 months, 5 years recurrence MDF distribution map

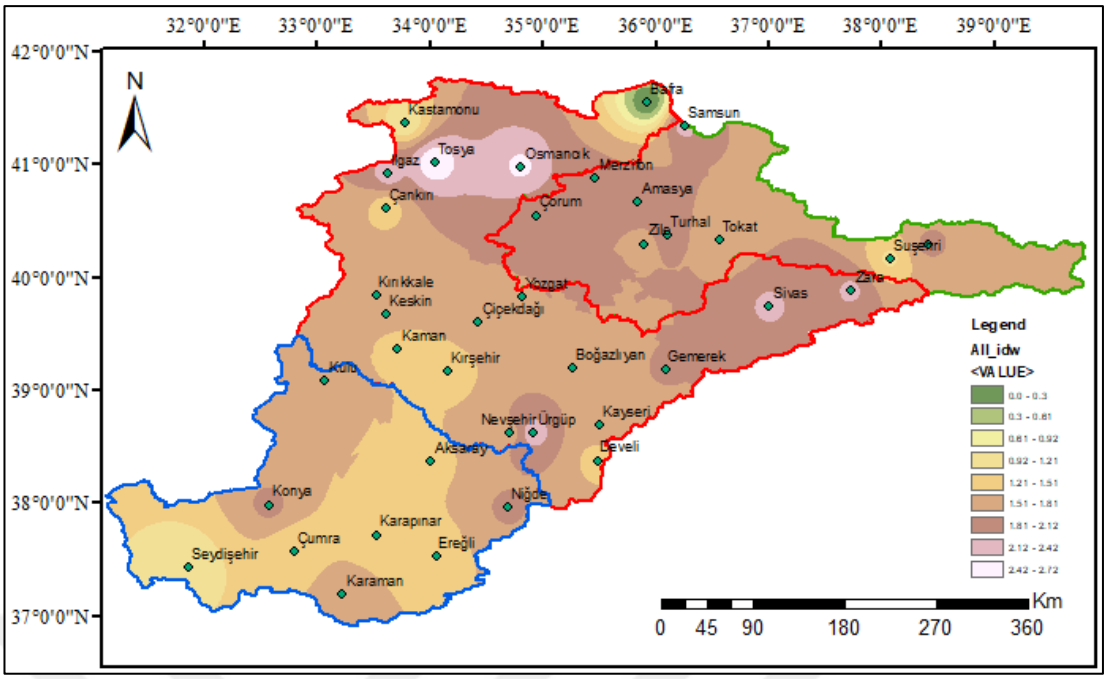


**Figure 4. 88.** All basins SPEI 3 bf, 4-6 months, 5 years recurrence MDF distribution map

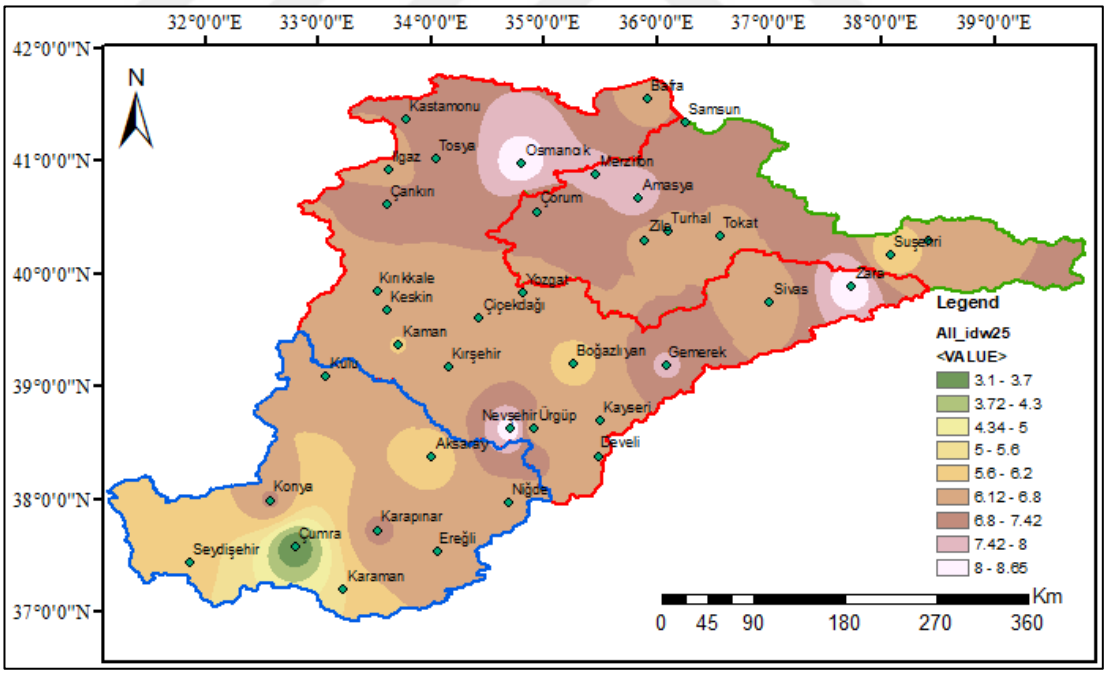


**Figure 4. 89.** All basins SPEI 3 bf, 4-6 months, 25 years recurrence MDF distribution map

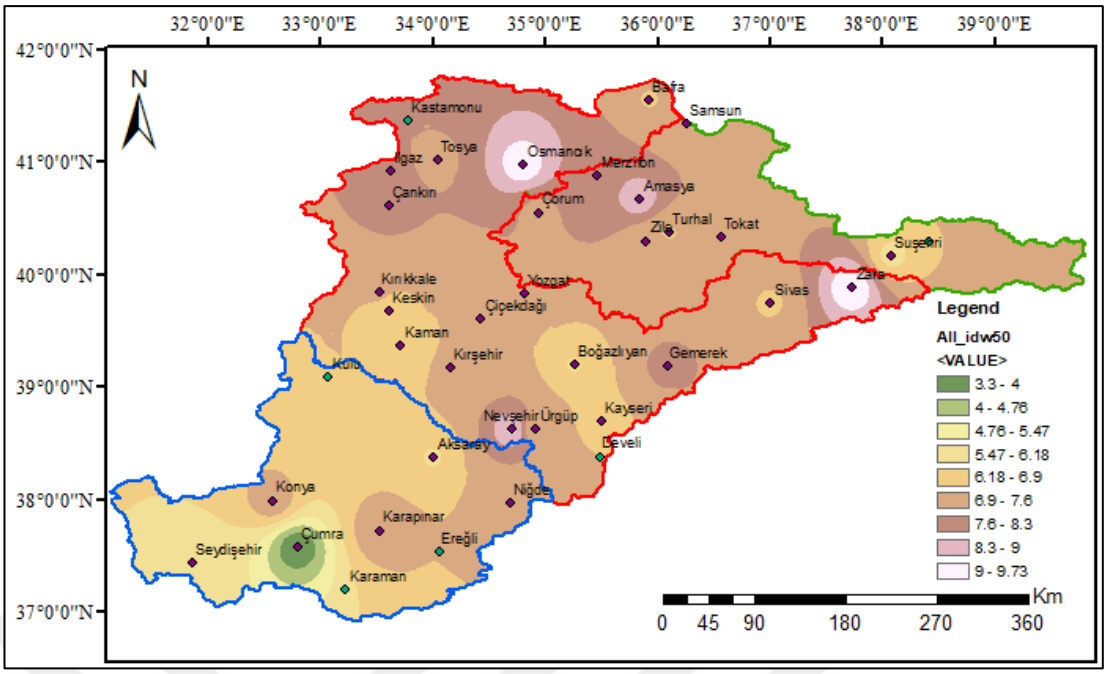


**Figure 4. 90.** All basins SPEI 3 bf, 4-6 months, 50 years recurrence MDF distribution map

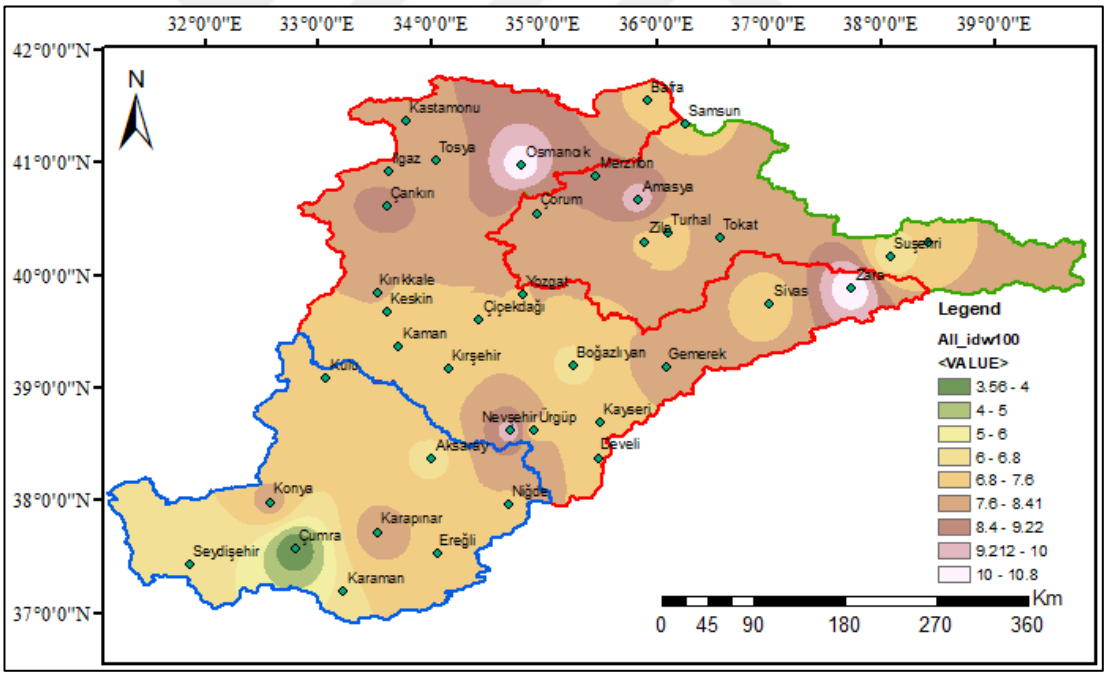


**Figure 4. 91.** All basins SPEI 3 bf, 4-6 months, *100* years recurrence MDF distribution map

The spatial variability of MDF distributions for the SPEI 3 bf method, including 4-6 months and 5, 25, 50, and 100 years of results, is depicted in the aforementioned figures. Figures 4.85-4.87 display the spatial distributions separately for the Yeşilırmak, Kızılırmak, and Konya closed basins. Figure 4.88-4.91 represents the

entire study area where all basins are examined together. These figures indicate the presence of a boundary condition that affects the calculated drought values when mapping the basins separately. However, this effect disappears when all basins are mapped together. Therefore, to evaluate the MDF effect and spatial variability, as well as to consider the spatial impacts of drought, analyses should be conducted over larger areas.

Figure 4.91 indicates that the drought magnitude (intensity) during drought events lasting 4 to 6 months with a return period of 100 years is lowest in Çumra, highest in Zara, and observed in Osmancık. The drought intensity appears to be higher in the northern regions and decreases as we move southward. Figures 4.88, 4.89, 4.90, and 4.91 demonstrate that the magnitude (intensity) of droughts lasting 4 to 6 months and with return periods of 5, 25, 50, and 100 years is highest in the northern part of the examined area, gradually decreasing towards the south. With the exception of the drought with a 5-year return period, the lowest intensity was observed in Çumra, while the highest magnitude was seen in Osmancık and Zara. For the drought event with a 5-year return period, the lowest magnitude was observed in Bafra.

# CHAPTER 5

# CONCLUSIONS

Within the scope of this thesis, meteorology stations with at least 30 years of rainfall data were identified for drought analysis of the Yeşilırmak, Kızılırmak, and Konya closed basins. Accordingly, drought analyses were conducted using the SPI, RDI, and SPEI methods for a total of 38 meteorology stations, consisting of 9 in the Yeşilırmak basin, 20 in the Kızılırmak basin, and 9 in the Konya closed basin. Nine stream flow stations were identified for the SRI method, which have at least 30 years of streamflow data. Of these, 5 are located in the Yeşilırmak basin, 4 are in the Kızılırmak basin, and no flow station was found in the Konya closed basin.

Firstly, drought analysis was conducted using the SPI method for 1, 3, 6, 9, 12, and 24-month consecutive totals by fitting all data to the gamma distribution. To determine how accurate the traditional Gamma distribution assumption is, the most appropriate theoretical distribution methods was determined for each station, and then the SPI drought analysis for 1, 3, 6, 9, 12, and 24-month totals of all rainfall stations were carried out. The results from traditional gamma and best-fit distributions were compared with each other. When analysing the SPI best-fit (bf) distributions, it was predominantly observed that the Weibull distribution was suitable for SPI 1 bf, SPI 3 bf, and SPI 12 bf, while the Generalized Extreme Value (GEV) distribution was appropriate for SPI 6 bf and SPI 9 bf. For SPI 24 bf, both the Weibull and GEV distributions were considered suitable. Stagge et al. (2015) found the Weibull distribution to be predominantly suitable for SPI 3 and SPI 12 in their study. Similarly, in this study, the Weibull distribution was predominantly determined to be the most appropriate distribution for SPI 3 bf and SPI 12 bf. These findings confirm the accuracy of the results obtained in this study. Histograms depicting the percentages of drought classifications based on the Gamma distribution and the best-fit distribution were provided for all stations, and they were interpreted accordingly.

Then, drought analysis was conducted using the RDI method for 3-, 6-, 9-, and 12-month totals, and significant results were obtained. Results were evaluated for each basin and station. When examining the correlation tables, it was generally observed that the RDI results had very low correlations with other indices. Therefore, it was

concluded that the RDI index was not entirely reliable for drought assessments. Histograms depicting the percentages of drought classifications were provided for all stations, and they were interpreted accordingly.

Drought analysis was conducted using the SPEI method for 3-, 6-, 9-, 12-, and 24-month totals by fitting all data to the GLOG distribution which was suggested by Vicente-Serrano et al. (2010). As in the SPI analysis, a comparison of the SPEI results obtained from the suggested GLOG distribution and the theoretical probability distribution that most approximately fitted the data was performed. As no critical conditions were observed in the data, it was concluded that this method was not accurate. Therefore, the SPEI drought was reanalyzed for 3-, 6-, 9-, 12-, and 24-month accumulations to determine the most appropriate distribution methods for the D values at each station. Thus, more meaningful results were obtained. Results were evaluated for each stations of the basins. When evaluating the SPEI best-fit (bf) distributions, it was predominantly observed that the Generalized Extreme Value (GEV) distribution was suitable for SPEI 3 bf and SPEI 12 bf. In their study, Stagge et al. (2015) also predominantly found the Generalized Extreme Value (GEV) distribution to be the most suitable distribution for SPEI. These findings confirm the accuracy of this thesis study. Histograms depicting the percentages of drought classifications based on the GLOG distribution and the best-fit distribution were provided for all stations, and they were interpreted accordingly.

Finally, drought analysis was conducted using the SRI method for 1-, 3-, 6-, 9-, 12-, and 24-month totals. The small number of stations and the insufficient length of the data did not make it possible to sufficiently draw meaningful conclusions for the area under study. For future studies, drought analyses can be conducted using different meteorological and streamflow data to better understand the differences between meteorological drought and streamflow drought. It is recommended to maintain regular streamflow data records.

After completing all drought analyses, correlation calculations were performed to understand the relationships between drought analyses for all meteorological stations. The correlations were calculated between SPI 1 G, SPI 3 G, SPI 6 G, SPI 9 G, SPI 12 G, SPI 24 G, SPI 1 bf, SPI 3 bf, SPI 6 bf, SPI 9 bf, SPI 12 bf, SPI 24 bf, SPEI 3 G, SPEI 6 G, SPEI 9 G, SPEI 12 G, SPEI 24 G, SPEI 3 bf, SPEI 12 bf, RDI

3, RDI 6, RDI 9, and RDI 12. Correlation values close to 1 indicate a high degree of relationship, while values close to 0 indicate a low degree of relationship.

Histograms of the 3-month and 12-month calculations of SPI Gamma, SPI Best Fit, SPEI Glog, SPEI Best Fit, and RDI indices were obtained for each station according to the severe drought (D3), moderate drought (D2), mild drought (D1), and extreme wetness (W3) classifications in order to understand the relationship between drought classifications. The graphs generally showed that the moderate drought classification was predominant.

To understand the impact of drought classifications evaluated on a station-by-station basis on a basin-wide scale, distribution maps of histograms were generated using the Inverse Distance Weighting (IDW) method for SPI G, SPI bf, SPEI G, SPEI bf, and RDI indices for 3-month and 12-month calculations, specifically for the D1, D2, D3, and W3 classifications. According to the obtained maps, the highest D1 percentage was observed in the RDI 3 method, the highest D2 percentage was observed in the SPI 3 bf method, the highest D3 percentage was observed in the RDI 12 method, and the highest W3 percentage was observed in the SPEI 12 bf method. The RDI 12 method yielded good results for extreme drought periods, while the SPEI 12 bf method had performance better for extreme wet periods.

Trend analyses were performed using the MK and ITA methods on precipitation data, SPI bf, RDI, and SPEI bf drought analysis results for 38 meteorological stations. The analyses were conducted considering a significance level of 5%. In the ITA method, both formula-based and graphical trend analyses were conducted. The graphical analysis was used for visual interpretation, while the statistical significance test was used to determine whether the trend is statistically significant or not. The trend results from MK and ITA were given on maps for each basin. To understand the numerical differences between MK and ITA, the numbers of decreasing trends, no trends, and increasing trends calculated by SPI bf, RDI, and SPEI bf for 3-month and 12-month drought periods were presented in the tables. For the 3-month droughts, the MK method predominantly identified "no trend" while the ITA method indicated "increasing trend." For the 12-month droughts, both MK and ITA methods yielded almost identical results. Dabanlı et al. (2016) found that the MK trend test yielded "no trend" results for all stations, indicating a lack of significant findings.

However, the ITA trend test produced a more diverse range of results, including "increasing trend," "no trend," and "decreasing trend." Thus, it can be interpreted that while the MK test yielded unreliable results for this study, the ITA test provided more reliable findings. In terms of the drought analysis results, the ITA test yielded more significant results for the 3-month drought analysis, while both the MK and ITA tests produced similar results for the 12-month drought analysis. These findings confirm the accuracy of the present thesis. For future studies, it is recommended to analyse the drought analysis results using other trend analysis methods and compare the outcomes.

Magnitude-Duration-Frequency (MDF) analyses were conducted to characterize drought and predict the duration of future drought magnitudes. The results of the 3-month Standardized Precipitation Index (SPI) best fit, Reconnaissance Drought Index (RDI), and 3-month Standardized Precipitation Evapotranspiration Index (SPEI) best fit methods were classified into 2-month periods. Based on these results, frequency intervals of 2, 5, 10, 25, 50, and 100 years were calculated for each station and presented in graphical form. Comparisons and interpretations were made among the drought indices for short, medium, and long-term periods.

After completing the MDF graphs, the MDF results for each station were combined, and MDF comparisons of each method for the stations were shown through graphs. To enhance the understanding of MDF comparisons, MDF comparison maps were obtained for each basin based on SPEI 3-month from best-fit distribution, 4-6-month, and 5, 25, 50, 100-year return periods. Initially, separate analyses were conducted for each basin, and it was observed that accurate results could not be obtained due to boundary conditions. Subsequently, all basins were merged, and the analyses were repeated after removing the boundary conditions. The regional MDF distributions were then represented by combining all basin maps. Maps showed that for the same recurrence intervals and similar durations, drought magnitudes (intensities) were higher for northern parts of the area under study than southern parts.

In light of the aforementioned explanations, to reduce drought risk and effectively utilize water resources in all three basins, irrigation methods with high water application efficiency such as drip irrigation and/or sprinkler irrigation should be encouraged and made mandatory for farmers. Alternative crop options that require

less water should be provided to farmers within the study area. Cultural studies involving all stakeholders should be conducted to raise awareness about drought. Furthermore, the ability of these indices used in the study area to represent natural conditions should be investigated in real-time, and subsequent studies should examine to what extent these indices reflect the natural conditions. Additionally, besides these indices, other indicators that can better represent the study area and drought analysis should be considered in future studies.

## REFERENCES


Abramopoulos, F., Rosenzweig, C. and Choudhury B. (1988). Improved Ground Hydrology Calculations For Global Climate Models (Gcms): Soil Water Movement And Evapotranspiration. *Journal Of Climate*, 1 (9), 921-941.

Afzali, A., Keshtkar, H., Pakzad, S., Moazami, N., Azizabadi Farahani, E., Golpaygani, A., Khosrojerdi, E., Yousefi, Z., TaghiNaghilou, M., "Spatio-Temporal Analysis of Drought Severity Using Drought Indices and Deterministic and Geostatistical Methods (Case Study: Zayandehroud River Basin)", Desert (Biaban), 21(2), 165–172 (2016).

Ahmad, M. I., Sinclair, C. D. and Werritty, A. (1988). Log-logistic Flood Frequency Analysis. *Journal of Hydrology*, 98 (3-4), 205-224.

Akbaş, A., (2014). Important Drought Years Over Turkey. Journal Of Geographical Sciences, *CBD 12* (2), 101- 118.

Akın, B., (2019). Drought Analysis of Tuz Gölü Basin, National Environmental Sciences Research Journal, *Issue 2*(1): 44-56.

Aksoy, H., Çetin, M., Önöz, B., Yüce, M. İ., Eriş, E., Selek, B., Aksu, H., Burgan, H. İ., Çavuş, Y., Eşit, M., Orta, S., (2019). Determination of Critical Drought Intensity-Duration-Frequency Curves by Using Frequency Analysis. 10. *National Hydrology Congress*, 9-12 October, 2019, Muğla Sıtkı Koçman University.

Aksoy, H., Önöz, B., Çetin, M., Yüce, M. İ., Eriş, E., Selek, B., Aksu, H., Burgan, H., İ., Eşit, M., Orta, S., Çavuş, Y., (2018). Drought Severity-Duration-Frequency Curves for Edirne. *National Hydrogeology and Water Resources Symposium*, 27-29 September 2018, Beytepe, Ankara.

Akşan, G. N., (2021). Drought Analysis In Turkey. *Pamukkale Unıversity Institute Of Science Civil Engineering*.

Albaqoul, A. A. A., (2022). Meteorological And Hydrological Drought Analysis Of Sinop, Kastamonu, Bartın Provinces In The Western Black Sea. *Karabük University The Institute of Graduate Programs The Department of Civil Engineering*.

Alley, W.M. (1984) “The Palmer Drought Severity Index: Limitations and Assumptions”, Journal of Climate and Applied Meteorology, (23), 1100-1109.

Anisfeld, S. C., 2011. Water resources: Island Press. 321p, Washington, DC.

Anlı, A. S., Apaydın, H., Öztürk, F., (2009). Regional Frequency Analysis of the Annual Maximum Precipitation Observed In Trabzon Province. *Journal Of Agricultural Sciences 2009*, 15 (3) 240-248. DOI: 10.1501/Tarimbil_0000001097.

Anlı, S., (2014). Temporal Variation of Reference Evapotranspiration (ET0) in Southeastern Anatolia Region and Meteorological Drought Analysis through RDI (Reconnaissance Drought Index) Method. *Journal of Agricultural Sciences 20* (2014) 248-260.

Arslan, O., Bilgil, A., Veske, O., (2016). Meteorological Drought Analysis In Kızılırmak Basin Using Standardized Precipitation Index Method. Nigde University *Journal of Engineering Sciences*, Volume 5, Number 2, (2016), 188-194.

Aslan, D., (2020). The Investigation Of Relations Between Large Scale Atmospheric Parameters And Drought Indices. *Dokuz Eylul University Graduate School of Natural and Applied Sciences, Department of Civil Engineering, Hydraulics - Hydrology and Water Resources Program*.

Bacanlı, U. G., Kargı, P. G., (2019). Drought Analysis in Long and Short Term Periods: Bursa Example, Research Article. *Journal of Natural Disasters and Environment*, 2019; 5(1): 166-174, DOI: 10.21324/dacd.429391.

Bacanli, U. G., and Saf, B., (2005). Investigation Of Drought Determination Methods İn The Case Of Antalya Province. *Civil Engineering Problems of Antalya Region Symposium*, Antalya, 22-25/09/2005.

Bakanoğulları, F., (2020). İstanbul-Damlıca Creek Using SPI And SPI Indis Analysis Of Drought İn Violence İn The Basin. *Toprak Su Journal*, 2020, 9 (1): (1-10).

Başak, A., (2020). Drought Analysis Of Five Province İn Lower Euphrates Basin And Estimation Of Drought İndices With Artificial Neural Network. *Harran*

*University, Graduate School of Natural and Applied Sciences, Department of Civil Engineering.*

Bayazıt, M. and Önöz, B., (2008). Flood and Drought Hydrology. *Istanbul Technical University.*

Bayçınar, M., (2019). Evaluation Of Common Use Of Drought Indices By Factor Analysis In The Example Of Konya Closed Basin. *Erzincan Binali Yıldırım University Graduate School of Natural and Applied Sciences Department of Civil Engineering*.

Baykal, T., Terzi, Ö., (2017). Flood Frequency Analysis of Kucuk Aksu River. *Cumhuriyet Sci. J*., Vol.38-4 (2017) 639-646.

Begueria, S., Serrano, S. M., Reig, F., Latorre, B., (2014). Standardized Precipitation Evapotranspiration İndex (SPEI) Revisited: Parameter Fitting, Evapotranspiration Models, Tools, Datasets And Drought Monitoring. *International Journal Of Climatology, Int. J. Climatol.* **34**: 3001–3023.

Bhunia, P., Das, P., & Maiti, R. (2019). Meteorological Drought Study Through SPI in Three Drought Prone Districts of West Bengal, India. *Earth Systems and Environment*. 4, 43-55.

Borgomeo, E., Pflug, G., Hall, J. W., Stigler, S., (2015) Assessing Water Resource System Vulnerability To Unprecedented Hydrological Drought Using Copulas To Characterize Drought Duration And Deficit. 10.1002/2015WR017324, doi:10.1002/2015WR017324.

Bölük, E., (2016). T.R. Ministry Of Forestry And Water Works General Directorate Of Meteorology, Turkish Climate According To Thornthwaite Climate Classification. *Research Department Climatology Branch Office*.

Büyükkaracığan, N., Kahya, E., (2009). Flood Frequency Analysis Of Annual Peak Flows In Konya Basin Streams. *Journal of Selcuk-Technic*. Volume 8, Number:3-2009.

Caloiero, T., Veltri, S., Caloiero, P., Frustaci, F., (2018). Drought Analysis in Europe and in the Mediterranean Basin Using the Standardized Precipitation Index. *Water* 2018, 10, 1043; doi:10.3390/w10081043.

Cheo, A. E., (2016), Understanding Seasonal Trend Of Rainfall For The Better Planning Of Water Harvesting Facilities İn The Far-North Region. Cameroon. *Water Utility Journal* 13: 3-11.

Çavuş, Y., Aksoy, M., (2019). Critical Drought Severity-Duration-Frequency Curves in Precipitation Deficit. *10. National Hydrology Congress*, 9-12 October, 2019, Muğla Sıtkı Koçman University.

Çeribası, G., Doğan, E., Sönmez, O., (2013). Evaluation of Sakarya River Streamflow and Sediment Transport With Rainfall Usage Trend Analysis. *Fresenius Environ Bull*. 22 (3A):846–852.

Dabanlı, İ., (2017). Climate Change Impact On Precipitation-Temperature In Turkey And Drought Analysis: Akarçay Case Study. *Istanbul Technıcal University Institute Of Natural Sciences.*

Dabanlı, İ., Şen, Z., Yeleğin, M. Ö., Şişman, E., Selek, B., Güçlü, Y. S., (2016), Trend Assessment by the Innovative-Şen Method. *Water Resour Management* 30:5193 –5203.

Demir, R., (2022). Optimization Of Eruh Water Distribition Networks Using Metaheuristic Methods. *Dicle University Institute Of Natural Sciences, Master of Science in Department of Civil Engineering*.

Dewes, C. F., Rangwala, I., Barsugli, J. J., Hobbins, M. T., and Kumar, S., "Drought risk assessment under climate change is sensitive tomethodological choices for the estimation of evaporative demand", PLoS One, 12(3), e0174045, (2017).

Dinç, N., Aydinşakir, K., Işık, M., Büyüktaş, D., (2016). Drought Analysis Of Antalya Province By Standardized Precipitation Index (SPI). *Derim,* 2016, 33 (2): 279- 298. DOI: 10.16882/Derim.2016.267912.

Dodangeh, S., Sattari, M. T., Seçkin, N., (2011). L-Moments Method of Minimum Currents Regional Frequency Analysis. *Journal of Agricultural Sciences* 17 (2011) 43-58.

Es Proje Mühendislik Müşavirlik, (2015). Detection Report Of Drought İndices, İndicators And Threshold Values. *Akarçay Basin Drought Management Plan*.

Geyikli, M. S., (2015). Determination Of Flood Risk Maps By Using GIS Software. *Inonu University, Graduate School of Natural and Applied Sciences, Department of Civil Engineering*.

Gibbs, W. J. and Maher, J. V., (1967). Rainfall Deciles As Drought Indicators. *Bureau Of Meteorology Bulletin*, No. 48. *Commonwealth of Australia*. Melbourne.

Guttman, N. B. (1998). Comparing The Palmer Drought İndex And The Standardized Precipitation Index. *Journal Of The American Water Resources Association,* 34 (1), 113-121.

Guttman, N. B. (1999). Accepting The Standardized Precipitation İndex: A Calculation Algorithm. *Journal Of The American Water Resources Association*, 35 (2), 311-322.

Gümüş, V. and Algin, H. M. (2017). Meteorological And Hydrological Drought Analysis Of Seyhan-Ceyhan River Basin, Turkey. *Meteorological Applications,* 24 (1), 62-73.

Gümüş, V., (2017). Hydrological Drought Analysis of Asi River Basin with Standardized Runoff Index . *GU J Sci, Part C*, 5(1): 65-73.

Gümüş, V., Başak, A., Oruç, N., (2016). Drought Analysis of Şanlıurfa Station by Standardized Precipitation Index (SPI) Method. *HU J. of Eng*. 01 (2016) p.36- 44

Gümüş, V., Yeardız, M. S., Şimşek, O., (2018). Hydrological Drought Assessment: Case Study of Murat River-Palu. *Harran University Journal of Engineering*, 3 (2018) p. 297-301.

Hejazizadeh, Z. and Javizadeh, S., (2011). Introduction to drought and its indices. *Samt Publications*. 358s, İran.

Hernandez, E. A., Uddamedi, V., (2014). Standardized Precipitation Evaporation İndex (SPEI)-Based Drought Assessment İn Semi-Arid South Texas. *Environ Earth Sci* (2014) 71:2491–2501. DOI 10.1007/s12665-013-2897-7.

Hezarani, A. B., (2018). Drought Analysis In The Yeşilırmak River Basin Using Various Methods. *University of Ondokuz Mayıs Institute of Sciences Civil Engineering Graduate Program*.

Hezeran, A. B., (2018). Drought Analysis In The Yeşilırmak River Basin Using Various Methods. *University of Ondokuz Mayıs, Institute of Sciences, Civil Engineering Graduate Program*.

Hınıs, M. A., (2009). Regional Frequency Analysis of Yearly Precipitation data In Konya Basın. *1st National Drought and Desertification Symposium*, 16-18 June 2009-Konya.

Hınıs, M., (2013). Hydrometeorological Drought Analysis in Aksaray with Integrated Drought Index. *Journal of Gazi Univ. Eng. Arct. Fac.*, Vol. 28, No. 4, 711-721.

Hobbins, M. T., Wood, A., McEvoy, D. J., Huntington, J. L., Morton, C., Anderson, M. and Hain C., "The evaporative demand drought index. Part I: Linking drought evolution to variations in evaporative demand", *J. Hydrometeorol.*, 17(6), 1745–1761, (2016).

Hu, Q., and G. D. Willson (2000). Effect Of Temperature Anomalies On The Palmer Drought Severity İndex İn The Central United States. *International Journal Of Climatology*, 20 (15), 1899-1911.

İvrem, A., Özbuldu, M., Çıplak, C., (2018). Drought Analysis By Using Stream Flow Data Of The Seyhan Göksu-Himmetli Sub-Basin. *Journal Of Agricultural Faculty Of Mustafa Kemal University.* 23(2):148-157.

Jamal, R., (2019). Trend Analysis Of The Drought Over Turkey. *Anadolu University, Graduate School, Department of Civil Engineering.*

Jones, J. R., Schwartz, J, S., Ellis, K. N., Hathaway, J. M., Jawdy, C. M., (2015). "Temporal Variability Of Precipitation İn The Upper Tennessee Valley". *Journal Of Hydrology: Regional Studies.* 3 125–138.

Kadıoğlu, M., (2001). Drought Breaker. Current Publishing, *Istanbul*, 125s.

Katipoğlu, O. M., (2020). Analysıs Of Meteorologıcal And Hydrologıcal Droughts In Euphrates Rıver Valley. *Atatürk University, Institute Of Natural Sciences, Civil Engineering Department.*

Kermen, Ç., (2019). Determination Of The Relationship Between Meteorological And Hydrological Drought In Küçük Menderes Basin. *Dokuz Eylul University Institute of Science, Master Thesis, Department of Civil Engineering, Hydraulics - Hydrology and Water Resources Program.*

Keskiner, A. D., Çetin, M., Uçan, M., Şimşek M., (2016). Meteorological Drought Analysis With Different Return Periods by Using Standardized Precipitation Index In Geographic Information Systems Environment: A Case Study In The Seyhan River Basin. *Çukurova J. Agric. Food Sci*. 31(2): 79-90, 2016.

Keyantash J, Dracup JA (2004). An Aggregate Drought İndex: Assessing Drought Severity Based On Fluctuations İn The Hydrologic Cycle And Surface Water Storage. *Water Resour Res.* **40** (9), W09304.

Kim, D. W., Byun, H. R., Choi, K. S. and Oh, S. B., "A spatiotemporal analysis of historical droughts in Korea", J. Appl. Meteorol. Climatol., 50(9), 1895–1912, (2011).

Kubat, C. (2019). MATLAB Artificial Intelligence and Engineering Applications (4th ed.). *Abakus Book Publication Distribution Services.*

Linsley, R. K., Jr., Kohler, M.A. and Paulhus, L.H., (1958). *Hydrology for Engineers*, McGraw-Hill, 340.

Lyon, B., "The strength of El Niño and the spatial extent of tropical drought", Geophys. Res. Lett., 31(21), 1–4 (2004).

McKee, T. B., Doesken, N. J. and Kleist J. (1995). Drought Monitoring With Multiple Time Scales. 9th Conference On Applied Climatology, 15-20 January 1995, Dallas, *American Meteorological Society*, 233-236.

McKee, T. B., Doesken, N. J., & Kleist, J. (1993). The Relationship Of Drought Frequency And Duration To Time Scales. *In Proceedings Of The 8th Conference On Applied Climatology*. **17** (22), 179–184.

Mishra, S. S. and Nagarajan, R., (2011). Spatio-Temporal Drought Assessment İn Tel River Basin Using Standardized Precipitation Index (SPI) and GIS. *Geomatics, Natural Hazards and Risk*, 2(1), 79-93.

Mohorji, A., M., Şen, Z., Almazroui, M., (2017). Trend Analyses Revision and Global Monthly Temperature Innovative Multi-Duration Analysis. *Earth Syst Environ* (2017) 1:9. DOI 10.1007/s41748-017-0014-x.

Morid, S., Smakhtin, V. and Moghaddasi, M., "Comparison of seven meteorological indices for drought monitoring in Iran", Int. J. Clim., 26(7), 971–985, (2006).

Nalbantis, I. (2008). Evaluation Of A Hydrological Drought İndex. *European Water* 23/24, 67-77.

Nalbantis, I. and Tsakiris, G. (2009). Assessment Of Hydrological Drought Revisited. *Water Resources Management*, 23 (5), 881–897.

Oğuz, İ., Yürekli, K., Öztürk, F., (2011). Frequency Analysis of Precipitation Erosion Index (R Factor) in Tokat Province. *Journal of Agricultural Sciences Research* 4 (2): 23-26.

Oğuztürk, G., (2017). Investigating The Effect Of Precipitation Deficits On Hydrological Systems İn Different Dam Basins Of Turkey. *Kırıkkale University, Institute of Science and Technology, Department of Civil Engineering*.

Ojara, M. A., Lou, Y., Aribo, L., Naumbia, S., Uddin, Md. J., (2020). Dry Periods And Probability Of Precipitation For The Lake Kyoga Basin İn Uganda, East Africa. *Natural Hazards*. 100: 493–514, https://doi.org/10.1007/s11069-019-03822-x.

Orhunbilge, N., (2017). Applied Regression And Correlation Analysis. *Nobel Academic Publishing.*

Oruç, N., (2017). Southeastern Anatolia Region Drought Analysis. *Pamukkale University Institute of Science Civil Engineering.*

Öney, M., (2020). Regional Drought Analysis İn The Gediz Basin With Standard Rainfall Evapotranspiration Index (SPEI). *Ankara University Institute of Science and Technology.*

Özfidaner, M., Şopalyo, D., Topaloğlu, F., (2018). Hydrological Drought Analysis of Seyhan Basin Flow Data. *Toprak Su Journal*, 2018, 7 (1): (57-64).

Öztopal, A., Şen, Z., (2016). Innovative Trend Methodology Applications to Precipitation Records in Turkey. *Water Resour Manage* (2016) 31:727–737. DOI 10.1007/s11269-016-1343-5.

Rao, A. R., Hamed, K. H., (2000). Flood Frequency Analysis. *CRC Press LLC.*

Reis, M., Dutal, H., Bolat, N., (2016). An Evaluation On IDI (Integrated Drought Index): The Case of Kahramanmaraş Province. *1st International Mediterranean Science and Engineering Congress*. Pages: 4650-4655, Paper ID: 1338, Adana.

Seçkin, N., Topçu, E., (2016). Regional Frequency Analysis Of Annual Maximum Precipitation İn Adana And Surrounding Provinces. *Journal Of The Faculty Of Engineering And Architecture Of Gazi University* 31:4 (2016) 1049-1062.

Sen, Z., (2009). Drought Disaster and Modern Calculation Methods. *Water Foundation Publications.* pp.248.

Serrano, S. M. V., Beguerıa, S., Lacruz J. L., Camarero, J. J., Moreno, J. I. L., Molina, C. A., Revuelto, J.; Tejeda E. M. and Lorenzo A. S. (2012). Performance Of Drought İndices For Ecological, Agricultural, And Hydrological Applications. *Earth Interactions*, 16 (10), 1-27.

Serrano, S. M., Begueria, S., Moreno, J. I.,. (2010). A Multiscalar Drought Index Sensitive to Global Warming: The Standardized Precipitation Evapotranspiration Index. *DOI*: 10.1175/2009JCLI2909.

Sırdas, S., (2002). Meteorological Drought Modeling And İts Application İn Turkey. *Istanbul Technical University, Institute Of Science And Technology*, PhD Thesis, 237s. Istanbul.

Stagge, J. H., Tallaksen, L. M., Xu, C. Y., Lanen, H. A. J., (2014). Standardized Precipitation-Evapotranspiration Index (SPEI): Sensitivity To Potential Evapotranspiration Model And Parameters. Hydrology In A Changing World: Environmental And Human Dimensions Proceedings Of FRIEND-Water 2014, *Montpellier, France*, October 2014 (IAHS Publ. 363, 2014).

Stagge, J. H., Tallaksen, L., Gudmundsson, L., Van Loon, A. F., Stahl, K., (2015). Candidate Distributions for Climatological Drought Indices (SPI and SPEI), *International Journal of Climatology, Int. J. Climatol*. 35: 4027–4040.

Şaplıoğlu, K., Kilit, M., Yavuz, B.K. (2014). Trend Analysis Of Streams İn The Western Mediterranean Basin Of Turkey". *Fresenius Environ Bull*. 23(1A):313–324.

Şaylan, L., Durak, M. and Şen, O., (1997). Drought and its effects, Proceedings of the Meteorological Characteristic. *Natural Disasters Symposium* (7-9 October 1997, Ankara), p. 433-444.

Şen, Z., (2001) Drought In Turkey And Our Water Resources. *Water Foundation Publications*, pp.140.

Şen, Z., (2017). Innovative Trend Significance Test And Applications. *Theor Appl Climatol* (2017) 127:939–947. DOI 10.1007/s00704-015-1681-x.

Şen, Z., (2017). Innovative Trend Significance Tests And Applications. *Theor Appl Climatol*. 127: 939–947, DOI 10.1007/s00704-015-1681-x.

Şen, Z., Şişman, E., Dabanlı, İ., (2019). Innovative Polygon Trend Analysis (IPTA) And Applications. *Journal of Hydrology* 575 (2019) 202–210.

Şen, Z., Şişman, E., Dabanlı, İ., (2020). Wet and Dry Spell Feature Charts For Practical Uses. *Natural Hazards* 104: 1975–1986, https://doi.org/10.1007/s11069-020- 04257-5.

Şişman, E., (2019). Piecewise Wet And Dry Spell Duration-Number Relationship And Possible Climate Change Impact İdentification In Turkey. *Arabian Journal of Geosciences* (2019) 12: 787. https://doi.org/10.1007/s12517-019-4973-0.

Temel, İ., (2016). Drought Analysis in Gediz Basin. *Ege University Institute of Natural Sciences.*

Thom, H. C. S. (1966). Distribution Of Maximum Annual Water Equivalent Of Snow On The Ground. *Monthly Weather Review*, 94 (4), 265-271.

Tigkas D, Vangelis H, Tsakiris G (2013). The RDI As a Composite Climatic Index. *European Water*. 41:17–22.

Tigkas, D., Vangelis, H., Tsakiris, G., (2015). DrinC: A Software For Drought Analysis Based On Drought Indices. *Earth Sci Inform* (2015) 8:697–709. DOI 10.1007/s12145-014-0178-y.

Topçu, E., (2018). Drought Analysis Of East Mediterranean, Seyhan, Ceyhan And Asi Basins By Using Various Methods. *Çukurova University, Institute of Science and Technology, Department of Civil Engineering*.

Tosunoğlu, F., (2014). Investigating The Relationship Between Atmospheric Oscillations And Meteorological And Hydrological Droughts In Turkey. *Atatürk University, Graduate School of Natural and Applied Sciences, Department of Civil Engineering*.

Tsakiris, G., Pangalou, D., Vangelis, H. (2007). Regional Drought Assessment Based On The Reconnaissance Drought Index (RDI). *Water Resources Management.* **21** (5), 821–833.

Turhan, E., Çulha, B. D., Değerli, S., Hydrological Evaluation of Standardized Runoff Index Method for Different Time Scales: A Case Study of Arsuz Plain, Turkey. *Journal of Natural Hazards and Environment*. 2022; 8(1): 25-36, DOI: 10.21324/dacd.903655.

Türkeş, M., (2011). Hydroclimatological And Time-Series Analysis Of Variations In Precipitation And Aridity İndex Series Of The Akhisar And Manisa Districts And Geographical Synthesis Of Their Consequences With Respect To Desertification. *Journal of Geographical Sciences, CBD* 9 (1), 79-99.

Türkeş, M., Akgündüz, S. A., Demirörs, Z., (2009). According To Palmer Drought Index, The Drought Periods And Drought İn The Konya Department Of The Central Anatolia Region And Drought. *Journal Of Geographical Sciences. CBD* 7 (2), 129-144.

URL-1. https://www.xlstat.com/en/

URL-2. https://drought.unl.edu/Education/DroughtIn-depth/TypesofDrought.aspx

Ünlükara, A., (2014). Use Of Solar Radiation Intensity And Relative Insurance Data In Reference Evapotranspiration Calculations. *12. National Culture-Technical Symposium*. 21-23 May 2014, Tekirdağ.

Wilhite D. A, Svoboda M. D., Hayes MJ (2007). Understanding The Complex İmpacts Of Drought: A Key To Enhancing Drought Mitigation And Preparedness. *Water Resour Manag*. **21**:763–774. doi:10.1007/s11269-006-9076-5.

Wilhite, D. A., (1995). Developing A Precipitation-Based İndex To Assess Climatic Condition Across Nebraska. *Final Report Submitted To The Natural Resources Commission.* Lincoln, Nebraska.

Wilks, Daniel S. (1999). Interannual Variability And Extreme Value Characteristics Of Several Stochastic Daily Precipitation Models. *Agricultural and Forest Meteorology*, 93 (3), 153-169.

Wu H, Hayes MJ, Wilhite DA, Svoboda MD. 2005. The Effect of The Length of Record on The Standardized Precipitation Index Calculation. *International Journal of Climatology*, 25 (4), 505-520.

Yeardırı, I., Aksoy, H., (2019). Determination Of Possibilities Of Crossing SPI Drought Classes In Gediz Basin. *10. National Hydrology Congress* 9-12 October, 2019. Muğla Sıtkı Koçman University.

Yeardız, F., (2017). Applicability Of Matlab Language To Parallel Programming For Nonlinear Seismic Analysis Of Structure. *Istanbul Technical University, Institute Of Natural Sciences*.

Yeardız, M., S., (2019). Hydrologıial Drought Analysis Of Euphrates Basin With Standardized Runoff Index Method. *Harran University, Graduate School of Natural and Applied Sciences, Department of Civil Engineering*.

Yu, M., Liu, X., Li, Q., (2019). Impacts Of The Three Gorges Reservoir On İts İmmediate Downstream Hydrological Drought Regime During 1950–2016. *Natural Hazards* (2019) 96:413–430. https://doi.org/10.1007/s11069-018-3549-8.

Yürekli, K., (2005). Regional Analysis of Monthly Rainfalls over Amasya Province via L-Moments Method. GOÜ. *Journal of Faculty of Agriculture*, 2005, 22 (2), 51-56.

Yürekli, K., (2005). Regional Frequency Analysis of Maximum Daily Rainfalls Based on L-Moment Approach. GOÜ. *Journal of the Faculty of Agriculture*, 2005, 22 (1), 37-44.

Yürekli, K., Köse, Ö., Hınıs, M. A., (2011). Regional Frequency Analysis of Annual maximum Rainfalls created Surface Drainage Problem. *Journal of Agricultural Sciences Research* 4 (2): 27-30.

Yürekli, K., Sattari, M. T., Anlı, A. S., Hınıs, M. S., (2012). Seasonal And Annual Regional Drought Prediction By Using Data-Mining Approach. *Atmósfera* 25(1), 85-105.

Yürekli, K., Ünlükara, A., Yeardırım, M., (2010). Drought Analysis of Karaman Province with Different Approaches. *Journal of Agricultural Sciences Research* 3 (1): 19-23.

Zang, Y., Li, W., Chen, Q., Pu, X., and Xiang, L., (2017). Multi-models for SPI drought forecasting in the 158orth of Haihe River Basin, China. *Stochastic Environmental Research and Risk Assess.* 31:2471–2481, DOI 10.1007/s00477-017-1437-5

Zhang, Y., Li, W., Chen, Q., Pu, X., Xiang, L., (2017). Multi-models for SPI drought forecasting in the 158orth of Haihe River Basin, China. *Stoch Environ Res Risk Assess* (2017) 31:2471–2481. DOI 10.1007/s00477-017-1437-5.

Zhu, Y., Liu, Y., Ma, X., Ren, L., Singh, V. P. (2018). Drought Analysis in the Yellow River Basin Based on a Short-Scalar Palmer Drought Severity Index. *Water* 2018, 10, 1526; doi:10.3390/w10111526.

# APPENDIX

**APPENDIX A-1**: Drought analysis histograms

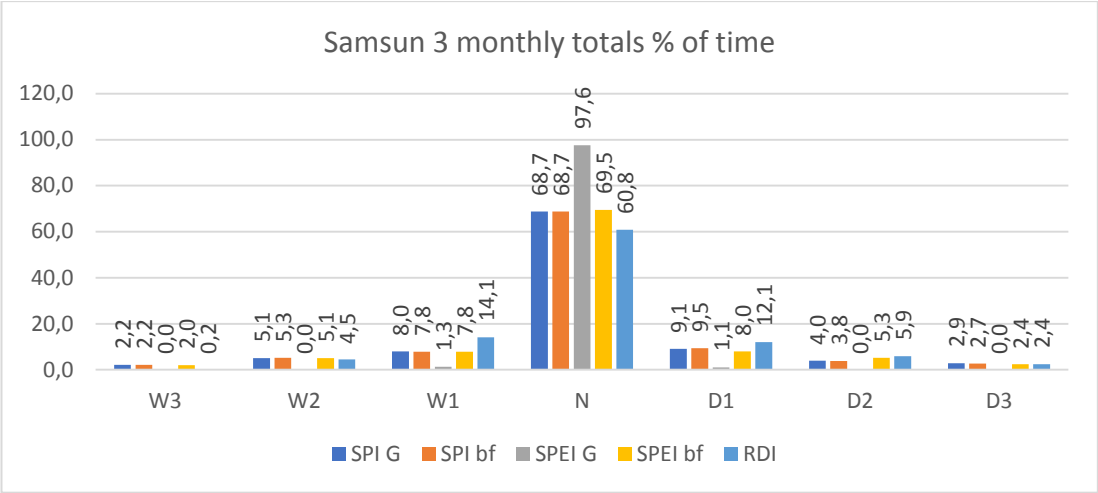


**APPENDIX A-1. 1.** Samsun 3 monthly totals % of time histogram

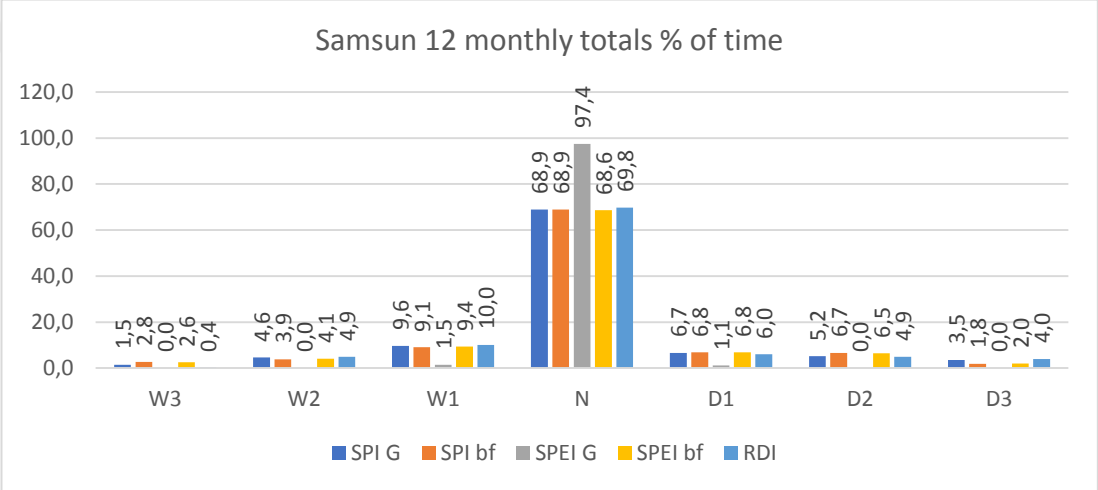


**APPENDIX A-1. 2.** Samsun 12 monthly totals % of time histogram

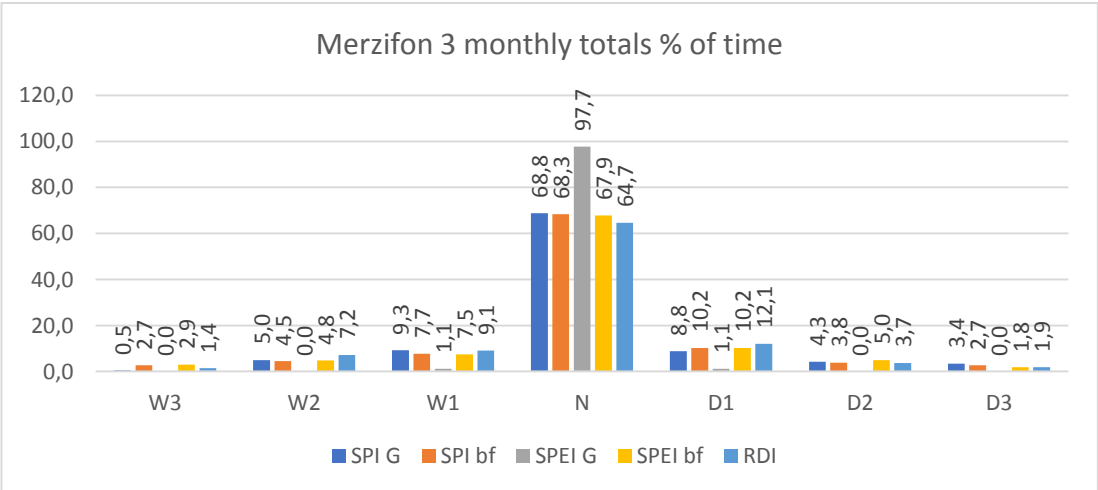


**APPENDIX A-1. 3.** Merzifon 3 monthly totals % of time histogram

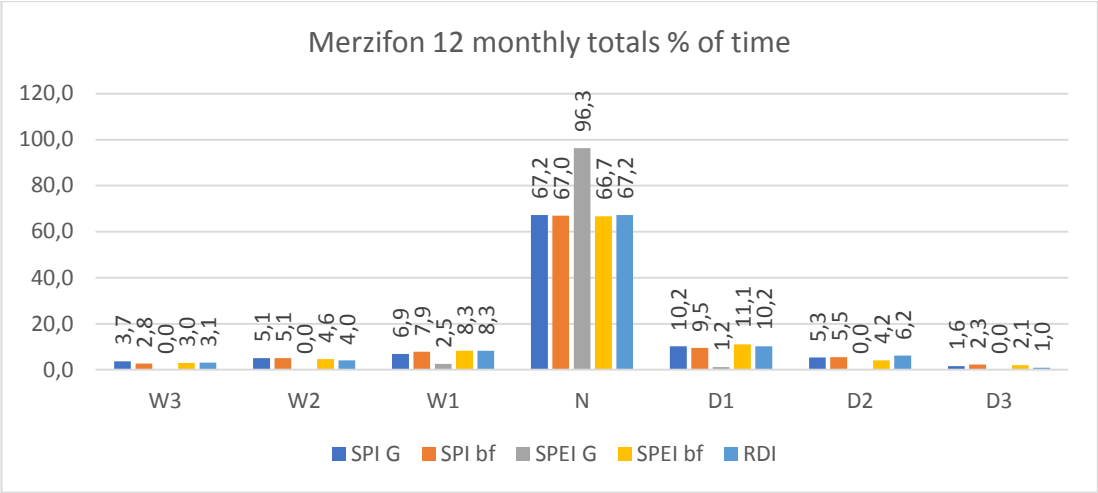


**APPENDIX A-1. 4.** Merzifon 12 monthly totals % of time histogram

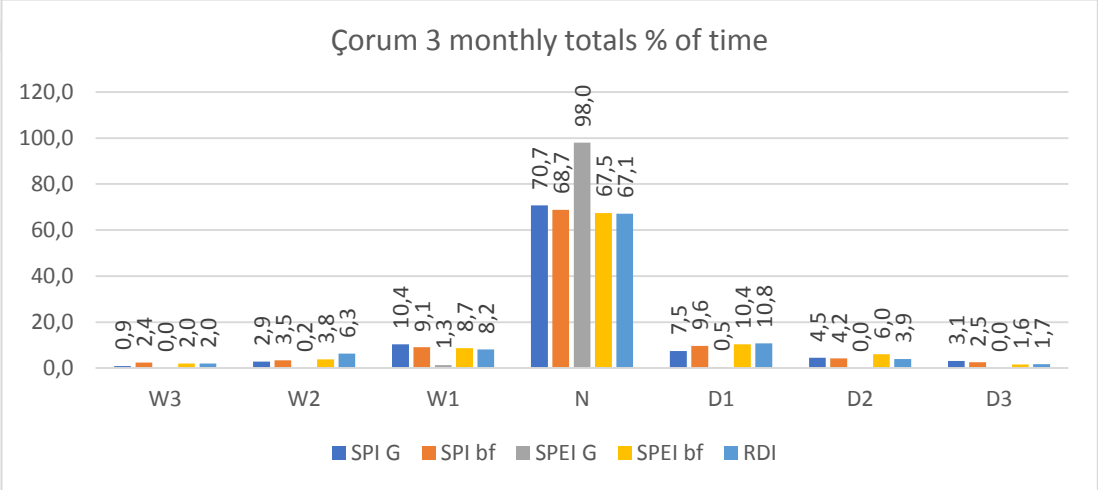


**APPENDIX A-1. 5.** Çorum 3 monthly totals % of time histogram

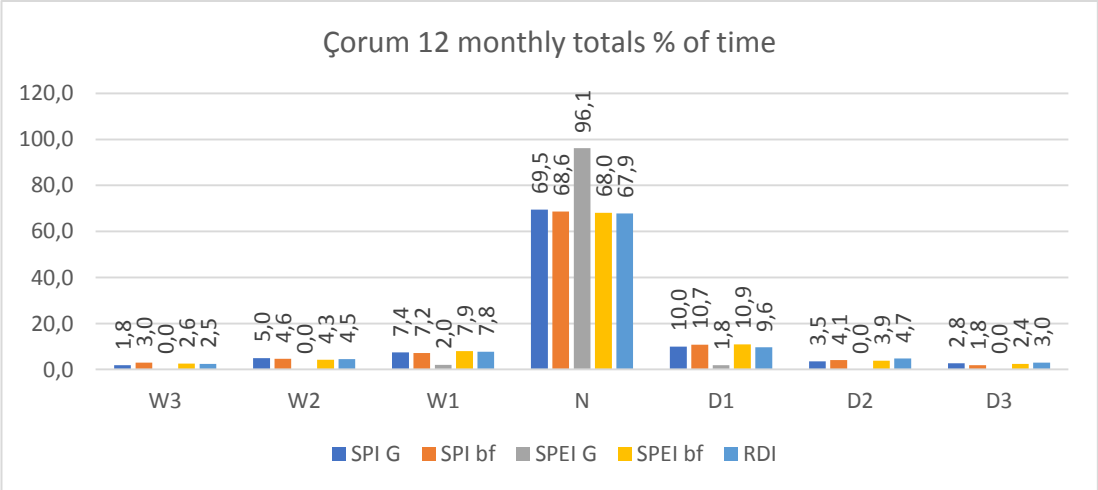


**APPENDIX A-1. 6.** Çorum 12 monthly totals % of time histogram

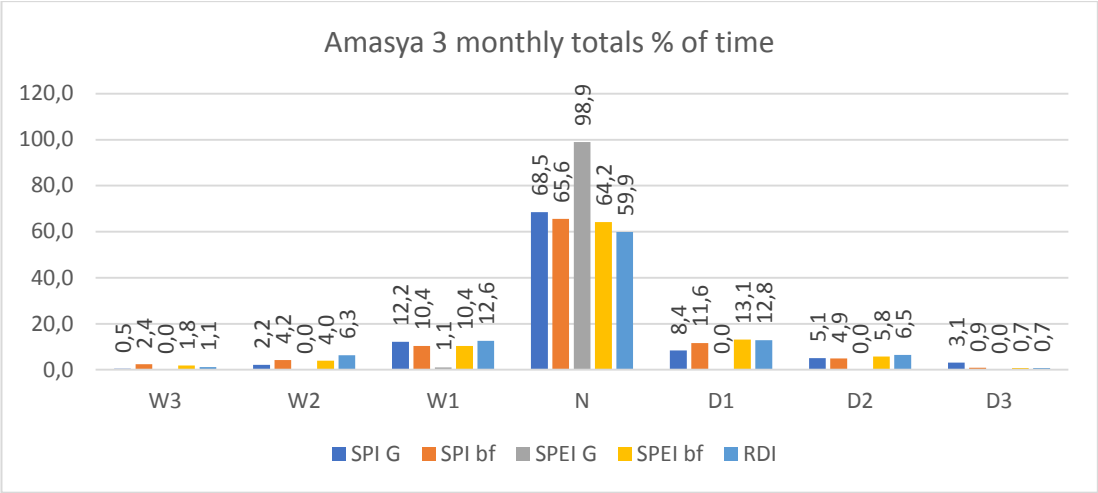


**APPENDIX A-1. 7.** Amasya 3 monthly totals % of time histogram

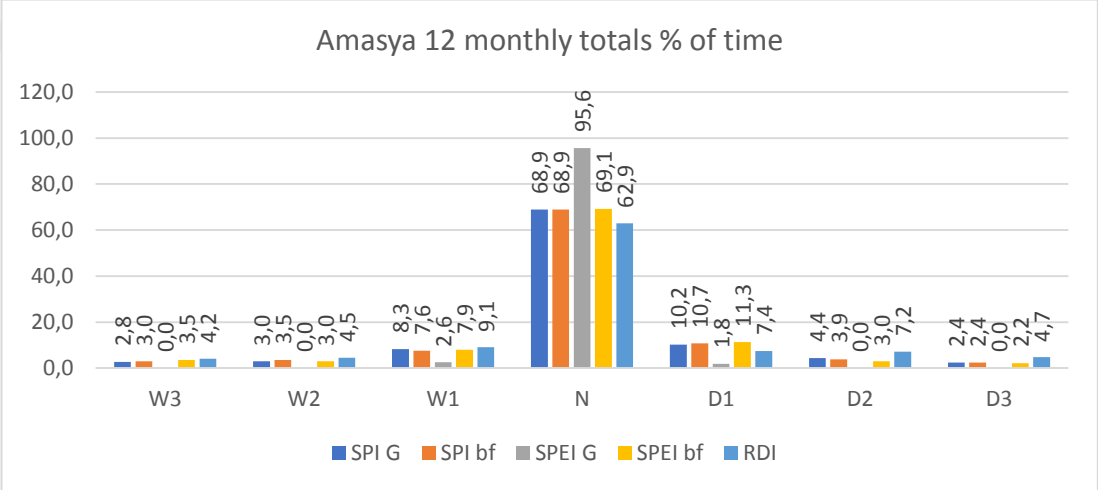


**APPENDIX A-1. 8.** Amasya 12 monthly totals % of time histogram

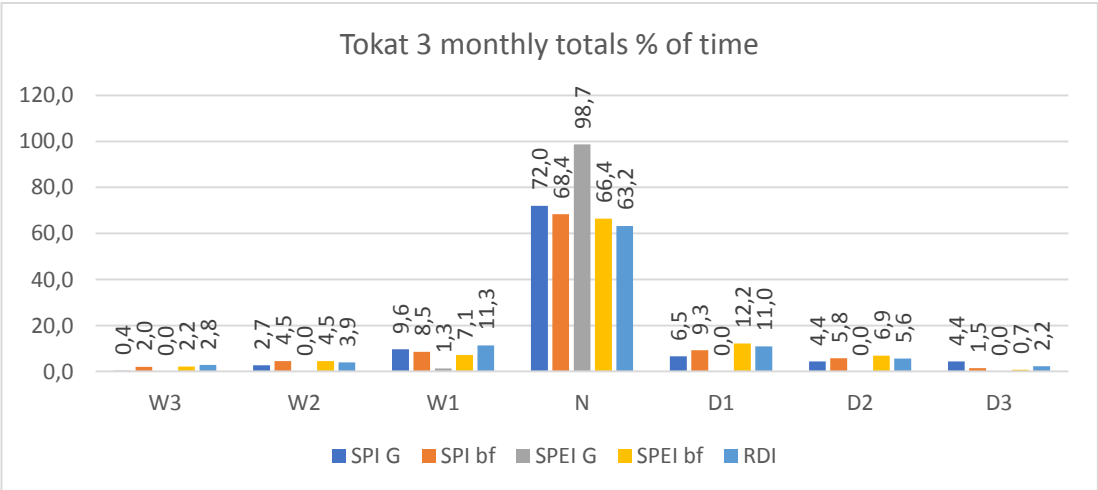


**APPENDIX A-1. 9.** Tokat 3 monthly totals % of time histogram

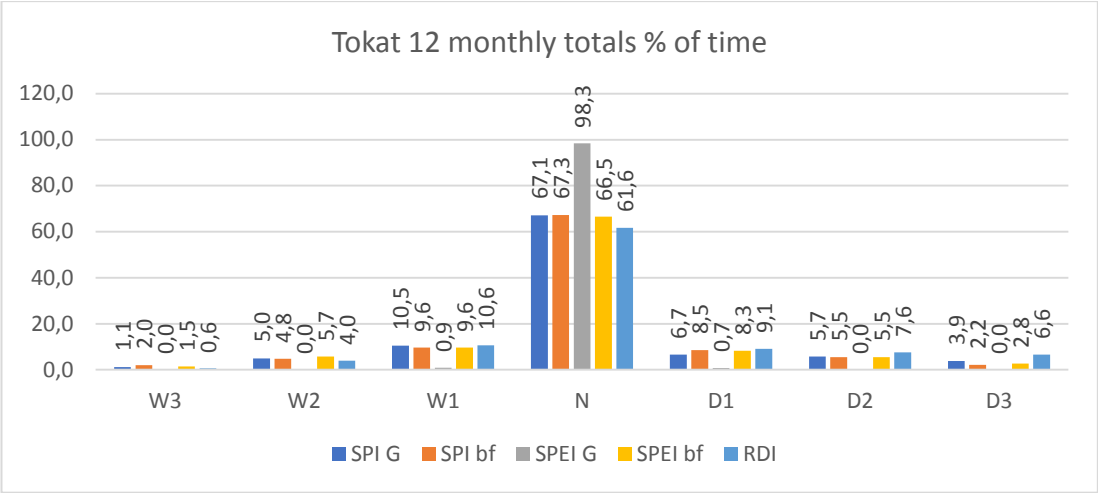


**APPENDIX A-1. 10.** Tokat 12 monthly totals % of time histogram

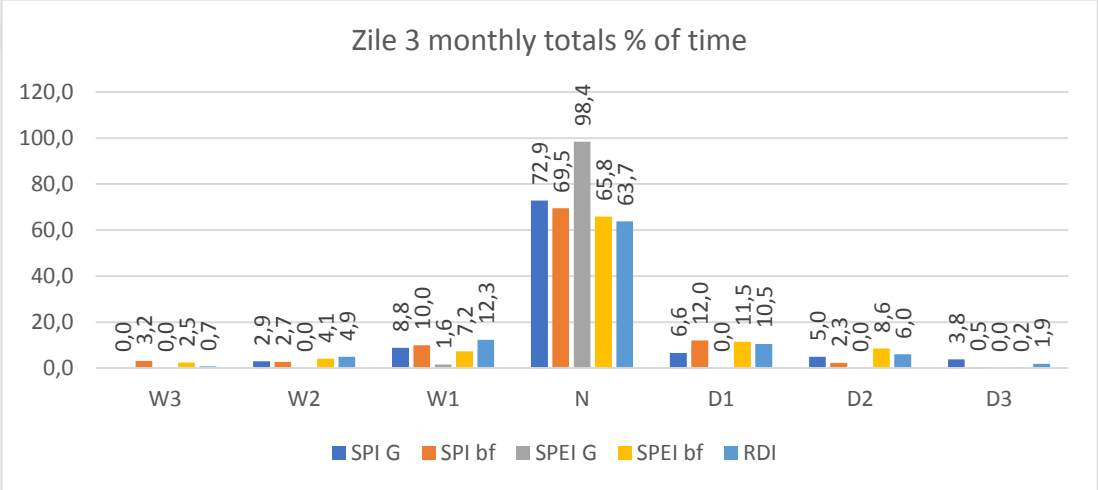


**APPENDIX A-1. 11.** Zile 3 monthly totals % of time histogram

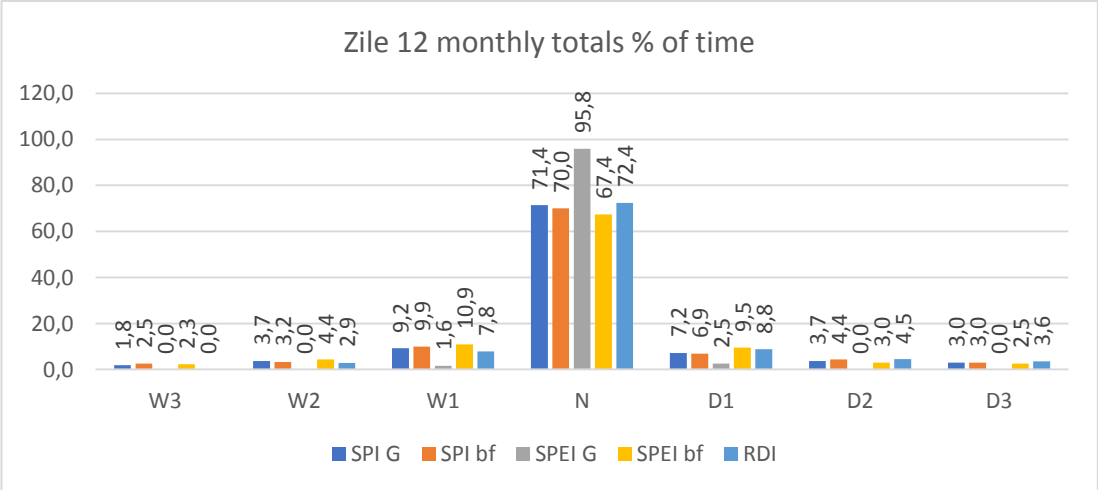


**APPENDIX A-1. 12.** Zile 12 monthly totals % of time histogram

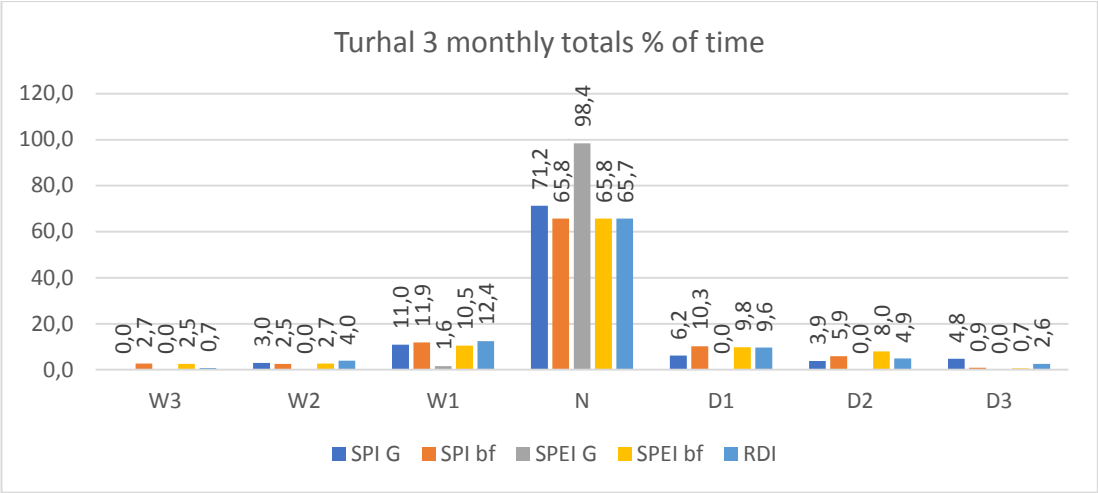


**APPENDIX A-1. 13.** Turhal 3 monthly totals % of time histogram

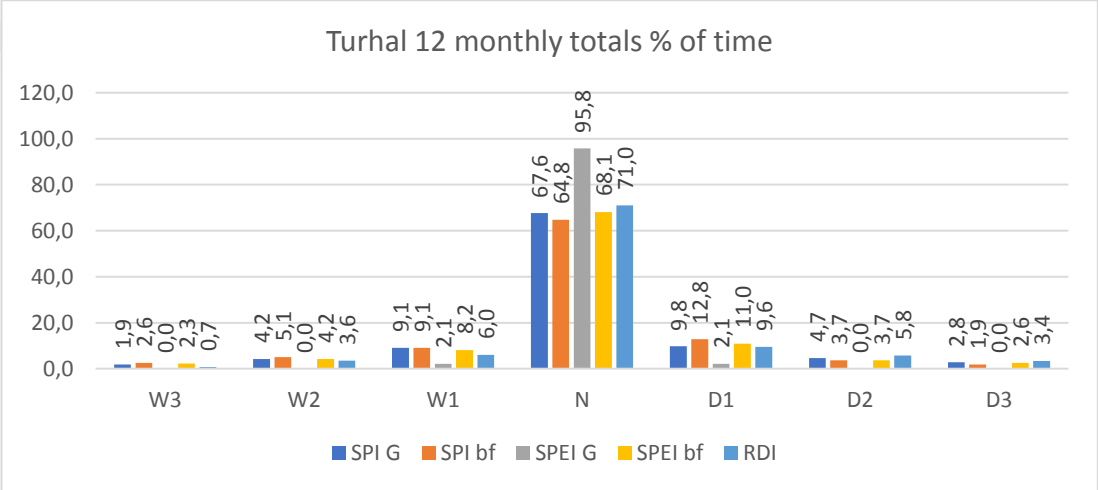


**APPENDIX A-1. 14.** Turhal 12 monthly totals % of time histogram

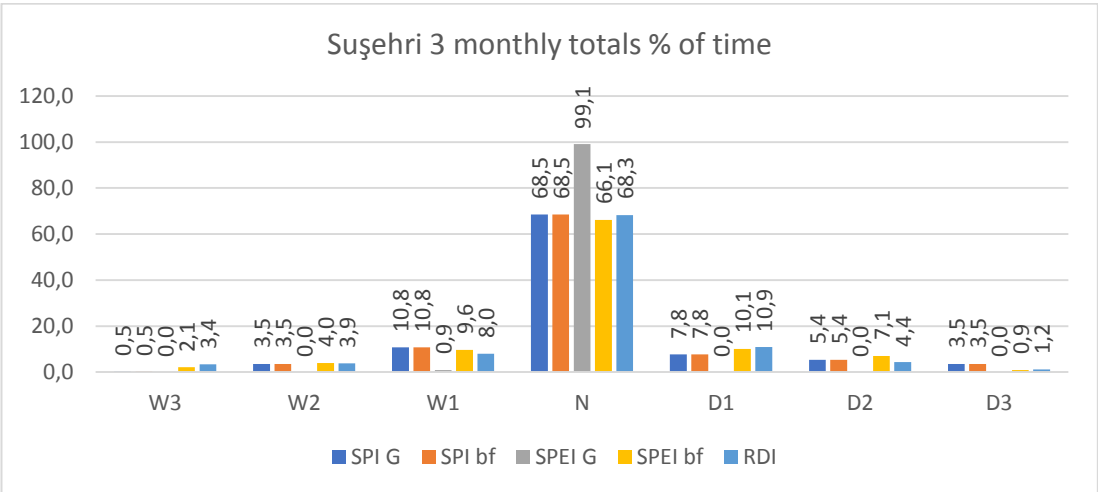


**APPENDIX A-1. 15.** Suşehri 3 monthly totals % of time histogram

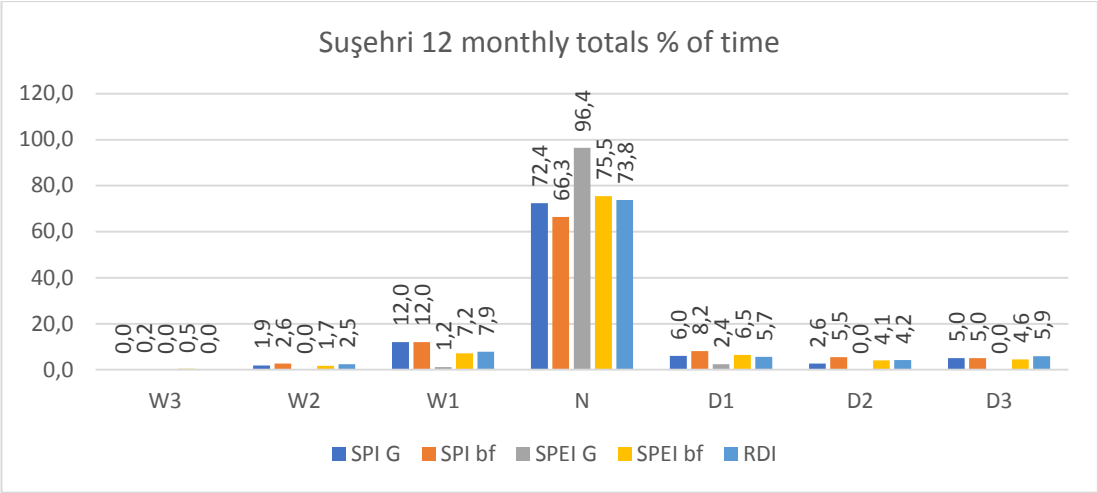


**APPENDIX A-1. 16.** Suşehri 12 monthly totals % of time histogram

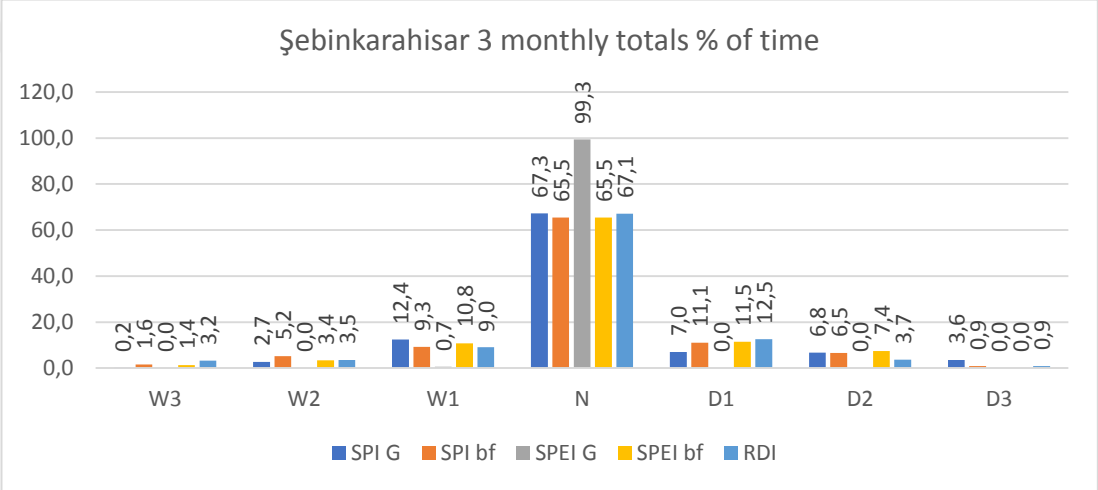


**APPENDIX A-1. 17.** Şebinkarahisar 3 monthly totals % of time histogram

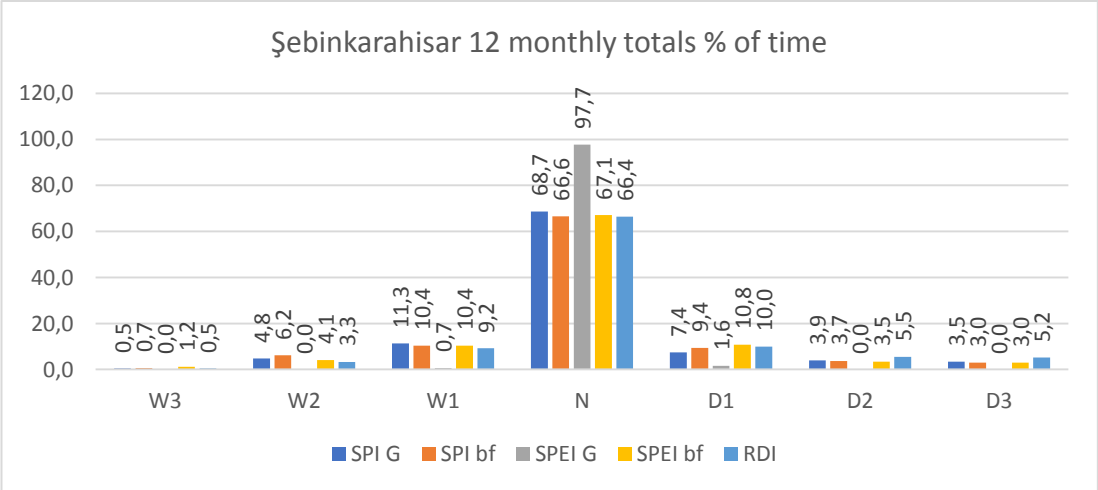


**APPENDIX A-1. 18.** Şebinkarahisar 12 monthly totals % of time histogram

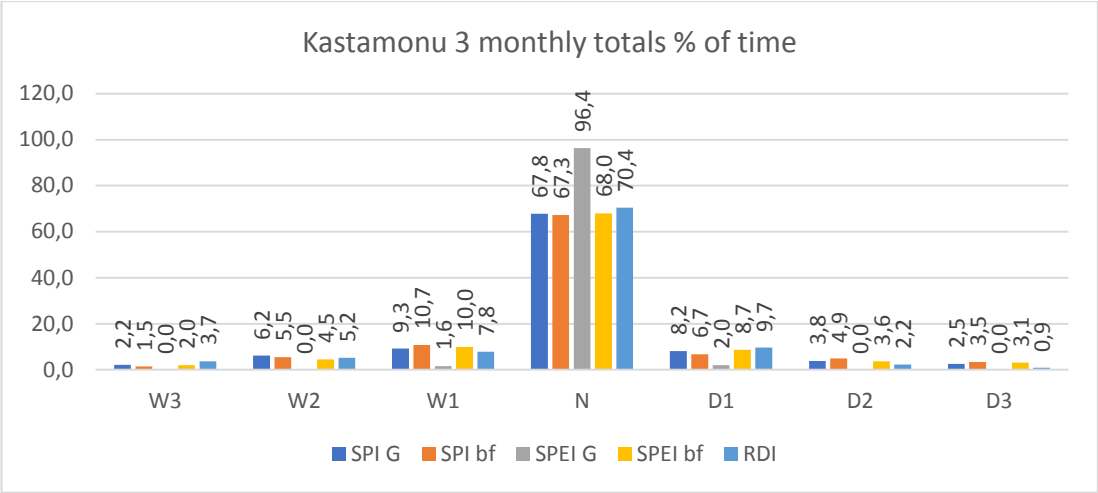


**APPENDIX A-1. 19.** Kastamonu 3 monthly totals % of time histogram

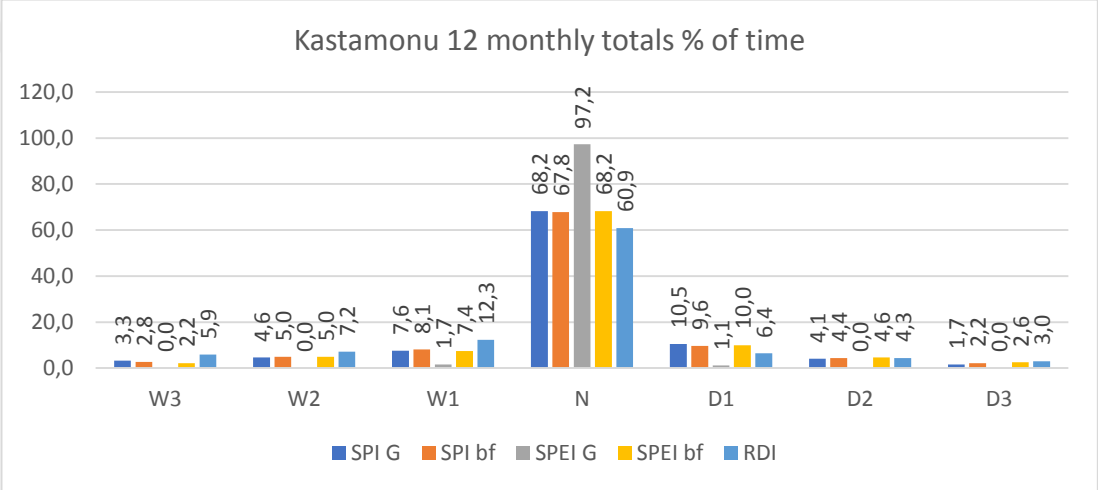


**APPENDIX A-1. 20.** Kastamonu 12 monthly totals % of time histogram

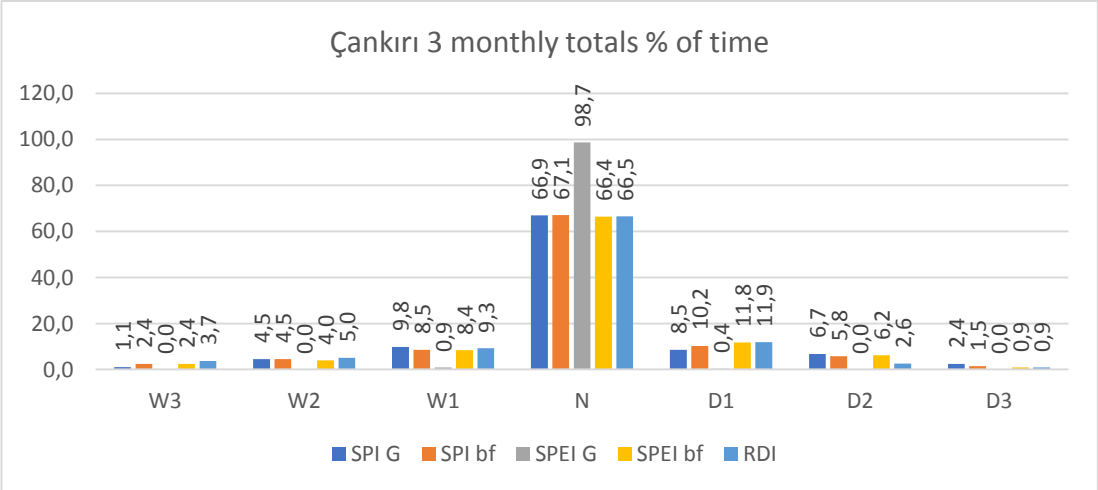


**APPENDIX A-1. 21.** Çankırı 3 monthly totals % of time histogram

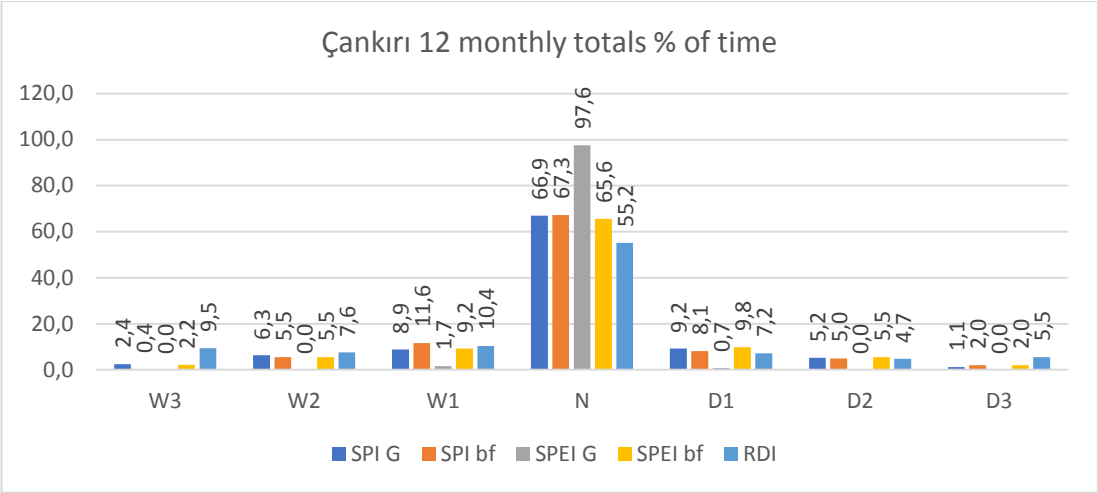


**APPENDIX A-1. 22.** Çankırı 12 monthly totals % of time histogram

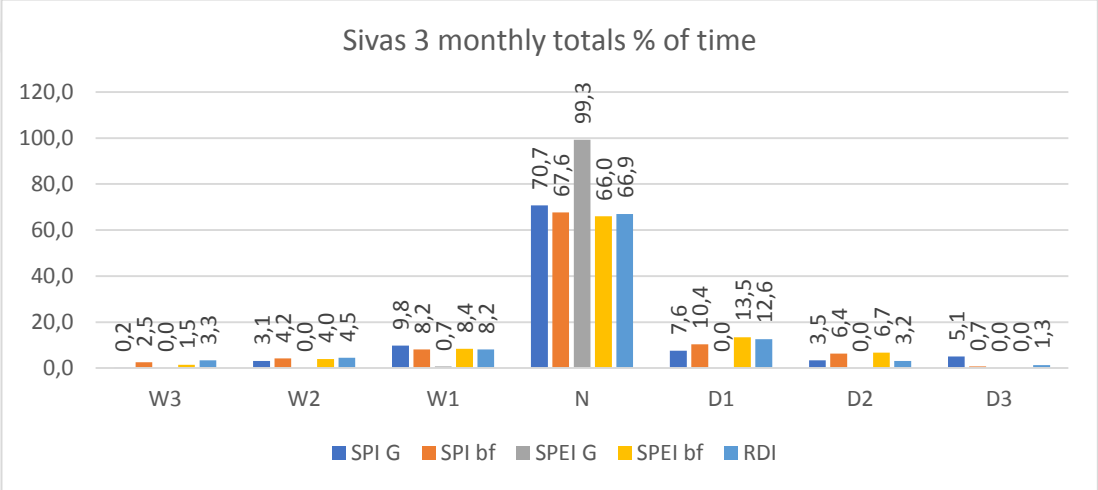


**APPENDIX A-1. 23.** Sivas 3 monthly totals % of time histogram

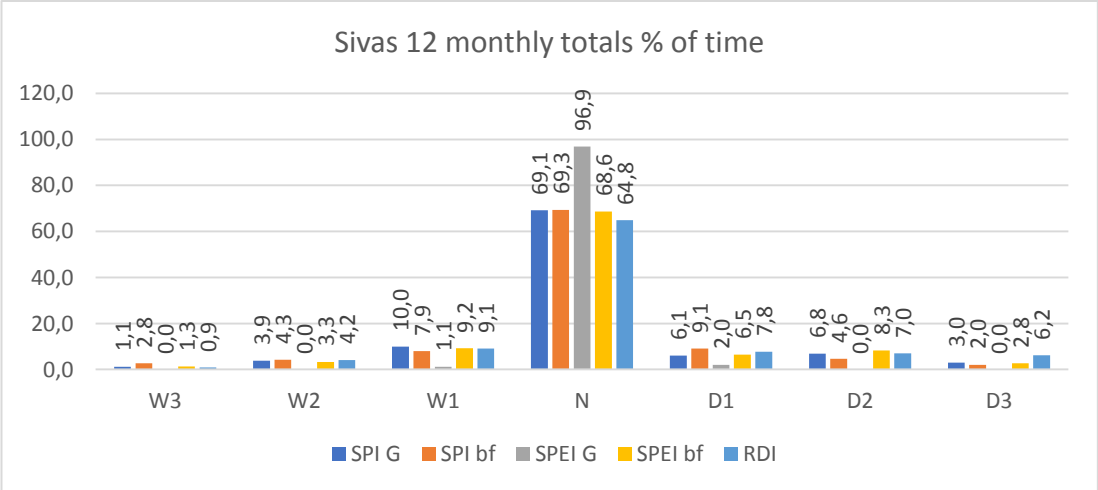


**APPENDIX A-1. 24.** Sivas 12 monthly totals % of time histogram

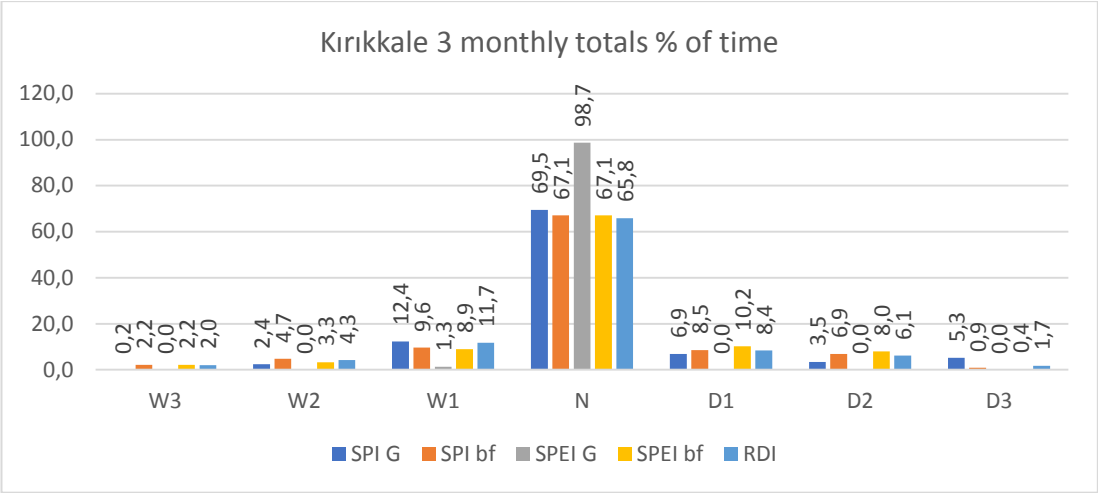


**APPENDIX A-1. 25.** Kırıkkale 3 monthly totals % of time histogram

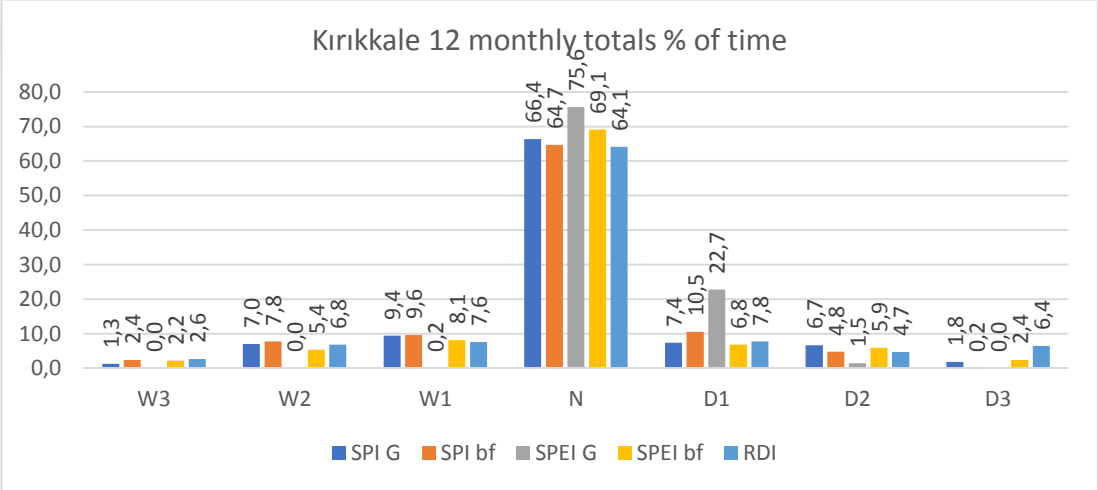


**APPENDIX A-1. 26.** Kırıkkale 12 monthly totals % of time histogram

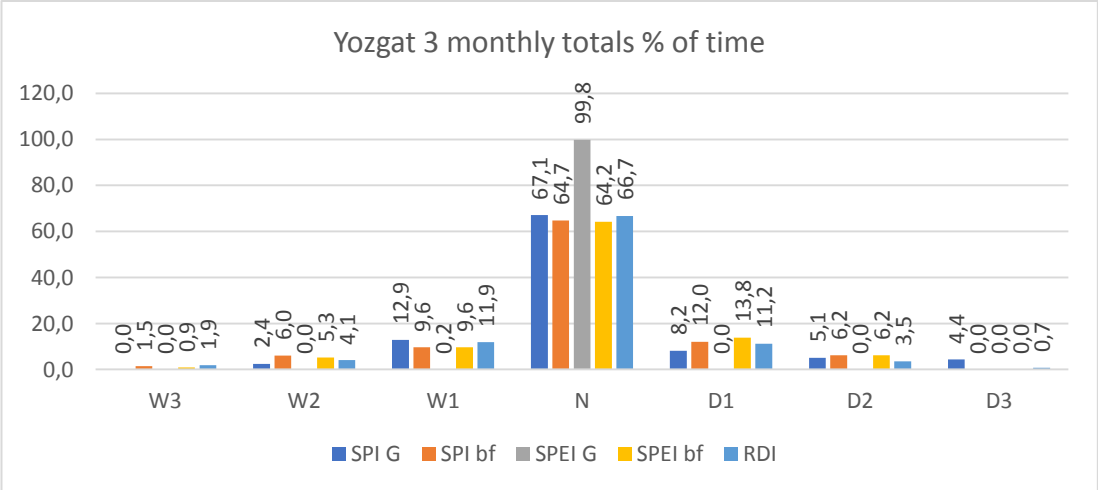


**APPENDIX A-1. 27.** Yozgat 3 monthly totals % of time histogram

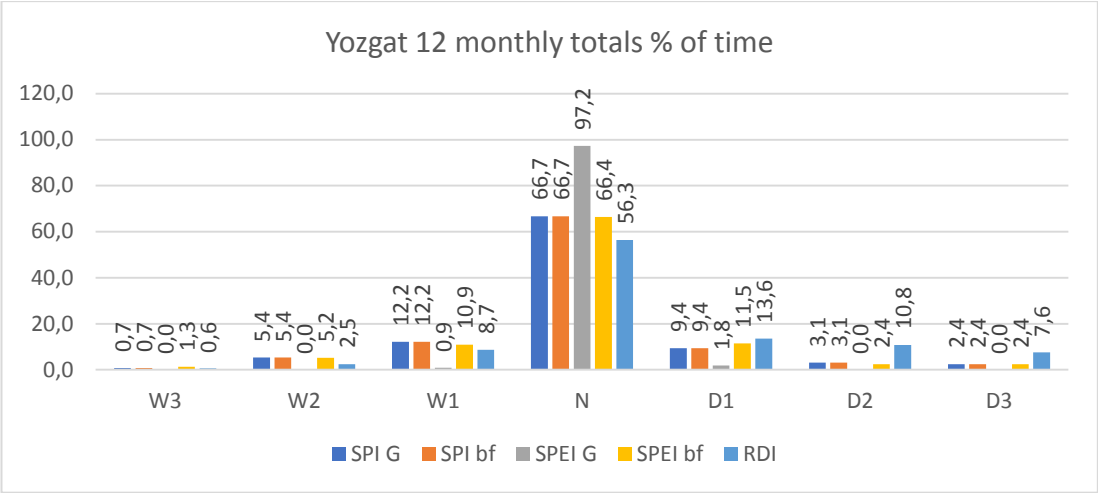


**APPENDIX A-1. 28.** Yozgat 12 monthly totals % of time histogram

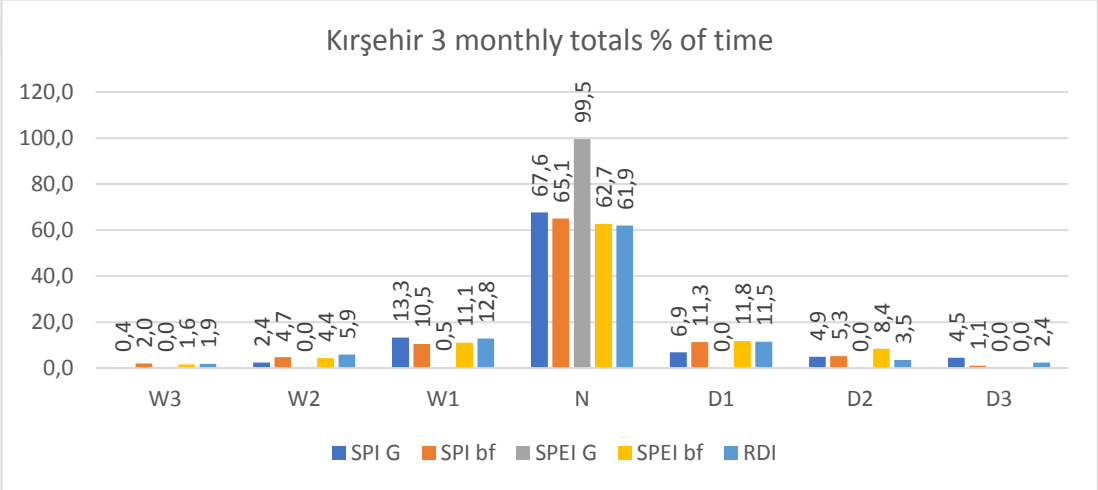


**APPENDIX A-1. 29.** Kırşehir 3 monthly totals % of time histogram

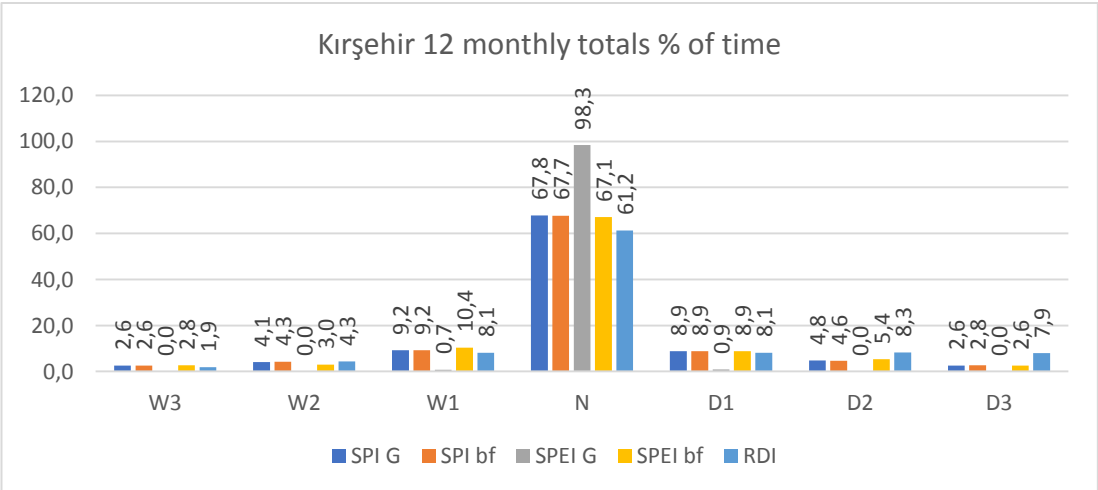


**APPENDIX A-1. 30.** Kırşehir 12 monthly totals % of time histogram

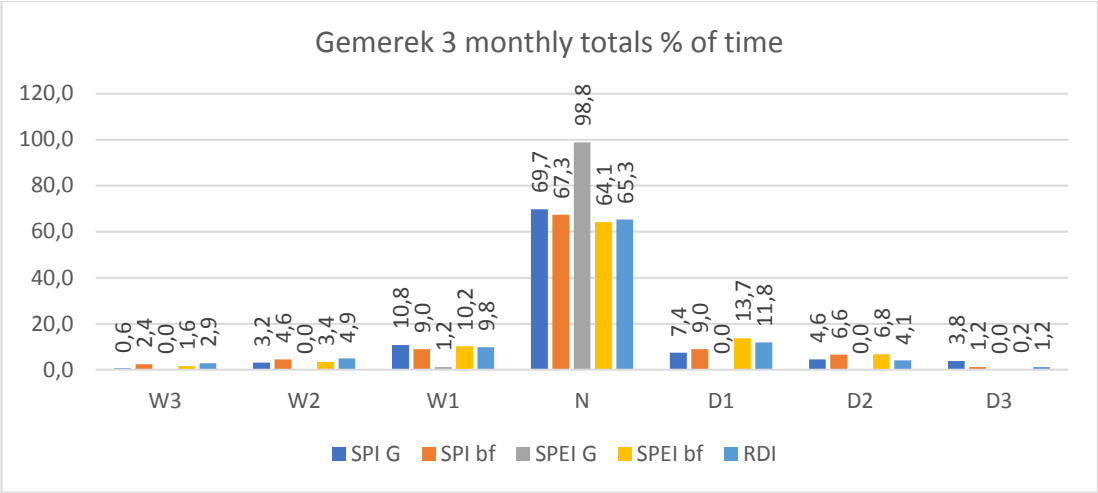


**APPENDIX A-1. 31.** Gemerek 3 monthly totals % of time histogram

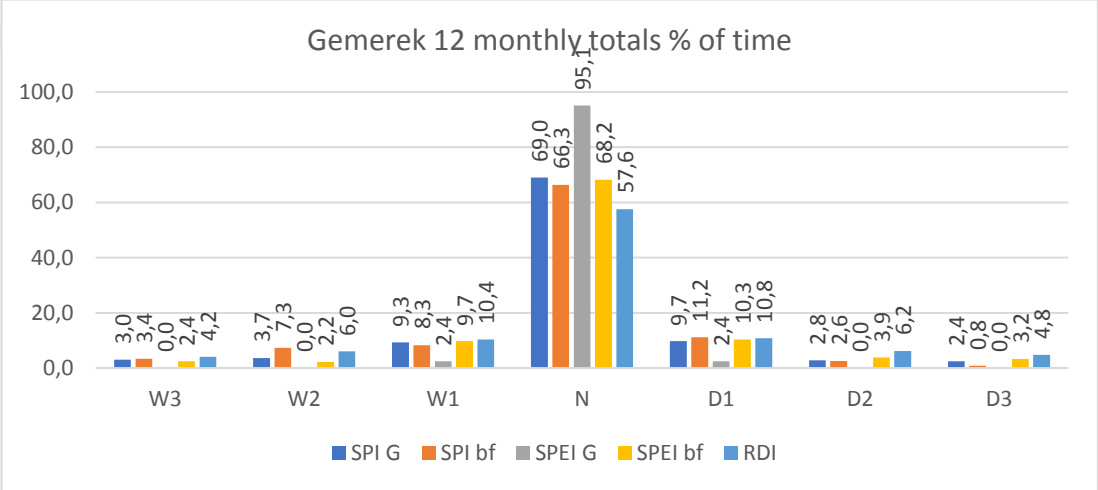


**APPENDIX A-1. 32.** Gemerek 12 monthly totals % of time histogram

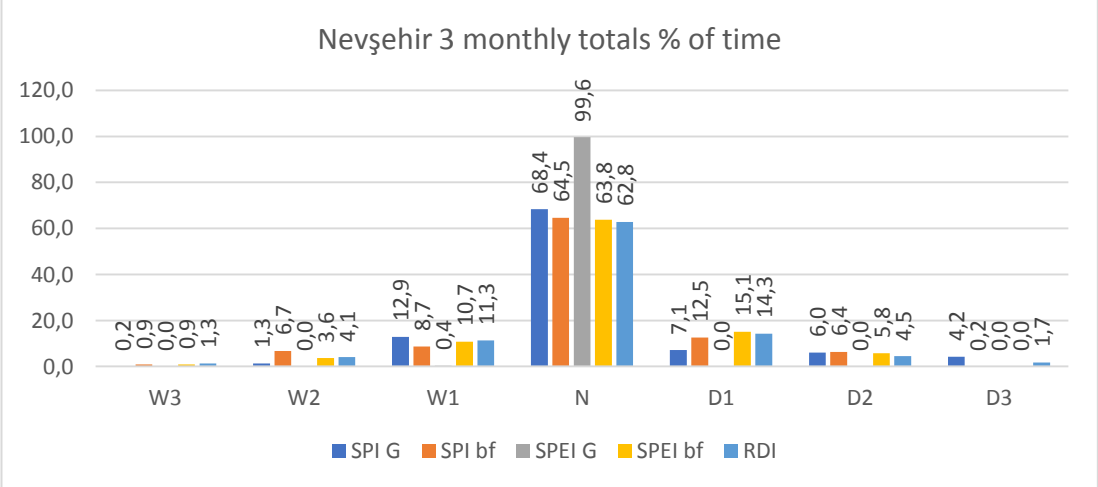


**APPENDIX A-1. 33.** Nevşehir 3 monthly totals % of time histogram

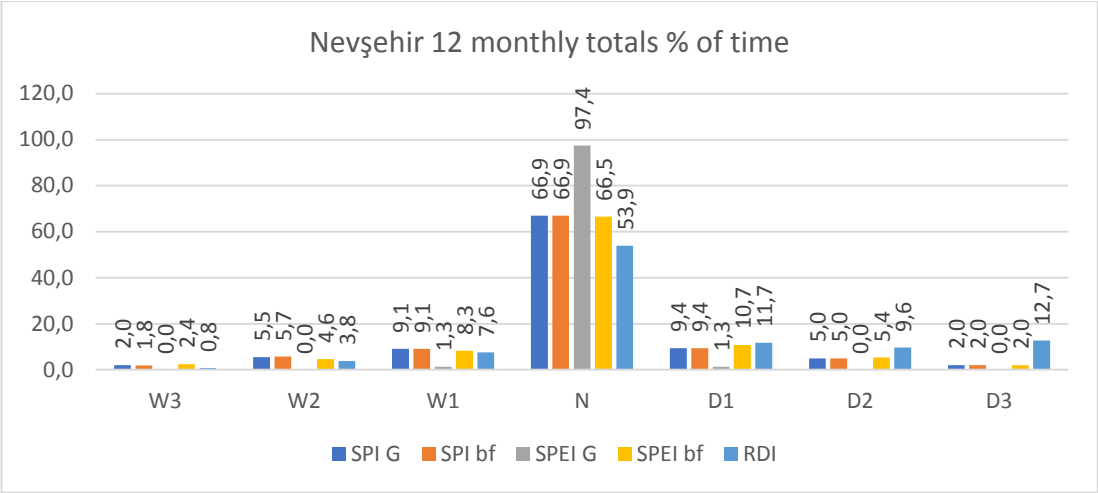


**APPENDIX A-1. 34.** Nevşehir 12 monthly totals % of time histogram

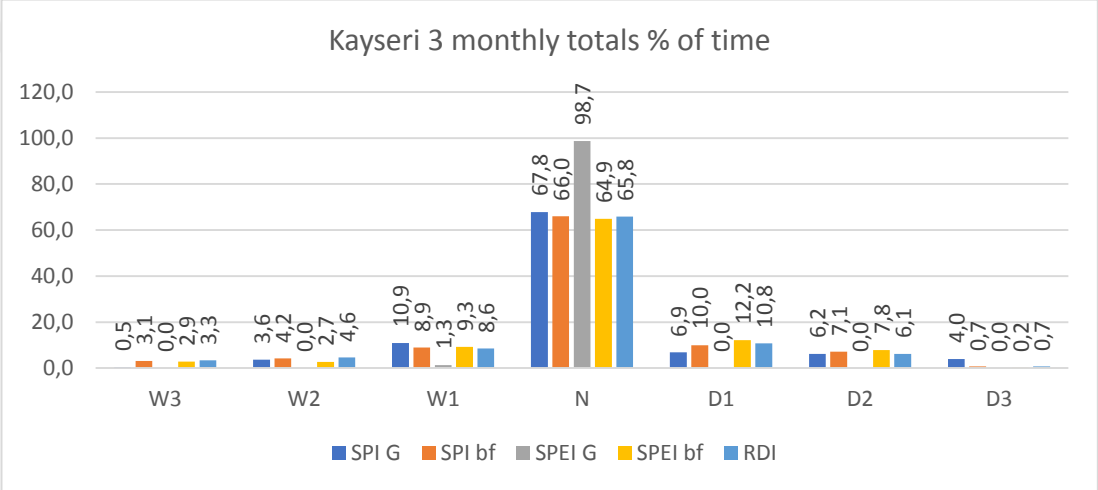


**APPENDIX A-1. 35.** Kayseri 3 monthly totals % of time histogram

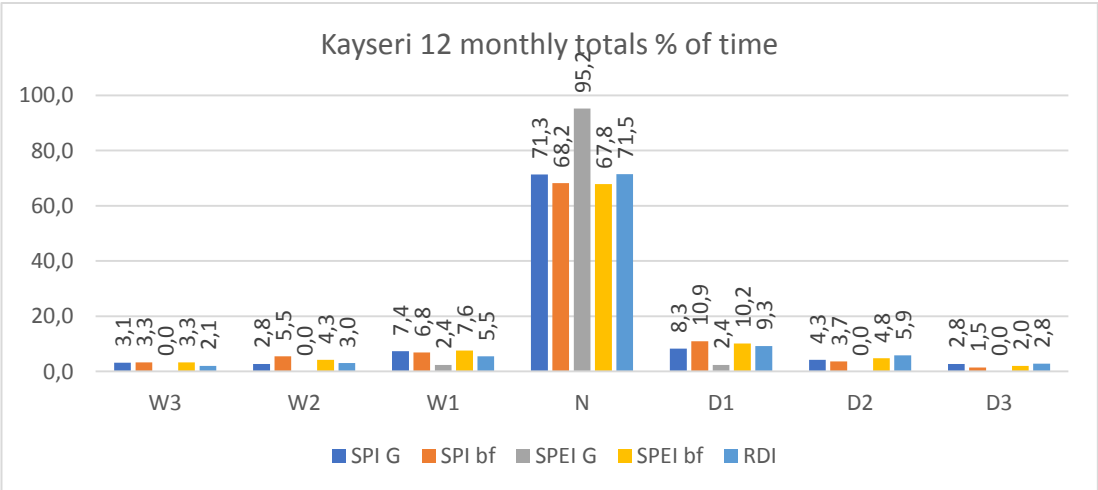


**APPENDIX A-1. 36.** Kayseri 12 monthly totals % of time histogram

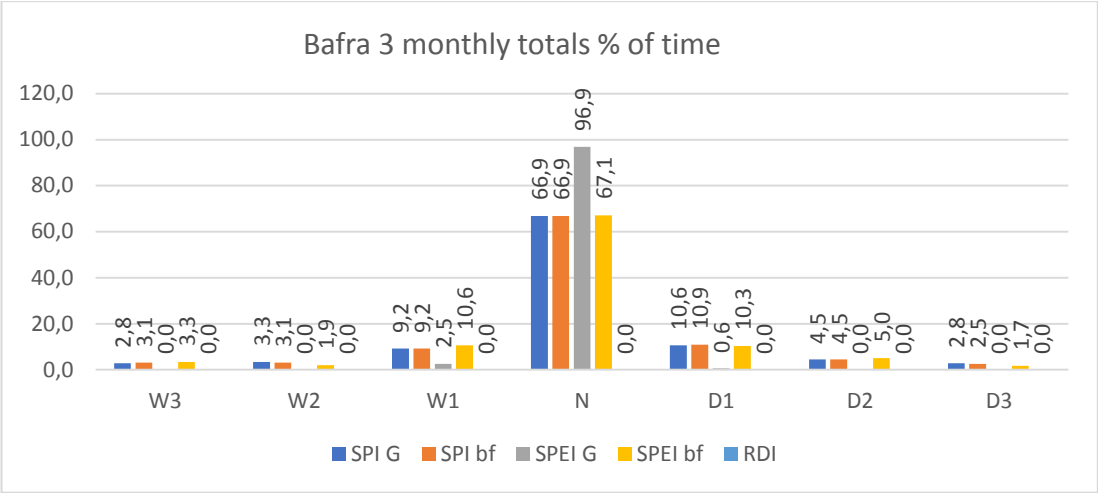


**APPENDIX A-1. 37.** Bafra 3 monthly totals % of time histogram

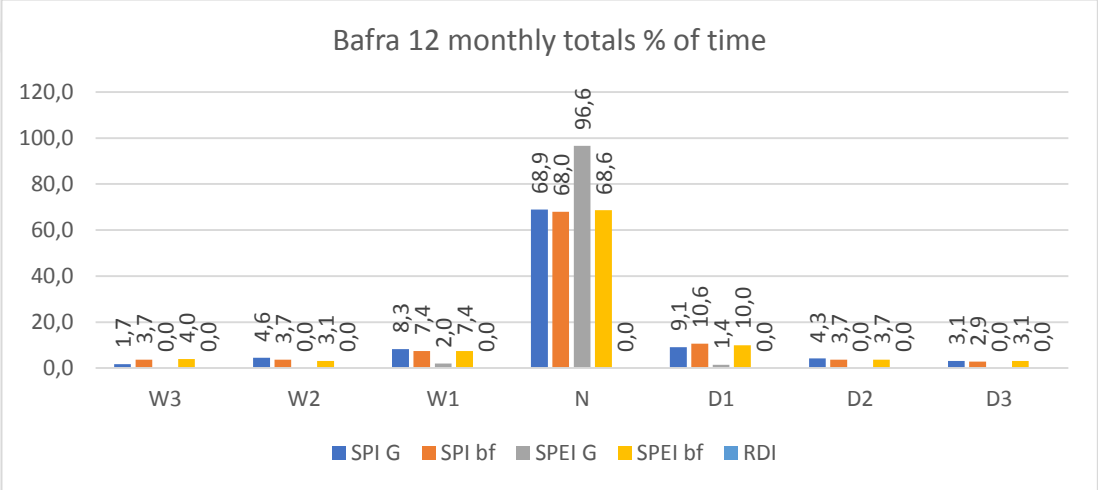


**APPENDIX A-1. 38.** Bafra 12 monthly totals % of time histogram

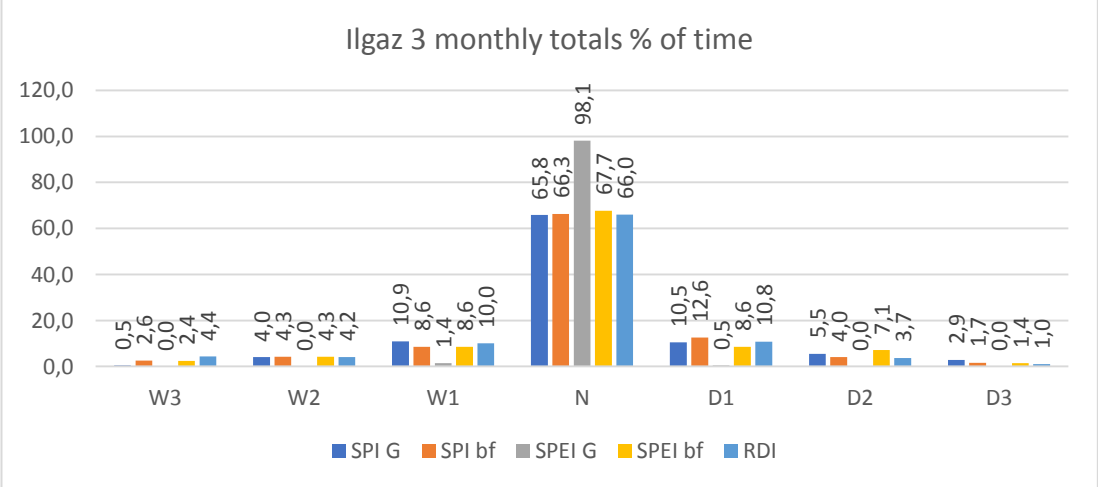


**APPENDIX A-1. 39.** Ilgaz 3 monthly totals % of time histogram

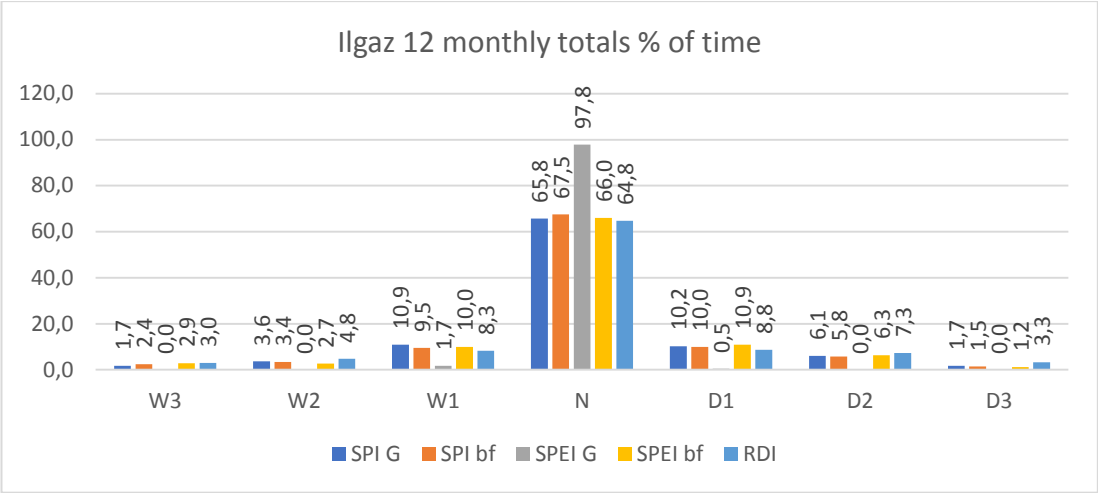


**APPENDIX A-1. 40.** Ilgaz 12 monthly totals % of time histogram

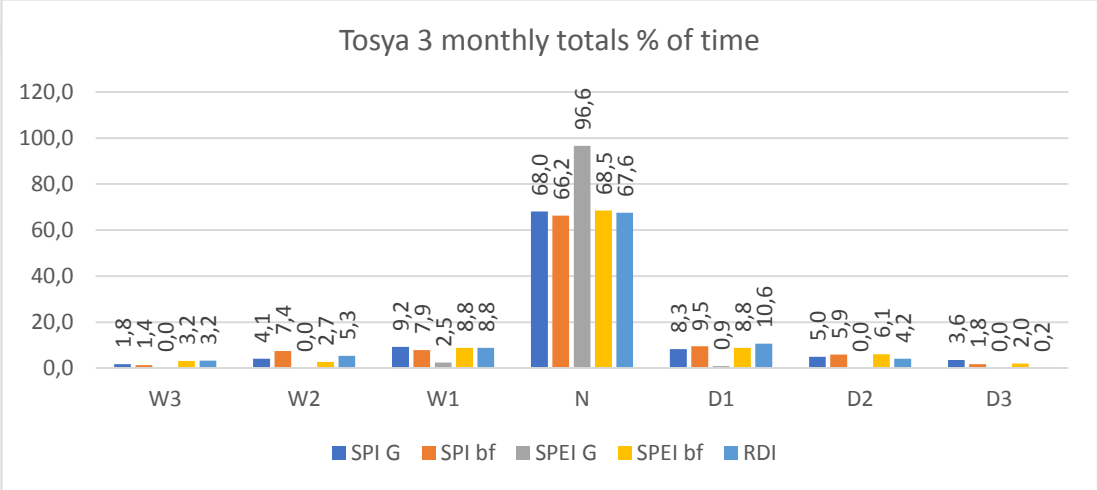


**APPENDIX A-1. 41.** Tosya 3 monthly totals % of time histogram

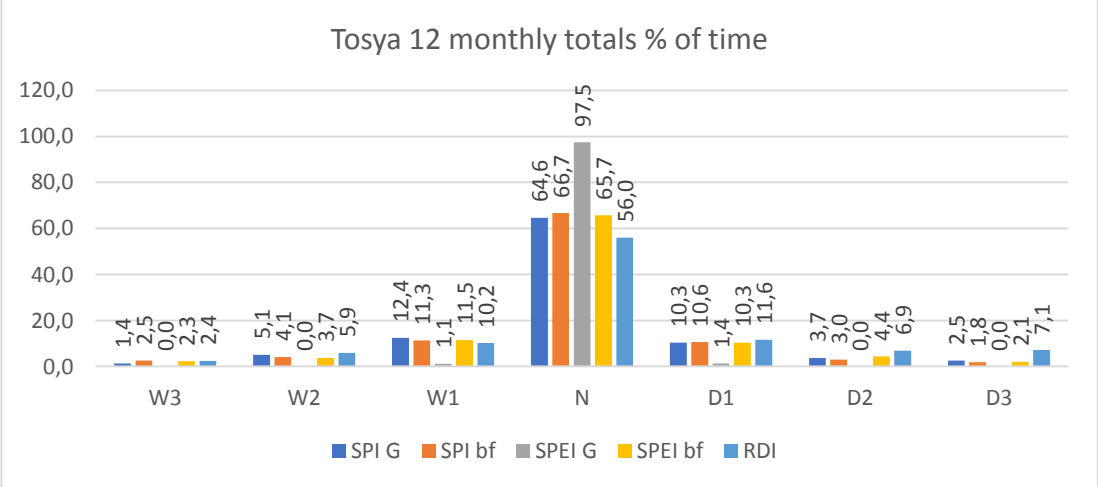


**APPENDIX A-1. 42.** Tosya 12 monthly totals % of time histogram

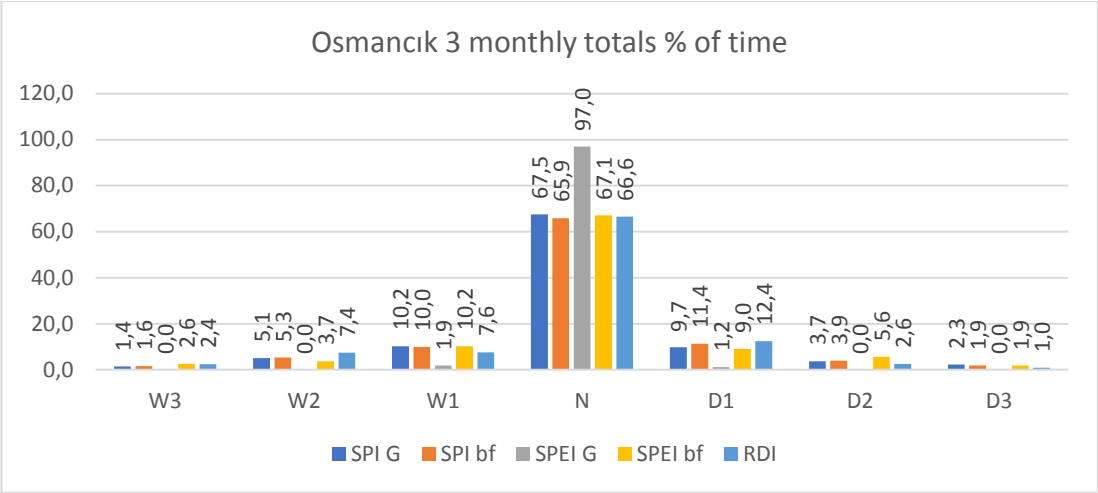


**APPENDIX A-1. 43.** Osmancık 3 monthly totals % of time histogram

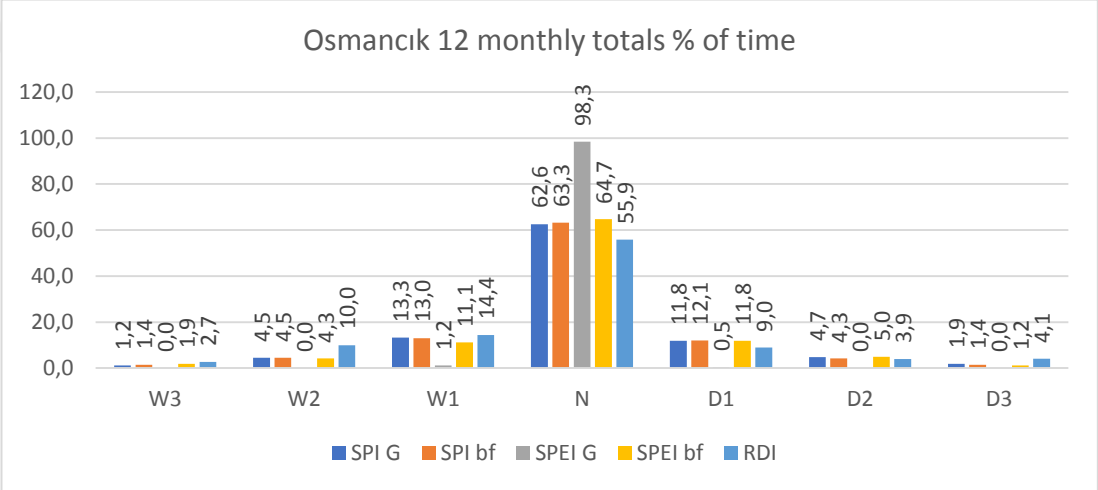


**APPENDIX A-1. 44.** Osmancık 12 monthly totals % of time histogram

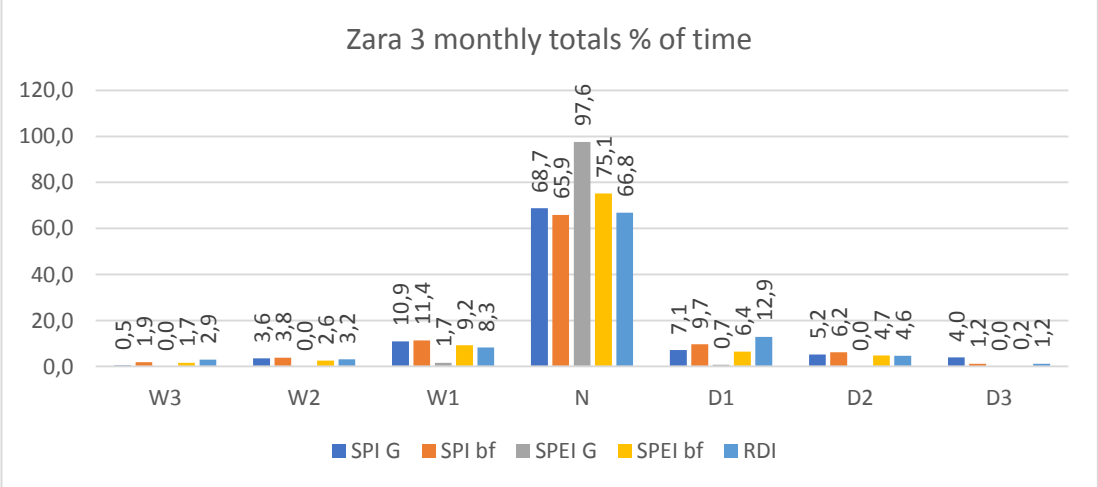


**APPENDIX A-1. 45.** Zara 3 monthly totals % of time histogram

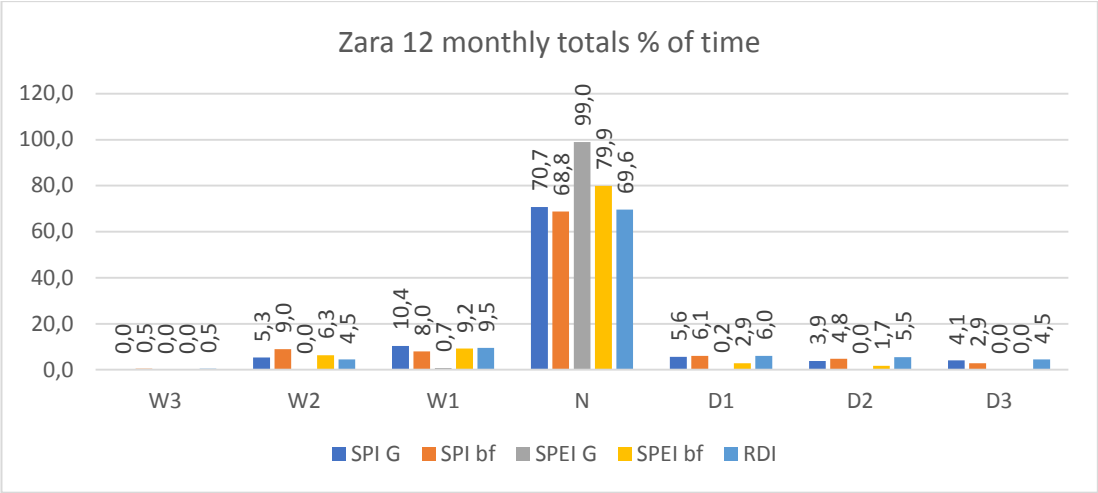


**APPENDIX A-1. 46.** Zara 12 monthly totals % of time histogram

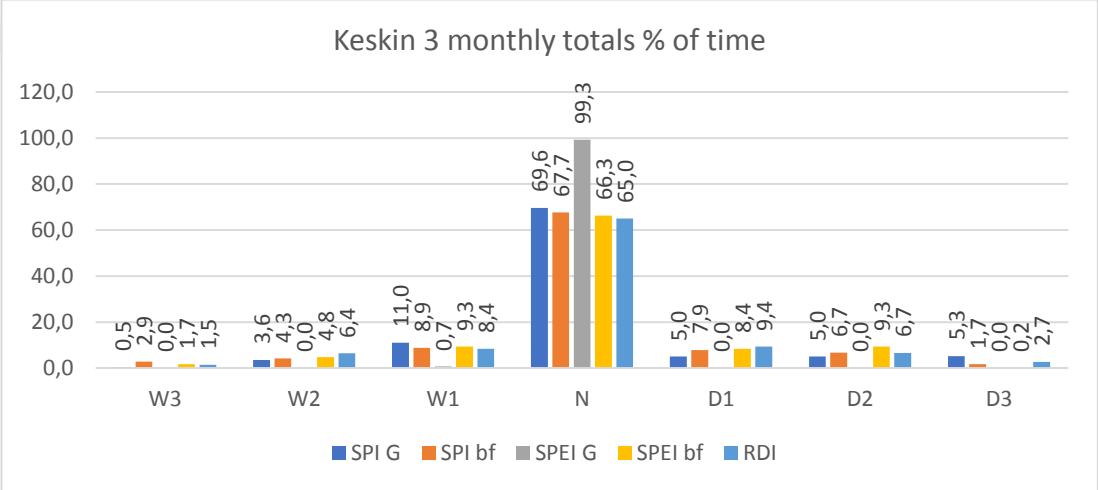


**APPENDIX A-1. 47.** Keskin 3 monthly totals % of time histogram

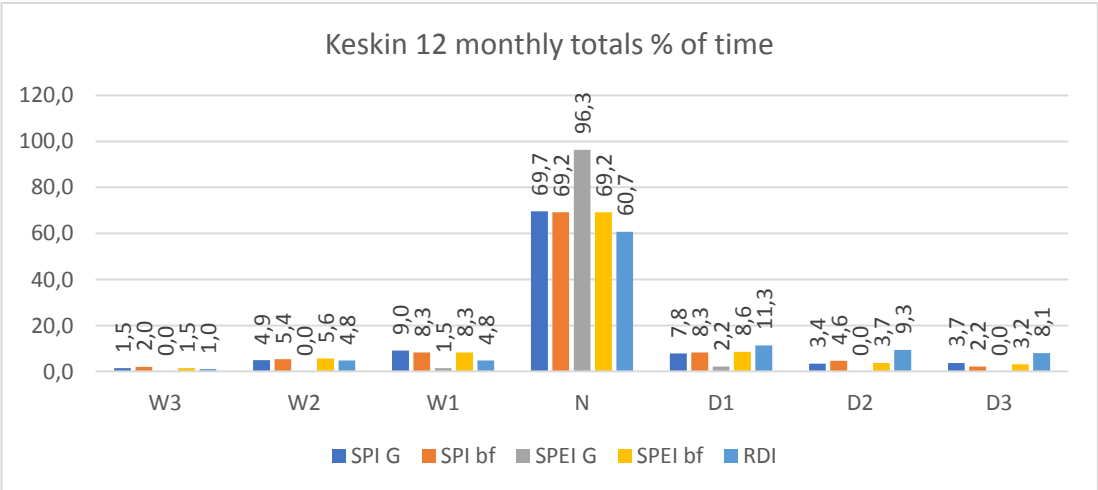


**APPENDIX A-1. 48.** Keskin 12 monthly totals % of time histogram

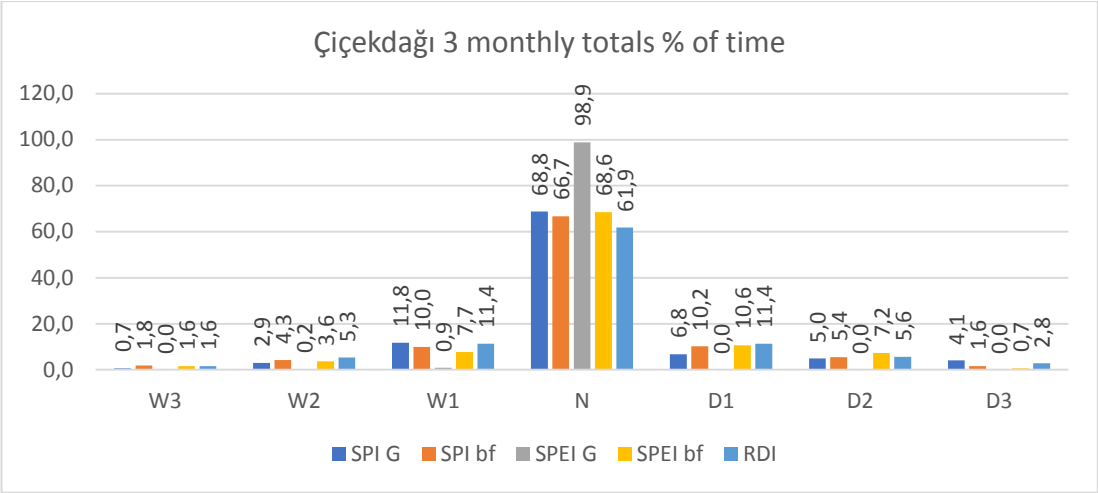


**APPENDIX A-1. 49.** Çiçekdağı 3 monthly totals % of time histogram

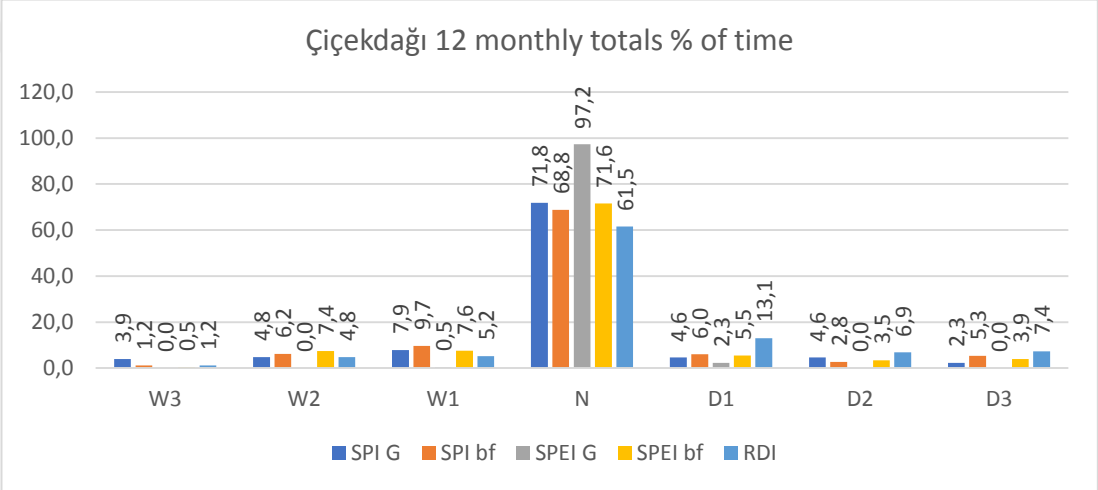


**APPENDIX A-1. 50.** Çiçekdağı 12 monthly totals % of time histogram

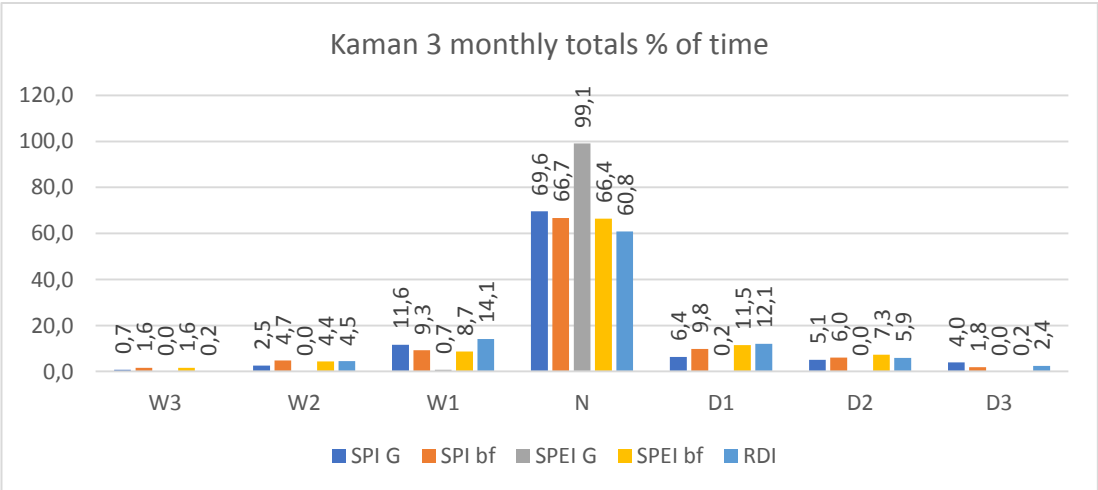


**APPENDIX A-1. 51.** Kaman 3 monthly totals % of time histogram

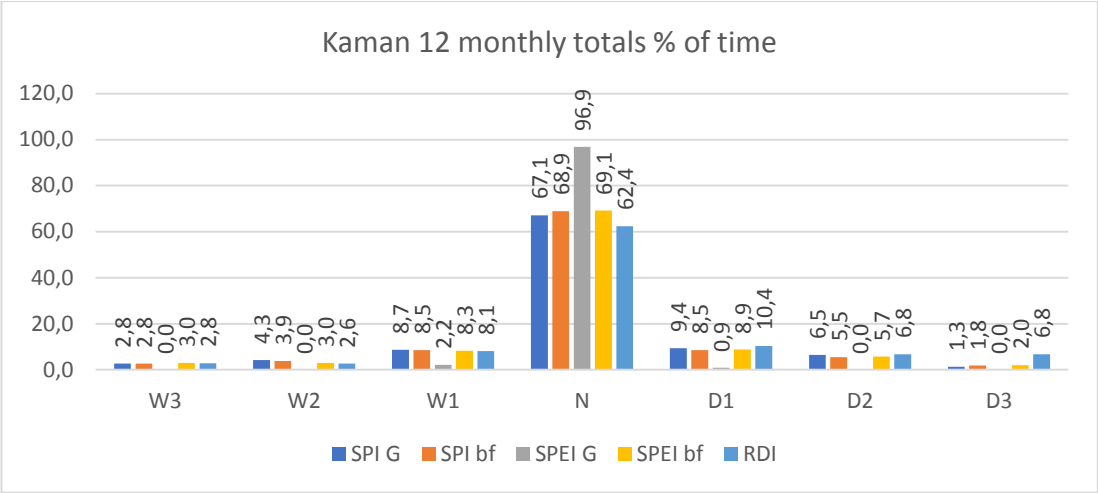


**APPENDIX A-1. 52.** Kaman 12 monthly totals % of time histogram

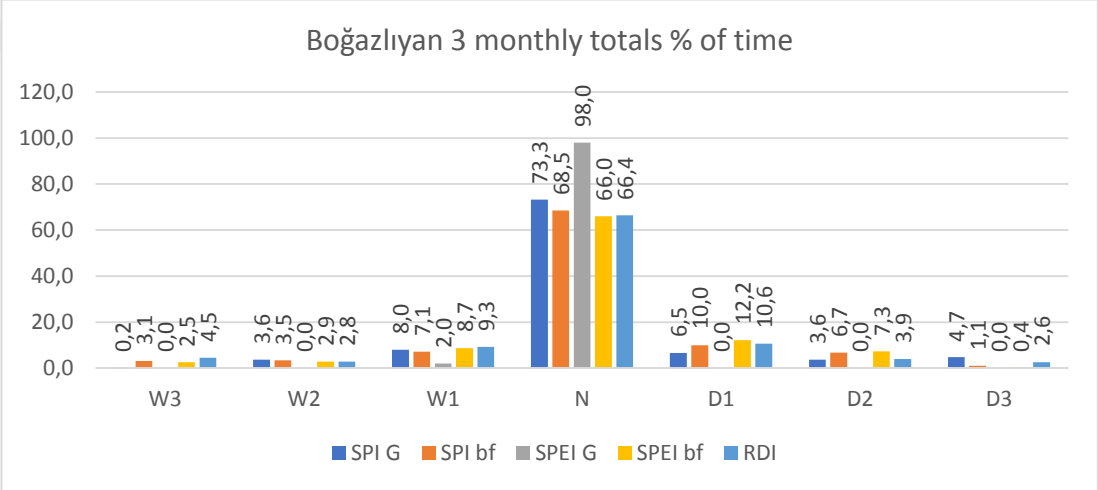


**APPENDIX A-1. 53.** Boğazlıyan 3 monthly totals % of time histogram

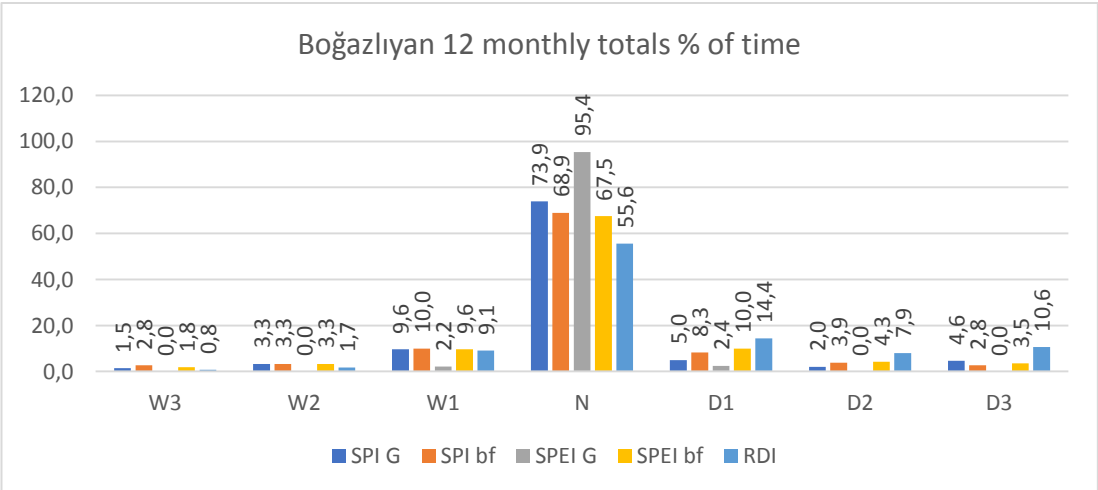


**APPENDIX A-1. 54.** Boğazlıyan 12 monthly totals % of time histogram

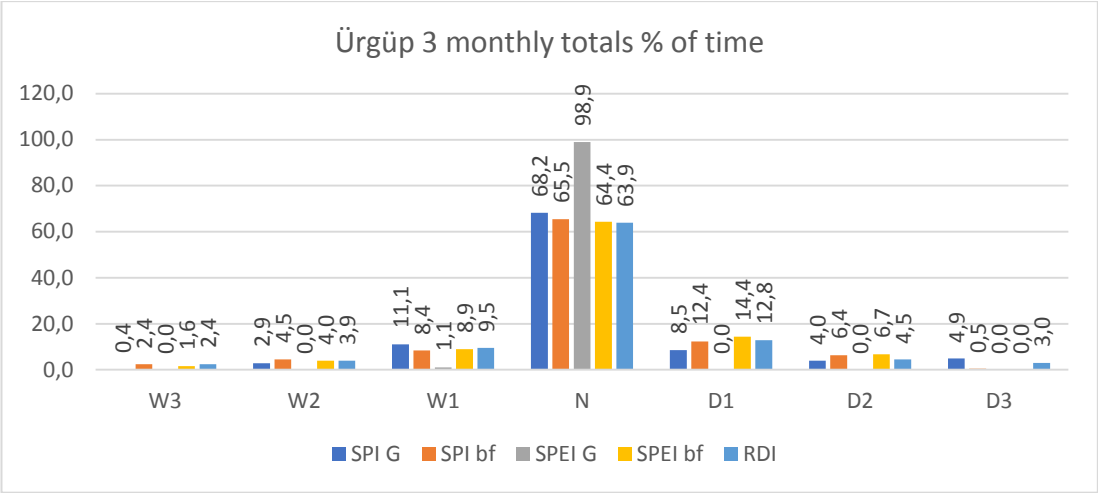


**APPENDIX A-1. 55.** Ürgüp 3 monthly totals % of time histogram

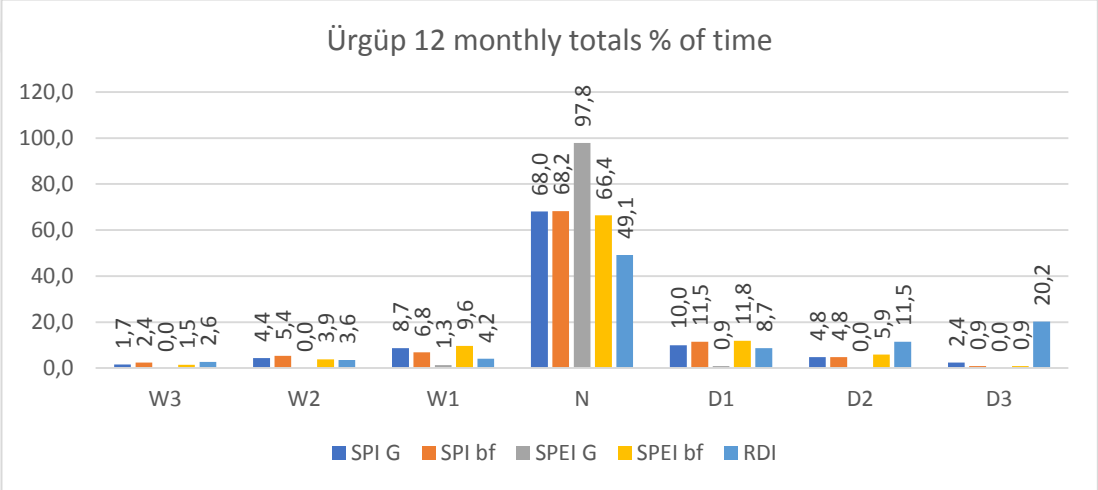


**APPENDIX A-1. 56.** Ürgüp 12 monthly totals % of time histogram

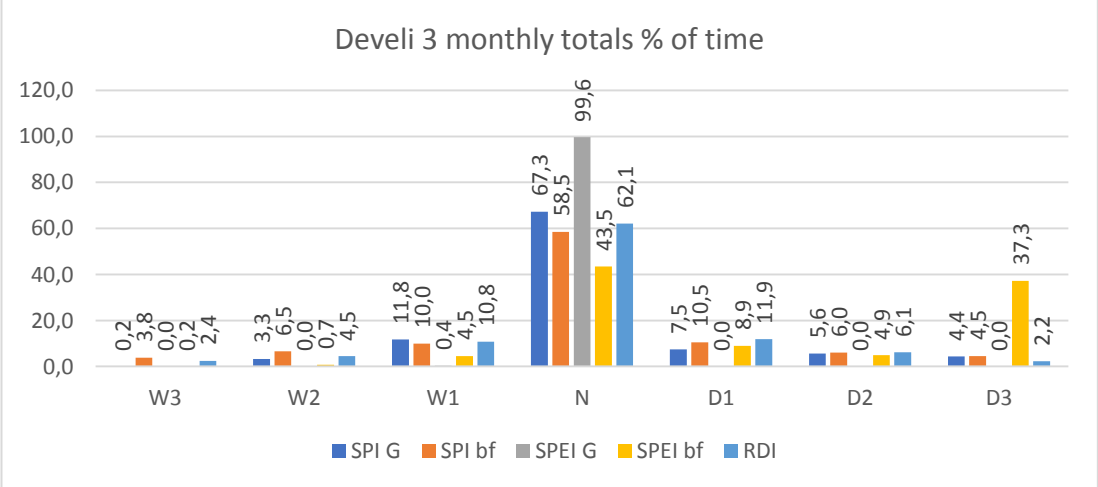


**APPENDIX A-1. 57.** Develi 3 monthly totals % of time histogram

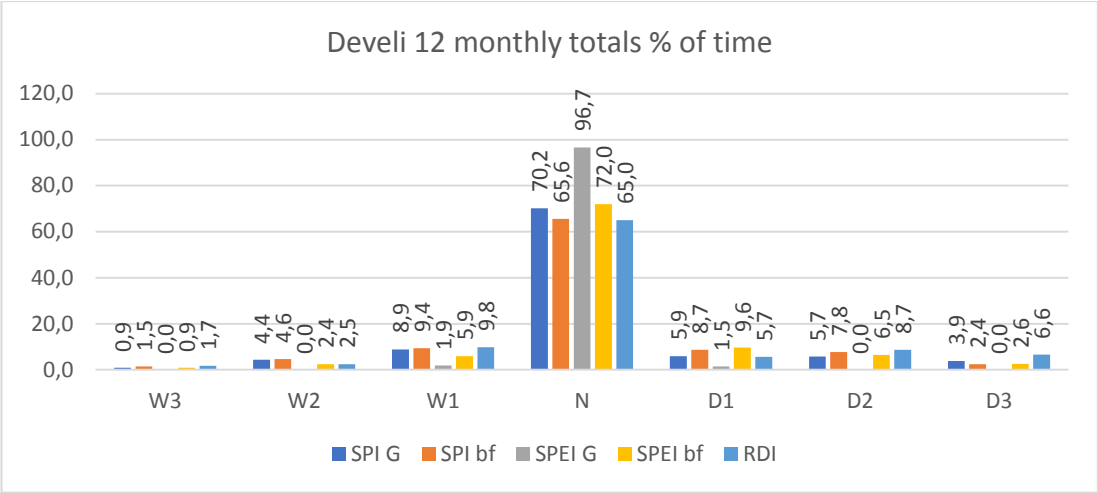


**APPENDIX A-1. 58.** Develi 12 monthly totals % of time histogram

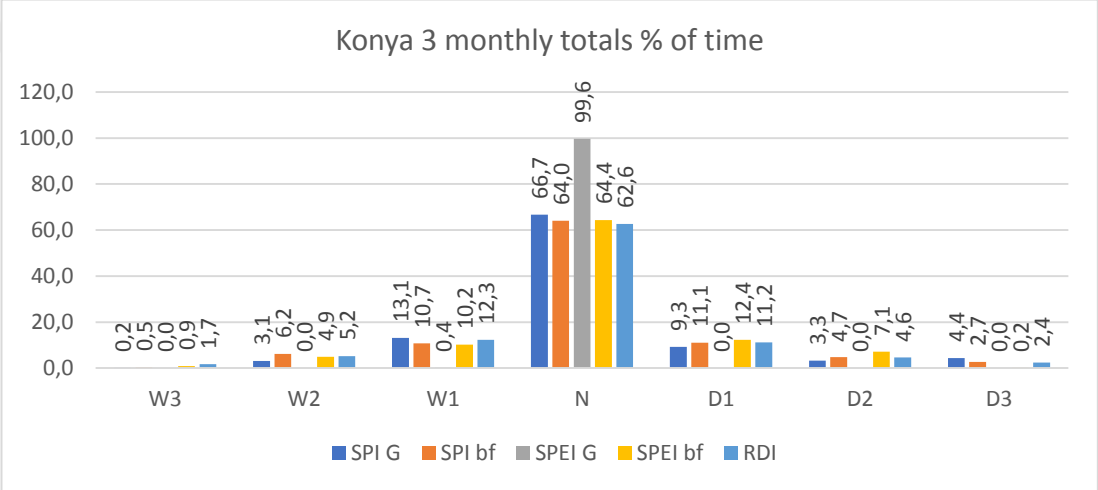


**APPENDIX A-1. 59.** Konya 3 monthly totals % of time histogram

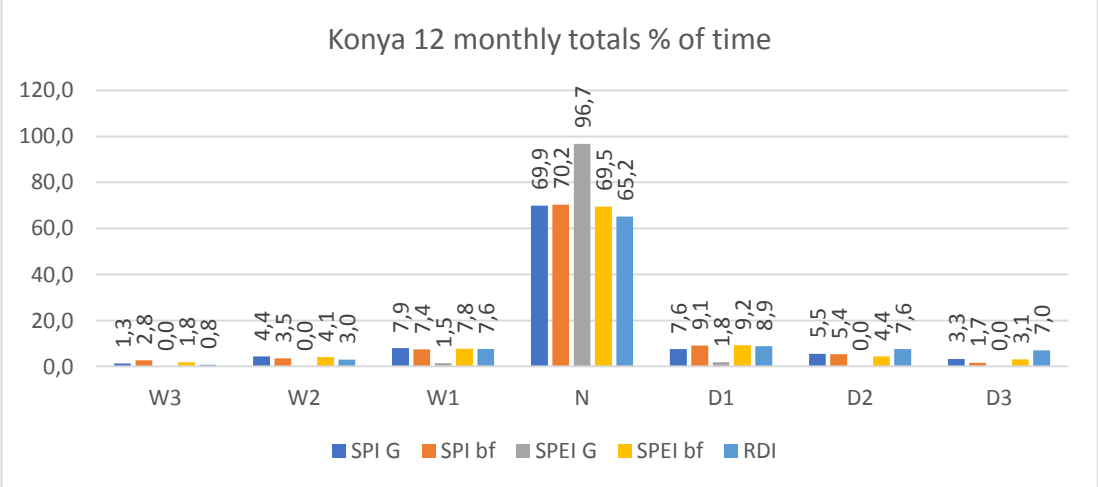


**APPENDIX A-1. 60.** Konya 12 monthly totals % of time histogram

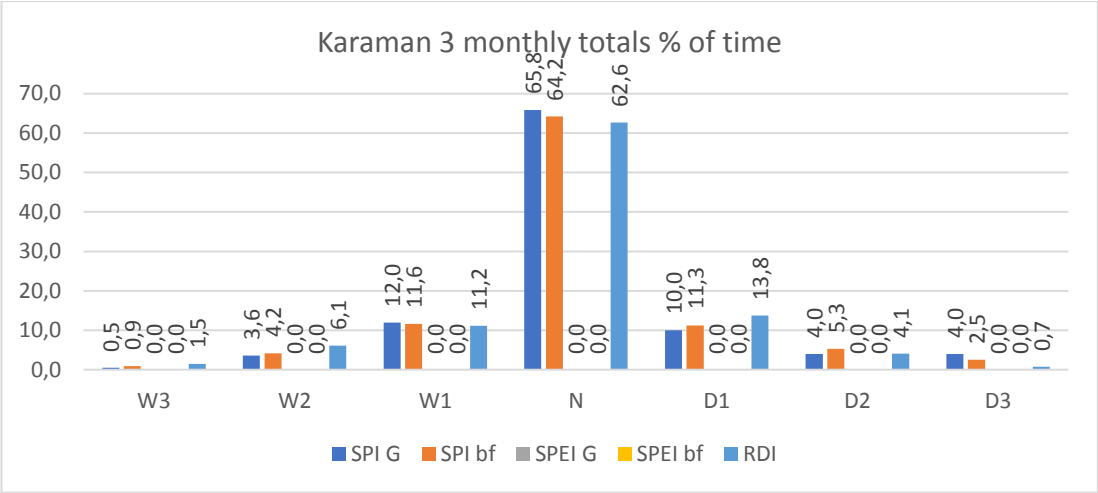


**APPENDIX A-1. 61.** Karaman 3 monthly totals % of time histogram

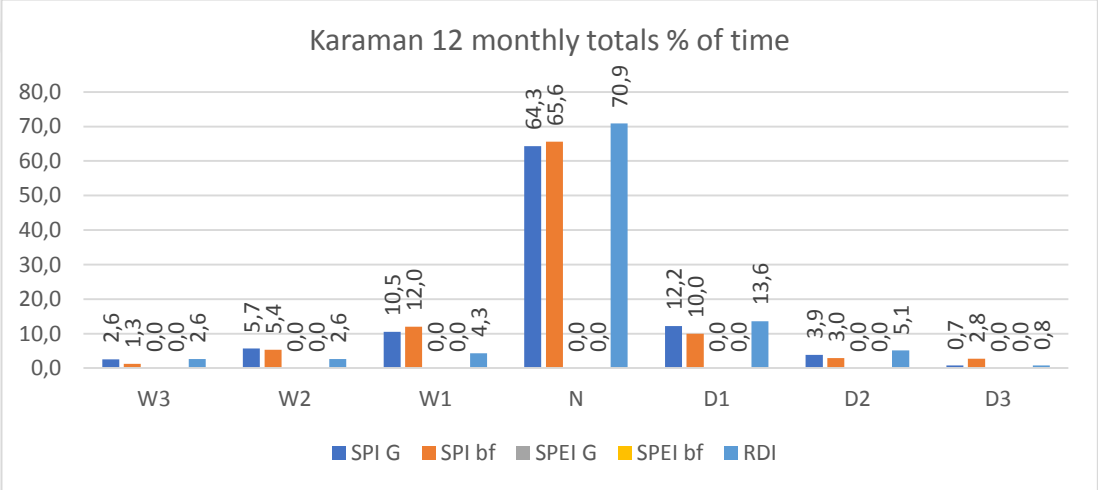


**APPENDIX A-1. 62.** Karaman 12 monthly totals % of time histogram

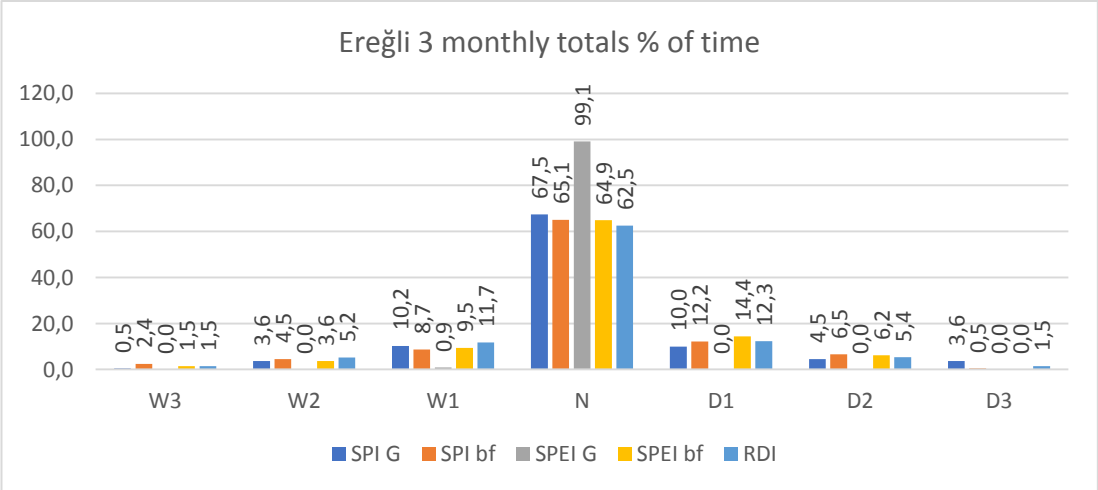


**APPENDIX A-1. 63.** Ereğli 3 monthly totals % of time histogram

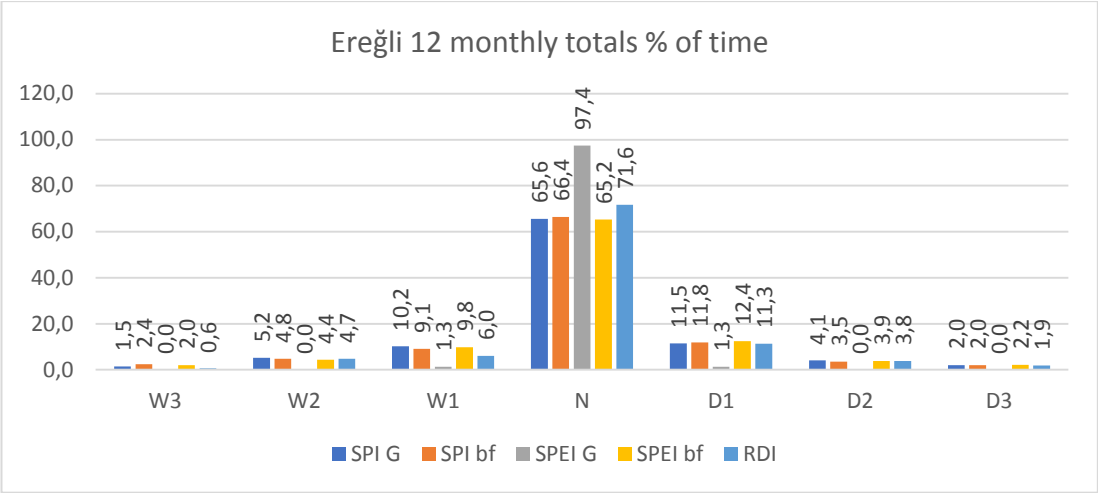


**APPENDIX A-1. 64.** Ereğli 12 monthly totals % of time histogram

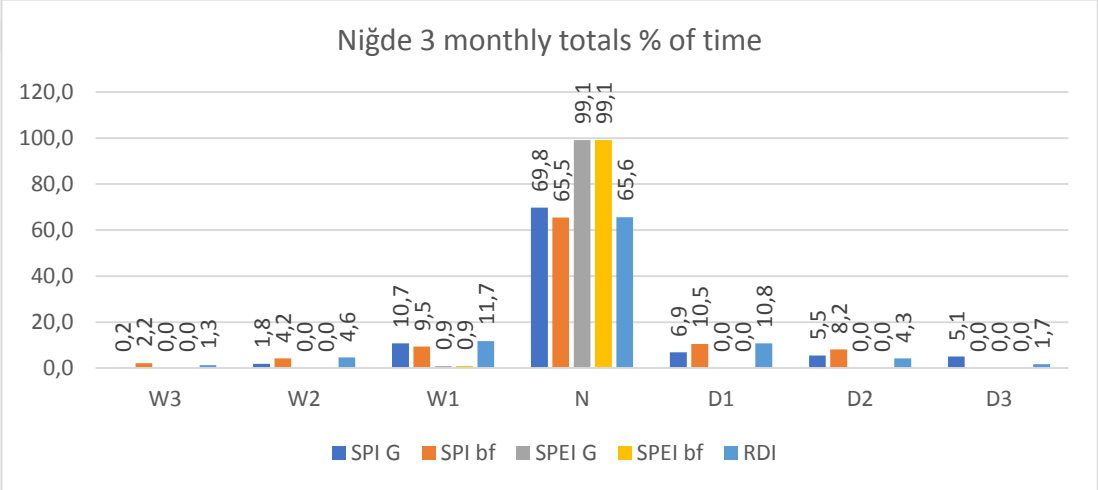


**APPENDIX A-1. 65.** Niğde 3 monthly totals % of time histogram

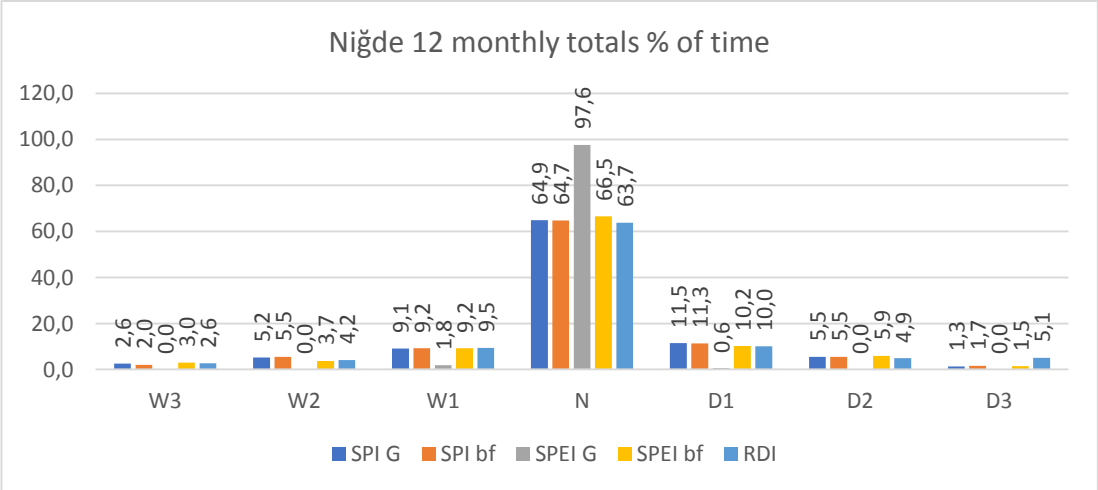


**APPENDIX A-1. 66.** Niğde 12 monthly totals % of time histogram

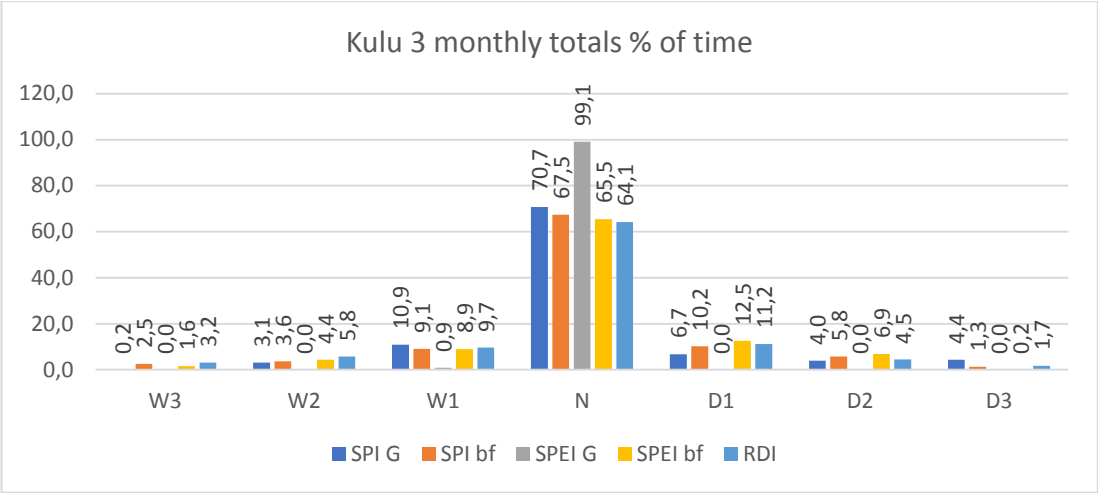


**APPENDIX A-1. 67.** Kulu 3 monthly totals % of time histogram

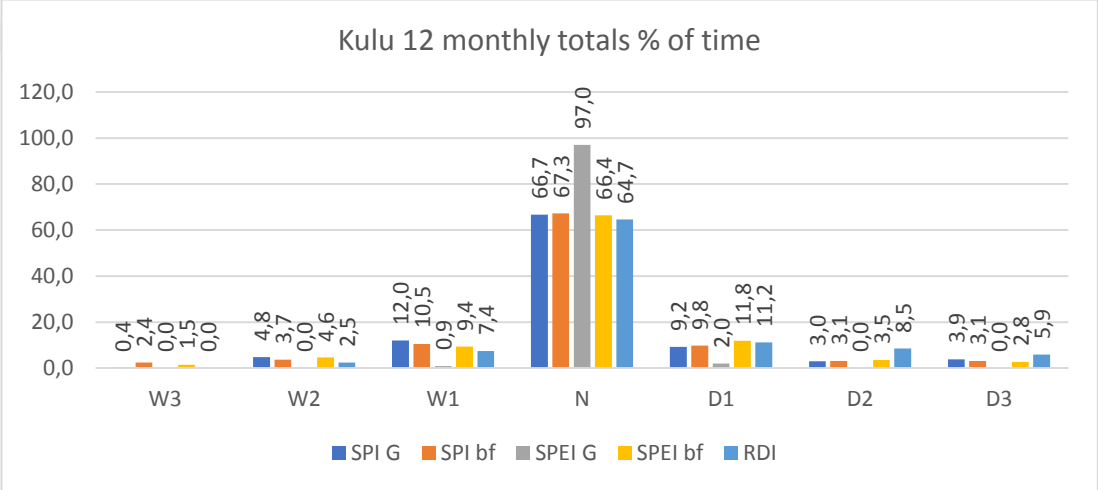


**APPENDIX A-1. 68.** Kulu 12 monthly totals % of time histogram

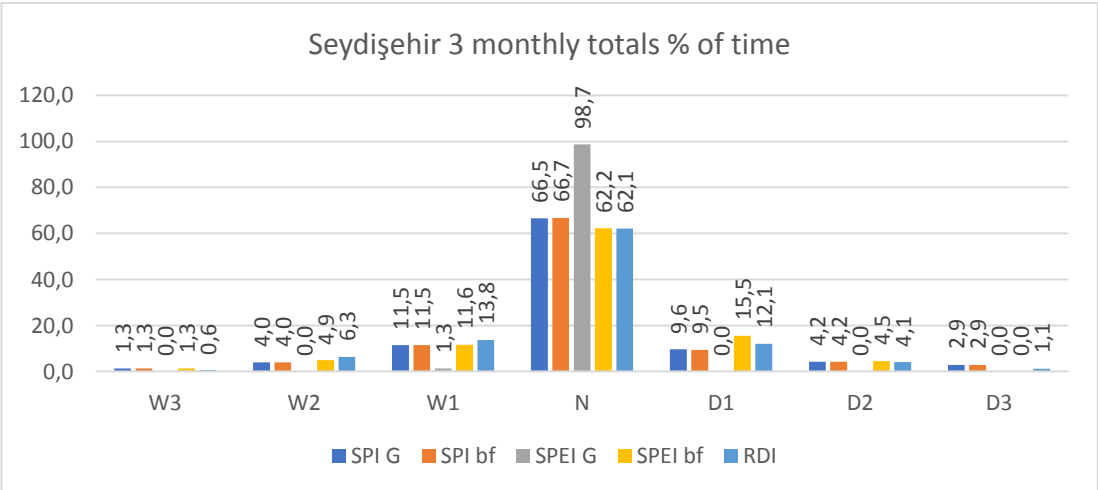


**APPENDIX A-1. 69.** Seydişehir 3 monthly totals % of time histogram

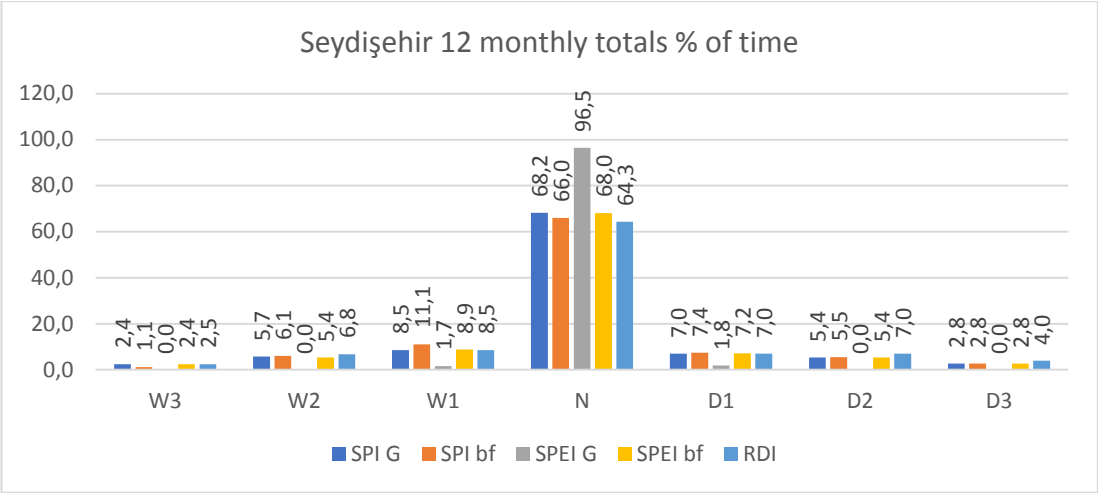


**APPENDIX A-1. 70.** Seydişehir 12 monthly totals % of time histogram

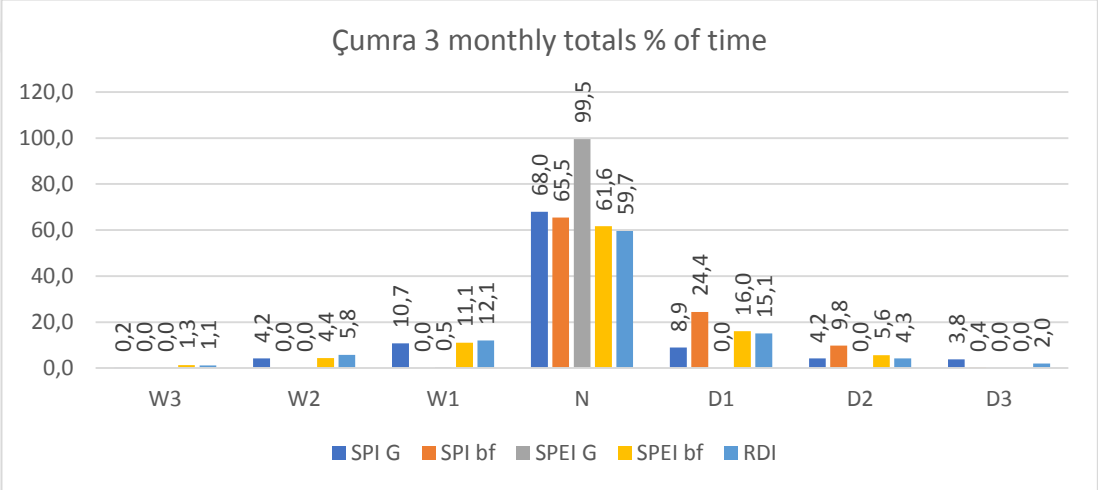


**APPENDIX A-1. 71.** Çumra 3 monthly totals % of time histogram

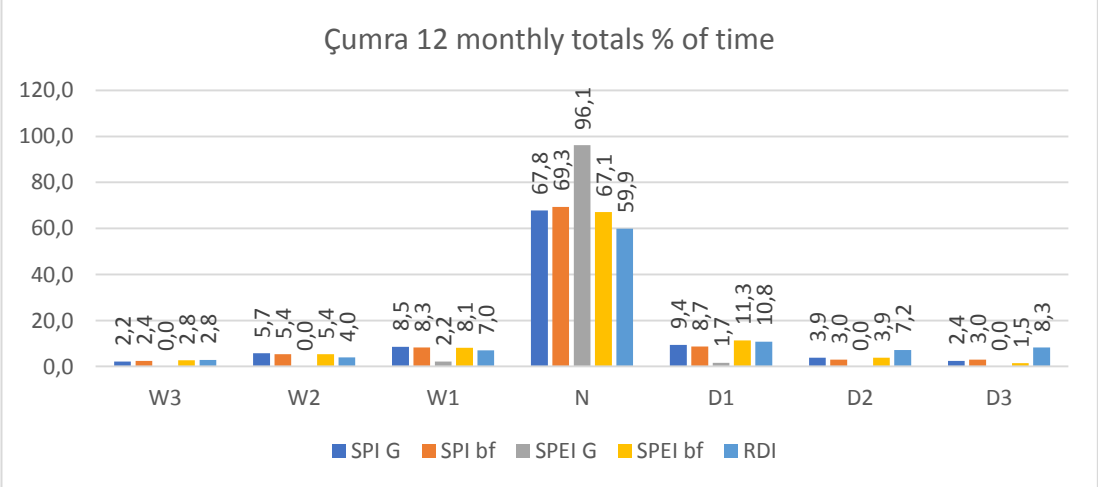


**APPENDIX A-1. 72.** Çumra 12 monthly totals % of time histogram

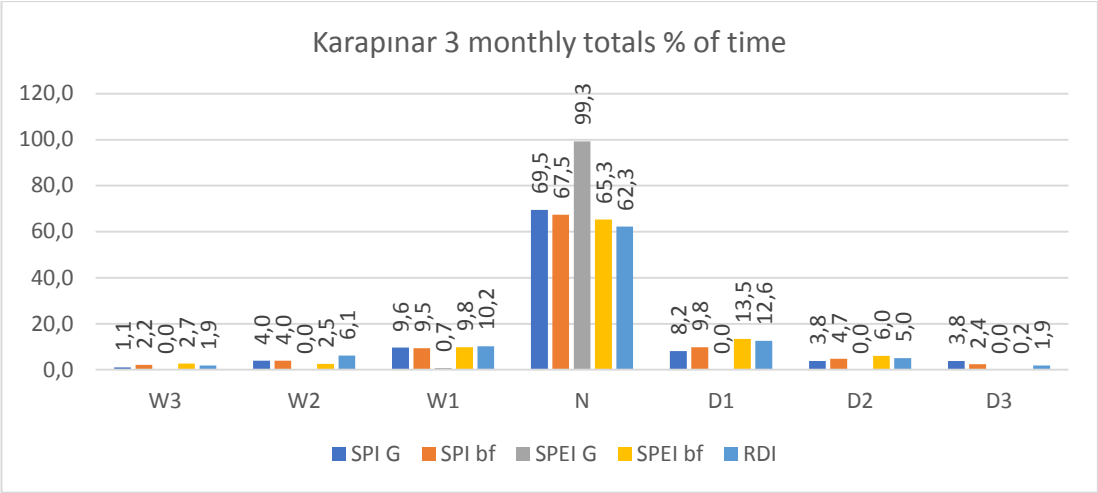


**APPENDIX A-1. 73.** Karapınar 3 monthly totals % of time histogram

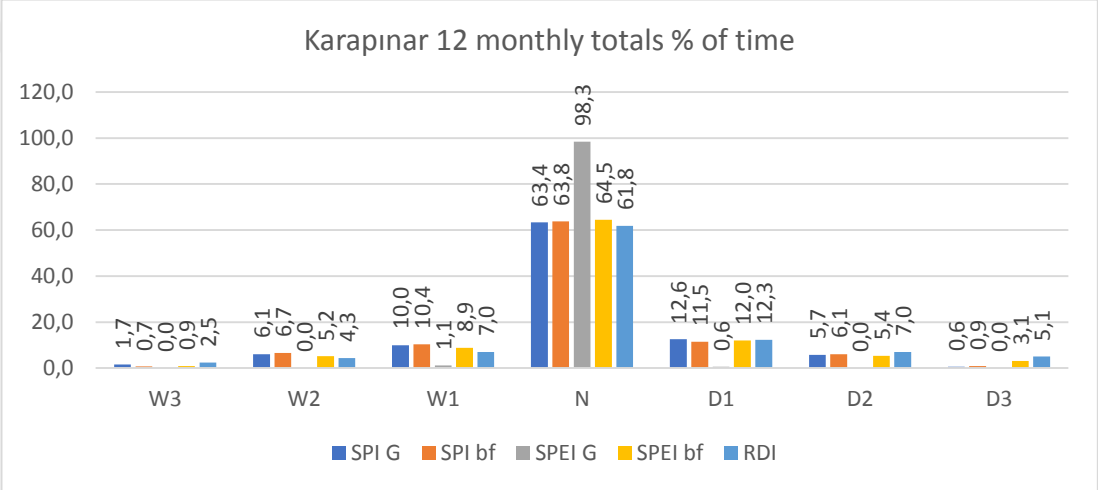


**APPENDIX A-1. 74.** Karapınar 12 monthly totals % of time histogram

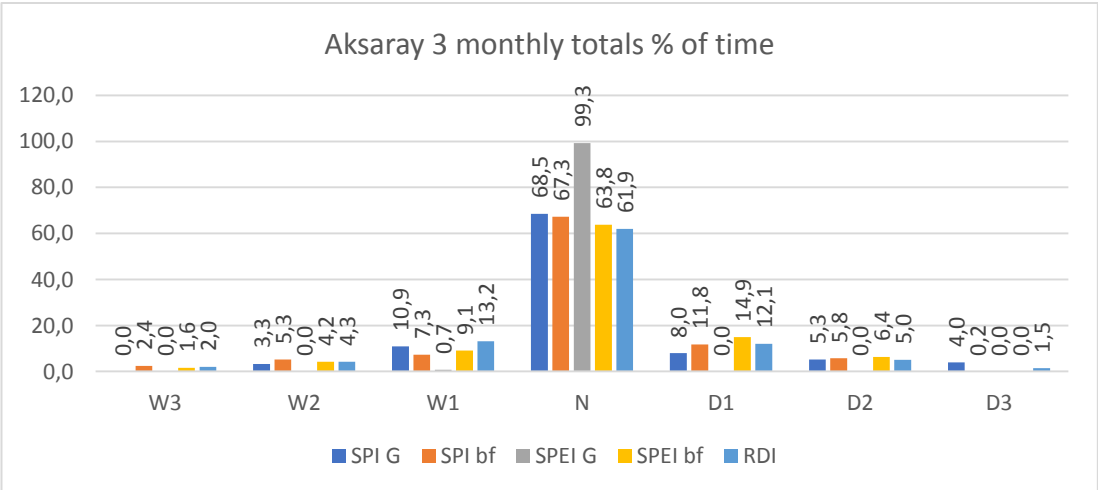


**APPENDIX A-1. 75.** Aksaray 3 monthly totals % of time histogram

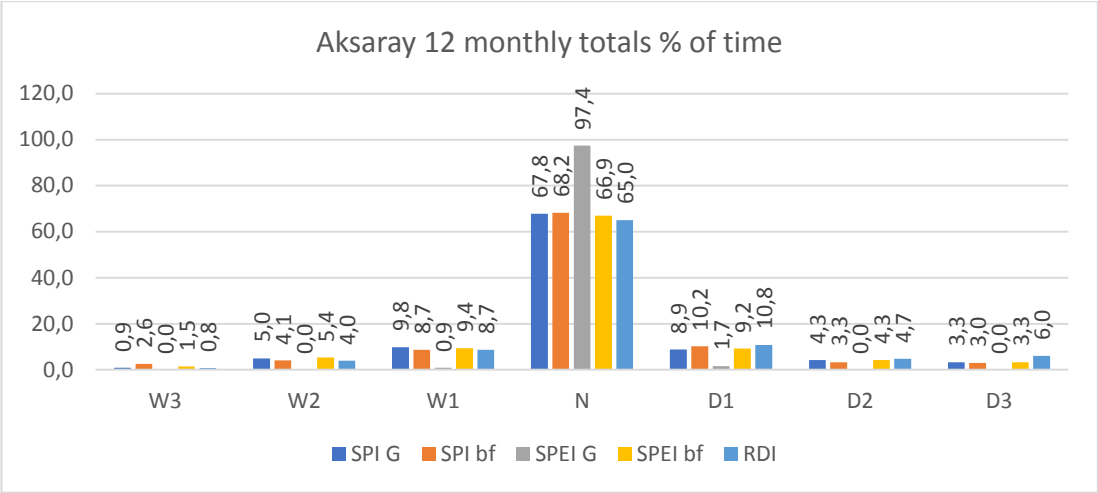


**APPENDIX A-1. 76.** Aksaray 12 monthly totals % of time histogram

## CURRICULUM VITAE

**Name and Surname** : Mehmet Selim GEYİKLİ

**Nationality** : Republic of Türkiye

**Education Information**

| | | |
|---|---|---|
| **Undergraduate** | : Gümüşhane University, | 2013 |
| **Master** | : İnönü University, | 2016 |
| **Ph. D.** | : Hasan Kalyoncu University, | 2023 |

**PROFESSIONAL EXPERIENCE**

Tokat Gaziosmanpaşa University / Research Assistant (2015-)

**PUBLICATIONS AND PRESENTATIONS**

- HINIS MEHMET ALİ, GEYİKLİ MEHMET SELİM, (2023). "Accuracy Evaluation of Standardized Precipitation Index (SPI) Estimation under Conventional Assumption in YeŞilırmak, Kızılırmak, and Konya Closed Basins, Turkey". Hindawi, Advances in Meteorology, Volume 2023, Article ID 5142965, 13 pages, https://doi.org/10.1155/2023/5142965
- GEYİKLİ MEHMET SELİM, HINIS MEHMET ALİ, YÜREKLİ KADRİ, (2022). "Drought Analysis With Two Different Indices İn Yeşilırmak Basin", Journal Of Agricultural Faculty Of Gaziosmanpasa University, 39(3), 151-160., Doi: 10.55507/gopzfd.1166245 (Yayın No: 8296536)
- GEYİKLİ MEHMET SELİM, HINIS MEHMET ALİ, YÜREKLİ KADRİ, YURTSEVER ADEM (2022). STANDARTLAŞTIRILMIŞ YAĞIŞ İNDEKSİ (SYİ) YÖNTEMİYLE KURAKLIK HESABI: TOKAT İLİ ÖRNEĞİ. 8. ULUSLARARASI MARDİN ARTUKLU BİLİMSEL ARAŞTIRMALAR KONGRESİ (Tam Metin Bildiri) (Yayın No:7865904)
- Değişli Beyza, Aksu Şeyma, Nergiz Nazlı, Göktaş Hilmi Emre, GEYİKLİ MEHMET SELİM, SEVİMLİ MEHMET FAİK, DEMİR VAHDETTİN (2022). Investigation of homogeneity test of annual total precipitation of

Konya Closed Basin with standard normal homogeneity test. 5th Advanced Engineering Days (AED) (Tam Metin Bildiri) (Yayın No:7998797)

- DEMİR VAHDETTİN, ÇITAKOĞLU HATİCE, GEYİKLİ MEHMET SELİM, KUYUCU HÜLYA (2017). Estimation of Digital Elevation Model by Artificial Intelligence Methods. 1st International Symposium on Multidisciplinary Studies and Innovative Technologies (Özet Bildiri) (Yayın No:3696111)
- ÇITAKOĞLU HATİCE, GEYİKLİ MEHMET SELİM, DEMİR VAHDETTİN (2017). Ege Bölgesi Yaz Ayları Buharlaşma Verilerine Trend Analizi. 5. Uluslararası Katılımlı Toprak ve Su Kaynakları Kongresi (Tam Metin Bildiri) (Yayın No:3598055)
- KUYUCU HÜLYA, DEMİR VAHDETTİN, GEYİKLİ MEHMET SELİM, ÇITAKOĞLU HATİCE (2017). Trend Analysis of Turkey Temperatures. 1st International Symposium on Multidisciplinary Studies and Innovative Technologies Proceedings (Tam Metin Bildiri) (Yayın No:3895963)
- ÇITAKOĞLU HATİCE, GEYİKLİ MEHMET SELİM (2017). Determination of Intensity-Duration-Frequency Relationship By Excel Solver In Inner Anatolia Region. 2nd INTERNATIONAL CONFERENCE ON CIVIL AND ENVIRONMENTAL ENGINEERING (Tam Metin Bildiri) (Yayın No:3568791)
- GEYİKLİ MEHMET SELİM, DEMİR VAHDETTİN, KİŞİ ÖZGÜR (2016). Orta Karadeniz Bölümünde Toplam Yağışlar Artıyor mu Azalıyor mu. International Symposium of Water and Wastewater Management (Tam Metin Bildiri) (Yayın No:2924033)
- GEYİKLİ MEHMET SELİM, DEMİR VAHDETTİN (2016). Orta Karadeniz Bölümünde Toplam Yağışlar Artıyor mu Azalıyor mu Does the Total Precipitation of Central Black Sea Region Increase Or Decrease. Uluslararası Kentsel Su ve Atıksu Yönetimi Sempozyumu (Tam Metin Bildiri) (Yayın No:2923614)
- AYDOĞDU MAHMUT, GEYİKLİ MEHMET SELİM (2016). Darende Nadir Köprüsü veTaşkın Durumlarının İncelenmesi. Uluslararası Kentsel Su ve Atıksu Yönetimi Sempozyumu (Tam Metin Bildiri) (Yayın No:2923622)

- DEMİR VAHDETTİN, GEYİKLİ MEHMET SELİM, KİŞİ ÖZGÜR (2016). Trend Analysis of Precipitation and Temperature in Tokat. International Conference on Natural Science and Engineering(ICNASE'16) (Tam Metin Bildiri) (Yayın No:2682009)
- GEYİKLİ MEHMET SELİM, DURSUN ÖMERUL FARUK (2015). Malatya İçme Suyu Kaynağı ve Şebekesinin Taşkın Risklerinin Değerlendirilmesi. 7. Kentsel Altyapı Sempozyumu (Tam Metin Bildiri) (Yayın No:2600248)